

# Modeling Rift Valley fever virus transmission dynamics

*insight from micro- to macro-scale studies*



*Hélène Cecilia*



# THESE DE DOCTORAT DE

ONIRIS

ECOLE DOCTORALE N° 600

*Ecole doctorale Ecologie, Géosciences, Agronomie et Alimentation*

Spécialité : Epidémiologie, évaluation des risques

Par

**Hélène CECILIA**

## **Modeling Rift Valley fever virus transmission dynamics**

Insight from micro- to macro-scale studies

Thèse présentée et soutenue à Nantes, le 28 octobre 2021

Unité de recherche : INRAE, Oniris, BIOEPAR, 44300 Nantes, France

### **Rapporteurs avant soutenance :**

Cécile Viboud Senior staff scientist, Fogarty International Center, National Institutes of Health, Etats-Unis

Samuel Alizon Directeur de recherche, CNRS Montpellier

### **Composition du Jury :**

Président : Frédérick Arnaud

Directeur de recherche cumulant à EPHE/INRAE Lyon

Examineurs : Catherine Linard

Professeure à l'Université de Namur, Belgique

Sebastian Lequime

Professeur assistant à l'Université de Groningen, Pays-Bas

Directrice de thèse : Pauline Ezanno

Directrice de recherche à INRAE Nantes

Co-encadrants de thèse : Raphaëlle Métras

Chargée de recherche à l'INSERM de Paris

Renaud Lancelot

Vétérinaire épidémiologiste au CIRAD de La Réunion



*La thèse c'est jongler entre l'espoir de ne pas être le génie que l'on espère et l'angoisse d'être  
l'abruti que l'on redoute.  
Marie-Hélène Douchez*



*À mon grand-père, Francis Cecilia.*





# Remerciements

Bonjour à toi, chère lectrice, cher lecteur, ou peut-être bonsoir. Je peux te tutoyer ? Il paraît que cette section sera certainement la plus lue de ma thèse. Je ne peux pas te promettre qu'elle répondra à toutes tes attentes. Si je ne te connais pas, j'imagine que tu es un·e étudiant·e ou (apprenti·e) chercheur·se, en train de procrastiner avant de te plonger dans la section que tu es réellement venu·e chercher. Si on se connaît, alors peut-être espères-tu voir apparaître ton nom quelque part sur cette page, tel un signe de reconnaissance. Si tu ne le trouves pas, pose toi les bonnes questions (je rigole). Trêve de plaisanteries, j'ai plein de gens à remercier, on va pas y passer la journée.

Tout d'abord, je voudrais sincèrement remercier Cécile Viboud et Samuel Alizon, d'avoir accepté d'être les rapporteurs de cette thèse. Merci pour votre disponibilité malgré un emploi du temps chargé, et pour la bienveillance de vos rapports qui m'a beaucoup touchée. Je tiens également à remercier Catherine Linard, Sebastian Lequime, et Frederick Arnaud, d'avoir accepté d'examiner mon travail et Frederick d'avoir présidé le jury. À tous les cinq, vos regards croisés sur ma recherche m'ont permis d'enrichir ma perspective, et pour cela, je vous remercie.

Les mots risquent de me manquer pour exprimer ma gratitude envers mes encadrant·e-s, Pauline, Raphaëlle, et Renaud. Je vais tâcher d'être brève, et pas trop mielleuse.

Pauline d'abord, directrice de thèse et mentor en cheffe ! Merci pour ton accompagnement et ta confiance qui, dès mon contrat d'ingénieure, m'ont permis de m'épanouir dans ce travail. Grâce à cela, j'ai pu m'engager en pleine conscience dans la thèse, déjà assurée que notre duo allait fonctionner, ce qui est un énorme avantage. Merci pour tes idées, souvent débitées à un rythme déconcertant, parfois intimidant, mais qui ont forgé mon esprit d'exploratrice de modèles ! Merci pour tes relectures bienveillantes et argumentées, jamais décourageantes, qui ont su laisser la place à mon propre style d'écriture. Merci d'avoir râbaché aussi souvent que nécessaire "C'est ta thèse, tu as le dernier mot, c'est toi qui connais le mieux ton sujet et l'important est que tu sois fière de ce que tu as produit." Ça a fini par rentrer !!

À Raphaëlle, avec qui je partage de bien trop nombreux points communs: marseillaise, ayant eu Mme Rouquerol en maîtresse de primaire, ayant fait ses études supérieures à Lyon et ayant vécu en Angleterre ! Comme quoi, ça devait être écrit ! Merci pour tes mots d'encouragements, qui, mêlés à ton management *à l'anglaise*, m'ont permis de gagner en autonomie tout en sachant que j'allais dans la bonne direction. Tes incitations régulières à "boire des coups pour fêter

ça” m’ont fait réaliser que chaque petite réussite peut et doit être célébrée pour rester motivée !

À Renaud, pour qui le premier qualificatif qui me vient est “puit de science”. Merci pour ce stock illimité d’hypothèses de travail sur la Rift au Sénégal, tes anecdotes de terrain, et ta connaissance politique du monde de la recherche, qui m’ont beaucoup enrichie.

À Quirine, avec qui je me suis dès le départ sentie collaboratrice et non étudiante. Merci pour ta confiance, ta gentillesse, pour m’avoir fait profiter de ton réseau sans réserve et pour tes conseils de carrière! Merci à toute l’équipe de WUR pour l’accueil, et merci à Pauline et Haniel pour les rires, les *lunch* et les pintes!

Aux membres de mon comité de suivi de thèse, Véronique, Benoit et Cyril, merci pour votre aiguillage. Un merci supplémentaire à Véronique et Benoit pour leur implication en tant que collaborateurs sur deux des chapitres de cette thèse. Cela m’amène à remercier Alex, qui a naïvement accepté de collaborer sur la revue de la littérature des modèles Rift, et qui ne se doutait probablement pas du travail que ça représentait. Merci pour tes GIF et tes punchlines sur le Slack, en tête desquelles : “J’estime que j’ai perdu environ 4 ans d’espérance de vie” et “Le moustique préfère-t-il un zébu tuberculeux ? Un beau sujet de thèse”. Cela a permis de mettre un peu de joie dans notre désarroi face à des articles pour lesquels les qualificatifs me manquent ...!

À Marie et Mathilde, mes co-bureau, co-café, co-runneuse, co-yoga, et *gossip girl* de choc! Merci pour les rires, les larmes, les coups de colère et les “crises de calme” de petit Bambou ! Merci d’avoir été la soupape de décompression dont tout-e doctorant-e a besoin. Merci à *mamène* Erwann, pilote de l’extrême, pour les moments *bitch*, les discussions féministes, la boîte à thé, les conseils vins, les calins, les gâteaux, les crêpes et les yaourts ! Merci aux docs de choc pour les repas, les foot, squash et autres moments détente. Merci à Mich-much, Sylvie et Juliette, pour leur appui sans faille. Merci enfin à toute l’équipe Dynamo, la Dynamo-cratie, où ça sait jouer collectif et ça fait du bien ! Merci à Vianney et Sébastien pour leurs blagues, jeux de mots et références historiques improbables. Merci à Sandie, codeuse/débuggeuse/wiki-euse formidable. Merci à Gaël, pour les gâteaux (encore!), les cafés, les points bricolo pendant nos travaux respectifs, et les conseils esthétiques pour les figures de papiers !

Merci à Maxime, coordinateur du projet FORESEE, concentré de gentillesse et de bienveillance ! Merci à Ibra , Moustafa et Diam Sow pour cette mission terrain que je n’oublierai jamais. Merci à l’ISRA pour l’accueil à Dakar et particulièrement à Assane pour sa disponibilité.

Merci à Blatteman<sup>1</sup> pour ses illustrations, en couverture et dans les chapitres 3 et 4 grand public.

Viennent désormais les remerciements à l'entourage non professionnel, qui contribue tout autant à la réussite d'une thèse, d'avantage sur le plan mental que scientifique ! Merci tout d'abord à mes parents, pour leur soutien et leur amour. Merci à maman, *coach* devoirs puis *coach* peinture, de m'avoir transmis le goût du travail bien fait et ce petit côté littéraire qui je l'espère rend cette thèse agréable à lire. Merci à papa de m'avoir transmis la curiosité scientifique, le goût de la résolution de problèmes, et un côté un peu *geek* ! Merci à Jeanne, petite soeur, petit carlin au grand coeur, Bloubie junior, d'avoir agrandi la diaspora Cecilia à Nantes, avec qui on peut parler de tout sans tabou, un petit bonbon au bambou !

Merci aux copains, celles qui se sont déplacées de loin pour la soutenance, "la colloc" pour les poireaux, les cointreau-basket, les Levrette café et autres soirées Miss France. Merci à Tim, mon fan number one, grâce à qui j'ai réalisé mon rêve de conduire une Audi TT. Merci aux vulgarisateur·rice·s du Labo des Savoirs, pour ces précieux moments radiophoniques. Merci aux Pintes à Vélo pour le rugby, la transpi, les toucher, les passes ratées, et qui m'ont permis de décompresser.

À Jean-Baptiste, qui me fait rire tous les jours, qui m'a permis de rester saine d'esprit dans un 28m<sup>2</sup> pendant le confinement, qui m'a embarquée dans le projet fou d'acheter un appartement avec travaux un an avant la fin de la thèse... Merci pour tout ça, pour ta méconnaissance du monde de la recherche, qui engendre des conseils parfois décalés, qui peuvent me faire pester mais qui m'ont permis de porter un nouveau regard sur certaines situations. Merci pour ton optimisme, ta présence, ta patience, ton soutien, tes "Ça va ?", tes blagues, tes chansons qui restent dans la tête, tes pas de danse, les parties de Mario Kart (et désormais de baby foot) endiablées. Merci pour cette complicité et cet amour qui m'ont permis d'avancer.

---

<sup>1</sup> Ses travaux sont à retrouver sur <https://twitter.com/BlatteManCorp> ou <https://blatteman182569782.wordpress.com/>



# Contents

<b>1</b>	<b>Introduction</b>	<b>1</b>
1.1	Vector-borne and zoonotic diseases . . . . .	1
1.2	Mathematical modeling in epidemiology . . . . .	2
1.3	Rift Valley fever virus . . . . .	9
1.4	The Sahelian setting . . . . .	12
1.5	Thesis objective and outline . . . . .	13
<b>2</b>	<b>Models of Rift Valley fever virus transmission dynamics - Systematic review</b>	<b>15</b>
2.1	Introduction . . . . .	15
2.2	Material and Methods . . . . .	17
2.2.1	Search strategy . . . . .	17
2.2.2	Inclusion and exclusion criteria . . . . .	17
2.2.3	Screening . . . . .	17
2.2.4	Model categories . . . . .	18
2.3	Results and discussion . . . . .	18
2.3.1	Study selection . . . . .	18
2.3.2	Context modeled . . . . .	20
2.3.3	Data . . . . .	23
2.3.4	Contribution to RVFV epidemiology . . . . .	24
2.3.5	Force of infection . . . . .	30
2.3.6	Diversity of assumptions . . . . .	32
2.3.7	Connected papers . . . . .	33
2.4	Conclusion . . . . .	34
2.5	Supplementary information . . . . .	36
<b>3</b>	<b>Epidemic potential in northern Senegal - Basic reproduction number</b>	<b>39</b>
3.1	[In French] Résumé grand public . . . . .	39
3.1.1	Potentiel épidémique : qu’entend-on par là ? Pourquoi l’estimer ? . . . . .	41
3.1.2	La métrique du $R_0$ comme outil . . . . .	43
3.1.3	Notre étude: comment créé-t-on une nouvelle information à partir de données existantes ? . . . . .	47
3.2	Article . . . . .	55
3.3	Supplementary Information . . . . .	66

<b>4</b>	<b>Transmission potential of livestock hosts - Within-host model</b>	<b>83</b>
4.1	[In French] Résumé grand public . . . . .	83
4.1.1	La multiplication du virus dans un hôte : comment ça marche ? . . . . .	84
4.1.2	Comment faire pour qu'un modèle mathématique reproduise fidèlement les données réelles ? . . . . .	88
4.1.3	Le voyage du virus dans un moustique . . . . .	92
4.1.4	Notre étude: les différentes espèces animales sont-elles toutes logées à la même enseigne pour transmettre la fièvre de la Vallée du Rift ? . . . . .	95
4.2	Article . . . . .	97
4.3	Supplementary Information . . . . .	120
<b>5</b>	<b>Role of seasonal herd movements - Metapopulation model</b>	<b>131</b>
5.1	Introduction . . . . .	131
5.2	Material and Methods . . . . .	133
5.2.1	Input data . . . . .	133
5.2.1.1	Patch selection . . . . .	133
5.2.1.2	Vector populations . . . . .	135
5.2.1.3	Host populations . . . . .	135
5.2.1.4	Hosts movements . . . . .	136
5.2.2	Metapopulation model . . . . .	138
5.2.2.1	Within-patch : RVF virus transmission dynamics . . . . .	138
5.2.2.2	Between-patch : animal mobility . . . . .	141
5.2.3	Scenarios of animal movements . . . . .	143
5.2.3.1	Raw movements . . . . .	143
5.2.3.2	Synthetic movements . . . . .	144
5.3	Results . . . . .	144
5.3.1	Raw movements . . . . .	144
5.3.2	Synthetic movements . . . . .	144
5.4	Discussion . . . . .	149
5.5	Supplementary information . . . . .	152
<b>6</b>	<b>Discussion</b>	<b>163</b>
6.1	Main contributions . . . . .	163
6.2	Implications . . . . .	165
6.3	Perspectives . . . . .	168
6.4	Questions pending . . . . .	170
6.5	Lessons learned from the community . . . . .	171
6.6	Conclusion . . . . .	172
	<b>Bibliography</b>	<b>173</b>
	<b>Appendices</b>	<b>198</b>

A	Article (co-author) - Over 100 years of Rift Valley fever : a patchwork of data on pathogen spread and spillover . . . . .	199
B	<i>Curriculum vitae</i> . . . . .	219
C	In French - Rapport de mobilité . . . . .	223
D	Conference poster - EEID 2021 . . . . .	225
E	Pictures taken during my field trip in Senegal - December 2019 . . . . .	227
F	PhD abstract . . . . .	233

# List of Figures

1.1	Maps of RVFV historical spread and recent outbreaks . . . . .	11
2.1	PRISMA flow diagram representing the selection process. . . . .	19
2.2	Location and number of RVFV models. Scale of applied and grey models . . . . .	21
2.3	Objective and main output of models, per category. . . . .	25
2.4	Functional forms (FFs) used by models for their force of infection (vectorial transmission only) . . . . .	32
3.1	Zone d'étude et schéma du modèle mathématique . . . . .	40
3.2	Distinction entre dynamique de la maladie (liée aux symptômes) et dynamique de la contagiosité. . . . .	42
3.3	Succession d'évènements nécessaires à la transmission du virus . . . . .	45
3.4	Schéma représentant l'inclusion de différents jeux de données dans notre formule du $R_0$ . . . . .	48
3.5	Répartition géographique des localisations présentant le plus fort potentiel épidémique, pour chaque saison des pluies étudiée. . . . .	51
3.6	Article - Figure 1: Study area and model diagram . . . . .	57
3.7	Article - Figure 2: September is the month of highest RVFV epidemic potential in northern Senegal . . . . .	60
3.8	Article - Figure 3: Zones of high RVFV epidemic potential change between rainy seasons . . . . .	61
3.9	Article - Figure 4: Decreased vector densities do not greatly reduce RVFV epidemic potential in at-risk locations . . . . .	62
3.10	Article - Figure 5: In both study areas an increase in the proportion of immune cattle decreases the number of pixels with high $R_0$ values ( $R_0 > Q_{3,year}$ ) more effectively than increasing the proportion of immune small ruminants . . . . .	62
3.11	Article - Figure 6: The feeding preferences and the gonotrophic cycle duration of the most abundant vector species are the most influential parameters on the epidemic potential at the regional scale . . . . .	63
4.1	Schéma du modèle intra-hôte (idem Figure 4.6) . . . . .	88
4.2	Titre infectieux au cours du temps mesuré chez les animaux à la suite de leur infection par le virus de la FVR . . . . .	89



4.3	Sensibilité du modèle au changement de valeurs des paramètres . . . . .	90
4.4	Représentation schématique des événements se déroulant dans le moustique de l'ingestion d'un repas de sang infecté à la retransmission du virus à un nouvel hôte. . . . .	93
4.5	Relation entre le titre infectieux de l'animal et la probabilité d'infecter un moustique qui viendrait le piquer . . . . .	95
4.6	Article - Figure 1 : Graphical representation of the within-host model . . . . .	100
4.7	Article - Figure 2: Viral load data and model fits . . . . .	102
4.8	Article - Figure 3: Outcome measures per host group . . . . .	103
4.9	Article - Figure 4: Dose-response relationships linking host infectious viral load to the probability to infect mosquito vectors . . . . .	105
4.10	Article - Figure 5: Net infectiousness of RVFV livestock host species . . . . .	105
5.1	Selected patches for the metapopulation model . . . . .	134
5.2	Density of nomadic individuals per patch, per species, during the wet season . . . . .	136
5.3	Description of the network, and resulting patch dynamics when applying the 2015 raw dataset . . . . .	137
5.4	Schematic representation of how the within-patch model incorporates heterogeneity between livestock hosts, in terms of infectious period duration and infectiousness to mosquitoes . . . . .	140
5.5	Maximum number of <i>Aedes</i> and <i>Culex</i> per patch in 2015. Corresponding beginning and end dates of the wet season . . . . .	141
5.6	Schematic representation of the targeted synthetic within-patch nomadic population dynamics . . . . .	142
5.7	Example of nomadic population dynamics per patch . . . . .	145
5.8	Example of variability in patch prevalence between 10 stochastic runs . . . . .	145
5.9	Number of infected sedentary and nomadic animals over time, per patch . . . . .	147
5.10	Example of host and vector contribution to infections and transmission . . . . .	148

# List of Tables

2.1	Characteristics of spatial models as well as non-spatial models with external renewal. . . . .	22
2.2	Vaccination strategies implemented in models and main results. . . . .	29
3.1	Article - Table 1: Parameter values of the basic reproduction number $R_0$ derived from the mechanistic RVF virus transmission model with two host and two vector populations . . . . .	58
4.1	Article - Table 1: Parameter estimates for selected models . . . . .	103
4.2	Article - Table 2: Parameters of the within-host model . . . . .	111
5.1	Parameter values of the within-patch model, added or modified compared to Chapter 3 . . . . .	139

# 1

## Introduction

### 1.1 Vector-borne and zoonotic diseases

Vector-borne diseases represent a major threat to public health around the world (IFAH, 2014; WHO, 2014, Leta et al., 2018). So far, such diseases were mainly constrained to tropical settings due to more suitable climatic conditions (Sellers, 1980; Fouque and Reeder, 2019). Poor countries suffer the most from disease burden, due to their overall socio-economic vulnerability, e.g the lack of access to adapted health services or surveillance systems (Wandiga et al., 2010; Tusting et al., 2013; Bardosh et al., 2017). The consequences of poor animal- (production loss, trade bans) and public-health (labour force loss, decreased school attendance) end up slowing down the economic development of affected countries, which often mostly relies on agriculture (Boutayeb, 2010; Grace et al., 2015; El Bcheraoui et al., 2020). Globalization has greatly eased the circulation of hosts and the pathogens they carry (Saker et al., 2004; Massó Sagüés et al., 2019), and climate change will increasingly impact the distribution of vector populations (Parham et al., 2015; Fouque and Reeder, 2019). Together, these phenomena create the perfect conditions for vector-borne diseases to establish in disease-free areas (Massó Sagüés et al., 2019; Metelmann et al., 2019), as can already be witnessed in southern France with the autochthonous circulation of dengue and chikungunya (Jourdain et al., 2020).

Among vector-borne pathogens, arthropod-borne viruses (arboviruses) are a particularly concerning category. Most arboviruses are RNA viruses (the only known exception is African Swine Fever). Such viruses exhibit higher mutation rates than DNA viruses, which might explain their ability to accommodate to both vertebrate and invertebrate hosts (Coffey et al., 2013; Duffy, 2018). Consequently, they are often suited to multi-host transmission, and can be zoonotic (with or without the intervention of a vector), as is the case for West Nile, Japanese

encephalitis, tick-borne encephalitis, and Crimean-Congo haemorrhagic fever viruses, to name a few (Gubler, 2006). First settled and identified in the tropics, many arboviruses have now evolved and established at temperate latitudes, causing large outbreaks (Weaver and Reisen, 2010).

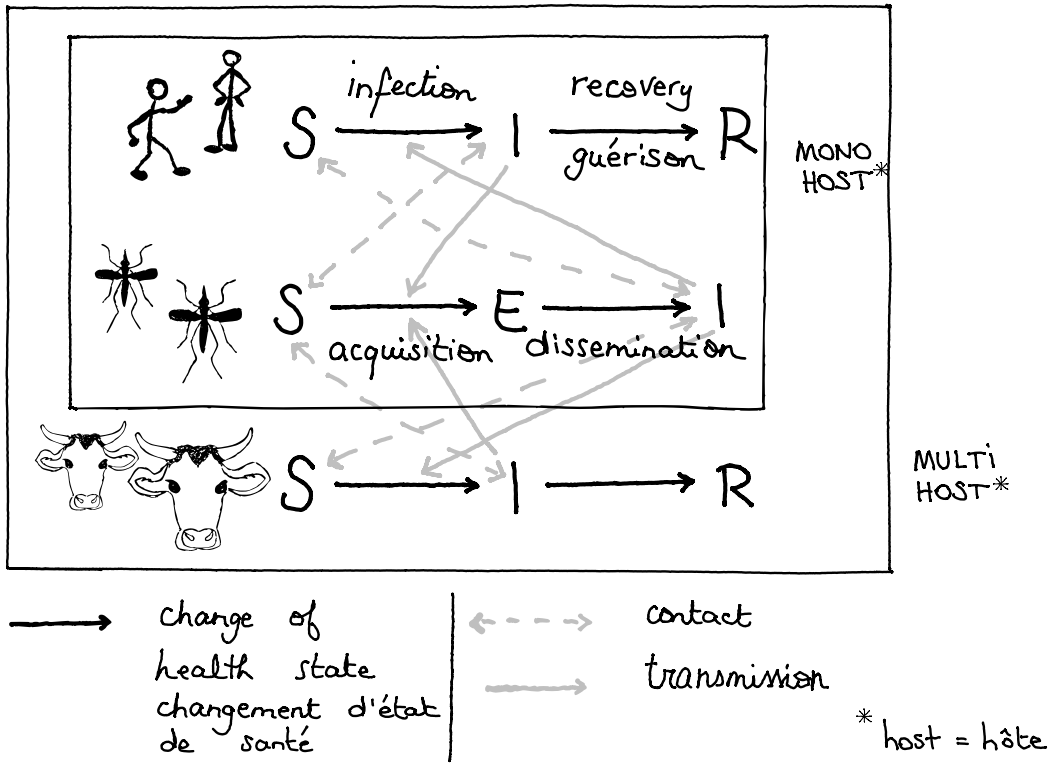
Zoonotic arboviruses transmission dynamics are shaped by complex interactions between the pathogen, vertebrate hosts, vectors, and the environment (Esser et al., 2019). To prevent and control outbreaks, an integrative approach must be adopted, to gain a deeper knowledge of all mechanisms underlying emergence, amplification, and spread of those diseases (Esser et al., 2019). Mathematical modeling is one possible tool to tackle this urgent challenge.

## 1.2 Mathematical modeling in epidemiology

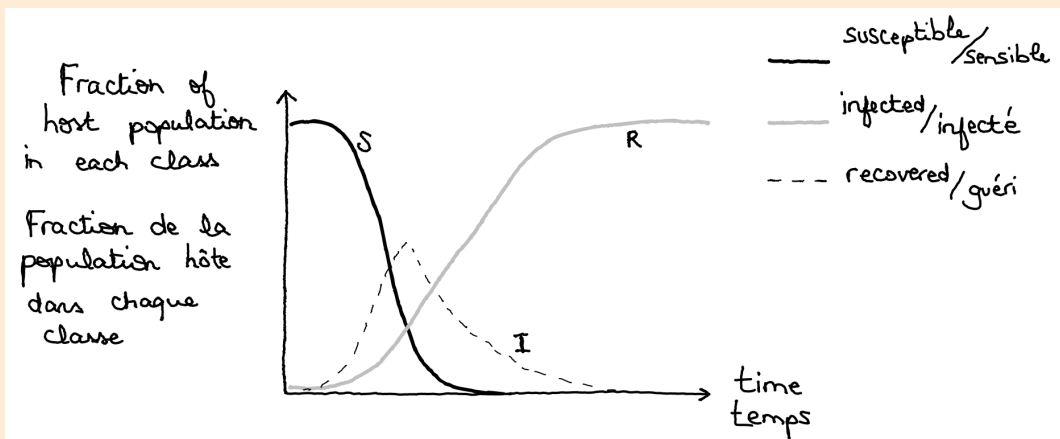
The use of mathematical models in epidemiology started long before modern computers could allow running large scale simulations in the blink of an eye, with Daniel Bernoulli demonstrating the advantages of smallpox inoculation in 1760 (Bacaër, 2011). One hundred and fifty years later, the first models developed for a vector-borne disease focused on ways to decrease transmission of malaria (Ross, 1908, 1911; Macdonald, 1956a,b; Macdonald and Gockel, 1964), which is still nowadays the deadliest vector-borne disease. Since then, this seemingly simple theoretical framework (Box 1.1, Keeling and Rohani, 2008) has provided critically important insights for the study of infectious diseases in general, although some sophistications have also been introduced in order to account for various sources of heterogeneity in the system (Reiner et al., 2013; Smith et al., 2014). In this section, I will first give a few definitions, then focus on some challenges modellers face when working on vector-borne and zoonotic diseases.

Box 1.1

Compartmental model applied to vector-borne diseases  
 Modèle à compartiments appliqué aux maladies vectorielles



Schematic diagram of a compartmental model intended for vector-borne diseases  
 Schéma d'un modèle à compartiments appliqué à une maladie vectorielle



Fraction of the population in each compartment over time : global dynamics when starting with a naive population, which is not replenished. Exact values depend on parameters of the model.  
 Fraction de la population dans chaque compartiment au cours du temps : dynamique globale lorsque la population n'a jamais été exposée à la maladie et qu'il n'y a pas d'entrée de nouveaux S dans le système au cours du temps. Les valeurs exactes dépendent des paramètres du modèle.

In compartmental models of infectious diseases, classes are built to contain the number of individuals in different health states. In its simplest form, such states are known as SIR : Susceptible, Infected, Recovered. When dealing with a vector-borne disease, the same reasoning is applied to the vector population, with a few adjustments. When infected, mosquitoes remain so until they die, hence the R compartment is removed. Besides, it takes time between the ingestion of a pathogen through a blood meal on an infected host, and the mosquito itself turning infectious. Therefore, an Exposed (E) compartment is added, to account for this delay, known as the extrinsic incubation period. In some cases, it can be relevant to account for different host (or vector) populations at once, each represented with their own set of compartments.

Model equations then aim at characterizing the rates at which individuals (hosts and vectors) go from one state to the other, on average, in order to reproduce the dynamics of an outbreak. In particular, the rate of contact between hosts and vectors will impact the rate at which individuals from both populations will get infected. Regarding vectors, the impact of meteorological conditions on their life cycle can be taken into account by setting their birth and death rates, as well as how often they are host-seeking, as temperature-dependent, for instance.

*Lorsqu'on cherche à développer un modèle à compartiment pour une maladie infectieuse donnée, on construit des catégories contenant le nombre d'individus dans différents états de santé. Le modèle le plus simple est appelé SIR, car les catégories en question sont Sensible, Infecté, et guéri (Recovered en anglais). Lorsque la maladie étudiée se transmet par un vecteur, le même raisonnement s'applique pour cette seconde population, avec quelques changements. En effet, les moustiques (par exemple), lorsqu'ils s'infectent, restent infectés jusqu'à leur mort, le compartiment R n'est donc pas nécessaire. De plus, après avoir ingéré un agent pathogène (un virus par exemple) en se nourrissant sur un hôte infecté, le moustique ne devient pas infectieux (càd contagieux) tout de suite. Un compartiment Exposé (E) est donc créé pour prendre en compte ce délai, que l'on appelle dans le jargon la période d'incubation extrinsèque. Par ailleurs, il est parfois utile de considérer plusieurs population d'hôtes (ou de vecteurs) simultanément dans un modèle. Dans ce cas, chaque population est associée à ses propres compartiments.*

*Les équations du modèle (que je ne montre pas ici) ont pour objectif de décrire ce qui déclenche les changements d'états de santé, et à quelle vitesse ceux-ci s'effectuent, en moyenne. C'est ce qui permet de reproduire la dynamique d'une épidémie dans le temps. En particulier, le taux de contact entre les hôtes et les vecteurs va influencer la propagation de l'agent pathogène dans ces populations. Pour les vecteurs, dont le cycle de vie est fortement dépendant des conditions météorologiques, le modèle peut être amélioré en considérant que la natalité, mortalité, ou encore l'"appétit" (nécessité de chercher un hôte pour se nourrir) des moustiques, est dépendant de la température, par exemple.*

In this dissertation, mathematical modeling is understood with a mechanistic intent, i.e the will to “explicitly include specific mechanisms (or processes) governing the system of interest, in order to allow the direct investigation of such mechanisms” (Handel et al., 2020). By contrast, phenomenological models (often called statistical models) aim to extract patterns, or at least information, from data (Handel et al., 2020). Such models can determine correlations, deduce potential causations, but cannot identify underlying mechanisms responsible for patterns found in the data. There are several possible uses of mechanistic models, but no unique way to categorize such uses (Box 1.2). Regarding the construction of mechanistic models, a good analogy to determine what is the right model and how detailed it should be is the use of maps (Box 1.2). Mechanistic modelling often goes hand in hand with systems thinking, which is “the concept that for systems with many components interacting in complex ways, studying only a small part of the system does not provide a full understanding of the overall system dynamics. Thus, to fully understand the system, one needs to study it in its entirety” (Handel et al., 2020).

Dealing with vector-borne or zoonotic diseases means that one will have to model interactions between different populations (insect vectors, domestic animals, wildlife, humans) with different characteristics with regards, for example, to their behaviour, biological needs, or vulnerability to environmental changes. Ultimately, the practical goal is often to protect a target population from being infected (Haydon et al., 2002). To have any chance at achieving this goal, one needs to disentangle the relative contributions of hosts, vectors, and transmission routes to the overall dynamics (Hollingsworth et al., 2015; Webster et al., 2017). Only then can key components be targeted by the relevant interventions to achieve disease control or elimination (Hollingsworth et al., 2015; Webster et al., 2017). This is easier said than done, of course, but fortunately this daunting task can usually be split into several research questions, each with a narrower focus, hopefully easier to tackle.

For vector-borne transmission to happen, hosts and vectors need to be present in the same place at the same time. This can seem obvious, yet, establishing where and when these populations can be found together already constitutes a challenge. Regarding vectors, their presence and their ability to transmit pathogens is tightly linked to climatic variables (Eckhoff et al., 2015; Mordecai et al., 2019) and is therefore often seasonal. Trapping methods are diverse and can sample different subsets of the mosquito community, therefore introducing bias (Gorsich et al., 2019). The present century has enabled a broader access to remotely-sensed meteorological data. This in turn improved our ability to map suitable habitats for vectors (Tourre et al.,

2012; Sedda et al., 2019), although spatio-temporal resolutions required for this kind of task are only starting to be achievable (Phiri et al., 2020). Several strategies can then be chosen from. One of them mostly aims at capturing broad dynamic patterns of vector densities and can directly use climatic variables as a proxy of these densities. Another will favour a thorough understanding of vector life cycle to identify possible drivers of transmission, and needs to be backed up by experimental and trap data to develop dedicated models (Eckhoff et al., 2015). Regarding vertebrate hosts, one could instinctively think that knowing their distribution, in particular domestic livestock and humans, would be easier than vectors'. In resource-poor settings though, census can be hard to access, and rarely structured according to epidemiologists expectations. In addition, a static view of host distribution would not be informative when we know host movements to be a driver of infectious diseases spread (Colizza et al., 2007; Balcan et al., 2009; Fritzsche McKay and Hoye, 2016). Livestock movements depend on husbandry practices, and so does their behaviour and exposure to vector bites. Remote-sensing technologies can once again help in that regard, characterizing pathogenic landscapes taking into account interactions between land, people, disease vectors, and their animal hosts (Lambin et al., 2010; Hollings et al., 2018). Overall, these different sources of spatial heterogeneity require spatial models, which can be harder to implement, slower to compute. These technical constraints as well as the lack of relevant data can influence the complexity of the model and urge to make parsimonious choices (Eckhoff et al., 2015).

One question modellers also need to ask themselves is “What is the contact structure between populations?” : how often do they interact, how does this scale with population size, is one population in need of contacts (e.g. vectors searching for a blood meal) while the other is merely a passive receiver (e.g. vertebrate hosts)? This contact structure will impact the mathematical formulation of the model and in particular, the force of infection, i.e the rate of appearance of new infections in the populations. This contact structure can be heterogeneous in space (exposure to vectors is higher in a rice field than a barn) or time (some vectors host-seek exclusively at night, dusk or dawn), so assumptions need to be tailored to the system at hand. These assumptions are always somewhat simplifying, and this is acceptable as long as the limits of a given choice are clearly stated and accounted for when interpreting results (Wonham et al., 2006; Smith et al., 2014).

To understand how contacts can result in transmission, one needs to dive into micro-scale processes, i.e. host-pathogen and vector-pathogen interactions. The term competence is used



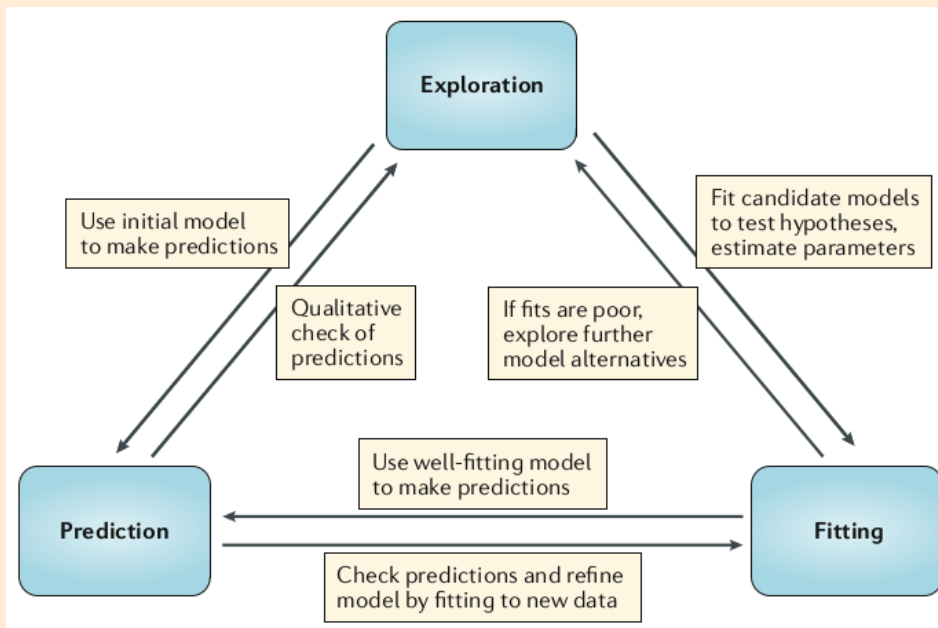
to define the ability to acquire and subsequently transmit a pathogen, and can be studied in both vectors and hosts (Azar and Weaver, 2019; Martin et al., 2019). In vectors, it requires to identify possible transmission bottlenecks between one blood meal and the next, but is often oversimplified as a static property (Gog et al., 2015; Fontaine et al., 2018; Lequime et al., 2020). In hosts, looking past clinical symptoms to estimate how infectiousness relates to pathogen load (Gog et al., 2015), and how some hosts might inherently be better pathogen amplifiers than others, is crucial yet understudied. Ultimately, combining within-host and within-vector viral dynamics with population-level ecological factors, such as vector preferences and host diversity (Thiemann et al., 2011; Simpson et al., 2012; Miller and Huppert, 2013; Zeilinger and Daugherty, 2014), might hold the key to identifying the Achilles' heel of multi-host vector-borne pathogens (Roche et al., 2014; Vazquez-Prokopec et al., 2016).

I have tried to give an overview of possible research focuses when studying the epidemiology of vector-borne and zoonotic diseases with mathematical modeling as the main tool. It is by no mean exhaustive nor the only way to categorize research questions. That being said, it is clear that while these three focuses (presence, contact, transmission), corresponding to different scales, can be first explored independently, they will ultimately need to be merged for their effects to interact and the overall dynamic patterns to emerge. Multi-scale models are a theoretical dream but a possible nightmare in practice. If one does not identify the major insights gained from each scale, extract its essence and think about efficient ways to link these together, dramatic increase in complexity are inevitable (Parham et al., 2015; Gog et al., 2015). This challenge will not be overcome without efficient interdisciplinarity (Ezanno et al., 2020).

In research, once you've laid down your question, there is no unique way to answer it. Even with mathematical modelling as your weapon of choice, several approaches are still on the table. The challenges I just presented can be tackled from a methodological viewpoint, using conceptual models to extract general trends. In this PhD however, we will focus on a specific pathogen, which, as you will soon understand, neatly exemplifies the issues faced with emerging, vector-borne, zoonotic diseases, and the modelling of their transmission dynamics: Rift Valley fever virus.

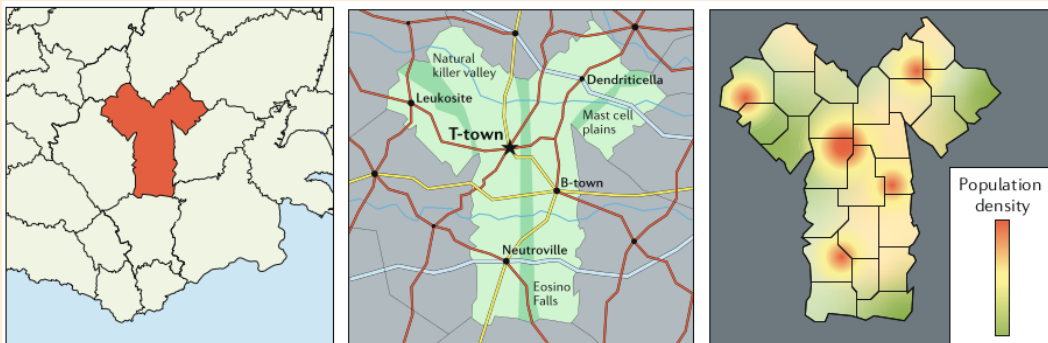
**Box 1.2 Model uses and complexity**

The following text and figures are directly reproduced from Handel et al., 2020.



Uses for mechanistic models. A schematic illustrating a way to categorize and conceptualize different uses of mechanistic models.

Maps are models of the real world. They serve specific purposes, and it is important that a given map be useful for the intended purpose. Consider the three maps (models) of the fictional country of Antibodia (see figure below). If you want to know where this country is located, the left map is useful. If instead you want to know how to drive from T-town to Dendriticella, the middle map would be the most useful. If you want to know where most people live in this country, the right map is most useful. It is the same ‘system’ under consideration (the country of Antibodia), but depending on the question, different maps (models) are needed. Analogously, for the same biological system under study (for example, a specific pathogen and host), different types of models that include and exclude different details of the systems are needed, depending on the question you want to answer. The usefulness of maps (and models) is that they capture the information that is needed for a specific situation, while ignoring details that are not important for a given question, thus producing the right level of complexity.



An analogy for determining the right model : the use of maps

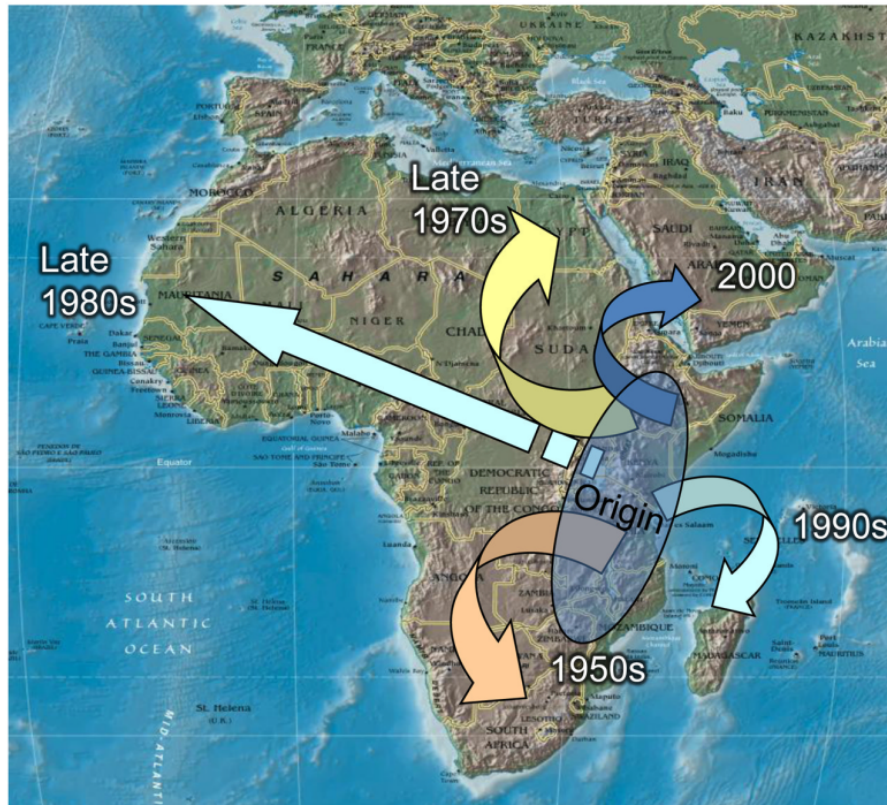
### 1.3 Rift Valley fever virus

Rift Valley fever virus (RVFV, family Bunyaviridae, genus Phlebovirus) is a pathogen causing a severe disease in livestock and a moderate to severe illness in people (Gerdes, 2004; Bird et al., 2009). RVFV is vector-borne, with mosquitoes as the main vectors, and zoonotic (Gerdes, 2004; Bird et al., 2009). Several mosquito species can transmit RVFV, pertaining to different genera: *Aedes*, *Culex*, *Mansonia*, *Anopheles* (Chevalier et al., 2004; Hanafi et al., 2010; Seufi and Galal, 2010; Linthicum et al., 2016); the degree to which RVFV vectors can successfully transmit virus varies between species (Ndiaye et al., 2016; Nepomichene et al., 2018). Sheep, goats, cattle, and camels are the main livestock hosts of RVFV (Davies and Martin, 2003; Hartman, 2017). The most ubiquitous sign of infection is a high rate of abortion at all stages of pregnancy, the strength of other symptoms and death rates vary with species and animal age (Pepin et al., 2010; Wright et al., 2019). Humans can be infected by handling infected animal tissue (Nicholas et al., 2014; Linthicum et al., 2016), through the consumption of raw milk (Grossi-Soyster et al., 2019), as well as from mosquito bites (LaBeaud et al., 2010; Linthicum et al., 2016; Lumley et al., 2017). When infected, humans can experience a wide spectrum of clinical outcomes, from self-limited febrile illness to hepatitis, ocular disease, encephalitis, haemorrhagic disease and death (Laughlin et al., 1979; Madani et al., 2003; LaBeaud et al., 2010).

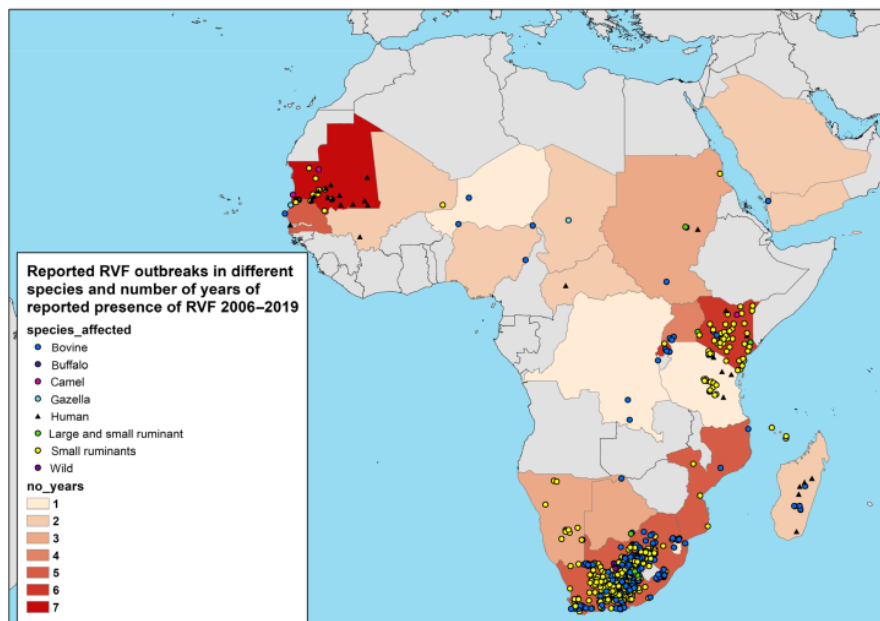
Other transmission routes and reservoirs might add complexity to the transmission cycle of RVFV. Direct transmission between animals, through contact with abortion or birth products, could explain the correlation between RVFV transmission and high densities of livestock, during unfavourable seasons for vectors (Nicolas et al., 2014; Olive et al., 2016). Evidence of vertical transmission in vectors exists in *Aedes* and *Culex* genera, but is limited (Linthicum et al., 1985; Romoser, 2011; Bergren et al., 2021). As for other arboviruses, assessing the importance of this transmission route in the field is challenging because of experimental limitations and the influence of environmental factors (Lequime et al., 2016; Lumley et al., 2017). Wild mammals could constitute a reservoir of infection, but studies are lacking to accurately estimate their role in RVFV epidemiology (Evans et al., 2008; Olive et al., 2012; Rostal et al., 2017; Walsh et al., 2017). Humans are usually considered dead-end hosts (Chevalier et al., 2010; Sindato et al., 2011; Lumley et al., 2017; Nielsen et al., 2020) but measures of high viral loads during the acute phase of infection question this hypothesis (St. Maurice et al., 2018).

The spread of RVFV through the African continent and outside was progressive throughout the 20th century. Rift Valley fever virus was first identified in 1930, in Kenya, after being described as an enzootic hepatitis of sheep (Daubney and Hudson, 1931). It was soon after reported in Tanzania, and reached South Africa 20 years later (Rissmann et al., 2020). Extensions of specific interest, in ecologically different areas, happened next (Figure 1.1a). The first RVFV outbreak in Northern Africa, in Egypt, occurred in 1977-1978 (Meegan, 1979), most likely due to the importation of infected livestock from Sudan (Napp et al., 2018). A decade later, the first outbreak in Western Africa occurred in the Senegal river basin, at the border between Senegal and Mauritania (Jouan et al., 1988). The first outbreak outside of African mainland took place in Madagascar in 1990-1991 (Morvan et al., 1991), followed by RVFV introduction outside the African continent in 2000 in Saudi Arabia and Yemen (Ahmad, 2000; Jupp et al., 2002; Madani et al., 2003). In the present century, newly affected countries include The Gambia, Botswana, and Niger (Rissmann et al., 2020). Mauritania, Kenya and South Africa had the most outbreaks in the last 15 years, with outbreak locations spread across the territory (Figure 1.1b). Evidence of human and/or animal seropositivity exists in the Maghreb and the Middle East, without official RVFV case report so far (Nielsen et al., 2020; Bron et al., 2021).

Preventing and controlling RVFV outbreaks is a challenging task. Vector control strategies exist in diverse forms (Achee et al., 2019) but are rarely used to decrease RVFV transmission, due to the number of competent mosquito species and the extension of breeding sites (Balenghien et al., 2013; Nielsen et al., 2020). Several animal vaccines are commercially available or in the final stages of validation (Nielsen et al., 2020). For now, drawbacks include the need for repeated vaccinations or residual virulence in newborn and gestating animals, depending on the vaccine used (Kortekaas et al., 2011; Njenga et al., 2015). Regarding the risk of human infection, information of people is crucial to ensure appropriate slaughtering and consumption practices (La Rocque and Formenty, 2014). A decision-support tool was developed for the Greater Horn of Africa (ILRI/FAO, 2008) after the 2006/2007 epizootic whose consequences were exacerbated by delays in decision-making. Intervention strategies need to account for different phases, all with adapted measures : forecasting and preparedness, alert, epidemic control and post epidemic (La Rocque and Formenty, 2014). It is recognized that a One Health approach should be privileged, requiring the coordination between public- and animal-health competent bodies (La Rocque and Formenty, 2014; Lancelot et al., 2019; Fawzy and Helmy, 2019).



(a)



(b)

**Figure 1.1** – Maps of RVFV historical spread and recent outbreaks. (a) Reproduced from Weaver and Reisen, 2010. Temporal patterns of dispersal by RVFV in Africa since 1930s to present. Dates indicate the earliest detection and possible establishment of virus in each area. (b) Reproduced from Nielsen et al., 2020. Number of years of reported presence of RVF and species affected in the outbreaks reported between 2006 and 2019 (OIE and WHO)

## 1.4 The Sahelian setting

Rift Valley fever virus has been reported in all Sahelian countries (Figure 1.1B). The Sahel is an arid to semi-arid region bridging the gap between the Sahara Desert and sub-humid/humid Africa, with a climate strongly influenced by the Atlantic Ocean (Giannini, 2003; Pomposi et al., 2016). The most recurring RVFV circulation happens on the Western end of the region (Figure 1.1B). The dominant livestock production system in this region is transhumant pastoralism, an extensive system in which herds move throughout the year to adapt to climatic conditions, looking for water sources and grazing areas (Apolloni et al., 2019). Movements can be national or transboundary (Apolloni et al., 2018; Belkhiria et al., 2019; Jahel et al., 2020), with the terminal market located on the coast, in Senegal (Apolloni et al., 2019).

Although the first Senegalese RVFV outbreak occurred in the Senegal river delta and valley (SRDV, Jouan et al., 1988), the Ferlo, a sylvopastoral northcentral region of Senegal, was quickly identified as another area of active RVFV circulation (Ksiazek et al., 1989; Wilson et al., 1994). In SRDV, achieving food self-sufficiency motivated the irrigation of extensive areas for agriculture (Bruckmann, 2018), in particular rice culture, and therefore modified the transmission of vector-borne diseases (Thonnon et al., 1999). There, sentinel herds spread across the region are used to detect seroconversions (Thiongane, 2000; Chevalier et al., 2005; Lancelot et al., 2019). In the Ferlo region, understanding RVFV circulation requires a fine knowledge of rainy season typology (Ndione et al., 2008; Bodian, 2014), which influences temporary ponds filling dynamics (Diop et al., 2003; Lacaux et al., 2007; Ndione et al., 2009; Soti et al., 2009), subsequently triggering vector emergence (Diallo et al., 2011; Tran et al., 2019). Targeted field studies identified the main competent mosquito species in the region (Ba et al., 2005; Ndiaye et al., 2016; Biteye et al., 2018), and characterized their behaviour (Ba et al., 2006; Ndiaye et al., 2006; Biteye et al., 2019). This seasonal dynamics also needs to be studied from the host perspective, with nomadic herders adapting their itinerary to climatic conditions (Adriansen, 2008; Oumar, 2015; Belkhiria et al., 2019).

Over the years, a vast amount of knowledge has been acquired on these different processes, often with the help of phenomenological or mechanistic modelling. Models first helped to understand the correlations between pairs of processes (rain-pond filling, Bop et al., 2014; Bicout et al., 2015; rain-vectors, Mondet et al., 2005; Guilloteau et al., 2014; Talla et al., 2014; pond-vectors, Tourre et al., 2008; Talla et al., 2016). Rift Valley fever could then be added to the mix, with different approaches spanning risk mapping to mechanistic transmission (Bicout

and Sabatier, 2004; Clements et al., 2007; Vignolles et al., 2009; Caminade et al., 2011; Soti et al., 2012, 2013; Durand et al., 2020). These models left several questions unanswered, either due to small spatial scales or important processes not being integrated, often because of the lack of relevant data. This PhD will aim at filling some of these knowledge gaps, using the strategy developed hereafter.

## 1.5 Thesis objective and outline

The aim of this thesis is to enhance knowledge about the eco-epidemiology of RVFV, in a region with recurring virus circulation. A special focus is put on the study of the relative contributions of the different livestock hosts (cattle, sheep, and goat) to disease dynamics, under the influence of environmental conditions, human activities, and individual competence. To do so, we use mechanistic modelling at different scales. The dissertation will be structured as follows:

Chapter 2 reviews mechanistic modelling work developed so far to study RVFV. The objective is to explore the diversity of mathematical implementations spanning a broad spectrum of conceptual to applied frameworks. Their hypotheses and contribution to the understanding of RVFV epidemiology might differ, but overall these different approaches complement and inspire each other.

Chapter 3 studies the local epidemic potential of RVFV in northern Senegal upon virus introduction. To do so, we map the basic reproduction number, obtained analytically, for introduction dates spanning 3 consecutive rainy seasons (2014-2016), in the Senegal river delta and valley and in the Ferlo. In this model, cattle and small ruminants differ in their densities, natural lifespan, disease-induced mortality rates and attractiveness to vectors, but not in their transmission potential.

Consequently, Chapter 4 aims at quantifying infectiousness of livestock host species. We develop a within-host model fitted to experimental data of host viral loads upon RVFV infection, to characterize differences between species. We conduct a review of the literature to estimate the relationship between a vertebrate host infectious titer and vector infection rates, for *Aedes* and *Culex* spp. vectors separately. Ultimately, we estimate the net infectiousness of livestock host species.

Chapter 5 then incorporates the findings of previous chapters in a metapopulation model of RVFV transmission dynamics in northern Senegal. The role of nomadic herd movements in the Ferlo is explored, in particular the synchronicity of transhumance with vector emergence as well as the importance of small-scale intra-Ferlo movements.

Last, a general discussion provides a summary of all findings, discuss the suitability of methodological approaches used, their limitations, implications of our results and recommendations for future research.

*Note: Each research chapter was written as a manuscript intended for publication in a peer-reviewed journal, hence some repetitions of background information throughout the thesis. Chapter 3 is published in *Epidemics*. Chapter 2 is intended for submission in *Plos Neglected Tropical Diseases*, Chapter 4 in *Elife* and Chapter 5 is more exploratory so far. In addition, Chapter 3 and 4 are preceded by a summary in French intended for a broad audience, hence the less formal tone.*



# 2

## Mechanistic models of Rift Valley fever virus transmission dynamics : A systematic review

An updated version can be found as a preprint

<https://www.medrxiv.org/content/10.1101/2022.03.28.22272741v1>

This paper has been submitted to Plos Neglected Tropical Diseases.

Hélène Cecilia<sup>1</sup>, Alex Drouin<sup>2,3</sup>, Raphaëlle Métras<sup>4,5</sup>, Thomas Balenghien<sup>2,6,7</sup>, Benoit Durand<sup>3</sup>, Véronique Chevalier<sup>2</sup>, Pauline Ezanno<sup>1</sup>

<sup>1</sup> INRAE, Oniris, BIOEPAR, 44300 Nantes, France

<sup>2</sup> Agricultural Research for Development (CIRAD), UMR ASTRE, F-34090 Montpellier, France

<sup>3</sup> Epidemiology Unit, Laboratory for Animal Health, French Agency for Food, environmental and Occupational Health and Safety (ANSES), University Paris-Est, 94700 Maisons-Alfort, France

<sup>4</sup> INSERM, Sorbonne Université, Institut Pierre Louis d'Épidémiologie et de Santé Publique (Unité Mixte de Recherche en Santé 1136), 75012 Paris, France

<sup>5</sup> Centre for the Mathematical Modelling of Infectious Diseases, Department of Infectious Disease Epidemiology, London School of Hygiene and Tropical Medicine, London WC1E 7HT, United Kingdom

<sup>6</sup> Cirad, UMR ASTRE, 10100, Rabat, Morocco

<sup>7</sup> Unité Microbiologie, immunologie et maladies contagieuses, Institut Agronomique et Vétérinaire Hassan II, 10100, Rabat-Instituts, Morocco

### 2.1 Introduction

Rift Valley fever (RVF-V) is a viral, vector-borne, zoonotic disease, first identified in Kenya in 1930 (Daubney and Hudson, 1931), which has since then been reported across the African continent, in the South West Indian Ocean islands, and in the Arabian Peninsula. RVFV is mostly transmitted by *Aedes* and *Culex* spp. mosquitoes (Chevalier et al., 2004), some of which are present in Europe and North America (Moutailler et al., 2008; Brustolin et al., 2017; Lumley

et al., 2018; Birnberg et al., 2019). In livestock, abortion storms and death can strongly impact the local economy (Davies, 2010; Rich and Wanyoike, 2010). The clinical spectrum in humans is broad, with a minority of deadly cases (Madani et al., 2003; Chevalier et al., 2010).

About 100 years after its first description, RVF outbreaks are still difficult to anticipate and contain, and the drivers of its endemicity not clearly understood. The multiplicity of vertebrate hosts and mosquito species involved, the diversity of affected ecosystems, each with their own environmental dynamics, as well as the impact of human activities, make this complex system hard to disentangle (Bird et al., 2009). The lack of suitable vaccines (Nielsen et al., 2020), coupled with the overall social vulnerability of affected regions (Sindato et al., 2011; Peyre et al., 2015), are also major obstacles. The pastoralist tradition, which constitutes the main production system in Africa's drylands (FAO, 2018), can induce delayed access to health care and hinder the traceability of animal movements. This in turn impacts the quality and availability of epidemiological data, which can be quite heterogeneous (Clark et al., 2018; Bron et al., 2021)<sup>1</sup>. As a result, it is often difficult to generalize local findings, unless a mechanistic understanding of epidemiological processes is acquired.

Mathematical models can be useful to project epidemiological scenarios, including control strategies, at large scales, be they temporal, spatial or demographic (Martens et al., 1995; Colizza et al., 2007). Powerful methods can now estimate the most likely drivers of observed outbreak patterns (Hartig et al., 2011; Endo et al., 2019), or point out to key processes needing further field or laboratory investigations (Marino et al., 2008). Phenomenological models (used here to avoid the often-used but misleading term 'statistical models', Handel et al., 2020) are effective to extract patterns from data. In contrast, mechanistic (or dynamical) models can adapt to data-scarce settings by exploring a complex system conceptually, in a hypothesis-based fashion (Cabral et al., 2017), e.g to see what ranges of behaviour can emerge from first principles, as is routinely done in ecology (Radchuk et al., 2019). This flexibility gives rise to an interesting variability in the way epidemiological mechanistic models are designed and used, spanning a broad spectrum from highly theoretical to closely mimicking field situations (Lessler et al., 2016).

Two existing reviews have focused on models developed to study RVF. The first one, by Métras et al., 2011, was a narrative review presenting modeling tools used to measure or model RVF risk in animals. At that time, only three mechanistic models were available and included in the study. The second one, by Danzetta et al., 2016, was a systematic review constrained to compartmental models, using RVF as a case study to present how the use of compartmental models can be helpful to investigate various aspects of vector-borne diseases transmission. A complementary paper, by Reiner et al., 2013, reviewed 40 years of mathematical models of mosquito-borne pathogen transmission, with a thorough and comprehensive reading grid. It

<sup>1</sup> I am a co-author of Bron et al. 2021, you can find the paper in Appendix A

did however only include three models on RVF.

To update the state of the art on RVF mechanistic models of transmission, we conducted a systematic review of mechanistic models of RVF transmission. We explored the diversity of methodological choices and assumptions made in theoretical and applied models. We discuss what they have in common, how they differ, if they inspire each other and their contribution to the understanding, anticipation, and control of RVF transmission and spread.

## 2.2 Material and Methods

### 2.2.1 Search strategy

This review was conducted according to the Preferred Reporting Items for Systematic reviews and Meta-Analyses (PRISMA) guidelines (Liberati et al., 2009). The research was performed in Scopus and Pubmed databases on 15 December 2020. No restriction on publication date was considered, and only papers written in English were selected. The following Boolean query was applied in both databases:

(rift AND valley AND fever) AND (mathematical OR epidem\* OR compartment\* OR sir OR seir OR metapopulation OR deterministic OR stochastic OR mechanistic OR dynamic\*) AND (model\*)

This query was used in the “title, abstract and keywords”, and “title and abstract” fields for Scopus and PubMed, respectively.

### 2.2.2 Inclusion and exclusion criteria

After removal of duplicates, articles were included in three steps: title screening, abstract screening and full text reading. In the first and second step, articles were selected if they appeared to present a RVF model using a mechanistic approach for at least one part of the model. Exclusion criteria were: irrelevant topic, reviews, cases report, serological studies and statistical studies. Articles selected in the first and second step went to a full text screening with the first set of exclusion criteria, with addition of: non-mechanistic models, models dealing with mosquitoes only, incomplete model description and theoretical paper without any RVF numerical application. Discussion among authors occurred in case of doubt to reach a consensus on final inclusions.

### 2.2.3 Screening

We designed a reading grid (Supplementary Information S.1), partially inspired by the one used in Reiner et al., 2013, to collect information from the articles. The context of the study (e.g location, presence of data), model components (e.g. host and vector species, infection states) and assumptions (e.g. vertical transmission in vectors), type of outputs (e.g  $R_0$ , parameter estimations, sensitivity analysis) and main results, were all recorded. Two authors took charge

of the systematic reading. To cross-validate the use of the grid, 3 papers were read by both authors and specific topics were regularly discussed to make sure a consensus was reached.

#### 2.2.4 Model categories

We defined three model categories : theoretical, applied, and grey models. **Theoretical** models do not use data and are not intended to represent a specific geographical location. **Applied** models represent a specific geographical context and use relevant data to tailor model development to their case study or to validate model outputs. Such data can be of several types, not necessarily epidemiological in the sense of seroprevalence or case reports. **Grey** models are those which do not fit into these black-and-white categories, either because authors do not use data but demonstrate a strong will to adapt their model to a specific geographical context, or because despite the use of data, the model developed is still very conceptual and insights remain distant from field preoccupations.

We compared the objectives, methodological and epidemiological contributions of these model categories and assessed whether these categories evolved separately or inspired each other. This inspiration was recorded if a model of a given category explicitly stated being adapted from a model from another category, then defined as a **parent** model.

## 2.3 Results and discussion

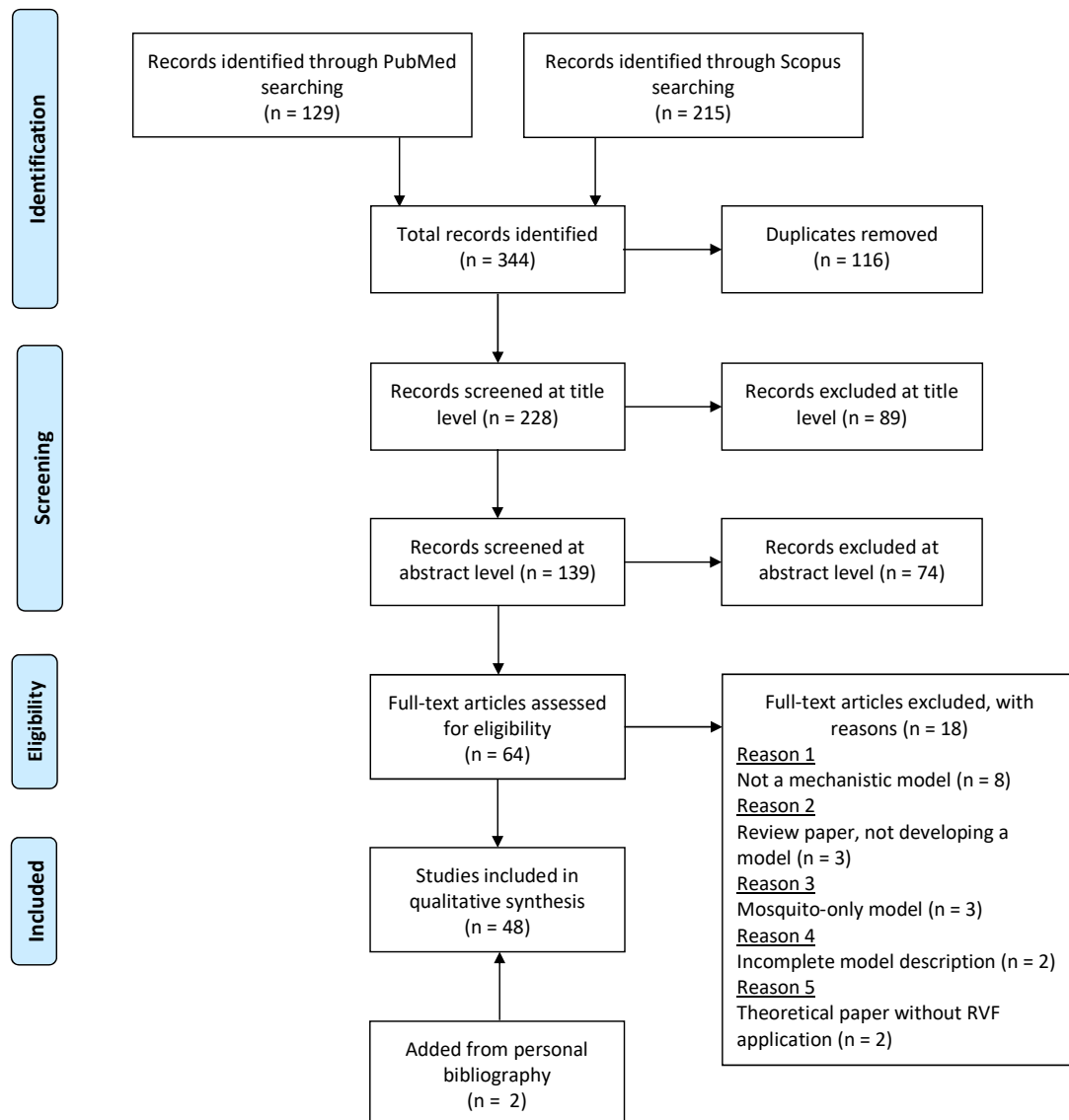
### 2.3.1 Study selection

A total of 344 studies were identified from the two databases. After removal of duplicates, 228 articles were screened at the title level, 139 at the abstract level and 64 were fully read. Eventually, 48 articles including 2 papers added from our personal bibliography, were kept for the present review (Figure 2.1). Among those, 26 papers were not present in the review by Danzetta et al., 2016.

*Note: In the present PhD chapter, unless stated otherwise, results are presented for 42 models, extracted from 41 papers (85%). The 7 remaining papers pertain to those not present in the review by Danzetta et al., 2016. The manuscript will be updated when the last papers are read to finalize the publication. We believe this will not change the overall message conveyed here.*



PRISMA 2009 Flow Diagram



From: Moher D, Liberati A, Tetzlaff J, Altman DG, The PRISMA Group (2009). *Preferred Reporting Items for Systematic Reviews and Meta-Analyses: The PRISMA Statement*. PLoS Med 6(7): e1000097. doi:10.1371/journal.pmed1000097

For more information, visit [www.prisma-statement.org](http://www.prisma-statement.org).

Figure 2.1 – PRISMA flow diagram representing the selection process.

### 2.3.2 Context modeled

We identified 17 applied models (40%), 13 theoretical models (31%), and 12 grey models (29%). Locations of applied and grey models are mapped in Figure 2.2A. The scale of applied and grey models varied from local to international (Figure 2.2B). The sub-national scale was the most prevalent in both applied (10/17) and grey models (4/11) (Figure 2.2B). The Netherlands and the US, both RVF-free, have had several specific models developed. Regarding zones with known presence of RVF, several countries reporting numerous outbreaks in the last 15 years (Nielsen et al., 2020) have had at least one specific model developed. However, regions with recurring virus circulation, such as Mauritania, Mozambique, Namibia or Botswana (Nielsen et al., 2020) are still left out from this modeling effort. Identifying the possible hurdles preventing model development is important.

Spatial models, with at least two distinct locations, represented 55% (n=23) of models (Table 2.1). Among those, 11 were applied, 3 theoretical, and 5 grey models (Table 2.1). Thirteen out of 23 spatial models incorporated connections between their spatial entities (Table 2.1): in 7 cases, vertebrate hosts moved, in 3 cases, vectors and hosts could move, and in 3 other cases, the connection was indirect, in the sense that the force of infection of one location was influenced by neighbors, taking into account distance, or just prevalence. All international models were spatialized, but among those, only grey models incorporated connections between their spatial entities (Figure 2.2B, Table 2.1). Three models were not spatialized but did include emigration and immigration of hosts into their model (Table 2.1).

Most models (27/42) included one vertebrate host, most of the time (19/27) broadly labeled as livestock. When two hosts were accounted for, it was most often done to add a human compartment (9/14). Fischer et al., 2013; Gachohi et al., 2016; Cecilia et al., 2020; Durand et al., 2020 grouped small ruminants (sheep and goats) together and differentiated them from cattle. In addition to livestock, Barker et al., 2013 included birds as incompetent hosts, used as alternate blood-feeding sources by vectors. The model by McMahon et al., 2014 was the only one explicitly including a wildlife compartment, but did not describe the way the associated carrying capacity was estimated based on land use data. Sumaye et al., 2019 included a probability to pick up infection from wildlife hosts with a single parameter. Beechler et al., 2015; Manore and Beechler, 2015 both modeled African buffaloes (*Syncerus caffer*), either captive or free-ranging.

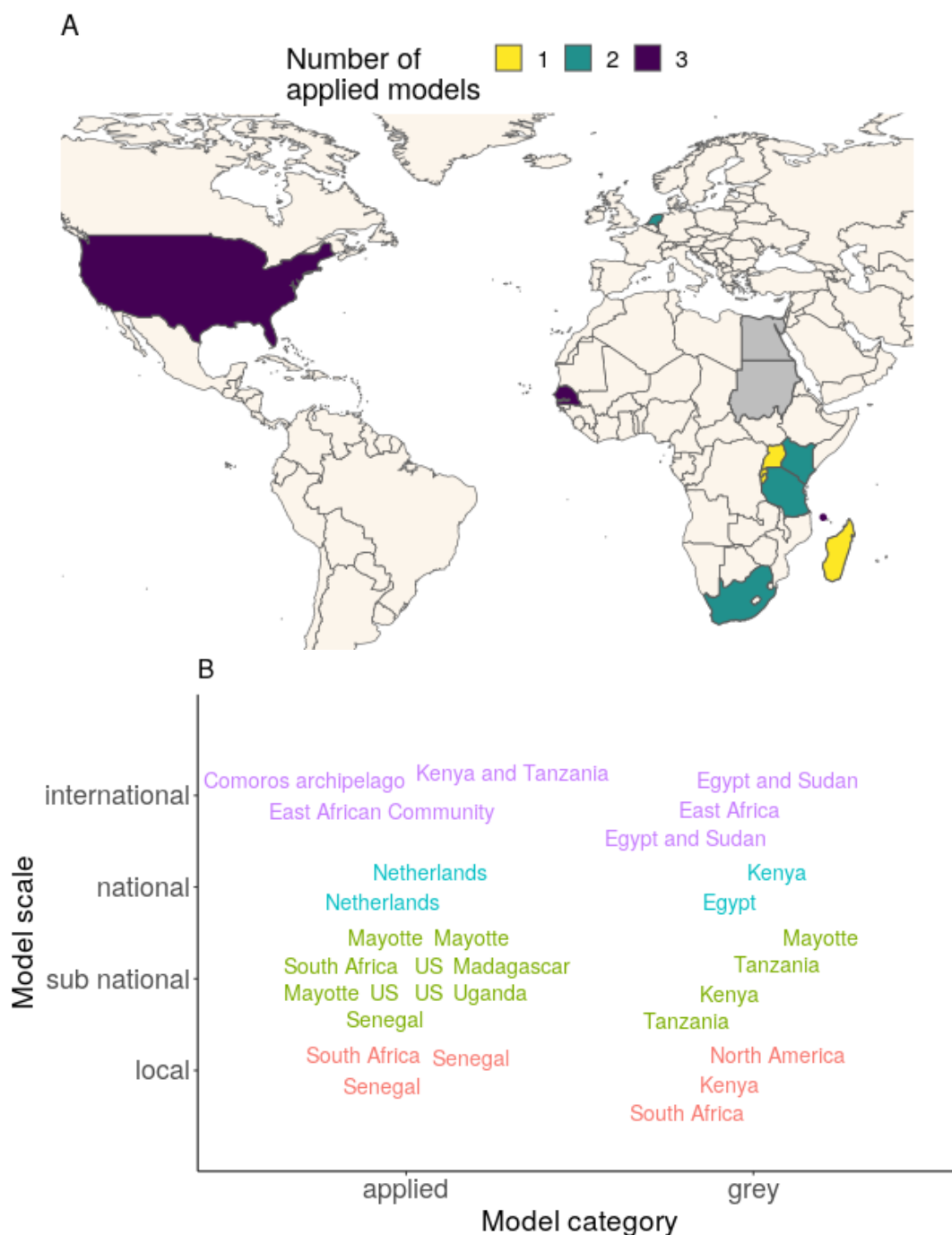


**Figure 2.2 – A** - Location and number of RVFV models. Grey models are mapped but not counted in totals because they sometimes refer to a non precise context (e.g. East Africa, North America, see B). Locations of grey models which are not also studied in applied models are shown in grey (Egypt, Sudan). The point north of Madagascar intends to locate Mayotte but is centered on Comoros. **B** - Scale of applied and grey models. Labels represent model locations. Labels are colored to help identify the scale (y-axis). East African Community = Burundi, Kenya, Rwanda, and Tanzania. Note that Mayotte is counted as sub-national because it is an overseas department of France, but all 4 models applied to Mayotte considered the whole island (374 sq. km).

Reference	Category	Location	Scale	Connection	Movement data / use of proxy
<b>Spatial models</b>					
Niu et al., 2012	theoretical		local	vectors and hosts move	None
Xue and Scoglio, 2013	theoretical		undetermined	hosts move	None
Paul et al., 2020	theoretical		local	hosts move	None
Gao et al., 2013	grey	Egypt and Sudan	international	hosts move	None
McMahon et al., 2014	grey	East Africa	international	indirect through FOI	None
Mpeshe et al., 2014	grey	Tanzania	sub-national	disconnected entities	None
Xiao et al., 2015	grey	Egypt and Sudan	international	hosts move	None
Sumaye et al., 2019	grey	Tanzania	sub-national	hosts move	None
					vectors : wind
Xue et al., 2012	applied	South Africa	sub-national	vectors and hosts move	livestock : animals sold, number in feedlots humans : distance, population, commuting and return rates
Xue et al., 2013	applied	US	sub-national	vectors and hosts move	maximum percentage of animals moving, extensive agricultural setting
Barker et al., 2013	applied	US	sub-national	disconnected entities	None
Fischer et al., 2013	applied	Netherlands	national	disconnected entities	None
Nicolas et al., 2014	applied	Madagascar	sub-national	hosts move	renewal practices of cattle breeders : trade, barter, number of animals, origin
Leedale et al., 2016	applied	Kenya and Tanzania	international	disconnected entities	None
Taylor et al., 2016	applied	East African Community	international	disconnected entities	None
Scoglio et al., 2016	applied	US	sub-national	hosts move	None
Sekamatte et al., 2019	applied	Uganda	sub-national	indirect through FOI	None
Cecilia et al., 2020	applied	Senegal	sub-national	disconnected entities	None
EFSA, 2020 Model 2	applied	Netherlands	national	indirect through FOI	None
<b>Non spatial, open models</b>					
Gil et al., 2016	grey	Egypt	national	hosts entry (importations)	None
Métras et al., 2017	applied	Mayotte	sub-national	hosts entry	unofficial trade
Durand et al., 2020	applied	Senegal	local	hosts in and out	survey of nomadic herders : main stops, dates

**Table 2.1** – Characteristics of spatial models as well as non-spatial models with external renewal.



Models with explicit vector compartments (37/42) included 1 ( $n = 16$ ), 2 ( $n = 19$ ) or more ( $n = 2$ ) vector taxa. Models with two taxa were all combining *Aedes* and *Culex* spp. vectors, while models with one taxon often (7/16) did not precise the type of vector studied. The diversity of vector species was important, with the most redundant being *Ae. vexans* ( $n = 4$ ) and *Cx. poicilipes* ( $n = 4$ ). Pedro et al., 2017 studied ticks (*Hyalomma truncatum*) in addition to *Aedes* and *Culex*. Sumaye et al., 2019 included *Ae. mcintoshi*, *Ae. aegypti* and two generic *Culex* vectors in their model.

### 2.3.3 Data

Data was used in 23 out of 42 (55%) models. Here, we define data as any raw information, as opposed to a readily available parameter value extracted from another study. Among grey models, 6 used data and 6 did not. Several types of data were represented: experimental (3/23), environmental (17/23), epidemiological (13/23), demographic (18/23), movements (5/23, Table 2.1), and geographical (5/23). Most (20/23) models used more than one type of data, and sometimes had several distinct datasets per type.

Only 38% of all datasets were spatialized, and 38% were time-series. Regarding epidemiological datasets, 19% were spatialized, and 57% were time-series. This is lower than environmental datasets, which were 46% spatialized and 65% time-series. This supports conclusions made in recent reviews on RVFV epidemiological data (Clark et al., 2018; Bron et al., 2021) on possible improvements on data collection. Most models with data used at least one spatialized dataset (61%) or time-series (87%). This indicates that mechanistic models can resort to all types of data to try and compensate the lack of precision in epidemiological reporting. Five papers used epidemiological data not published elsewhere (Cavalerie et al., 2015; Beechler et al., 2015; Métras et al., 2017, 2020; Durand et al., 2020), showing that modeling studies can also be seen as a way to valorize new datasets.

We categorized data use into 3 categories : calibration, input, and model assessment. Calibration was defined as the parametrization of one process or initial condition of the model, transforming the data in some way. This was done in 11 cases. Input was the fact of using the raw data directly as a parameter or initial condition of the model. This was done in 18 cases. Model assessment could refer either to parameter inference or qualitative estimation looking to maximize similarity between model outputs and data. This was done in 11 cases.

Ultimately, building accurate models helpful for policy makers requires the support of data. However, for RVFV as well as other infectious diseases, no single data source can be expected to inform each relevant parameter, hence, the integration of information from many heterogeneous sources of data has become the norm (De Angelis et al., 2015). This is a challenging task, as different datasets will be of different quality, potentially dependent, or in conflict (De Angelis

et al., 2015). Regarding quality, model-driven data collection can be a solution, but remains the exception rather than the rule, due to technical and cultural issues (Lessler et al., 2015).

#### 2.3.4 Contribution to RVFV epidemiology

Three main scientific objectives were identified : exploring epidemiological mechanisms (**understand**,  $n = 30$ ), examining consequences of hypothetical outbreaks (**anticipate**,  $n = 5$ ), and assessing control strategies, which we labeled **prevent** ( $n = 7$ ), although it can refer to actions taken before or during an outbreak. In the present section, we focus on key features identified per objective. In addition, in  $>30\%$  of cases, model development in itself seemed to be a leading objective of the paper. In such cases, contributing to RVFV epidemiology was as important as contributing methodologically to RVFV mechanistic modeling, by including for the first time a given compartment, parameter, or by developing a method to integrate data.

The main output of a model, holding the paper's key message, could pertain to one of 4 categories : i) parameter estimation ( $n = 7$ ), ii) risk maps ( $n = 7$ ), iii) comparison of scenarios, defined as a small set of simulations with specific parameters varied (or processes turned off) across a small set of values ( $n = 19$ ), and iv) sensitivity analysis, where a large subset (if not all) of parameters are varied across a large set of values (e.g. using factorial design), ususally to produce an index quantifying the impact of a given parameter on selected model outputs ( $n = 9$ ). A given paper could have produced several of these outputs but we tried to identify, with an inevitable part of subjectivity, the one standing out as the main output.

The most common primary scientific objective of models was to understand epidemiological processes, in all model categories (from 69% of theoretical models to 83% of grey models, Figure 2.3). Although in 9 cases, those models also aimed to anticipate or prevent outbreaks, in a secondary part (Gaff et al., 2007; McMahon et al., 2014; Chamchod et al., 2014; Pedro et al., 2016; Scoglio et al., 2016; Métras et al., 2017; Sekamatte et al., 2019; Métras et al., 2020; Cecilia et al., 2020). The main model output varied according to the model category and their primary objective (Figure 2.3). Scenario comparison was the only output used by all model categories (Figure 2.3). Indeed, this type of analyses are quite flexible and can be tailored to a model's features easily. Risk maps were only produced by applied models, and was the most common output for models with the aim to anticipate (Figure 2.3). Sensitivity analyses were mostly used by theoretical models (6/9), and not at all by applied models (Figure 2.3, 3/9 by grey models). Parameter estimation were mostly performed by applied models (5/7), and not at all by theoretical models (Figure 2.3, 2/7 by grey models). By nature, sensitivity analyses and parameter estimation are primary done to understand the system better. Here, we highlight that theoretical and applied model can use different tools to contribute to a common objective. In 2 cases, parameter estimations were used further in the same model to help anticipate (Métras et al., 2017) or prevent (Métras et al., 2020) outbreaks, as a secondary

objective. Fifty percent of models provided an estimation of a type of reproduction number ( $R_0, R_e, R_{st}, R_T$ ), most of which obtained analytically (19/21).

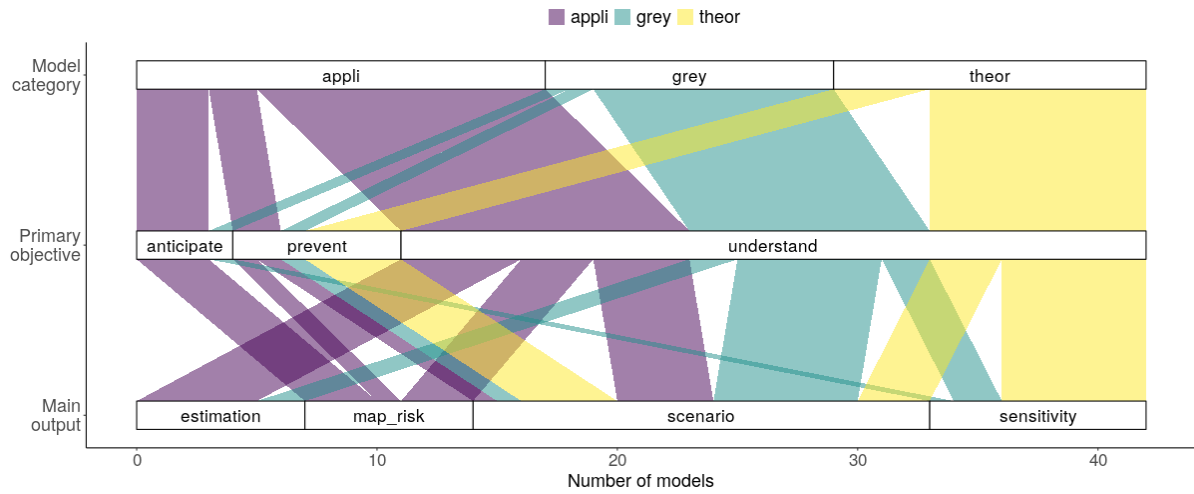


**Figure 2.3** – Objective and main output of models, per category.

Vertical transmission in vectors was included in around 50% of models, which seems representative of the state of evidence currently available on the role of this process in field situations. Three models centered their research question on the quantification of this role, one in each category. Chitnis et al., 2013 (theoretical) showed that while the vertical transmission rate does not impact  $R_0$ , it can contribute significantly to inter-epidemic persistence. Manore and Beechler, 2015 (grey) focused on inter-epidemic activity in Kruger National Park (South Africa) and estimated that realistic vertical transmission rates should be combined with the presence of alternate hosts to allow RVFV persistence. Durand et al., 2020 (applied) concluded that vertical transmission cannot be ruled out but is not necessary to explain endemic circulation in Senegal.

Ten models reflected on possible vaccination strategies (Table 2.2), in all categories (3 applied, 5 theoretical, 2 grey). Such strategies were shaped by parameters such as the time to build-up immunity, vaccine efficacy, coverage, and regimen (Table 2.2). Most models insisted on the need for vaccination to happen before outbreaks or quickly after the first cases are detected, to have a significant impact (Table 2.2). Métras et al., 2020; Gachohi et al., 2016, EFSA, 2020 Model 1 incorporated constraints on the number of individuals vaccinated per day, so that a given coverage is reached at a realistic pace. Regarding the choice of hosts to vaccinate, Gachohi et al., 2016 highlighted that while small ruminants need a smaller coverage than cattle to achieve a given reduction of incidence, the vaccination of cattle provided the benefit of protecting both host populations. Métras et al., 2020 estimated that to reduce human cases, the vaccination of livestock required less doses than human vaccination, taking into account human exposure to livestock in their risk of infection. Adongo et al., 2013 showed that optimal strategies differ depending on whether one prioritizes the minimization of costs (doses) or infections, but failed to convey their results in a way that would benefit policy mak-

ers. Chamchod et al., 2016 explored differences between the use of live and killed vaccines, estimating that even with  $R_0 < 1$ , RVFV becomes endemic when live vaccines are implemented.

Some research questions and model features stood out from the rest. Beechler et al., 2015 studied the impact of co-infections with another pathogen (Bovine tuberculosis, BTB). Their data highlighted that RVFV infection was twice as likely in BTB+ than BTB- individuals, which once incorporated in a model, proved to have a global, non linear effect on outbreak size in both BTB populations. Pedro et al., 2017 looked at the possible role of ticks as vectors, and concluded that if ticks were capable of carrying and transmitting RVFV, they could increase the size of outbreaks, accelerate them and reduce their duration. Tuncer et al., 2016 developed an immuno-epidemiological model in which pathogen load impacts transmission rate, and focused on the identifiability of parameters (i.e the uniqueness of parameter values able to reproduce a given model trajectory) rather than the epidemiological impact of such an hypothesis. In Métras et al., 2017, 2020, the lack of data on vector densities urged the authors to use an environmental proxy (NDVI or rainfall) to drive vectorial transmission, without including an explicit vector compartment.

Model	Category	Vaccine-related health state(s)	Time to build-up immunity	Efficacy	Coverage	Target specific hosts	Vaccination regimen
Gaff et al., 2011	theoretical	explicit compartment : only from $S$	Yes	Yes	Yes	No	periodic vs one-time vs constant
<u>Main results:</u> Most efficient strategy tested is preventive vaccination of 100% of livestock with 85% vaccine efficacy via a 28-day continuous campaign							
Adongo et al., 2013	theoretical	explicit compartment : only from $S$	No	No	Yes (optimized in time through objective functional)	No	Optimal (objective functional, no delay)
<u>Main results:</u> Optimal strategy varies with the weight put on cost-minimization (number of vaccinated) vs minimizing the infected class							
Chamchod et al., 2014	theoretical	$S \rightarrow R$ transition	No	No	Yes (optimized in time through objective functional)	No	optimal (objective functional, start with delay)
<u>Main results:</u> i) vaccinating at a strong rate before the outbreak is the most efficient strategy ii) if delay $\geq 2$ months epidemic size is not decreased							
Chamchod et al., 2016	theoretical	explicit compartment ; Live vaccines : probability of reversion to virulence and possible abortions ; Killed vaccines : need of a booster to acquire lifelong immunity	Yes	Yes	Yes	No	periodic (start with delay)

Main results: i) introduction of ruminants vaccinated by live vaccines in RVFV-free areas may cause an outbreak and RVFV may become endemic if there is sustained use of live vaccines ii) if delay  $\geq 3$  months epidemic size is not decreased

---

Yang and Nie, 2016	theoretical	explicit compartment : only from $S$	No	No	Yes	No	impulsive (length of cycle)
--------------------	-------------	--------------------------------------	----	----	-----	----	-----------------------------

Main results: i) a short period of pulsing or a large pulse vaccination rate are sufficient conditions for the eradication of RVFV ii) RVFV is uniformly persistent if the vaccination rate is low and vaccination period is too long

---

Gachohi et al., 2016	grey	unknown	Yes	Yes	Yes (reached progressively, not pulse event)	Yes (cattle vs small ruminants)	periodic vs reactive
----------------------	------	---------	-----	-----	--	---------------------------------	----------------------

Main results: i) similar coverage induce stronger reduction of incidence in small ruminants than in cattle ii) vaccinating cattle protects both cattle and small ruminants while vaccinating small ruminants only protects small ruminants iii) authors provide a relationship between level of reactive vaccination required to stop an outbreak, given a specific level of periodic vaccination implemented

---

McMahon et al., 2014	grey	explicit compartment	Yes	Yes	No	No	reactive, with delay
----------------------	------	----------------------	-----	-----	----	----	----------------------

Main results: For a 45 day rainy season, 3 week window of opportunity to vaccinate to impact ongoing epidemic. Otherwise, benefits of vaccination primarily occur in years subsequent to the vaccination effort

---

Métras et al., 2020	applied	explicit compartment	Yes	Yes	Yes	Yes (livestock vs human)	reactive, mass vaccination, with delay
---------------------	---------	----------------------	-----	-----	-----	--------------------------	--

Main results: i) vaccinating 20% of livestock immediately after first human case is reported reduces human cases by 30% ii) waiting one more month requires 50% more vaccine doses to achieve similar impact

---

EFSA, 2020 Model 1	applied	explicit compartment	No	Yes	No (nb of animals vaccinated per day until 100% is reached)	No	continuous, starting before or after RVFV incursion
-----------------------	---------	----------------------	----	-----	---	----	---

Main results: i) the vaccination is more effective when applied early before the start of the epidemic and quickly implemented throughout the population ii) vaccine effectiveness has a minor effect on the reduction of infections iii) Vaccinating 200 to 2000 animals a day guarantees the epidemic is halted within 1 year, regardless whether vaccination starts before or after RVFV incursion. With 20 animals vaccinated per day, the epidemic continues for more than 2 years, and the whole population eventually gets infected.

EFSA, 2020 Model 2	applied	reduce probability of transmission (vector to host and host to vector)	Yes	Yes	No (infected premises eventually 100% vaccinated)	No	reactive, without delay
-----------------------	---------	--	-----	-----	---	----	-------------------------

Main results: vaccination in a 50-km radius around detected farms is among the most effective strategies (other, not involving vaccination, are compared)

**Table 2.2** – Vaccination strategies implemented in models and main results.

### 2.3.5 Force of infection

We chose to make a focus on the diversity of functional forms (FFs) used in the models for the force of infection related to vectorial transmission. This applied only to model explicitly including a vector compartment. Among those, a majority (23/37) did not justify their choice of FF, even though the force of infection, as a disease transmission term, encapsulates authors' assumption on the host-vector interaction and therefore influence their predictions (Wonham et al., 2006). Six FFs were found in reviewed models (Figure 2.4 + see *Note*). We detail them in Eq 2.1-2.6, expressed as transmission rates, which in model equations are multiplied by the number of susceptible of the relevant group. In Eq. 2.1-2.3,  $\beta_{hv}$  and  $\beta_{vh}$  are aggregated terms, sometimes called adequate contact rates as in Gaff et al., 2007, which can be decomposed into several parameters with a more focused biological meaning in some papers. The reservoir frequency-dependent (FR,  $n = 11$ , Eq. 2.1), infectious frequency-dependent (FI,  $n = 11$ , Eq. 2.2), and mass action (MA,  $n = 7$ , Eq. 2.3), are defined as in Wonham et al., 2006. Such FFs can only apply biologically at certain population densities, outside which they can generate aberrant values and therefore erroneous predictions (Wonham et al., 2006). Three alternative FFs were found in RVFV models to prevent this issue (Figure 2.4 + see *Note*). Those FFs require additional parameters to constrain the contact rate between populations.

$$FR_{h \rightarrow v} = \beta_{hv} \cdot \frac{I_h}{N_h} \quad (2.1)$$

$$FR_{v \rightarrow h} = \beta_{vh} \cdot \frac{I_v}{N_h}$$

$$FI_{h \rightarrow v} = \beta_{hv} \cdot \frac{I_h}{N_h} \quad (2.2)$$

$$FI_{v \rightarrow h} = \beta_{vh} \cdot \frac{I_v}{N_v}$$

$$MA_{h \rightarrow v} = \beta_{hv} \cdot I_h \quad (2.3)$$

$$MA_{v \rightarrow h} = \beta_{vh} \cdot I_v$$

The first alternative FF (Eq. 2.4, Hybrid1 in Figure 2.4,  $n = 7$ ) was first used in RVFV models by Chitnis et al., 2013, who previously formulated it in a model of malaria transmission (Chitnis et al., 2006).

$$Hyb_{1,h \rightarrow v} = \frac{\sigma_v \sigma_h \cancel{N_h}}{\sigma_v N_v + \sigma_h N_h} \cdot \alpha_{hv} \frac{I_h}{\cancel{N_h}} \quad (2.4)$$

$$Hyb_{1,v \rightarrow h} = \frac{\sigma_v \sigma_h \cancel{N_v}}{\sigma_v N_v + \sigma_h N_h} \cdot \alpha_{hv} \frac{I_v}{\cancel{N_v}}$$

In Eq. 2.4,  $\alpha_{hv}$  and  $\alpha_{vh}$  refer to probabilities of successful transmission given contact, from host to vector and vice versa.  $\sigma_v$  is defined as the maximum number of times a mosquito would



bite a host per unit time, if freely available. This is a function of the mosquito's gonotrophic cycle and its preference for a given host species.  $\sigma_h$  is the parameter added to avoid abnormally high contact rates and represent the maximum number of bites sustained by a host per unit time. Although  $\sigma_h$  seems virtually impossible to estimate in the field, this alternative FOI can efficiently prevent erroneous model predictions and has therefore been often reused in RVFV models. It is also the most justified FF (5/7, Figure 2.4). Some slight variations in its mathematical formulation can be found in Sumaye et al., 2019.

Another alternative FF was used by McMahon et al., 2014 (Eq. 2.5, Hybrid2 in Figure 2.4, n = 1).

$$\begin{aligned}
 Hyb_{2,h \rightarrow v} &= inf_h.sus_v.e^{-r/a}.I_h \\
 Hyb_{2,v \rightarrow h} &= inf_v.sus_h.e^{-r/a}.I_v \\
 r &= -\sqrt{\frac{N_v + N_h}{A}}
 \end{aligned} \tag{2.5}$$

Here, *inf* and *sus* refer to a vector or host infectivity and susceptibility, respectively. The contact rate is formulated as  $e^{-r/a}$ , with  $a$  the characteristic length of local spread. In  $r$ ,  $A$  is the patch area.

*Note* : Another alternative FF was used in Lo Iacono et al., 2018 (Eq. 2.6), a paper included in the final review but not described in this version.

$$\begin{aligned}
 Hyb_{3,h \rightarrow v} &= \alpha_{hv}.\tilde{\theta} \frac{I_h}{N_h} \\
 Hyb_{3,v \rightarrow h} &= \alpha_{vh}.m.\tilde{\theta} \frac{I_v}{N_v} \\
 \tilde{\theta} &= \frac{\theta}{1 + \frac{m}{q}} \\
 m &= p_f \cdot \frac{N_v}{N_h}
 \end{aligned} \tag{2.6}$$

$p_f$  is the proportion of the mosquito population able to detect and feed on the host species under consideration.  $m$  is therefore an “effective” vector-to-host ratio.  $\tilde{\theta}$  is the biting rate, function of the rate of completion of the gonotrophic cycle,  $\theta$ ,  $m$ , and  $q$ , the vector-to-host ratio for which vector fecundity is divided by 2.

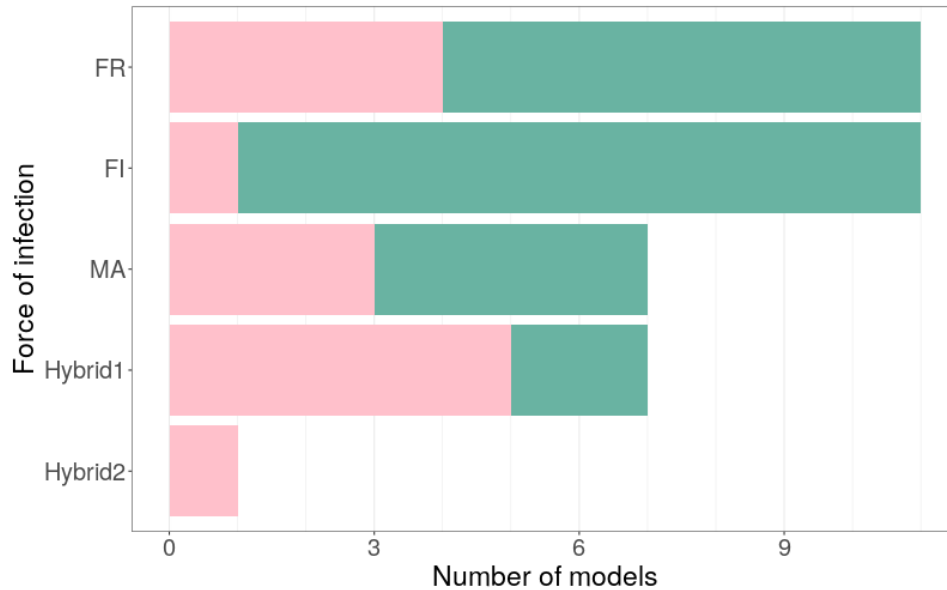


**Figure 2.4** – Functional forms (FFs) used by models for their force of infection (vectorial transmission only). The sum of the pink and green bars represents the number of models using a given FF, the pink bars represent the number of models properly justifying their choice of FF. See Eq 2.1-2.6 for details on each FF.

Several reviews concluded that the choice of functional form for the force of infection could greatly affect model behaviour. McCallum et al., 2001; Begon et al., 2002; Hoch et al., 2018 focused on non-vectorial transmission. Hopkins et al., 2020 focused on parasite transmission, which could be through a vector, but did not include possible variations in frequency-dependent functions. Wonham et al., 2006 focused on FFs used to model vectorial transmission of West Nile virus and also noticed an important diversity. A comparison of the hybrid FF listed presently would be useful. This could be done through theoretical scenarios or by fitting them to a common empirical dataset, selecting the best-performing FF for a given case study.

### 2.3.6 Diversity of assumptions

In hosts, assumptions regarding the clinical expression of the disease varied. Chitnis et al., 2013; Pedro et al., 2014; McMahan et al., 2014 included an asymptomatic state in hosts. Gachohi et al., 2016; Leedale et al., 2016; Taylor et al., 2016; Durand et al., 2020 distributed hosts in age classes, which differed in disease-induced mortality. Cavalerie et al., 2015; Chamchod et al., 2014, 2016; Sumaye et al., 2019; Durand et al., 2020 incorporated abortion in livestock hosts due to RVFV.

Ten models (24%) incorporated the influence of abiotic factors on vectors' life cycle and competence, with dedicated equations. Fischer et al., 2013; Mpeshe et al., 2014; Leedale et al., 2016; Cecilia et al., 2020, EFSA, 2020 Model 2 took into account the influence of temperature and/or rainfall on adult vectors' lifespan. Xue et al., 2012, 2013; Mpeshe et al., 2014; Gachohi et al., 2016; Leedale et al., 2016 took into account the influence of temperature and/or rainfall on the egg laying rate and the development or survival of aquatic stages. Fischer et al., 2013;

Barker et al., 2013; Mpeshe et al., 2014; Cecilia et al., 2020 took into account the influence of temperature on the extrinsic incubation period (EIP) and biting rate (Durand et al., 2020 and EFSA, 2020 Model 2 on EIP only, Leedale et al., 2016 on biting rate only).

In terms of transmission routes, Nicolas et al., 2014; Cavalerie et al., 2015; Durand et al., 2020 included the possibility of direct transmission between vertebrate hosts, while Mpeshe et al., 2014; Sumaye et al., 2019 considered human-to-mosquito transmission (compared to 9 models incorporating mosquito-to-human transmission).

### 2.3.7 Connected papers

Nineteen models (45%) declared a parent model. In 13 cases (68%), a model and its parent shared at least one author. In 12 cases, a model and its parent belonged to the same category (5 applied, 1 grey, 6 theoretical). One grey model (Manore and Beechler, 2015) was the parent of an applied model (Beechler et al., 2015). In 4 cases, a theoretical model (Gaff et al., 2007 twice, Mpeshe et al., 2011; Chitnis et al., 2013) was a parent of a grey model (Miron et al., 2016; Cavalerie et al., 2015; Mpeshe et al., 2014; Manore and Beechler, 2015, respectively). Lastly, Gaff et al., 2007, a theoretical model, was parent of 2 applied models (Barker et al., 2013; Xue et al., 2012).

The model by Gaff et al., 2007 is a clear example of a theoretical model laying the groundwork for future model developments. It was first modified to explore control strategies of several types in Gaff et al., 2011. Adongo et al., 2013 then elaborated on Gaff et al., 2011 to explore sophisticated vaccination strategies. Another modification of Gaff et al., 2007 model was its spatialization in Niu et al., 2012.

In 84% of cases (16/19), a model used the same functional form (FF) for its force of infection as its parent model. A change of FF induced a justification in 2/3 cases. When keeping the same FF as the parent model, 8/16 models did not provide a justification, even though the parent model had no justification either in 7/8 cases.

Other examples can give an overview of the continuity between a model and its parent. Métras et al., 2020 added a human compartment to the model of Métras et al., 2017 and ran the parameter estimation algorithm on a new outbreak dataset. One of the two models described in EFSA, 2020 then made a stochastic model based on Métras et al., 2017, 2020. Taylor et al., 2016 used the model by Leedale et al., 2016 to explore a new research question (anticipate the effect of climate change) in an expanded region (East African Community compared to Kenya and Tanzania). Xiao et al., 2015 modified the model by Gao et al., 2013 to include seasonality through time-varying parameters.

*Note: Overall, the reasons why a given model is used as parent of another remain unknown. To go further, it would be interesting to see if other potential parent models had closer characteristics than the one used, creating a model tree for instance, as done in Andraud et al., 2012; Courtejoie et al., 2018; Hayes et al., 2021.*

## 2.4 Conclusion

In the last five years, more mechanistic models of RVFV transmission dynamics have been published than in the ten previous years combined. This possibly indicates a growing interest for RVFV epidemiology, although it is known that the number of publications is continuously growing, in all fields (Larsen and Ins, 2010; Bornmann and Mutz, 2015). An interesting trend is the evolution of modeling papers' objectives, which increasingly include the prevention and anticipation of RVF outbreaks (13/20 papers in 2016-present, 7/22 papers in 2004-2015). Research on RVFV, through mathematical modeling and other methods, has deeply enhanced our understanding of underlying epidemiological mechanisms, which now allows model to focus on more operational aspects. However, this review also highlighted important knowledge gaps, rarely addressed in mechanistic models of RVFV transmission dynamics.

A single model (Taylor et al., 2016) has looked at the possible effect of climate change on RVF risk, in Eastern Africa. This likely does not reflect a lack of interest for this issue, but could rather indicate that mechanistic modeling is not the preferred method to study such trends, compared to phenomenological (i.e statistical) models (Anyamba et al., 2009, 2012; Caminade et al., 2011; Caminade et al., 2014). Such phenomenological approaches can deepen our understanding of the effect of climate change on individual processes independently (e.g host mobility, vector habitat, Metelmann et al., 2019), a pre-requisite before developing integrative, disease-specific models (Bartlow et al., 2019). Still, how to prioritize research on livestock and human health in the context of climate change is up to debate (Campbell-Lendrum et al., 2015; Özkan et al., 2016). In their review, Métras et al., 2011 had highlighted the widespread use of phenomenological models to assess RVF risk across spatio-temporal scales. Mechanistic and phenomenological approaches can be seen as complementary ways to build a comprehensive view of the RVFV pathosystem.

The role of wildlife also seemed largely understudied. Contacts between livestock and wildlife are hard to observe and quantify (Bacigalupo et al., 2020), and modeling a higher biodiversity could result in amplification or dilution effects (Roberts and Heesterbeek, 2018). Studying the competence of local wildlife species for RVFV transmission, along with their attractiveness to mosquitoes, is a pre-requisite to determine the relevance of this question in a given territory (Evans et al., 2008; Olive et al., 2012; Rostal et al., 2017; Huyvaert et al., 2018).

*Note: This review also confirms that the models developed in this PhD were needed. At the within-host scale, only one model was developed so far (Tuncer et al., 2016), and brought limited mechanistic insight into the drivers of RVFV viral dynamics, which we address in Chapter 4. In Senegal, a model at large scale was lacking (the model at sub-national scale in Figure 2.2A is the one developed in Chapter 3), and the role of host movements has not yet been studied in this region, which we address in Chapter 5. More globally, the heterogeneity between livestock hosts, and how this could impact RVFV transmission dynamics, is also understudied, and is the common focus throughout this PhD.*

## 2.5 Supplementary information

### S.1 Reading grid

#### **Research questions, context, main analyses and results**

Main modeling objective (primary/secondary possible) : understand ; anticipate ; prevent

Model category : theoretical ; applied ; grey

Geographical location : if applicable, precise if zone with history of RVF or RVF-free

Context under study : hypothetical incursion or real world setting ; endemic or epidemic scenario ; other

Geographical scale : international ; national ; sub-national ; local

Is a parent model clearly stated?

What is common/different from the parent model?

Indicators of disease spread : R (any type of reproductive ratio, precise if analytical, from data, by simulation) ; number of individuals in a given health state ; summary statistic ; other

Model outputs : spatial patterns ; temporal patterns ; sensitivity of the model to parameters/hypothesis ; parameter estimation ; other

Control measures tested

Model selection performed?

Sensitivity analysis performed? If yes, which type: one-at-a-time ; global

Main results

Limits of the model (as presented in the paper)

#### **Data**

If presence of data,

Type of data : experimental ; environmental ; epidemiological ; clinimal ; demographic ; movement ; other

Is the data spatialized?

Is the data presented as time-series?

Use of data : calibration ; model selection ; input ; inference/model assessment

Origin of data : all published or open access ; some are published for the first time in peer review

#### **Hosts**

How many vertebrate taxa were considered?

What taxa?

What health states?

Is there population renewal?

Were age class considered? If yes, what type of age classes

Is the herd/human population detailed further (male/female ; pregnant ; occupation ; other)?

Important differences between host taxa or host types within a taxa : population density/dynamics ; movement patterns ; attractiveness to mosquitoes ; infectiousness/susceptibility ; clinical outcome ; duration of latent/infectious period ; development of immunity ; some were dead-end hosts ; other

Clinical outcomes described : asymptomatic/symptomatic ; mild/severe ; disease-induced mortality ; abortion ; none/other

### Vectors

How was the vector component modeled : implicitly (no state variable) ; explicitly (at least one state variable)

How many taxa?

What taxa?

Main characteristics of the vector population and differences between taxa, precise when driven by abiotic factor : life cycle (emergence, feeding behaviour) ; infection (probability, extrinsic incubation period) ; transmission (probability, vertical transmission)

What health states?

How were aquatic population modeled : not at all ; implicitly (emergence rate of adults described by a parameter or function) ; explicitly (at least one state variable) ; other (e.g. extracted from an external model)

If implicit aquatic population, type of parameter/function : constant ; forced (e.g. sinusoidal, precise if informed by data) ; input-dependent (e.g. abiotic variable) ; other

If explicit aquatic population, features (which state, influence of abiotic factors, possible dormancy etc.)

Bloodmeal frequency : constant ; variable (precise with what factor) ; not a parameter

Bloodmeal distribution among hosts : homogeneous ; heterogeneous ; not a parameter

Is there an explicit factor besides host taxa driving heterogeneous biting (host size, behaviour, infection status etc.)?

### Spatio-temporal dynamics and modeling paradigm

How many spatial locations : one with no immigration or emigration/location was undefined or vaguely defined (spaceless model) ; more than one location or model included terms describing immigration or emigration

Type of spatial model : discrete number of locations/pixels ; continuous space ; connectivity network among individual hosts ; other

Resolution (surface covered by one pixel, if applicable)

What moves : nothing ; vertebrate hosts ; vectors ; both

If hosts move, what type of movement : commercial ; nomadic ; other

If vectors move, what type of movement : follow hosts ; random ; other (e.g. wind)

Duration of simulations, and if known, time period (month, year)

Timestep

Characteristics of the model : deterministic/stochastic ; agent-based/compartamental  
If stochastic : what is stochastic, number of runs etc.

### **Transmission and infection**

Functional form of the force of infection (FOI, for vector-host transmission)

Is the choice of functional form justified/discussed?

Transmission parameter : aggregated, constant ; aggregated with variation (function with no clear biological translation, e.g proxy for seasonality) ; decomposed (different parameters for biological processes such as biting rate, proba of successful transmission, feeding preferences etc.)

Other routes of transmission (precise FOI if applicable) : mosquito-mosquito ; livestock-livestock ; mosquito-human (1 way or 2 ways) ; livestock-human (1 way)

Hypothesis for time spent in E/I/R state, for hosts/vectors : exponential ; other (precise if driven by abiotic factor)



# 3

## Epidemic potential of RVFV in northern Senegal

### 3.1 [In French] Résumé grand public

Le premier article issu de ma thèse s'intitule, si on le traduit : "Il est risqué d'errer en Septembre: modéliser le potentiel épidémique de la fièvre de la Vallée du Rift dans un contexte Sahélien." Ce résumé devrait vous permettre de comprendre ce qui a motivé cette étude, la méthodologie utilisée, les résultats clés et leur implication. Dans ce qui suit, j'utiliserai FVR pour désigner la fièvre de la Vallée du Rift, et hôte(s) pour qualifier les animaux à risque d'infection par la FVR.

Dans le Sahel Ouest-Africain, plusieurs épidémies de FVR ont eu lieu depuis la fin des années 1980, principalement au Sénégal et en Mauritanie. Le nord du Sénégal représente un cas d'étude intéressant car il comprend deux écosystèmes distincts:

- la vallée et le delta du fleuve Sénégal, espace frontalier avec la Mauritanie, où la présence d'eau favorise l'agriculture irriguée et permet ainsi la cohabitation des hôtes et moustiques toute l'année (Figure 3.1A, en bleu).
- la région du Ferlo, où la saison des pluies déclenche l'émergence<sup>1</sup> de moustiques suite à la création de mares temporaires, qui sont également des points de rassemblement pour les animaux transhumants<sup>2</sup> (Figure 3.1A, en rouge).

---

<sup>1</sup> Passage du stade aquatique au stade aérien. Avant de devenir un insecte volant, le moustique passe nécessairement par un stade larvaire qui s'effectue dans l'eau.

<sup>2</sup> Au Sahel, l'élevage se pratique de manière extensive : faible densité d'animaux, répartis sur de grands espaces et se basant sur l'exploitation des ressources naturelles (eau, pâturage). La disponibilité des ressources est très variable du fait de contraintes climatiques (alternance saison sèche et saison humide), ce qui amène les éleveurs à se déplacer sur de grandes distances avec leurs animaux pour s'adapter. C'est ce qu'on appelle la transhumance.

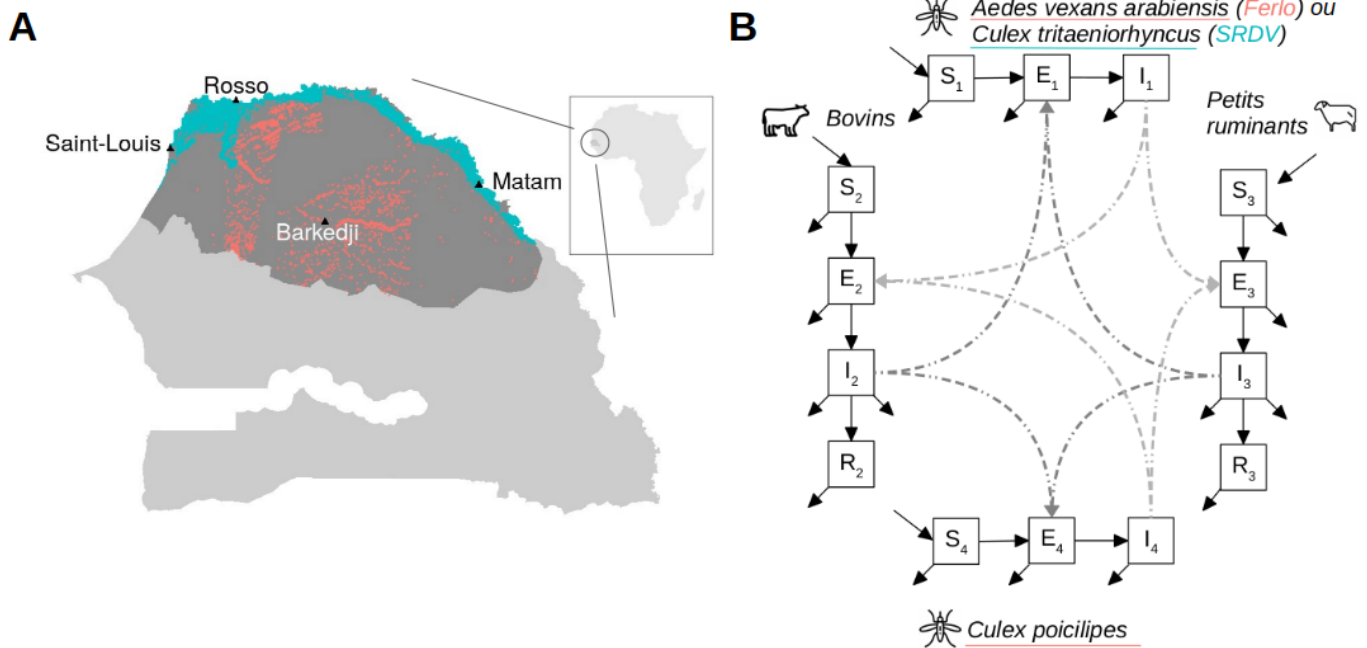
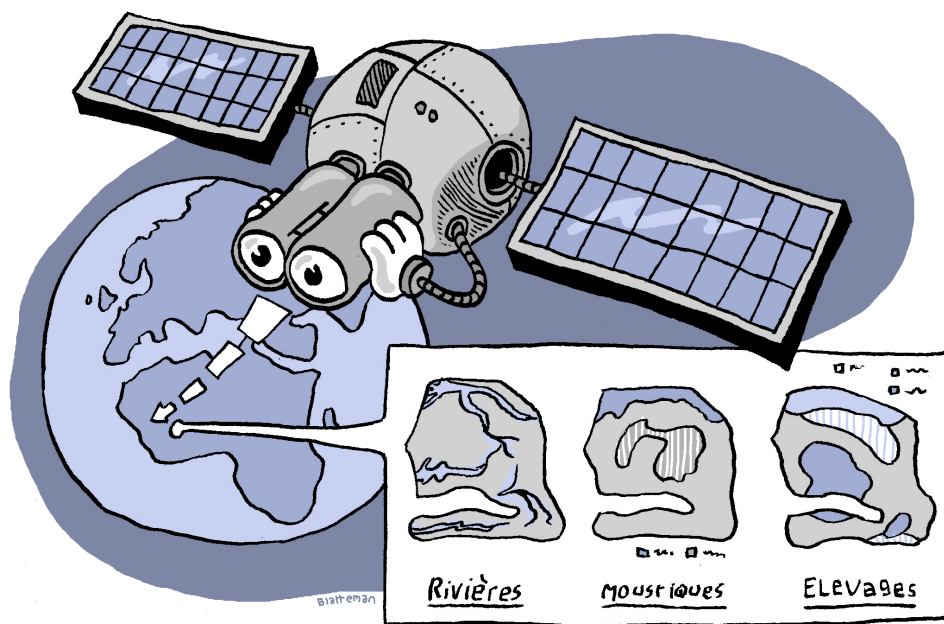


**Figure 3.1** – A – Zone d'étude, nord du Sénégal. Points bleus: vallée et delta du fleuve Sénégal. Points rouge: région du Ferlo.

B – Schéma du modèle mathématique utilisé pour représenter la transmission de la FVR. Deux espèces de moustiques, différentes en fonction des régions, interagissent avec deux catégories d'hôtes, bovins et petits ruminants (chèvres, moutons). Seule la transmission moustiques-hôtes est retenue. Etats de santé représentés: sensible ( $S$ ), exposé ( $E$ ), infectieux ( $I$ ), guéri/immunisé ( $R$ ). Se référer à la Box 1.1 du Chapitre 1 pour une explication simple du principe des modèles à compartiments.

Il nous a semblé important de mieux comprendre ce qui pouvait favoriser le démarrage d'une épidémie dans ces deux zones. En effet, différents mécanismes entrent en œuvre, et on ne sait pas dire avec certitude lesquels sont prépondérants, d'autant que cela peut varier dans le temps et dans l'espace. Ainsi, grâce à la modélisation mathématique, couplée à l'utilisation de données satellitaires, nous avons pu représenter sur des cartes le potentiel épidémique pendant trois saisons des pluies consécutives, de 2014 à 2016.

### 3.1.1 Potentiel épidémique : qu'entend-on par là ? Pourquoi l'estimer ?

Le terme épidémie provient de la combinaison du grec *epi*, “dans, parmi” et *démos*, “la population”. Il s'agit donc de quelque chose qui est présent dans la population, pas nécessairement un agent pathogène<sup>3</sup>. Le potentiel épidémique peut dès lors être défini comme la possibilité d'apparaître dans une population<sup>4</sup>. C'est donc un concept assez vague, et si on l'interprète dans le cas d'un virus, comme celui de la FVR, on comprend qu'il recouvre plusieurs mécanismes, plus ou moins imbriqués. En effet, si je vous demande “quels sont les facteurs qui contribuent à l'apparition d'une épidémie<sup>5</sup>?”, vous pouvez penser, entre autres, à:

#### *Le potentiel épidémique vise à mesurer les différents facteurs pouvant favoriser le démarrage d'une épidémie*

1. **Le virus doit être introduit dans la population** : par le biais d'un “cas zéro” ou seulement du fait de sa présence dans l'environnement, avant même que quelqu'un ne “l'attrape”.

*Sans cas zéro, pas d'épidémie.*

2. **Le virus doit se multiplier<sup>6</sup> dans la personne infectée, et la rendre contagieuse, donc capable de transmettre à son tour** : de manière générale, il existe d'abord une période de latence (Figure 3.2), pendant laquelle le virus se multiplie dans l'organisme, jusqu'à être présent dans des quantités suffisantes pour être transmis. Selon les virus, le lieu de multiplication privilégié n'est pas le même (goutelettes, sperme, sang), ce qui

---

<sup>3</sup> L'épidémiologie est donc un vaste domaine qui ne se limite pas à l'étude de la propagation des maladies contagieuses. Elle s'intéresse aussi par exemple au diabète, cancer, obésité, suicide, burnout etc.

<sup>4</sup> Plusieurs échelles de population peuvent être étudiées, avec chacune leurs implications et leur pertinence selon la question qu'on se pose: école, hôpital, ville, région, pays, monde...

<sup>5</sup> Ce qui est décrit ici pour un virus est généralisable aux autres types d'agents infectieux: bactéries, parasites, champignons, et protozoaires.

<sup>6</sup> Les virus sont incapables de se reproduire sans un hôte, car ils ont besoin d'exploiter sa machinerie cellulaire pour copier le matériel génétique (sous forme d'ADN ou d'ARN selon les virus) qu'ils contiennent. Ce n'est pas le cas des autres types d'agents infectieux, plus autonomes. C'est cette caractéristique des virus qui explique pourquoi il y a débat sur le fait de les classer dans le règne du vivant.

influe sur le mode de contagion : par aérosol, sexuelle, vectorielle (par insecte qui se nourrit de sang) etc. Des stratégies différentes existent selon les virus : la vitesse de multiplication, la durée de survie dans l'organisme, la vulnérabilité à la réponse immunitaire etc. peuvent grandement varier et influencer la vitesse à laquelle on devient contagieux et combien de temps on le reste. En effet, la plupart du temps, la contagiosité dure un temps limité, car la quantité de virus finit par diminuer, notamment grâce à l'action du système immunitaire. Enfin, il est important de préciser que la contagiosité n'est pas nécessairement liée à la manifestation de symptômes (Figure 3.2), ce qui peut poser des problèmes de détection des cas.

*Si le cas zéro n'est pas contagieux, pas d'épidémie.*

3. **La personne infectieuse adopte un comportement ou se trouve dans un environnement propice à la transmission** : la voie de transmission influe sur ce qui constitue un comportement ou un environnement "à risque".

*Si le cas zéro est contagieux mais que les conditions sont réunies pour éviter qu'il ne transmette, pas d'épidémie.*

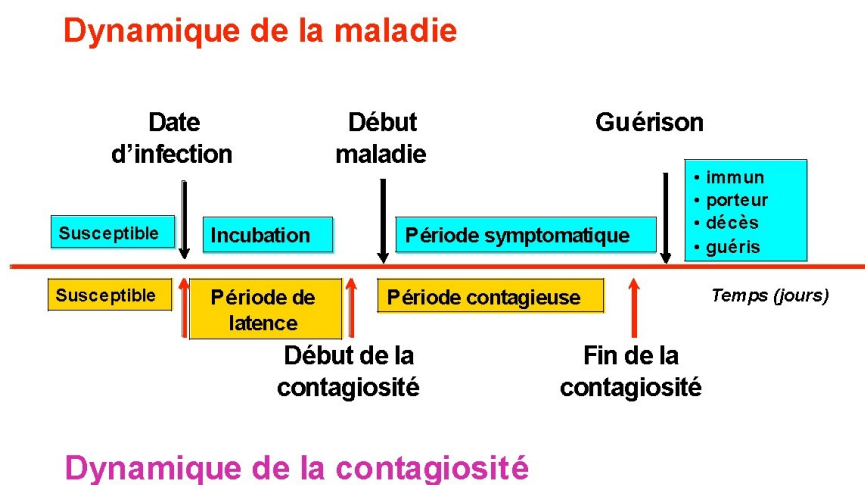


**Figure 3.2** – Distinction entre dynamique de la maladie (liée aux symptômes) et dynamique de la contagiosité. Ce qui est observable cliniquement (symptôme) n'est pas forcément synchronisé avec la contagiosité : les personnes asymptomatiques (porteurs sains, qui ne manifesteront jamais de symptômes) peuvent parfois être contagieuses. Il est également possible que certains individus commencent à être contagieux avant de développer des symptômes (transmission présymptomatique). Enfin, une personne qui présente toujours des symptômes peut ne plus être contagieuse, car l'agent infectieux a été éliminé mais le corps lutte toujours contre les séquelles de l'infection. Figure extraite de Fontenille et al., 2009 *La lutte antivectorielle en France*.

Ces trois conditions doivent donc être réunies pour que la possibilité d'une épidémie soit à envisager. Ce sont des conditions nécessaires, mais pas suffisantes! Pour qu'il y ait un réel

emballement, et que le nombre de cas ne reste pas anecdotique, il faut que les conditions 2 et 3 se réalisent également pour les cas créés par le cas zéro, et ainsi de suite<sup>7</sup>.

Estimer le potentiel épidémique revient donc à mesurer les différents facteurs pouvant favoriser le démarrage d'une épidémie. Les différents processus listés ci-dessus (1,2,3) peuvent être étudiés séparément, de manière plutôt fondamentale, notamment lorsqu'on a affaire à un virus mal connu. Mais sur le terrain, c'est leur combinaison qui déclenche des épidémies. Par conséquent, lorsque nous disposons de suffisamment d'informations, comme ça nous a semblé être le cas grâce aux précédentes études menées sur la FVR au nord du Sénégal, il est possible d'étudier ces trois facteurs ensemble, de façon intégrée.

*Cette connaissance est importante dans une optique de surveillance, de prévention, et de maîtrise*

Nous nous sommes donc attelés à étudier un indicateur global (le nombre de reproduction de base,  $R_0$ , présenté dans la section suivante), incluant les différents processus intervenant dans la transmission du virus au démarrage d'une potentielle épidémie. Nous avons également la volonté de représenter comment cet indicateur varie dans l'espace et dans le temps, pour mieux comprendre comment le risque varie entre régions du Sénégal et entre saisons des pluies.

Cette connaissance est importante dans une optique de (i) surveillance: à quels endroits et à quels moments faut-il être le plus attentif à une potentielle flambée du virus, (ii) de prévention: comment rendre l'environnement moins favorable à l'installation du virus dans la population, et (iii) de maîtrise: quelles actions mettre en place pour endiguer une transmission déjà en cours.

### 3.1.2 La métrique du $R_0$ comme outil

Il nous arrive souvent de vouloir résumer des phénomènes complexes par des métriques (du grec *metrikós*, "qui peut être mesuré"). Simples, faciles à comprendre, elles nous donnent l'impression de pouvoir quantifier précisément les choses: les kilo-calories de votre repas, les kilogrammes de CO<sub>2</sub> émis pendant votre trajet en voiture, ou encore une note sur 20 attribuée au devoir de votre enfant. Ces métriques, permettent de faire des statistiques: comparer, classer, moyenner... Là où les choses se corsent, c'est quand ces statistiques sont utilisées pour émettre des recommandations, des réglementations, créer des labels... On s'expose alors à la

---

<sup>7</sup> On pourrait imaginer qu'un cas zéro contamine à lui seul des centaines de personnes qui elles-mêmes ne seraient pas contagieuses, ce qui constituerait aussi une épidémie, mais avouez qu'il s'agit d'un scénario un peu extrême et rarement observé ;-)

possibilité d'une mauvaise interprétation des métriques par ceux qui ne savent pas (ou ont oublié) qu'elles ne reflètent pas toute la complexité du phénomène que l'on cherchait initialement à évaluer: les qualités nutritionnelles d'un plat, l'impact sur l'environnement d'un moyen de transport, ou les capacités intellectuelles d'un enfant.

*$R_0$  se définit comme le nombre moyen de nouveaux cas engendrés par un cas zéro introduit dans une population qui n'a jamais été exposée à la maladie en question*

Pour évaluer le potentiel épidémique de la FVR au Sénégal, j'ai fait appel à une métrique classiquement utilisée en épidémiologie, et qui a été mise en avant par les médias grand public dans le contexte de la pandémie de Sars-Cov2 : le nombre de reproduction de base, communément appelé  $R_0$  (à prononcer R-zéro en français, R-naught en anglais).

$R_0$  se définit comme le nombre moyen de nouveaux cas engendrés par un cas zéro introduit dans une population qui n'a jamais été exposée à la maladie en question. On dit que cette population est entièrement sensible. On ne compte que les cas directement engendrés par le cas zéro, et pas les cas suivants. Le décompte s'arrête donc lorsque le cas zéro n'est plus contagieux (parce qu'il a guéri ou parce qu'il est mort). Il ne s'agit alors pas d'estimer la taille d'une potentielle épidémie mais seulement un cycle, une génération, de nouveaux cas. On comprend cependant intuitivement que si un seul cycle permet de créer plusieurs nouveaux cas, il y a fort à parier que le risque d'épidémie est non négligeable. Et en effet, mathématiquement, si ce  $R_0$  est supérieur à 1, on est face à ce qu'on appelle une croissance exponentielle des cas, et donc une épidémie probable. J'ai bien dit probable, et pas certaine, je vous expliquerai plus loin pourquoi. Le seuil de 1 est donc classiquement utilisé comme seuil d'alerte.

Comment peut-on estimer ce  $R_0$ ? Intuitivement, il semblerait que des données d'épidémie réelle (ou de transmission expérimentale) soient nécessaires, avec des informations sur la date de survenue des cas et du traçage de "qui a infecté qui?". Mais avoir accès à ce genre de données relève plus de l'exception que de la règle, pour des raisons logistiques, éthiques, diagnostiques... et parfois même politiques! Pour faire sans, une des solutions consiste à faire appel à la modélisation. Un modèle étant une représentation simplifiée de la réalité, il faut d'abord décider de ce qui doit être inclus pour capturer la complexité du potentiel épidémique (Figure 3.1B). Dans notre cas, il nous a semblé important d'incorporer la diversité des hôtes et des moustiques pouvant prendre part à la transmission du virus de la FVR au nord du Sénégal. Nous avons donc distingué les bovins des petits ruminants (chèvres, moutons), car leur répartition varie

géographiquement et ils n'ont pas la même durée de vie (que ce soit en bonne santé ou une fois malades). En terme de moustiques, il existe différentes espèces avec des cycles de vie différents, qui font qu'elles ne sont pas présentes aux mêmes endroits aux mêmes moments. Nous avons choisi trois espèces, qui sont les plus abondantes dans nos régions d'étude et dont il est avéré qu'elles peuvent transmettre le virus de la FVR. Dans la vallée et le delta du fleuve Sénégal, nous avons distingué les *Culex poicilipes* des *Culex tritaeniorhynchus*. Dans le Ferlo, nous avons inclus les *Culex poicilipes* et les *Aedes vexans arabiensis*<sup>8</sup>. Ensuite, un ensemble d'équations reproduit les différents événements qui concourent à la transmission du virus de la FVR : naissance, mort, contact entre hôte et moustique lors d'une piqure, période d'incubation et de contagiosité. Une partie de la complexité de ce système est schématisé dans la Figure 3.3.

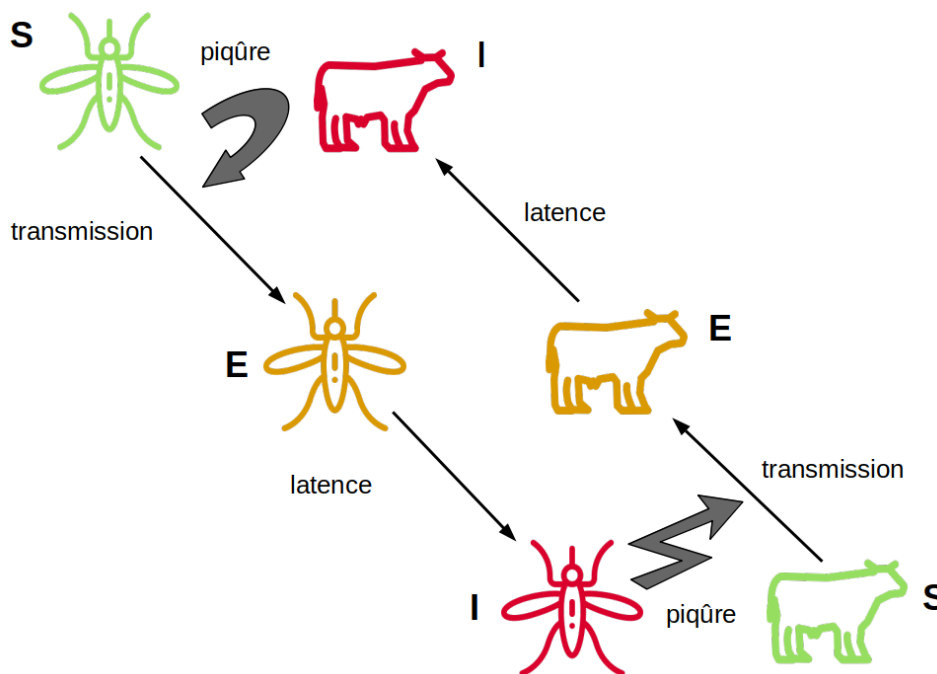


**Figure 3.3** – Succession d'évènements nécessaires à la transmission du virus. Chaque évènement correspond à un des paramètres du modèles et est inclus dans la formule du  $R_0$ : fréquence à laquelle le moustique recherche un hôte à piquer, probabilité de transmettre le virus lors d'une piqure, probabilité de survivre jusqu'à la fin de la période de latence.

Ce qu'il est important de retenir:

- Une fois infecté, un moustique peut transmettre le virus jusqu'à sa mort, il ne guérit pas, contrairement aux animaux.
- La seule voie de transmission retenue est vectorielle, c'est-à-dire la transmission du virus de l'hôte au moustique et vice-versa.

<sup>8</sup> *Aedes* et *Culex* sont deux genres de moustiques ayant un cycle de vie un peu différent. Les *Aedes* sont plutôt présents la première moitié de la saison des pluies, et les *Culex* la deuxième.

- Nous n'avons pas représenté la transmission entre animaux (par contact avec les avortons par exemple) ni la transmission d'un moustique à sa descendance. Ces voies de transmission peuvent exister, mais nous avons considéré qu'elles jouaient un rôle marginal dans le potentiel épidémique, et pouvaient donc être négligées.
- Les contacts entre moustiques et hôtes se font de la manière suivante: un moustique a besoin d'un repas de sang entre chaque ponte, et le prend donc sur un hôte<sup>9</sup>. Un animal va recevoir un nombre de piqûres proportionnel au nombre de moustiques présents. Ces derniers se répartissent équitablement sur l'ensemble des hôtes disponibles, en fonction de leur préférence pour les bovins et les petits ruminants.

$R_0$  se présente finalement sous forme d'une formule donnant le nombre de cas moyens résultant de tous les cas de figures autorisés par le modèle (ici pour l'exemple du Ferlo):

- Bovin(s) infecté(s) par un *Aedes*
- Petit(s) ruminant(s) infecté(s) par un *Aedes*
- Bovin(s) infecté(s) par un *Culex*
- Petit(s) ruminant(s) infecté(s) par un *Culex*
- *Aedes* infecté(s) par un bovin
- *Aedes* infecté(s) par un petit ruminant
- *Culex* infecté(s) par un bovin
- *Culex* infecté(s) par un petit ruminant

Le potentiel épidémique, par le biais du  $R_0$ , est ensuite quantifié indépendamment dans chacun des pixels de notre carte, chaque semaine, pendant les trois saisons des pluies étudiées. Nous estimons donc, dans une localisation donnée, pour une date d'introduction du virus de la FVR donnée, si le démarrage d'une épidémie est possible. Il y a cependant des cas de figures que notre analyse ne permet pas de capturer:

- Plusieurs introductions successives de la FVR, même si chacune indépendamment n'aurait pas généré assez de cas ( $R_0 < 1$ ), peuvent finalement déclencher une épidémie.

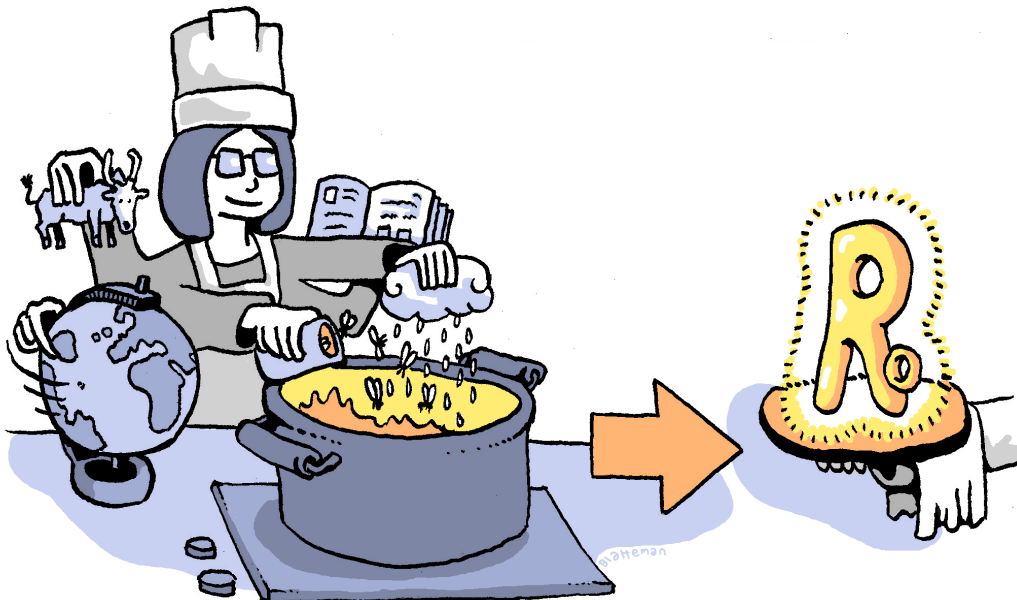
---

<sup>9</sup> Exceptionnellement deux lorsqu'il n'a pas pu récupérer la quantité de sang suffisante sur un seul hôte (parce que l'hôte s'est défendu par exemple).



- Une introduction dans des conditions de démarrage favorables ( $R_0 > 1$ ) peut ne pas déclencher d'épidémie si les conditions deviennent brusquement défavorables à la transmission: les cas générés par le cas zéro ne peuvent transmettre efficacement.

Une fois le modèle défini et la formule du  $R_0$  trouvée, le challenge est de savoir quelles valeurs donner à toutes les inconnues, ou paramètres, présents dans cette formule. Comme le but est de cartographier le potentiel épidémique pendant plusieurs saisons des pluies, il est important de distinguer les paramètres du modèle que l'on pense faire varier dans le temps et/ou dans l'espace de ceux que l'on va considérer comme constants. Je m'attarde plus en détails sur ce qui varie dans la section suivante, et qui constitue la réelle plus-value de ce travail.



### 3.1.3 Notre étude: comment cré-t-on une nouvelle information à partir de données existantes ?

La Figure 3.4 présente l'inclusion des différents jeux de données ayant permis de représenter la variabilité dans le temps et l'espace du  $R_0$  :

- La pluviométrie journalière (symbole gouttes d'eau, grille verte) est issue de données météorologiques satellitaires spécifiquement dédiées au continent africain, et parfois de stations météo directement présentes sur le terrain. En complément, des données satellitaires de dernière génération permettent de situer précisément les plans d'eau de notre zone d'étude, notamment les mares temporaires, très nombreuses et très variables en taille. Ces données alimentent un modèle hydrologique permettant de calculer la surface

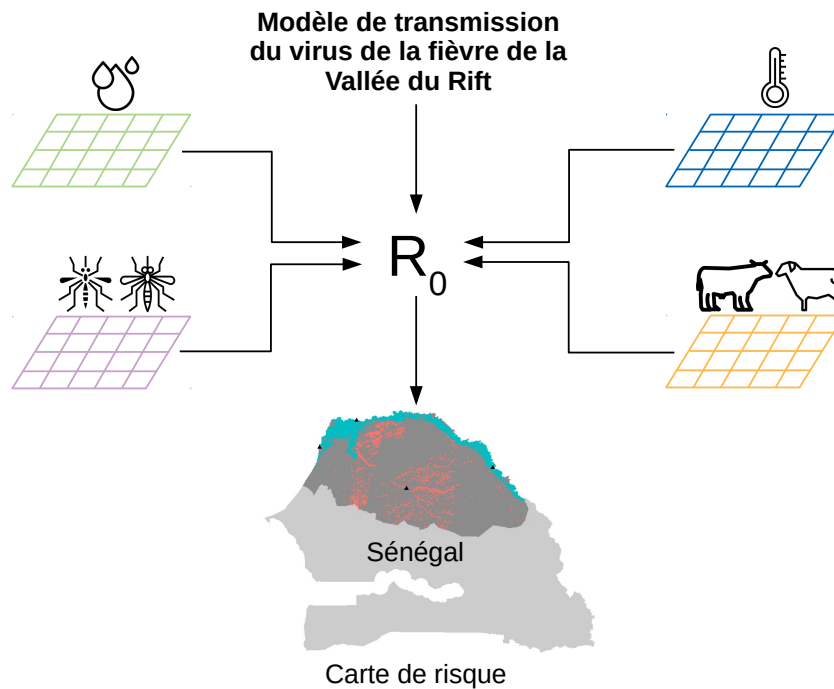


**Figure 3.4** – Schéma représentant l’inclusion de différents jeux de données dans notre formule du  $R_0$ . Ces jeux de données sont la source de la variabilité spatiale et temporelle du potentiel épidémique.

recouverte d’eau dans les pixels de notre carte au cours de la saison des pluies, ce qui va directement impacter les populations de moustiques<sup>10</sup>.

- Les données de température (symbole thermomètre, grille bleue) sont issues du centre européen pour les prévisions météorologiques à moyen terme. Ce sont des données satellitaires également, et ce sont plus précisément les températures minimum et maximum par décade (période de 10 jours) qui sont utilisées. Elles permettent de calculer le taux d’humidité relative, qui influe sur la longévité des *Culex*. La température impacte également la transmission du virus de la FVR, puisqu’elle influe sur la période d’incubation extrinsèque des moustiques<sup>11</sup>.
- Les densités de moustiques (symbole moustique, grille violette) sont variables dans le temps et dans l’espace, avec des dynamiques différentes selon les espèces. Nous avons utilisé les résultats d’un modèle mathématique déjà existant, nous permettant d’avoir le nombre de femelles en recherche d’un repas de sang (et donc d’un hôte), dans chaque pixel,

<sup>10</sup> Les plans d’eau constituent les gîtes de ponte des moustiques: à la surface pour les *Culex*, aux bords pour les *Aedes*.

<sup>11</sup> Il s’agit du temps entre l’infection du moustique lorsqu’il pique un hôte infecté et la présence du virus dans sa salive, lui permettant de transmettre à son tour. Expérimentalement, on est capable de détecter le passage du virus dans l’abdomen, le thorax, la tête, les pattes, et les ailes du moustique. Mais tant qu’il n’est pas dans la salive, pas de transmission possible! S’il n’y parvient jamais, on dit que l’espèce n’est pas compétente.

chaque semaine, pour les 3 espèces étudiées. Ce modèle utilise directement la dynamique de surface en eau évoquée précédemment, ainsi que les variations de température, qui impactent la biologie des moustiques<sup>12</sup>. Il a été validé grâce à des données de captures réalisées sur le terrain.

- Les densités d'hôtes (symbole vache et mouton, grille orange) proviennent d'un jeu de données mondial de l'Organisation des Nations Unies pour l'alimentation et l'agriculture (FAO). Il s'agit des résultats d'un modèle statistique existant, qui utilise les recensements officiels des pays, fournis par unité administrative (type région, département). Ce modèle répartit ensuite ces densités animales dans l'espace de manière plus précise. A partir de données environnementales diverses (topographie, utilisation des sols, etc.), il déduit là où il semble plus vraisemblable que les animaux soient situés. Nous avons utilisé les jeux de données pour les bovins, les chèvres et les moutons, ces deux derniers ayant été regroupés dans une même catégorie "petits ruminants" dans notre modèle. Cette source permet de représenter la répartition géographique des hôtes mais pas les variations temporelles de ces densités. La grille est donc constante dans le temps. Cela revient à faire l'hypothèse que les animaux sont toujours répartis de la même manière sur le territoire, ce qu'on sait être inexact, notamment du fait de la transhumance dans la région du Ferlo. C'est donc une des limitations de notre étude.

Une fois toutes ces données injectées dans notre formule du  $R_0$ , que nous a révélé notre cartographie qui n'était pas visible dans les données initiales? Qu'a apporté cet indicateur, qui lie les différents processus impliqués dans la transmission?

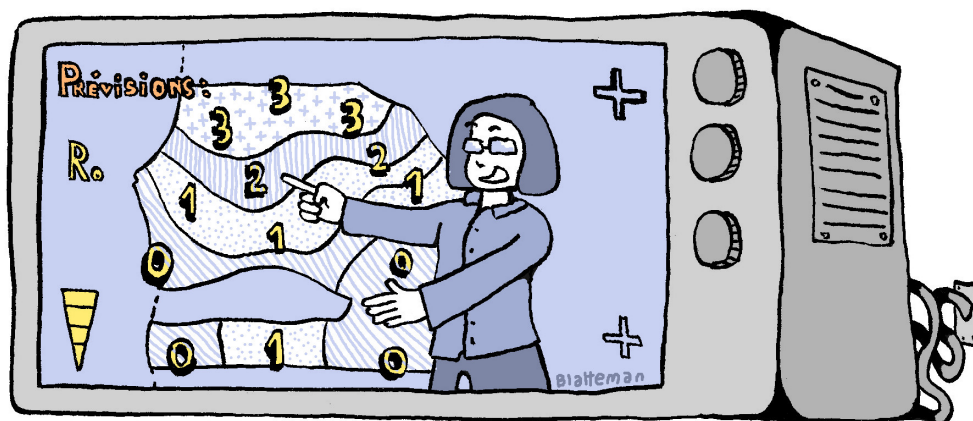
- **C'est en septembre que l'introduction du virus est la plus à risque de provoquer le démarrage d'une épidémie au nord du Sénégal.** En effet, pour les saisons des pluies 2014 à 2016, c'est systématiquement en septembre qu'est atteint le nombre maximum de pixels avec un  $R_0 > 1$ . La dynamique diffère entre nos deux régions d'étude. Dans la vallée et le delta du fleuve Sénégal, le potentiel épidémique est fort tout au long de la saison des pluies. Dans le Ferlo, la saisonnalité est beaucoup plus marquée, avec un risque maximum en septembre tous les ans malgré des profils de température et de densités de moustiques variables entre années.
- **La date d'introduction engendrant le risque maximal est atteinte plus tôt chaque année.** Le 22 septembre en 2014, le 14 septembre en 2015 et le 5 septembre en

---

<sup>12</sup> La température influe sur la durée de développement et mortalité des différents stades du cycle de vie des moustiques (oeuf, larve, puppe, adulte), ainsi que la fréquence des repas de sang pour engendrer de nouvelles pontes.

2016. Cette tendance n'ayant été calculée que sur 3 ans, elle mérite qu'on élargisse la fenêtre de temps étudiée pour l'infirmier ou la confirmer, et incite également à se projeter pour anticiper l'impact des changements climatiques globaux sur le risque épidémique de FVR au nord du Sénégal.

- **Les localisations les plus à risque de constituer des foyers épidémiques varient selon les années (Figure 3.5). Une fois de plus c'est dans le Ferlo que la variabilité est la plus forte.** En 2014, la majorité des mares dans les latitudes au sud de Barkedji ont présenté un potentiel épidémique élevé dans la saison, et ce pendant en moyenne 7 semaines, soit un tiers de la saison des pluies. En 2015 et 2016 le nombre de localisations à haut risque tend à diminuer et à se concentrer dans les longitudes à l'est de Barkedji, pour une durée plus limitée (4 à 5 semaines). Dans la vallée et le delta du fleuve Sénégal, la région dans son ensemble présente un fort potentiel épidémique, pendant 8 à 9 semaines dans la saison en moyenne. Seule la zone autour de Matam présente des variations entre années, avec une plus grande concentration de localisations à risque en 2015-2016 qu'en 2014.



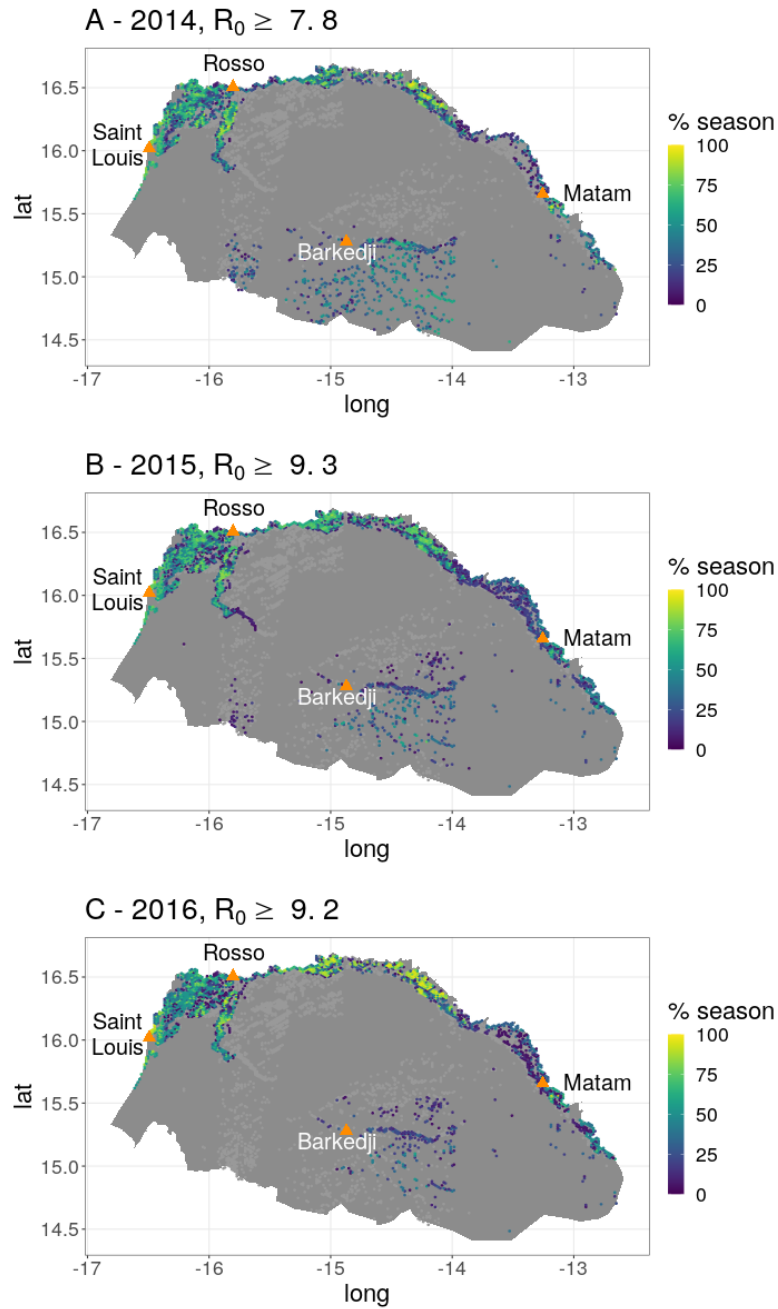


**Figure 3.5** – Répartition géographique des localisations présentant le plus fort potentiel épidémique, pour chaque saison des pluies étudiée.

- Dans ces localisations à risque, les densités de moustiques sont telles que la diminution de leur population ne constitue pas une piste viable de réduction du risque. A Barkedji par exemple, que ce soit en début de saison des pluies quand les *Aedes* sont les plus nombreux, ou en seconde moitié de saison quand les *Culex* prennent le relais, la diminution de l'une ou de l'autre espèce ne permet pas de faire redescendre le  $R_0$  en dessous de 1, à moins d'appliquer une diminution extrême de la population (plus de 80% sur chaque espèce), ce qui n'est pas réalisable en pratique.

- **Par contre, accroître l'immunité des bovins permettrait de réduire la transmission du virus de manière plus avantageuse qu'une action sur celle des petits ruminants.** Ce résultat est plutôt contre-intuitif car les petits ruminants sont plus nombreux que les bovins dans la quasi-totalité des pixels étudiés (Figure 3.5A, points non bleu). Mais en fait, les bovins sont malgré eux un maillon clé de la transmission. Je m'explique:

  - Nous avons considéré dans notre modèle que pour un même nombre de bovins et de petits ruminants disponibles, les moustiques préfèrent largement se nourrir sur les bovins, ce qui correspond à ce qui a été montré dans plusieurs études du comportement trophique (expression compliquée pour désigner les habitudes alimentaires) des moustiques.
  - Ainsi, en concentrant une plus grande partie des piqûres, les bovins ont plus de chances de subir une première piqûre qui les infecte et une seconde qui infecte un moustique qui ira transmettre le virus à son tour.
  - Dès lors, avoir des bovins immunisés (par vaccination ou par guérison d'une précédente infection de FVR) réduit la population de bovins sensibles disponibles et court-circuite de potentielles chaînes de transmission, faisant baisser le potentiel épidémique.
  - Bien sûr, il existe un seuil au-delà duquel une plus grande abondance de petits ruminants peut surpasser l'effet de la préférence naturelle des moustiques, mais nos calculs montrent que ce seuil n'est pas franchi à l'échelle régionale.
- **Les préférences trophiques des moustiques ainsi que la fréquence de leur repas en fonction de la température sont des paramètres clés nécessitant une estimation précise.** Ceci a été montré par le biais d'une analyse de sensibilité, capitale pour savoir si un modèle est fiable. En effet, les valeurs choisies pour les paramètres ne sont pas parfaites<sup>13</sup>. L'idée est alors de faire varier la valeur de tous les paramètres de notre modèle pour trouver les paramètres dont la variation a le plus fort impact sur les résultats énoncés précédemment. On vérifie ainsi que les résultats clés de nos analyses ne sont pas remis en cause par un léger changement de valeur des paramètres. Dans notre cas, les conclusions sur les périodes et lieux les plus à risque sont robustes, mais

---

<sup>13</sup> Certains paramètres sont très difficiles à estimer par des expériences ou études de terrain, et sont donc emprunts d'une grande incertitude, car les données sont rares. Pour d'autres, les données existent mais des erreurs de mesures ne peuvent être exclues. Il arrive souvent également de reprendre une valeur de paramètre provenant d'une autre zone ou espèce d'étude, à défaut d'une connaissance plus précise.

on note tout de même que les préférences alimentaires des moustiques et la fréquence de leur repas sont les paramètres pouvant le plus impacter le nombre de pixels avec  $R_0 > 1$ . Comme ce sont des paramètres difficiles à estimer, nous recommandons donc que plus d'études se penchent sur la question pour accroître la précision des modèles à venir.

#### A garder en tête

- Lorsque les données épidémiologiques sont rares, disparates, ou qu'elles ne correspondent pas exactement à ce qu'on aimerait quantifier, on peut faire appel à la modélisation mathématique pour estimer le potentiel épidémique d'une maladie.
- Le modèle doit être adapté à la maladie étudiée, mais la méthode pour en extraire la formule du  $R_0$  est la même quel que soit le modèle.
- La valeur du  $R_0$  dépend du contexte (lieu, moment), particulièrement pour les maladies vectorielles, pour lesquelles le climat joue un rôle important. Il faut donc éviter les valeurs de  $R_0$  uniques et globales, qui cachent toute la variabilité du potentiel épidémique.
- Pour capturer la variabilité du  $R_0$ , les données satellitaires sont d'une grande aide pour aboutir à de larges échelles de temps et d'espace, quasiment impossibles à obtenir avec les seules études de terrain, pour des raisons de temps et de moyens, financiers et humains.
- Les études de terrain et les données expérimentales sont indispensables pour garantir le réalisme des modèles. Les résultats des modèles peuvent à leur tour suggérer de nouvelles choses à tester sur le terrain ou en laboratoire. Des allers-retours sont alors possibles entre les approches.







## It's risky to wander in September: Modelling the epidemic potential of Rift Valley fever in a Sahelian setting

Hélène Cecilia<sup>a,b,c,\*</sup>, Raphaëlle Métras<sup>d</sup>, Assane Gueye Fall<sup>e</sup>, Modou Moustapha Lo<sup>e</sup>,  
Renaud Lancelot<sup>b,c</sup>, Pauline Ezanno<sup>a</sup>

<sup>a</sup> INRAE, Oniris, BIOEPAR, 44300, Nantes, France

<sup>b</sup> UMR ASTRE, CIRAD, Montpellier, France

<sup>c</sup> ASTRE, Montpellier University, CIRAD, INRAE, Montpellier, France

<sup>d</sup> Inserm, Sorbonne Université, Institut Pierre Louis d'Epidémiologie et de Santé Publique (IPLESP), F-75012, Paris, France

<sup>e</sup> Institut Sénégalais de Recherches Agricoles/Laboratoire National de l'Élevage et de Recherches Vétérinaires, BP 2057, Dakar-Hann, Senegal

### ARTICLE INFO

#### Keywords:

Rift Valley fever virus  
Basic reproduction number  
Mathematical modelling  
Vector-borne disease  
Risk map

### ABSTRACT

Estimating the epidemic potential of vector-borne diseases, along with the relative contribution of underlying mechanisms, is crucial for animal and human health worldwide. In West African Sahel, several outbreaks of Rift Valley fever (RVF) have occurred over the last decades, but uncertainty remains about the conditions necessary to trigger these outbreaks. We use the basic reproduction number ( $R_0$ ) as a measure of RVF epidemic potential in northern Senegal, and map its value in two distinct ecosystems, namely the Ferlo and the Senegal River delta and valley. We consider three consecutive rainy seasons (July–November 2014, 2015 and 2016) and account for several vector and animal species. We parametrize our model with estimates of *Aedes vexans arabiensis*, *Culex poicilipes*, *Culex tritaeniorhynchus*, cattle, sheep and goat abundances. The impact of RVF virus introduction is assessed every week over northern Senegal. We highlight September as the period of highest epidemic potential in northern Senegal, resulting from distinct dynamics in the two study areas. Spatially, in the seasonal environment of the Ferlo, we observe that high-risk locations vary between years. We show that decreased vector densities do not greatly reduce  $R_0$  and that cattle immunity has a greater impact on reducing transmission than small ruminant immunity. The host preferences of vectors and the temperature-dependent time interval between their blood meals are crucial parameters needing further biological investigations.

### 1. Introduction

Vector-borne diseases (VBDs) represent a growing threat to animal and human health worldwide. They account for 17 % of all infectious diseases, affecting more than one billion people each year (World Health Organization (WHO), 2014). Their presence in livestock can dramatically impact food production locally and hamper exports (Davies and Martin, 2003). This burden mostly affects low-income countries and their socio-economic development (World Health Organization (WHO), 2014). In addition, climate change, along with increased human and livestock mobility, create opportunities for vectors and their pathogens to establish in new areas, as was the case for West Nile virus in the United States of America (Calisher, 2000). Developing efficient countermeasures against VBDs requires a good understanding of their

transmission dynamics. This remains a major challenge considering the complexity of the biological system formed by pathogens, hosts, vectors and their relation to the environment (Parham et al., 2015).

Rift Valley fever virus (RVFV, Bunyaviridae: *Phlebovirus*) is a zoonotic and vector-borne pathogen, present throughout Africa, in the Arabian Peninsula and in the South West Indian Ocean islands. Mosquitoes of the *Aedes* and *Culex* genus are the main vectors (Chevalier et al., 2010), some of which are suspected to transmit the virus transovarially (Linthicum et al., 1985). They transmit it to a variety of domestic host species, including cattle, goats, sheep and camels, causing storms of abortions and a high mortality in young animals (Pepin et al., 2010). Human infection can occur through mucous membrane exposure or inhalation of viral particles (Davies and Martin, 2003). Most cases are limited to mild ‘flu-like’ symptoms (Laughlin et al., 1979), but severe

\* Corresponding author at: INRAE, Oniris, BIOEPAR, 44300, Nantes, France.

E-mail addresses: [helene.cecilia@oniris-nantes.fr](mailto:helene.cecilia@oniris-nantes.fr), [helene.cecilia3@gmail.com](mailto:helene.cecilia3@gmail.com) (H. Cecilia), [raphaelle.metras@inserm.fr](mailto:raphaelle.metras@inserm.fr) (R. Métras), [agueyefall@yahoo.fr](mailto:agueyefall@yahoo.fr) (A.G. Fall), [moustaphalo@yahoo.fr](mailto:moustaphalo@yahoo.fr) (M.M. Lo), [renaud.lancelot@cirad.fr](mailto:renaud.lancelot@cirad.fr) (R. Lancelot), [pauline.ezanno@inrae.fr](mailto:pauline.ezanno@inrae.fr) (P. Ezanno).

<https://doi.org/10.1016/j.epidem.2020.100409>

Received 17 February 2020; Received in revised form 27 August 2020; Accepted 16 September 2020

Available online 21 October 2020

1755-4365/© 2020 The Authors.

Published by Elsevier B.V. This is an open access article under the CC BY-NC-ND license

(<http://creativecommons.org/licenses/by-nc-nd/4.0/>).

forms of the disease can be fatal. The case fatality rate is usually below 1 % (Madani et al., 2003) but tends to increase in recent outbreaks (Chevalier et al., 2010). Spillover into human population mainly concerns people working in close contact with animals such as pastoralists, butchers or veterinarians (Anyangu et al., 2010; Linthicum et al., 2016), but can be a concern for the general population, e.g. in a context of livestock slaughters during religious festivals (EMPRES, 2003; Lancelot et al., 2019). Vector-to-human transmission is possible but does not seem to be the major route of infection (Gerdes, 2004). Animal-to-animal transmission by direct contact seems possible but is not yet confirmed (Chevalier et al., 2010). Since 2015, RVF is part of the R&D Blueprint program of the World Health Organization (Mehand et al., 2018), a list of top emerging diseases likely to cause major epidemics, and for which few or no medical countermeasures exist.

Models are a powerful tool to explore pathogen transmission dynamics, and several approaches have already been used to answer questions about RVFV emergence and spread (Métras et al., 2011; Danzetta et al., 2016). Statistical models demonstrated an association between El Niño/Southern Oscillation phenomena and RVF occurrence in the Horn of Africa in 2007 (Anyamba et al., 2009), as well as the link between rainfall patterns and population dynamics of RVF vectors (Mondet et al., 2005). Network models highlighted factors influencing host mobility in regions affected by RVF (Apolloni et al., 2018; Kim et al., 2018; Belkhiria et al., 2019). The use of remote-sensing and geographic information systems (GIS) enabled the identification of landscape properties associated with RVF virus transmission (Tourre et al., 2009; Tran et al., 2016). However, prior to studying the transmission dynamics of a pathogen at large time- and spatial- scale, it is critical to understand the short-term consequences of its local introduction and in particular, its potential to trigger the onset of an epidemic.

The use of compartmental models together with the next generation matrix provides a way to estimate the basic reproduction number  $R_0$  and gain a deeper understanding of the underlying processes contributing to the epidemic potential (Hartemink et al., 2008).  $R_0$  represents the average number of secondary cases produced by one infected individual introduced in an entirely susceptible population over the course of its infectious period. Several mechanistic models have been proposed to formulate  $R_0$  for RVF (Gaff et al., 2007; Niu et al., 2012; Xue and Scoglio, 2013; Pedro et al., 2016), but they remain theoretical and have not been applied in a spatially-explicit way using validated input data. In addition,  $R_0$  is context-specific and studies mapping  $R_0$  in space and time using data on hosts and vectors were primarily conducted for RVF-free regions, such as the Netherlands (Fischer et al., 2013) or the United States of America (Barker et al., 2013). In regions with regular RVF outbreaks, such as the West African Sahel, modelling  $R_0$  could explain, upon a new introduction of the virus, what locally drives the rapid increase in RVF incidence and creates amplification hotspots.

Senegal and Mauritania have experienced several outbreaks since 1987. Most cases were reported in the Sahel region, more specifically in northern Senegal and southern Mauritania (Caminade et al., 2014; Sow et al., 2016). This region encompassing semi-arid to arid climate bridges the gap between the Sahara Desert and the tropical rainforests of equatorial Africa. In northern Senegal, RVF outbreaks have mainly been reported in two distinct ecosystems, along the Senegal River and in the Ferlo region. RVF epidemic potential is assumed to differ between these two study areas. Indeed, along the Senegal River, the availability of river water enabled the development of irrigated agriculture (Bruckmann, 2018), and therefore the continuous contact between vectors (mainly *Culex*) and hosts. In contrast, the Ferlo is much dryer. When the rainy season starts in July, temporary ponds are flooded. *Aedes* eggs, laid at the edges of ponds the year before, and which can resist desiccation, hatch and induce a rapid and massive emergence of adult mosquitoes (Ndione et al., 2008). In the meantime, vegetation grows and creates the suitable conditions for nomadic herds to stop along their transhumance pathway (Adriansen, 2008). Therefore, convergence of mosquitoes and

livestock, which are both capable of introducing the virus, create opportunities for RVF outbreaks.

Previous studies mapping RVF risk in West African Sahel overlapped climate anomalies and host densities, but they did not investigate the underlying mechanisms responsible for the disease outcome (Caminade et al., 2011, 2014). At very local scales, in particular around the village of Barkedji in the Ferlo region of Senegal, different approaches such as remote-sensing (Lacaux et al., 2007; Ndione et al., 2009) or statistical models (Bicout and Sabatier, 2004; Vignolles et al., 2009; Talla et al., 2016) were used. These studies focused on the link between landscape features (typically ponds, Soti et al., 2013; Bop et al., 2014) and vector abundance. Therefore, there is still a need for a mechanistic approach integrating all the major processes that may play a role in RVF epidemic potential.

The aim of the present paper is to map the epidemic potential of RVF virus in a Sahelian setting during the rainy season, comparing two different study areas, namely the Senegal River delta and valley, and the Ferlo. For this, we use an expression of  $R_0$  in a multi-species (2 hosts and 2 vectors) context, accounting for vector feeding preferences. We identify parameters varying in time and space as well as relevant data sources to map contact zones between hosts and vectors. Next, the epidemic potential is quantified in independent spatial units, assuming each week of the rainy season to be a possible date of introduction, assessed separately. We identify locations and introduction times with higher epidemic potential. We assess the role of vector densities and herd immunity to reduce  $R_0$ . Eventually, we test the robustness of our results through a sensitivity analysis.

## 2. Material and methods

We built a compartmental, mechanistic model of RVF virus (RVFV) transmission with 2 host and 2 vector populations (Fig. 1, Eqs. S.1–S.3). We only included mechanisms accurately occurring at the onset of a potential epidemic, locally, upon the introduction of the virus, resulting from the introduction of an infected host or an infected vector. The model was used to obtain the next-generation matrix. We derived the expression of the basic reproduction number  $R_0$  by using the method by van den Driessche and Watmough (2002), which averages the result of amplification following the two possible routes of virus introduction (infected host or infected vector, Supplementary Information 2). The value of  $R_0$  was computed across each area (pixel resolution 3.5 km<sup>2</sup>), and for weekly dates of virus introduction spanning three rainy seasons (July to November) of 2014, 2015, and 2016. These years corresponded to a period of evidenced RVFV circulation (Durand et al., 2020), along with the overlap of data source availability. Dates and location of RVFV introduction were assumed independent from each other. In addition, host infectious period is rather short (around a week) and temperatures did not strongly vary in our study area (interquartile range [29.1–31.4 °C], Fig. S.2) over the course of a vector lifetime (around a month). Thus, parameters were kept constant within each  $R_0$  computation (i.e. each date and location of introduction) for the whole duration of secondary case generation, but were updated at each new computation.

### 2.1. Model structure and assumptions

Vectors were modelled using susceptible ( $S_i$ ), latently infected ( $E_i$ ), and infectious ( $I_i$ ) health states,  $i \in \{1,4\}$ . In the Ferlo, vector species considered were *Aedes vexans arabiensis* (subscript 1) and *Culex poicilipes* (subscript 4). In the Senegal River delta and valley (SRDV), vector species considered were *Culex tritaeniorhynchus* (subscript 1) and *C. poicilipes* (subscript 4). This was based on previous entomological studies conducted in both areas (Diallo et al., 2011; Fall et al., 2011; Biteye et al., 2018). *Ae. v. arabiensis* and *C. poicilipes* are confirmed vectors of RVFV in Senegal (Fontenille et al., 1998; Diallo et al., 2000; Ndiaye et al., 2016). *C. tritaeniorhynchus* is highly abundant and was

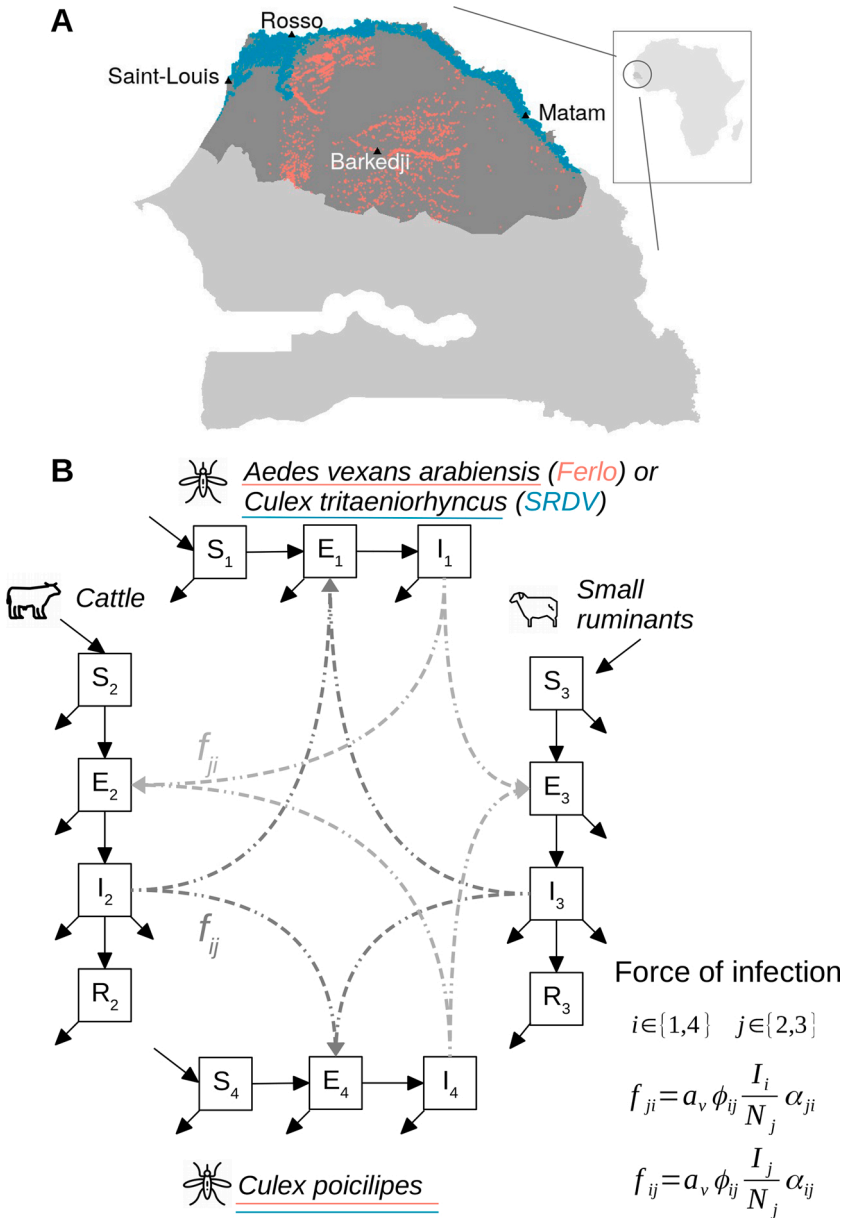


**Fig. 1. Study area and model diagram.** A – Study area, northern Senegal. Pixels highlighted correspond to locations with hosts and vectors at least once in the 3 rainy seasons, the color indicating the region and thus the vector species they contain. Ferlo (pink),  $n = 1702$ , Senegal River delta and valley (SRDV),  $n = 2676$ . B – Flow diagram of the RVFV mechanistic model used to obtain the next-generation matrix and derive the analytical formula of the basic reproduction number  $R_0$ . Formulas give the force of infection in host populations (from vectors)  $f_{ji}$  (light grey) and in vector populations (from hosts)  $f_{ij}$  (dark grey).

identified as a RVFV vector in the 2000 outbreak in Saudi Arabia (Jupp et al., 2002). In the model, vectors were assumed to become infected either after biting infectious cattle or small ruminants, but could not transmit the virus transovarially. Whilst limited evidence of vertical transmission of RVFV in mosquitoes is available (Linthicum et al., 1985), we assumed that this mechanism would be related to inter-annual patterns, rather than epidemic potential during a given rainy season (Lumley et al., 2017).

Host populations contained susceptible ( $S_j$ ), latently infected ( $E_j$ ), infectious ( $I_j$ ), and recovered (with immunity,  $R_j$ ) individuals,  $j \in \{2,3\}$ . They were stratified into cattle (subscript 2) and small ruminants (i.e. goats and sheep, subscript 3). Livestock could only be infected by the bites of infectious vectors. Animal-to-animal transmission by direct contact was here considered marginal compared to vector transmission, playing a minor role at the onset of a potential epidemic. Even though it might explain observed endemic patterns observed in unfavorable areas for mosquitoes (Nicolas et al., 2014), this transmission route has yet to be documented.

Mosquito biting rate, mortality and extrinsic incubation period (defined as the time between infection through a blood meal and virus

presence in the salivary glands) were assumed to be temperature-dependent for all vector species. In addition, we assumed that a proportion  $c_i$  of mosquito populations  $i$  could have double, partial, blood meals (Table 1, Supplementary Information 1.2). Transmission was modelled as reservoir frequency-dependent (Fig. 1, Eq. S.1), as defined by Wonham et al. (2006). In other words, an individual vector was considered to have a constant contact rate (biting rate + feeding preferences) with livestock populations regardless of surrounding densities, whereas an individual host had a contact rate with vectors dependent on the vector-to-host ratio in the area (Gubbins et al., 2008). This type of transmission function can induce unrealistically high  $R_0$  values when livestock densities are too low or vector densities are too high (Wonham et al., 2006). Therefore, for each introduction date, we removed pixels with vector-to-host ratio  $(N_1 + N_4) / (N_2 + N_3) > 1000$ . This threshold was chosen to significantly drop the highest values of  $R_0$  without removing too many points (Table S.1). The force of infection included the relative preference of vectors for both livestock populations ( $\pi_{ij}$ , Table 1) combined with relative abundance of hosts to compute the proportion of blood meals taken on each host population (parameter  $\phi_{ij}$ , Table 1). Parameter values and references are in Table 1, Supplementary

**Table 1**

Parameter values of the basic reproduction number  $R_0$  derived from the mechanistic RVF virus transmission model with two host and two vector populations. Durations are in days, rates in days<sup>-1</sup>. †: to the best of our knowledge. ECMWF: European Center for Medium Range Weather Forecasts.

Definition	Value	Source
<b>Vector populations</b>		
	subscripts $i \in \{1, 4\}$ $i = 1$ : <i>Ae. v. arabiensis</i> (Ferlo), <i>C. tritaeniorhynchus</i> (SRDV) $i = 4$ : <i>C. poicilipes</i>	
$N_i$	number of host-seeking female mosquitoes	Tran et al. (2019)
$a_i$	biting rate	$\frac{1 + c_i}{17\%}$
$c_i$	proportion of double blood meals	Ba et al. (2006)
$g_i(T)$	duration of gonotrophic cycle	$\frac{1}{(0.0173 \times (T - 9.6))}$
$1/\varepsilon_i$	extrinsic incubation period	$\frac{1}{(0.0071T - 0.1038)}$
$\phi_{ij}$	proportion of blood meals taken on host population $j$	$\frac{\pi_{ij}N_j}{\pi_{i2}N_2 + \pi_{i3}N_3}$ , $j \in \{2, 3\}$ , $\pi_{i2} + \pi_{i3} = 1$
$\pi_{ij}$	relative preference for host population $j$	0.843 for $j = 2$ , 0.157 for $j = 3$
$1/d_i$	vector lifespan	$\frac{1}{(0.000148T^2 - 0.00667T + 0.1)}$ $i = 1$ , Ferlo $\frac{1}{(0.000148T^2 - 0.00667T + 0.1) \times (1 - 0.016H)}$ $i = 1$ , SRDV, $i = 4$
<b>Host populations</b>		
$N_j$	Number of hosts	Gilbert et al. (2018)
$p_j$	proportion of immune individuals at disease-free equilibrium	0
$1/\varepsilon_j$	incubation period	2
$1/\gamma_j$	infectious period	6
$1/d_j$	Host natural lifespan	$8 \times 365$ , $j = 2$ $2400$ , $j = 3$
$\mu_j$	RVF-induced mortality rate	0.0176 for $j = 2$ , 0.0312 for $j = 3$
<b>Transmission</b>		
$\alpha_{ij}$	host-to-vector successful transmission probability	0.6
$\alpha_{ji}$	vector-to-host successful transmission probability	0.4
T	temperature (°C)	$(T_{min} + T_{max})/2$
H	relative humidity (%)	$100 \cdot \frac{\exp\left(\frac{17.27(T_{min} - 2)}{T_{min} - 2 + 237.3}\right)}{\exp\left(\frac{17.27T_{max}}{T_{max} + 237.3}\right)}$

information 1.2.

**2.2. Input data**

A schematic representation of data inclusion into our modelling framework, along with other parametrization aspects, can be found in Supplementary Information 1.2.

**2.2.1. Spatio-temporal data on vector abundance**

The vector abundance in space and time was derived from the predictions of a mechanistic model of mosquito population dynamics developed by Tran et al. (2019). This model provides the abundance of host-seeking female mosquitoes for the three vector species and the two regions of interest. Mosquito abundance is driven by rainfall, temperature, location of waterbodies, and the surface dynamics of ponds throughout the year. This model uses satellite-derived meteorological data and multispectral images to assess the habitat suitability for vectors. Tropical Applications of Meteorology using SATellite data (TAM-SAT) daily rainfall estimates are used (<http://www.tamsat.org.uk/cgi-bin/data/index.cgi>), along with the European Centre for Medium Range Weather Forecasts (ECMWF) 10-daily minimum and maximum temperatures (<https://confluence.ecmwf.int>). Water bodies are detected using cloud-free Sentinel 2 scenes (level 1-C, <https://earthexplorer.usgs.gov/>). Their filling dynamics is estimated with an existing hydrologic model (Soti et al., 2010). The predictions of this model have been validated against entomological data collected in several sites in our study area (Biteye et al., 2018). We used weekly mosquito abundance for three consecutive rainy seasons (July to November 2014, 2015 and

2016, downloaded from <https://doi.org/10.18167/DVN1/IQ2J1L>). Our spatial units were hexagonal pixels of 1 km radius ( $\approx 3.5\text{km}^2$ ) as in Tran et al. (2019).

**2.2.2. Spatial distribution of livestock**

For livestock host densities, we used the Gridded Livestock of the World database (GLW 3, downloaded from [https://dataverse.harvard.edu/dataverse/glw\\_3](https://dataverse.harvard.edu/dataverse/glw_3), Gilbert et al., 2018), which provides sub-national livestock distribution data for 2010, at a spatial resolution of 0, 083333° (approximately 10 km at the equator). We used the distributions of cattle and small ruminants (goats and sheep) based on Gilbert et al. (2018) dasymetric product, which disaggregates census data according to weights established by statistical models using high resolution spatial covariates (land use, climate, vegetation, topography, human presence). This dataset was downscaled to match Tran et al. (2019) model pixel size by homogeneously distributing animals in smaller space units. The GLW 3 dataset is an average snapshot and does not provide time series of animal densities.

**2.3. Analytical expression of the basic reproduction number**

$R_0$  was computed only for pixels in which both hosts and vectors were present. We considered the chosen spatial resolution large enough to neglect vector dispersal among pixels, in agreement with entomological studies conducted in the Ferlo and SRDV which show that vectors rarely disperse further than 1 km from ponds (Ba et al., 2005; Diallo et al., 2011; Fall et al., 2013). In addition, quantitative information on seasonal variations in livestock abundance at large scale was not

available. As a result, we considered that pixels were disconnected and that animal densities remained constant.

$R_0$  is the dominant eigenvalue of the next generation matrix of our model (Eqs. 1–5). The details of its computation can be found in Supplementary Information 2. Compared to the expression derived by Turner et al. (2013) for bluetongue, we accounted for an incubation period, a natural mortality rate and a proportion of immune individuals at the disease-free equilibrium in livestock hosts. We also considered transmission probabilities (vector-to-host and host-to-vector) to be host-population specific and not only vector-population specific.

$$R_0 = \sqrt{\frac{1}{2} \left[ (R_{11} + R_{44}) + \sqrt{(R_{11} + R_{44})^2 - 4(R_{11}R_{44} - R_{14}R_{41})} \right]} \quad (1)$$

$$R_{11} = \frac{\varepsilon_1}{(d_1 + \varepsilon_1)d_1} \times \left( \frac{\frac{N_1}{N_2} \varepsilon_2 \alpha_{21} \alpha_{12} (\phi_{12} a_1)^2}{(d_2 + \varepsilon_2)(d_2 + \gamma_2 + \mu_2)} (1 - p_2) + \frac{\frac{N_1}{N_3} \varepsilon_3 \alpha_{31} \alpha_{13} (\phi_{13} a_1)^2}{(d_3 + \varepsilon_3)(d_3 + \gamma_3 + \mu_3)} (1 - p_3) \right) \quad (2)$$

$$R_{44} = \frac{\varepsilon_4}{(d_4 + \varepsilon_4)d_4} \times \left( \frac{\frac{N_4}{N_2} \varepsilon_2 \alpha_{24} \alpha_{42} (\phi_{42} a_4)^2}{(d_2 + \varepsilon_2)(d_2 + \gamma_2 + \mu_2)} (1 - p_2) + \frac{\frac{N_4}{N_3} \varepsilon_3 \alpha_{34} \alpha_{43} (\phi_{43} a_4)^2}{(d_3 + \varepsilon_3)(d_3 + \gamma_3 + \mu_3)} (1 - p_3) \right) \quad (3)$$

$$R_{14} = \frac{\varepsilon_4}{(d_4 + \varepsilon_4)d_4} \times \left( \frac{\frac{N_1}{N_2} \varepsilon_2 \alpha_{21} \alpha_{42} \phi_{12} \phi_{42} a_1 a_4}{(d_2 + \varepsilon_2)(d_2 + \gamma_2 + \mu_2)} (1 - p_2) + \frac{\frac{N_1}{N_3} \varepsilon_3 \alpha_{31} \alpha_{43} \phi_{13} \phi_{43} a_1 a_4}{(d_3 + \varepsilon_3)(d_3 + \gamma_3 + \mu_3)} (1 - p_3) \right) \quad (4)$$

$$R_{41} = \frac{\varepsilon_1}{(d_1 + \varepsilon_1)d_1} \times \left( \frac{\frac{N_4}{N_2} \varepsilon_2 \alpha_{24} \alpha_{12} \phi_{12} \phi_{42} a_1 a_4}{(d_2 + \varepsilon_2)(d_2 + \gamma_2 + \mu_2)} (1 - p_2) + \frac{\frac{N_4}{N_3} \varepsilon_3 \alpha_{34} \alpha_{13} \phi_{13} \phi_{43} a_1 a_4}{(d_3 + \varepsilon_3)(d_3 + \gamma_3 + \mu_3)} (1 - p_3) \right) \quad (5)$$

#### 2.4. Spatio-temporal pattern of $R_0$

First, we identified dates and locations of RVFV introduction with high epidemic potential. For each area under study, we examined which

introduction date resulted in the highest number of pixels with  $R_0 > 1$ , each season. For clarity hereinafter,  $pxl_t$  is the number of pixels with  $R_0 > 1$  at a given introduction date. For each season, we computed an  $R_0$  threshold corresponding to the value of the third quartile, independently of the study area and date of introduction within a given season,  $Q_{3, year}$ . We mapped pixels for which  $R_0 > Q_{3, year}$  at least once within the season; we also recorded the number of times (i.e. weeks) it happened during the season. This was made to highlight high-risk areas. For two specific locations, namely Rosso in SRDV and Barkedji in the Ferlo, we normalized  $R_0$  values (dividing them by the maximum  $R_0$  value of the season) in order to compare seasonal patterns without focusing on absolute  $R_0$  values.

We then investigated the role of vector and host populations on the epidemic potential. We inspected how the relative abundances of vector

populations changed over time within pixels with  $R_0 > 1$ . We focused on three specific dates of virus introduction in Barkedji, in 2015. This was done to specifically understand whether lower vector densities (without any modification of their lifespan parameters) could significantly decrease  $R_0$  values. We also aimed to identify which species had the most impact on  $R_0$  when decreased, and whether this was influenced by the vector composition, quantified with  $\log_{10}(N_{C. poicillipes}/N_{Ae. v. arabiensis})$ . The first date we chose corresponded to the maximum  $pxl_t$  in the Ferlo over the season. The other two dates both induced  $R_0 > 1$  in Barkedji but exhibited diametrically opposed vector composition. Similarly, we assessed the effect of herd immunity, which could be acquired either through vaccination or previous exposure to RVFV, on the number of pixels with  $R_0 > Q_{3, year}$  per study area and season.

Finally, we performed a variance-based global sensitivity analysis

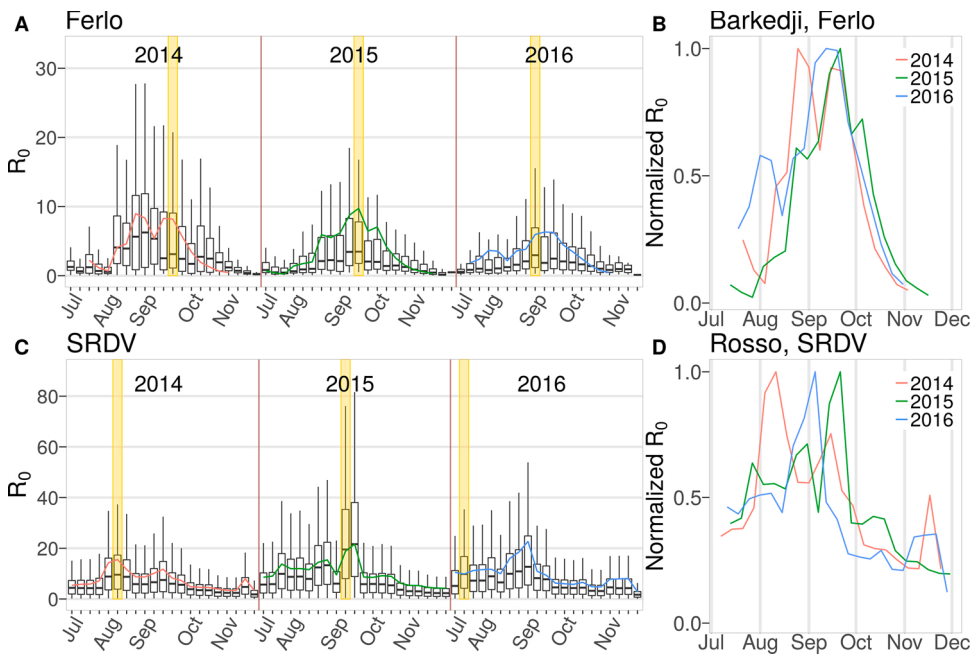


**Fig. 2. September is the month of highest RVFV epidemic potential in northern Senegal.** A, C:  $R_0$  distribution by introduction date for 3 consecutive rainy seasons, spatially aggregated by region (A: Ferlo, C: SRDV).  $R_0$  values are computed independently for each introduction date, assuming constant parameters over the course of the secondary case generation. Colored lines show the temporal patterns for Barkedji (Ferlo) and Rosso (SRDV). Yellow bands highlight the introduction dates inducing the highest number of pixels with  $R_0 > 1$ , for each rainy season. Northern Senegal (Ferlo + SRDV): 2014-09-22,  $n = 3557$ , 2015-09-14,  $n = 3944$ , 2016-09-05,  $n = 3411$ . Ferlo: 2014-09-22,  $n = 1313$ , 2015-09-21,  $n = 1527$ , 2016-09-05,  $n = 1022$ . SRDV: 2014-08-11,  $n = 2352$ , 2015-09-14,  $n = 2482$ , 2016-07-18,  $n = 2397$ . The median  $R_0$  value is 1.51 in the Ferlo, 4.95 in SRDV. B, D: Comparison of yearly  $R_0$  pattern for Barkedji and Rosso. Values are normalized by the maximum of each rainy season. In the boxplots, box boundaries indicate the 25th (bottom) and 75th (top) percentiles. The line within the box marks the median. Whiskers above and below the box indicate the 10th and 90th percentiles. Outliers outside the 10th and 90th percentiles are not shown to ease figure reading. (For interpretation of the references to colour in this figure legend, the reader is referred to the web version of this article).

using a Fourier Amplitude Sensitivity Testing (FAST, Saltelli et al., 2008). This method was used to quantify first order effects of parameters but also interactions between parameters varying simultaneously, which is not possible with “one-at-a-time” sensitivity analyses (Saltelli et al., 2019). Parameters varied within a 10 % range using scaling factors (reference value of 1). A given set (scenario) of scaling factors was applied to all  $R_0$  computations of a given study area and rainy season, to maintain the spatial heterogeneity as well as the relative temporal dynamics of vector densities and temperature-dependent parameters. Temperature-dependent function formulas were kept, and temperature was not varied. We sampled 10,000 values per parameter. We tested whether introduction dates and locations with high epidemic potential were robust to these parameter variations.

### 3. Results

Overall, there are 2.5 times more  $R_0$  values computed in the Senegal River delta and valley (SRDV) than in the Ferlo. Initially, input data covers a total surface of  $\sim 15,500 \text{ km}^2$ , comprised of 4419 independent pixels (1702 in the Ferlo, 2717 in SRDV) containing both hosts and vectors at least once in the 63 introduction dates (21 per season) studied. Over the 235,449 possible  $R_0$  computations, 3.7 % are discarded because the local vector-to-host ratio is too high (Supplementary Information 3). This mainly affects SRDV, where 41 pixels are entirely removed from the study because their ratio never goes below the chosen threshold during the 3 rainy seasons (Supplementary Information 3). We end up with a stable surface where  $R_0$  is computed per time step in SRDV (between 90 % and 100 % of the possible surface available in the data), whereas this proportion largely varies within a season in the Ferlo (from 0.1 % to 100 %). In addition, the number of pixels with  $R_0 > 1$  per introduction date ( $pxl_I$ ) never goes below 1767 for any date of introduction in SRDV (always  $> 66$  % of  $R_0$  computations in this study area), and reaches its absolute maximum on 2015-09-14 ( $n = 2482$ ). In the Ferlo,  $pxl_I$  can go from 0 for introductions in November (2014-11-24, 2015-11-30, 2016-11-21, and 2016-11-28) to 1527 (93 % of  $R_0$  computations) on 2015-09-21.

September is the month of highest RVF epidemic potential in northern Senegal for the three studied rainy seasons. The two study areas exhibit different epidemic potential temporal patterns. In the Ferlo, the epidemic potential is seasonal (median  $R_0 = 1.51$ ), and September is systematically highlighted as the period of highest RVFV epidemic potential (Fig. 2A) despite some variability in temperature and mosquito abundances between years (Figs. S.2, S.4). In the Senegal River delta and valley, the epidemic potential is high throughout the rainy seasons (median  $R_0 = 4.95$ ), with overall 90 % of  $R_0$  values above 2 in the whole studied period. The temporal pattern in two specific locations is similar to the one observed at the respective regional scale (Fig. 2). The pixel closest to Rosso has its  $R_0 > 1$  for every possible date of introduction over the three consecutive rainy seasons, which is not the case for the pixel closest to Barkedji (Fig. 2A, C, colored lines).

In northern Senegal, for the three years studied, the introduction date of highest epidemic potential is reached earlier every year (2014-09-22,  $pxl_I = 3557$ , 2015-09-14,  $pxl_I = 3944$ , 2016-09-05,  $pxl_I = 3411$ ). This trend is robust to the parameter variations tested in our sensitivity analysis, as well as the dates of maximum  $pxl_I$  within each study area (Table S.9).

The map of areas with highest epidemic potential varies across the three rainy seasons of 2014, 2015 and 2016 (Fig. 3). In the Ferlo, the south-west of Barkedji exhibits a high epidemic potential in 2014 but not in 2015–2016. Conversely, the north-east of Barkedji exhibits a high epidemic potential in 2015–2016 but not in 2014. In SRDV, around Matam, there is a strong density of pixels with  $R_0$  above the third quartile of the season ( $Q_{3, \text{year}}$ ) in 2015–2016 but less so in 2014. Overall, SRDV accounts for a larger proportion of pixels with  $R_0 > Q_{3, \text{year}}$  than the Ferlo, every season (at least three times more, Table S.8). In addition, the frequency of these high  $R_0$  values is lower per pixel in the Ferlo than in SRDV, every season (Fig. 3, pixels ranging from green to yellow, Table S.8). These results are also robust to parameter variations (Fig. S.9).

In the Ferlo, *Ae. v. arabiensis* tends to be the most abundant vector population within pixels with  $R_0 > 1$  at the beginning of the rainy season, while *C. poicilipes* is the most abundant later in the season (Figs. 4A,

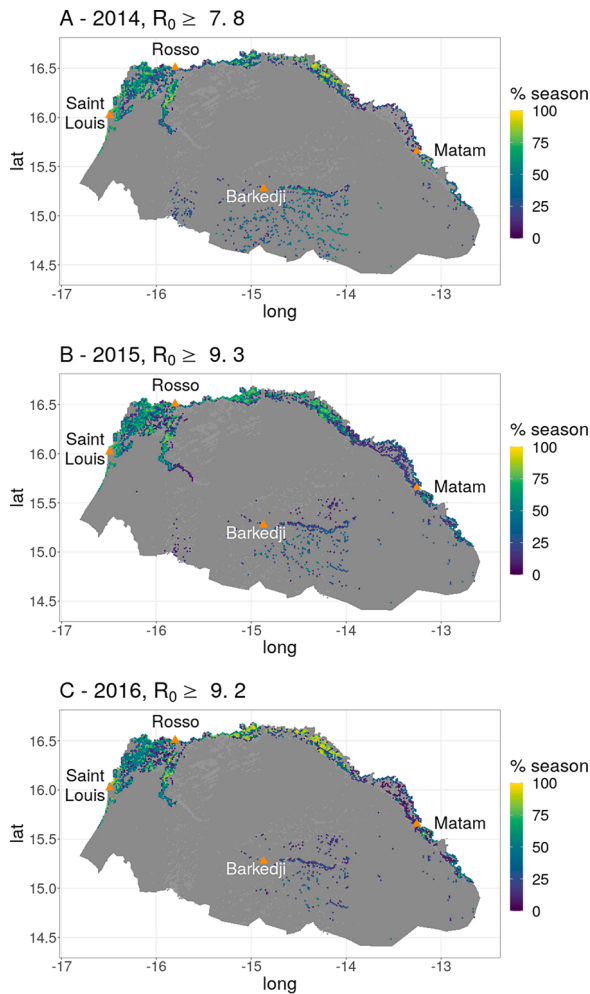


**Fig. 3.** Zones of high RVF epidemic potential change between rainy seasons. Map of northern Senegal showing pixels with  $R_0 > Q_{3, \text{year}}$  (third quartile of  $R_0$  values) at least once in the season. Pixels are colored by percentage of season spent above the threshold (1 to 21 weeks). Orange points are important locations to ease figure reading. Light grey pixels are other pixels where  $R_0$  is computed during the season.

S.4). Nonetheless, the vector composition shows a large variability between pixels for a same date of introduction. For instance, on October 12th 2015, minimum and maximum relative abundances are  $\log_{10}(N_{C. poicilipes}/N_{Ae. v. arabiensis}) = -3.74$  and  $\log_{10}(N_{C. poicilipes}/N_{Ae. v. arabiensis}) = 4.44$  respectively (Fig. 4A). In addition, inspecting dates resulting in the highest  $pxl_1$ , *Ae. v. arabiensis* is on average the most abundant in pixels with  $R_0 > 1$  in 2014 (2014-09-22, Fig. S.4), while *C. poicilipes* is on average the most abundant in pixels with  $R_0 > 1$  in 2015 and 2016 (2015-09-21, 2016-09-05, Figs. 4A, S.4). In Barkedji, diametrically opposed vector compositions can induce  $R_0 > 1$ , such as August 24th 2015 when  $\log_{10}(N_{C. poicilipes}/N_{Ae. v. arabiensis}) = -1.08$  and October 12th 2015 when  $\log_{10}(N_{C. poicilipes}/N_{Ae. v. arabiensis}) = 1.08$  (Fig. 4A, B, D). In SRDV, *C. tritaeniorhynchus* is always the most abundant species in every pixel with  $R_0 > 1$ , but the gap between population densities is less important than in the Ferlo (Fig. S.4).

Decreased vector densities do not greatly reduce  $R_0$  values of at-risk pixels below 1 (Fig. 4). In Barkedji, this is observed regardless of RVFV introduction date and whichever species is the most abundant. In addition, the vector composition is not an indicator of which population, if decreased, will more strongly affect  $R_0$ . Indeed, for RVFV introductions on August 24th 2015 and September 21st 2015, decreasing the density of the most abundant vector population has the strongest effect on  $R_0$  value (Fig. 4A-C). This is not observed on October 12th

2015, when *C. poicilipes* are more numerous than *Ae. v. arabiensis* in Barkedji (Fig. 4A, third red star), but decreasing the density of *Ae. v. arabiensis* has the strongest impact on  $R_0$  (Fig. 4D).

In both study areas, an increase in the proportion of immune cattle decreases the number of pixels with high  $R_0$  values ( $R_0 > Q_{3, \text{year}}$ ) more effectively than increasing the proportion of immune small ruminants (Figs. 5B, C, S.5). In most pixels ( $4302/4367 = 98.5\%$ ), the number of small ruminants is higher than the number of cattle (Fig. 5A). However, the difference in host populations sizes is smaller in SRDV than in the Ferlo. Indeed, there are on average 7.5 times more small ruminants than cattle in the Ferlo, and only twice more in SRDV. This is related to the presence of both very low cattle densities and very high small ruminant densities in the Ferlo, while the range of SRDV host distributions is narrower (Fig. S.3). As a consequence, cattle are in fewer numbers than small ruminants while being the preferred host of all vector species studied (Table 1, Supplementary information 1.2). Therefore, they are more likely to get bitten more than once. These bites, provided they result in successful transmission (first to the host, then to a vector), can strongly contribute to RVF epidemic potential.

Finally, the feeding preferences and the gonotrophic cycle duration of the most abundant vector species are the most influential parameters on the epidemic potential in the Ferlo (Figs. 6, S.6). In 2015, the first order effects of these parameters explain respectively 47 % and 19 % of the variance observed in the maximum  $pxl_1$  of the season. In SRDV, the maximum  $pxl_1$  does not vary much in our sensitivity analysis (maximum 2.4 % from the reference value in 2016, Fig. S.7), because it quickly reaches the total number of pixels where  $R_0$  is computed for the study area. It is nonetheless influenced by the same parameters as highlighted for the Ferlo (Fig. S.7). Specifically, the more the feeding preference of the most abundant vector population is skewed towards cattle, and the more often these vectors have to take a new blood meal, the higher  $pxl_1$ .

#### 4. Discussion

The results of our analyses show that an introduction of Rift Valley fever virus in September has the potential to trigger an epidemic almost everywhere in northern Senegal. In the Ferlo region, there is a clear seasonality of the epidemic potential, and the most at-risk ponds change between rainy seasons. In contrast, but as expected, the Senegal River delta and valley contains areas with high epidemic potential during most of the rainy season, as it is a persistent conducive vector habitat. In addition, the period of highest epidemic potential tends to be reached earlier each year. This trend deserves to be investigated further once data becomes available. These results are robust to parameter variations tested in our sensitivity analysis, following a global variance-based approach most appropriate for models with nonlinearities and interactions (Saltelli et al., 2019).

Our work is applied to Senegal, western Africa, at a larger scale than most of previous published RVF works conducted here. A previous study produced a spatial risk assessment of RVF in Senegal, at the country-level (Clements et al., 2007), using statistical methods on serology data. However, serological data points are scarce in the Ferlo region, while we did show that this region is periodically suitable for foci of infection. By using a mechanistic approach instead of a statistical one, and integrating the most trustworthy sources of input data, we build a new step towards a better understanding of the spatio-temporal dynamics of RVF in a Sahelian setting. In the absence of validation data regarding the time, location, and number of cases, the current study is not meant to directly inform decision-makers.

We provide the first mapping of RVF epidemic potential in the West African Sahel using the basic reproduction number. We achieve better spatial and temporal resolutions than previous studies in RVF-free regions (Barker et al., 2013; Fischer et al., 2013), which was made possible by the use of satellite Sentinel 2 images by Tran et al. (2019) along with ground truth validation data and a precise knowledge of temporary ponds filling dynamics. However, host densities, which do not stand out

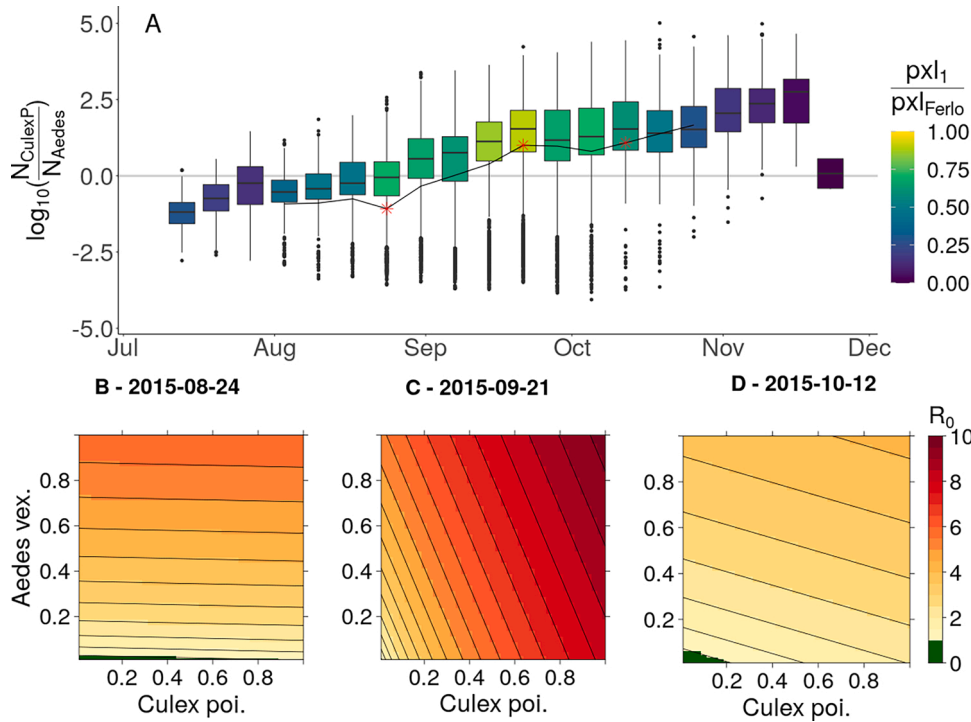


**Fig. 4. Decreased vector densities do not greatly reduce RVF epidemic potential in at-risk locations.** Example of Ferlo 2015. A: Relative abundance of vector populations  $\log_{10}(N_{C. poicillipes}/N_{Ae. v. arabiensis})$  within pixels having  $R_0 > 1$  over time. Light grey line indicates equal densities. For boxplots, see legend of Fig. 2. Outliers are shown. Colors inside boxplots indicate the number of pixels with  $R_0 > 1$  ( $pxl_1$ , min 4, max 1527) at each introduction date, normalized by the total number of pixels in the Ferlo (1702). Black line corresponds to the particular value of the ratio in Barkedji, for introduction dates inducing  $R_0 > 1$ . Stars are positioned at introduction dates 2015-08-24, 2015-09-21 and 2015-10-12. 2015-09-21 corresponds to the maximum  $pxl_1$  in the Ferlo this season. The other two dates both induce  $R_0 > 1$  in Barkedji but exhibit diametrically opposed vector composition. B-D: Variation of  $R_0$  in Barkedji when decreasing vector densities, for 3 different dates of introduction. Axes represent the proportion of initial vector density applied for the  $R_0$  computation; the reference is at the top right corner (1,1).

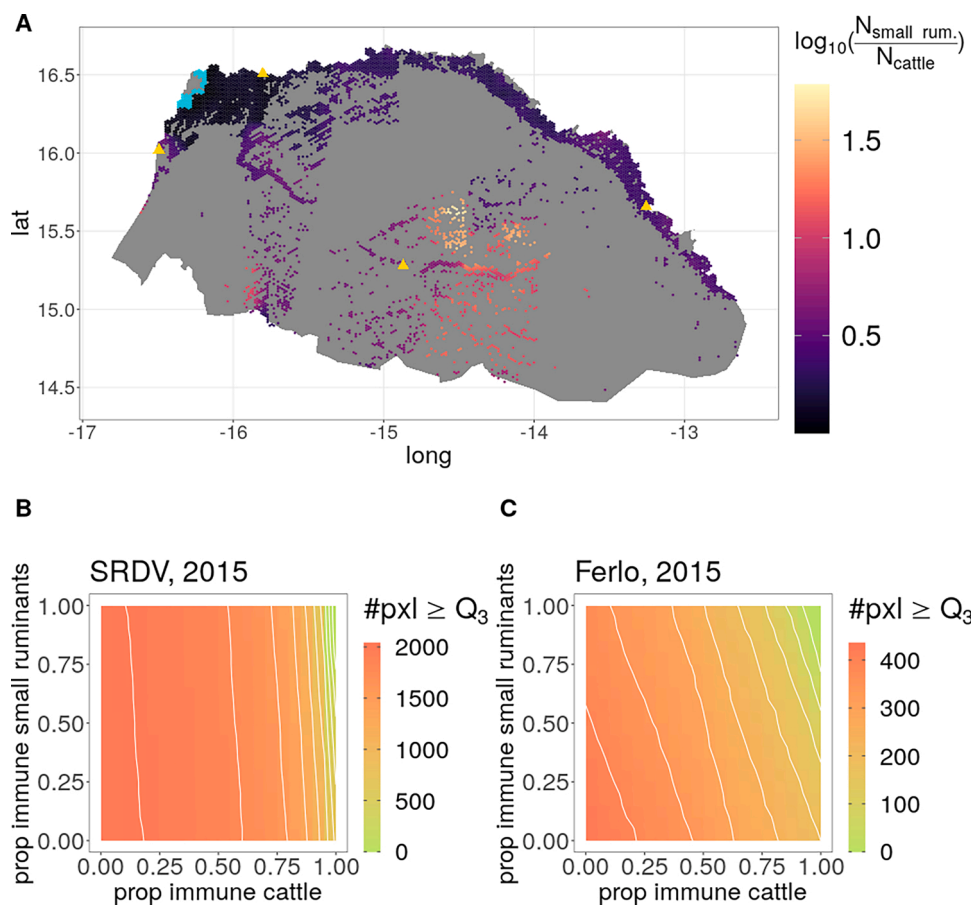


**Fig. 5. In both study areas, an increase in the proportion of immune cattle decreases the number of pixels with high  $R_0$  values ( $R_0 > Q_3, year$ ) more effectively than increasing the proportion of immune small ruminants.** A - Map of relative densities of hosts  $\log_{10}(N_{small\ ruminants}/N_{cattle})$  within pixels of our study area. Blue pixels have more cattle than small ruminants, the biggest difference being  $\log_{10}(N_{small\ ruminants}/N_{cattle}) = -0.08$ . B-C - Effect of increasing host immunity on the number of pixels with  $R_0 > Q_3, 2015$  by study area (B: SRDV, C: Ferlo). Axis represents the proportion of immune hosts applied for the  $R_0$  computation. The reference is the absence of herd immunity (0,0) in the bottom left corner. (For interpretation of the references to colour in this figure legend, the reader is referred to the web version of this article).

in our sensitivity analysis, may vary beyond the range presently allowed. Indeed, their temporal dynamics, mostly driven by animal mobility, is not incorporated into GLW 3 data, and might affect the

population-specific contact rate with vectors and therefore  $R_0$  values. Remote-sensing methods are considered a promising tool to measure human mobility (Bharti and Tatem, 2018), but we also need qualitative



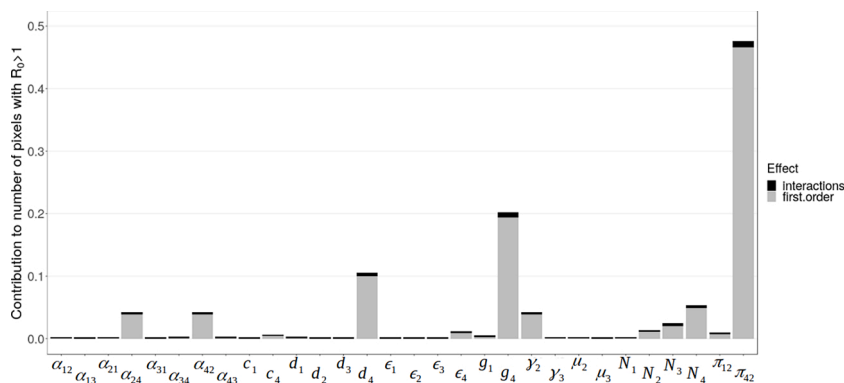


**Fig. 6.** The feeding preferences and the gonotrophic cycle duration of the most abundant vector species are the most influential parameters on the epidemic potential at the regional scale. Example of Ferlo, 2015. Results of the FAST sensitivity analysis showing contribution of model parameters to the maximum number of pixels with  $R_0 > 1$  ( $pxl_1$ ) in the season. Sensitivity indices for principal effect in grey and for interactions in black. Definition and reference values of parameters can be found in Table 1. The introduction date inducing the highest  $pxl_1$  during the 2015 rainy season is 09-21 for 299,999 scenarios and 09-14 for one scenario (Table S.9). At these dates, *C. poicilipes* is on average the most abundant vector population in the Ferlo within pixels with  $R_0 > 1$  (Fig. S.4).

data on factors guiding decisions of nomadic herders in order to include animal mobility in a mechanistic way (Apolloni et al., 2018; Belkhiria et al., 2019). Future work could expand our framework to longer periods of time, provided host and vector densities can be estimated, as was the case in a recent study using the same entomological model as we did, in a more constrained area (Durand et al., 2020).

The mechanistic approach used in this paper is the best suited to describe the complexity of RVF epidemic potential in our study region. Indeed, neither host nor vector densities alone are sufficient to predict the local epidemic potential, contrary to what was implied by previous mappings and statistical studies (Bicout and Sabatier, 2004; Caminade et al., 2011). It is actually the process of blood feeding, during which host and vector populations interact, which should accurately be described to achieve the most reliable estimates of RVF epidemic potential. We account for the influence of temperature in our model, which is known to strongly influence the risk of vector-borne diseases transmission (Kamiya et al., 2020; Mordecai et al., 2017, 2019). Important changes in temperature along with rainfall are expected in the future, but simulating the consequences of such changes is beyond the scope of this study. The adequate contact rate, an aggregated parameter used in previous models (Gaff et al., 2007; Mpeshe et al., 2014), is decomposed here to assess the importance of each of its components, as in Turner et al. (2013). Based on our sensitivity analysis, we recommend that future biological investigations focus on the feeding preferences of vectors and the duration of their gonotrophic cycle, in relation with temperature.

The inclusion of two host and two vector populations provides new insights on RVF epidemic potential, and this structure should be kept for future models studying RVF in the region. We show that decreased vector densities are not sufficient to limit the epidemic potential of RVF, regardless of the introduction date considered. Indeed, vector abundances are not always a good predictor of RVF epidemic potential, with high  $R_0$  values sometimes driven by the least abundant vector population. Moreover, cattle contribute strongly to RVF transmission and their immune status is likely to influence the epidemic potential at the regional scale. Favoring vaccination of cattle over small ruminants is not what is usually done in the field. Veterinary services, along with herders, tend to promote small ruminant vaccination as they are more likely to die from the disease and thus need more protection (Sow et al., 2016). The importance of small ruminant trade, particularly around the Tabaski festival, might also justify this approach (Lancelot et al., 2019). Operational decisions regarding targeted vaccination campaigns should therefore consider the potential benefits of cattle immunity at the population scale.

In the present study, we provide a better understanding of conditions which could trigger the onset of an epidemic. However, this should be interpreted with caution, and should not be considered as an indicator of epidemic size. Indeed, multiple introductions or sudden unfavorable conditions might lead to diseases persisting with  $R_0 < 1$  or dying out with  $R_0 > 1$  (Li et al., 2011). In addition, our results could be used as

initial conditions for a stochastic mechanistic model of spatio-temporal transmission, which would include processes underlying epidemic dynamic after RVFV introduction, such as animal mobility. Such a model would benefit from an increased availability of epidemiological data for validation and parametrization, which are necessary to unravel the underlying mechanisms driving the spatio-temporal dynamics of RVF in the West African Sahel.

#### Data and code accessibility

Input data and scripts are available online: <https://sourcesup.renatech.fr/projects/rvf-r0-senegal/>

#### Funding

This work was part of the FORESEE project funded by INRAE metaprogram GISA (Integrated Management of Animal Health). HC was funded by INRAE, Région Pays de la Loire, CIRAD.

#### CRediT authorship contribution statement

**Hélène Cecilia:** Conceptualization, Data curation, Formal analysis, Funding acquisition, Methodology, Software, Validation, Visualization, Writing - original draft, Writing - review & editing. **Raphaëlle Métras:** Conceptualization, Methodology, Supervision, Visualization, Writing - original draft, Writing - review & editing. **Assane Gueye Fall:** Resources, Writing - review & editing. **Modou Moustapha Lo:** Resources, Writing - review & editing. **Renaud Lancelot:** Conceptualization, Funding acquisition, Project administration, Supervision, Writing - review & editing. **Pauline Ezanno:** Conceptualization, Funding acquisition, Methodology, Project administration, Resources, Supervision, Validation, Visualization, Writing - original draft, Writing - review & editing.

#### Declaration of Competing Interest

The authors declare no conflict of interest.

#### Acknowledgments

We thank Cyril Caminade, Véronique Chevalier, Benoît Durand and Maxime Ratinier for helpful discussions. We thank Annelise Tran for providing input data and help for its use. We are grateful to the INRAE MIGALE bioinformatics facility (MIGALE, INRAE, 2020. Migale bioinformatics Facility, doi: 10.15454/1.5572390655343293E12) for providing computing and storage resources.

#### Appendix A. Supplementary data

Supplementary material related to this article can be found, in the

online version, at doi:<https://doi.org/10.1016/j.epidem.2020.100409>.

## References

- Adriansen, H.K., 2008. Understanding pastoral mobility: the case of Senegalese Fulani. *Geogr. J.* 174 (3), 17.
- Anyamba, A., Chretien, J.-P., Small, J., Tucker, C.J., Formenty, P.B., Richardson, J.H., Britch, S.C., Schnabel, D.C., Erickson, R.L., Linthicum, K.J., 2009. Prediction of a Rift Valley fever outbreak. *Proc. Natl. Acad. Sci. U. S. A.* 106 (3), 955–959. <https://doi.org/10.1073/pnas.0806490106>.
- Anyangu, A.S., Gould, L.H., Sharif, S.K., Nguku, P.M., Omolo, J.O., Mutonga, D., Rao, C. Y., Lederman, E.R., Schnabel, D., Paweska, J.T., Katz, M., Hightower, A., Njenga, M. K., Feikin, D.R., Breiman, R.F., 2010. Risk factors for severe Rift Valley fever infection in Kenya, 2007. *Am. J. Trop. Med. Hyg.* 83, 14–21. <https://doi.org/10.4269/ajtmh.2010.09-0293>.
- Apolloni, A., Nicolas, G., Coste, C., EL Mamy, A.B., Yahya, B., EL Arbi, A.S., Gueya, M.B., Baba, D., Gilbert, M., Lancelot, R., 2018. Towards the description of livestock mobility in Sahelian Africa: some results from a survey in Mauritania. *PLoS One* 13 (1). <https://doi.org/10.1371/journal.pone.0191565> e0191565.
- Ba, Y., Diallo, D., Kebe, C.M.F., Dia, I., Diallo, M., 2005. Aspects of bioecology of two Rift Valley fever virus vectors in Senegal (West Africa): *Aedes vexans* and *Culex poicilipes* (Diptera: Culicidae). *J. Med. Entomol.* 42 (5), 12.
- Ba, Y., Diallo, D., Dia, I., Diallo, M., 2006. Comportement trophique des vecteurs du virus de la fièvre de la vallée du Rift au Sénégal : implications dans l'épidémiologie de la maladie. *Bull. Soc. Pathol. Exot.* 99 (4), 283–289.
- Barker, C.M., Niu, T., Reisen, W.K., Hartley, D.M., 2013. Data-driven modeling to assess receptivity for Rift Valley fever virus. *PLoS Negl. Trop. Dis.* 7 (11), e2515. <https://doi.org/10.1371/journal.pntd.0002515>.
- Belkhiria, J., Lo, M.M., Sow, F., Martínez-López, B., Chevalier, V., 2019. Application of exponential random graph models to determine nomadic herders' movements in Senegal. *Transbound. Emerg. Dis.* 66, 1642–1652. <https://doi.org/10.1111/tbed.13198>.
- Bharti, N., Tatem, A.J., 2018. Fluctuations in anthropogenic nighttime lights from satellite imagery for five cities in Niger and Nigeria. *Sci. Data* 5, 180256. <https://doi.org/10.1038/sdata.2018.256>.
- Bicot, D.J., Sabatier, P., 2004. Mapping Rift Valley fever vectors and prevalence using rainfall variations. *Vector Borne Zoonotic Dis.* 4 (1), 33–42. <https://doi.org/10.1089/153036604773082979>.
- Bird, B.H., Ksiazek, T.G., Nichol, S.T., MacLachlan, N.J., 2009. Rift Valley fever virus. *J. Am. Vet. Med. Assoc.* 234 (7), 883–893.
- Biteye, B., Fall, A.G., Ciss, M., Seck, M.T., Apolloni, A., Fall, M., Tran, A., Gimonneau, G., 2018. Ecological distribution and population dynamics of Rift Valley fever virus mosquito vectors (Diptera, Culicidae) in Senegal. *Parasit. Vectors* 11 (1), 27. <https://doi.org/10.1186/s13071-017-2591-9>.
- Bop, M., Amadou, A., Seidou, O., Kèbè, C.M.F., Ndione, J.A., Sambou, S., Sanda, I.S., 2014. Modeling the hydrological dynamic of the breeding water bodies in Barkedji's zone. *J. Water Resource Prot.* 06 (08), 741–755. <https://doi.org/10.4236/jwarp.2014.68071>.
- Bruckmann, L., 2018. Crue et développement rural dans la vallée du Sénégal : entre marginalisation et résilience. *Belgeo* 2. <https://doi.org/10.4000/belgeo.23158>.
- Calisher, C.H., 2000. West Nile virus in the new world: appearance, persistence, and adaptation to a new ecniche—an opportunity taken. *Viral Immunol.* 13 (4), 411–414. <https://doi.org/10.1089/vim.2000.13.411>.
- Caminade, C., Ndione, J.A., Kebe, C.M.F., Jones, A.E., Danuor, S., Tay, S., Tourre, Y.M., Lacaux, J.-P., Vignolles, C., Duchemin, J.B., Jeanne, I., Morse, A.P., 2011. Mapping Rift Valley fever and malaria risk over West Africa using climatic indicators. *Atmos. Sci. Lett.* 12 (1), 96–103. <https://doi.org/10.1002/asl.296>.
- Caminade, C., Ndione, J., Diallo, M., MacLeod, D., Faye, O., Ba, Y., Dia, I., Morse, A., 2014. Rift Valley fever outbreaks in Mauritania and related environmental conditions. *Int. J. Environ. Res. Public Health* 11 (1), 903–918. <https://doi.org/10.3390/ijerph110100903>.
- Cavalerie, L., Charron, M.V.P., Ezanno, P., Dommergues, L., Zumbo, B., Cardinale, E., 2015. A stochastic model to study Rift Valley fever persistence with different seasonal patterns of vector abundance: new insights on the endemicity in the tropical island of Mayotte. *PLoS One* 10 (7). <https://doi.org/10.1371/journal.pone.0130838> e0130838.
- Chevalier, V., Pépin, M., Plée, L., Lancelot, R., 2010. Rift Valley fever - a threat for Europe? *Clin. Microbiol. Infect.* 19 (8), 705–708. <https://doi.org/10.1111/1469-0691.12163>.
- Clements, A.C., Pfeiffer, D.U., Martin, V., Pittiglio, C., Best, N., Thiongane, Y., 2007. Spatial risk assessment of rift valley fever in Senegal. *Vector-borne Zoonotic Dis.* 7 (2), 203–216. <https://doi.org/10.1089/vbz.2006.0600>.
- Danzetta, M.L., Bruno, R., Sauro, F., Savini, L., Calistri, P., 2016. Rift Valley fever transmission dynamics described by compartmental models. *Prev. Vet. Med.* 134, 197–210. <https://doi.org/10.1016/j.prevetmed.2016.09.007>.
- Davies, F.G., Martin, V., 2003. Recognizing Rift Valley fever. *FAO Animal Health Manual* 17.
- Diallo, M., Lochouart, L., Ba, K., Sall, A.A., Mondo, M., Girault, L., Mathiot, C., 2000. First isolation of the Rift Valley fever virus from *Culex poicilipes* (Diptera: culicidae) in nature. *Am. J. Trop. Med. Hyg.* 62 (6), 702–704. <https://doi.org/10.4269/ajtmh.2000.62.702>.
- Diallo, D., Talla, C., Ba, Y., Dia, I., Sall, A.A., Diallo, M., 2011. Temporal distribution and spatial pattern of abundance of the Rift Valley fever and West Nile fever vectors in Barkedji. *Senegal. Journal of Vector Ecology* 36 (2), 426–436. <https://doi.org/10.1111/j.1948-7134.2011.00184.x>.
- Durand, B., Lo Modou, M., Tran, A., Ba, A., Sow, F., Belkhiria, J., Fall, A.G., Biteye, B., Grosbois, V., Chevalier, V., 2020. Rift Valley fever in northern Senegal: a modelling approach to analyse the processes underlying virus circulation recurrence. *PLoS Negl. Trop. Dis.* 14 (6) <https://doi.org/10.1371/journal.pntd.0008009> e0008009.
- EMPRES, 2003. Early Warning Message: Rift Valley Fever in the Gambia; Tabaski Is Approaching. URL (Accessed 17 February 2020). <http://www.fao.org/AG/AGAlno/programmes/en/empres/earlywarning/ew14.html>.
- Fall, A.G., Diàité, A., Lancelot, R., Tran, A., Soti, V., Etter, E., Konaté, L., Faye, O., Bouyer, J., 2011. Feeding behaviour of potential vectors of West Nile virus in Senegal. *Parasit. Vectors* 4 (1), 99. <https://doi.org/10.1186/1756-3305-4-99>.
- Fall, A., Diàité, A., Seck, M., Bouyer, J., Lefrançois, T., Vachière, N., Aprelon, R., Faye, O., Konaté, L., Lancelot, R., 2013. West Nile virus transmission in sentinel chickens and potential mosquito vectors, Senegal River delta, 2008–2009. *Int. J. Environ. Res. Public Health* 10 (10), 4718–4727. <https://doi.org/10.3390/ijerph10104718>.
- Fischer, E.A., Boender, G.-J., Nodelijk, G., de Koeijer, A.A., van Roermund, H.J., 2013. The transmission potential of Rift Valley fever virus among livestock in the Netherlands: a modelling study. *Vet. Res.* 44 (1), 58. <https://doi.org/10.1186/1297-9716-44-58>.
- Fontenille, D., Traore-Laminaza, M., Diallo, M., Thonnon, J., Digoutte, J.P., Zeller, H.G., 1998. New vectors of Rift Valley fever in West Africa. *Emerging Infect. Dis.* 4 (2), 289–293. <https://doi.org/10.3201/eid0402.980218>.
- Gaff, H.D., Hartley, D.M., Leahy, N.P., 2007. An epidemiological model of Rift Valley fever. *Electronic Journal of Differential Equations* 2007 (115), 1–12.
- Gerdes, G.H., 2004. Rift Valley fever. *Rev. sci. tech. Off. int. Epiz.* 23 (2), 613–623.
- Gilbert, M., Nicolas, G., Cinardi, G., Van Boeckel, T.P., Vanwambeke, S.O., Wint, G.R.W., Robinson, T.P., 2018. Global distribution data for cattle, buffaloes, horses, sheep, goats, pigs, chickens and ducks in 2010. *Sci. Data* 5, 180227. <https://doi.org/10.1038/sdata.2018.227>.
- Gubbins, S., Carpenter, S., Baylis, M., Wood, J.L., Mellor, P.S., 2008. Assessing the risk of bluetongue to UK livestock: uncertainty and sensitivity analyses of a temperature-dependent model for the basic reproduction number. *J. R. Soc. Interface* 5 (20), 363–371. <https://doi.org/10.1098/rsif.2007.1110>.
- Hammami, P., Lancelot, R., Lesnoff, M., 2016. Modelling the dynamics of post-vaccination immunity rate in a population of Sahelian sheep after a vaccination campaign against Peste des Petits Ruminants virus. *PLoS One* 11 (9). <https://doi.org/10.1371/journal.pone.0161769> e0161769.
- Hartemink, N.A., Randolph, S.E., Davis, S.A., Heesterbeek, J.A.P., 2008. The basic reproduction number for complex disease systems: defining  $R_0$  for tick-borne infections. *Am. Nat.* 171 (6), 743–754. <https://doi.org/10.1086/587530>.
- Jupp, P.G., Kemp, A., Grobbelaar, A., Leman, P., Burt, F.J., Alahmed, A.M., Mujalli, D.A., Khamees, M.A., Swanepoel, R., 2002. The 2000 epidemic of Rift Valley fever in Saudi Arabia: mosquito vector studies. *Med. Vet. Entomol.* 16 (3), 245–252. <https://doi.org/10.1046/j.1365-2915.2002.00371.x>.
- Kamiya, T., Greischer, M.A., Wadhawan, K., Gilbert, B., Paaijmans, K., Mideo, N., 2020. Temperature-dependent variation in the extrinsic incubation period elevates the risk of vector-borne disease emergence. *Epidemics* 30, 100382. <https://doi.org/10.1016/j.epidem.2019.100382>.
- Kim, Y., Dommergues, L., M'sa, A.B., Mérot, P., Cardinale, E., Edmunds, J., Pfeiffer, D., Fournié, G., Métras, R., 2018. Livestock trade network: potential for disease transmission and implications for risk-based surveillance on the island of Mayotte. *Sci. Rep.* 8, 11550. <https://doi.org/10.1038/s41598-018-29999-y>.
- Lacaux, J., Tourre, Y., Vignolles, C., Ndione, J., Lafaye, M., 2007. Classification of ponds from high-spatial resolution remote sensing: application to Rift Valley fever epidemics in Senegal. *Remote Sens. Environ.* 106 (1), 66–74. <https://doi.org/10.1016/j.rse.2006.07.012>.
- Lancelot, R., Cetre-Sossah, C., Hassan, O.A., Yahya, B., Ould Elmamy, B., Fall, A.G., Lo, M.M., Apolloni, A., Arsevska, E., Chevalier, V., 2019. Rift Valley fever: One Health at play? In: Kardjadj, M., Diallo, A., Lancelot, R. (Eds.), *Transboundary Animal Diseases in Sahelian Africa and Connected Regions*. Springer International Publishing, Cham, pp. 121–148. [https://doi.org/10.1007/978-3-030-25385-1\\_8](https://doi.org/10.1007/978-3-030-25385-1_8). ISBN 978-3-030-25384-4 978-3-030-25385-1.
- Laughlin, L.W., Meegan, J.M., Strausbaugh, L.J., Morens, D.M., Watten, R.H., 1979. Epidemic Rift Valley fever in Egypt: observations of the spectrum of human illness. *Trans. R. Soc. Trop. Med. Hyg.* 73 (6), 630–633. [https://doi.org/10.1016/0035-203\(79\)90006-3](https://doi.org/10.1016/0035-203(79)90006-3).
- Li, J., Blakeley, D., Smith, R.J., 2011. The failure of  $R_0$ . *Comput. Math. Methods Med.* 17 <https://doi.org/10.1155/2011/527610>, 2011.
- Linthicum, K.J., Davies, F.G., Kairo, A., Bailey, C.L., 1985. Rift Valley fever virus (family Bunyaviridae, genus Phlebovirus). Isolations from Diptera collected during an interepizootic period in Kenya. *J. Hyg. (Lond)* 95 (01), 197–209. <https://doi.org/10.1017/S0022172400062434>.
- Linthicum, K.J., Britch, S.C., Anyamba, A., 2016. Rift Valley fever: an emerging mosquito-borne disease. *Annu. Rev. Entomol.* 61 (1), 395–415. <https://doi.org/10.1146/annurev-ento-010715-023819>.
- Lumley, S., Horton, D.L., Hernandez-Triana, L.L.M., Johnson, N., Fooks, A.R., Hewson, R., 2017. Rift Valley fever virus: strategies for maintenance, survival and vertical transmission in mosquitoes. *J. Gen. Virol.* 98 (5), 875–887. <https://doi.org/10.1099/jgv.0.000765>.
- Madani, T.A., Al-Mazrou, Y.Y., Al-Jeffri, M.H., Mishkhas, A.A., Al-Rabeah, A.M., Turkistani, A.M., Al-Sayed, M.O., Abodahish, A.A., Khan, A.S., Ksiazek, T.G., Shobokshi, O., 2003. Rift Valley fever epidemic in Saudi Arabia: epidemiological, clinical, and laboratory characteristics. *Clin. Infect. Dis.* 37 (8), 1084–1092. <https://doi.org/10.1086/378747>.
- Madder, D., Surgeoner, G., Helson, B., 1983. Number of generations, egg production, and developmental time of *Culex pipiens* and *Culex restuans* (Diptera: Culicidae) in

- Southern Ontario. *J. Med. Entomol.* 20 (3), 275–287. <https://doi.org/10.1093/jmedent/20.3.275>.
- Mehand, M.S., Al-Shorbaji, F., Millett, P., Murgue, B., 2018. The WHO R&D Blueprint: 2018 review of emerging infectious diseases requiring urgent research and development efforts. *Antiviral Res.* 159, 63–67. <https://doi.org/10.1016/j.antiviral.2018.09.009>.
- Metras, R., Collins, L.M., White, R.G., Alonso, S., Chevalier, V., Thurani-McKeever, C., Pfeiffer, D.U., 2011. Rift Valley fever epidemiology, surveillance, and control: what have models contributed? *Vector-borne Zoonotic Dis.* 11 (6), 761–771. <https://doi.org/10.1089/vbz.2010.0200>.
- Mondet, B., Diaité, A., Ndione, J.-A., Fall, A.G., Chevalier, V., Lancelot, R., Ndiaye, M., Ponçon, N., 2005. Rainfall patterns and population dynamics of *Aedes (Aedimorphus) vexans arabiensis*, Patton 1905 (Diptera: Culicidae), a potential vector of Rift Valley fever virus in Senegal. *J. Vector Ecol.* 30 (1), 5.
- Mordecai, E.A., Cohen, J.M., Evans, M.V., Gudapati, P., Johnson, L.R., Lippi, C.A., Miazgowicz, K., Murdock, C.C., Rohr, J.R., Ryan, S.J., Savage, V., Shocket, M.S., Ibarra, A.S., Thomas, M.B., Weikel, D.P., 2017. Detecting the impact of temperature on transmission of Zika, dengue, and chikungunya using mechanistic models. *PLoS Negl. Trop. Dis.* 11 (4) e0005568.
- Mordecai, E.A., Caldwell, J.M., Grossman, M.K., Lippi, C.A., Johnson, L.R., Neira, M., Rohr, J.R., Ryan, S.J., Savage, V., Shocket, M.S., Sippy, R., Stewart Ibarra, A.M., Thomas, M.B., Villena, O., 2019. Thermal biology of mosquito-borne disease. *Ecol. Lett.* <https://doi.org/10.1111/ele.13335>.
- Mpeshe, S.C., Luboobi, L.S., Nkansah-Gyekye, Y., 2014. Modeling the impact of climate change on the dynamics of Rift Valley fever. *Comput. Math. Methods Med.* 12 <https://doi.org/10.1155/2014/627586>, 2014.
- Ndiaye, E.H., Fall, G., Gaye, A., Bob, N.S., Talla, C., Diagne, C.T., Diallo, D., Ba, Y., Dia, I., Kohl, A., Sall, A.A., Diallo, M., 2016. Vector competence of *Aedes vexans* (Meigen), *Culex poicilipes* (Theobald) and *Cx. quinquefasciatus* Say from Senegal for West and East African lineages of Rift Valley fever virus. *Parasit. Vectors* 9, 94. <https://doi.org/10.1186/s13071-016-1383-y>.
- Ndione, J.-A., Diop, M., Lacaux, J.-P., Gaye, A.T., 2008. Variabilité intra-saisonnière de la pluviométrie et émergence de la fièvre de la Vallée du Rift dans la vallée du fleuve Sénégal : nouvelles considérations. *Climatologie* (5), 83–97. <https://doi.org/10.4267/climatologie.794>.
- Ndione, J.-A., Lacaux, J.-P., Tourre, Y., Vignolles, C., Fontanaz, D., Lafaye, M., 2009. Mares temporaires et risques sanitaires au Ferlo: contribution de la télédétection pour l'étude de la fièvre de la Vallée du Rift entre août 2003 et janvier 2004. *Secheresse* 20 (1), 153–160. <https://doi.org/10.1684/sec.2009.0170>.
- Nicolas, G., Chevalier, V., Tantely, L.M., Fontenille, D., Durand, B., 2014. A spatially explicit metapopulation model and cattle trade analysis suggests key determinants for the recurrent circulation of Rift Valley fever virus in a pilot area of Madagascar highlands. *PLoS Negl. Trop. Dis.* 8 (12), e3346. <https://doi.org/10.1371/journal.pntd.0003346>.
- Niu, T., Gaff, H.D., Papelis, Y.E., Hartley, D.M., 2012. An epidemiological model of Rift Valley fever with spatial dynamics. *Comput. Math. Methods Med.* 12 <https://doi.org/10.1155/2012/138757>, 2012.
- Parham, P.E., Waldock, J., Christophides, G.K., Hemming, D., Agosto, F., Evans, K.J., Fefferman, N., Gaff, H., Gumel, A., LaDeau, S., Lenhart, S., Mickens, R.E., Naumova, E.N., Ostfeld, R.S., Ready, P.D., Thomas, M.B., Velasco-Hernandez, J., Michael, E., 2015. Climate, environmental and socio-economic change: weighing up the balance in vector-borne disease transmission. *Philos. Trans. Biol. Sci.* 370, 20130551 <https://doi.org/10.1098/rstb.2013.0551>.
- Pedro, S.A., Abelman, S., Tonnang, H.E.Z., 2016. Predicting Rift Valley fever inter-epidemic activities and outbreak patterns: insights from a stochastic host-vector model. *PLoS Negl. Trop. Dis.* 10 (12) <https://doi.org/10.1371/journal.pntd.0005167> e0005167.
- Pepin, M., Bouloy, M., Bird, B.H., Kemp, A., Paweska, J., 2010. Rift Valley fever virus (Bunyaviridae: Phlebovirus): an update on pathogenesis, molecular epidemiology, vectors, diagnostics and prevention. *Vet. Res.* 41 (6), 61. <https://doi.org/10.1051/vetres/20100033>.
- Saltelli, A., Chan, R., Scott, F.M., 2008. *Sensitivity Analysis*. Wiley. ISBN 978-0-470-74382-74389.
- Saltelli, A., Aleksankina, K., Becker, W., Fennell, P., Ferretti, F., Holst, N., Li, S., Wu, Q., 2019. Why so many published sensitivity analyses are false: a systematic review of sensitivity analysis practices. *Environ. Model. Softw.* 114, 29–39. <https://doi.org/10.1016/j.envsoft.2019.01.012>.
- Soti, V., Puech, C., Lo Seen, D., Bertran, A., Vignolles, C., Mondet, B., Dessay, N., Tran, A., 2010. The potential for remote sensing and hydrologic modelling to assess the spatio-temporal dynamics of ponds in the Ferlo Region (Senegal). *Hydrol. Earth Syst. Sci.* 14 (8), 1449–1464. <https://doi.org/10.5194/hess-14-1449-2010>.
- Soti, V., Chevalier, V., Maura, J., Bègué, A., Lelong, C., Lancelot, R., Thiongane, Y., Tran, A., 2013. Identifying landscape features associated with Rift Valley fever virus transmission, Ferlo region, Senegal, using very high spatial resolution satellite imagery. *Int. J. Health Geogr.* 12, 10. <https://doi.org/10.1186/1476-072X-12-10>.
- Sow, A., Faye, O., Ba, Y., Diallo, D., Fall, G., Faye, O., Bob, N.S., Loucoubar, C., Richard, V., Dia, A.T., Diallo, M., Malvy, D., Sall, A.A., 2016. Widespread Rift Valley fever emergence in Senegal in 2013–2014. *Open Forum Infect. Dis.* <https://doi.org/10.1093/ofid/ofw149>.
- Spickler, A.R., 2015. Rift Valley Fever. URL (Accessed 17 February 2020). [http://www.cfsph.iastate.edu/Factsheets/pdfs/rift\\_valley\\_fever.pdf](http://www.cfsph.iastate.edu/Factsheets/pdfs/rift_valley_fever.pdf).
- Talla, C., Diallo, D., Dia, I., Ba, Y., Ndione, J.-A., Morse, A.P., Diop, A., Diallo, M., 2016. Modelling hotspots of the two dominant Rift Valley fever vectors (*Aedes vexans* and *Culex poicilipes*) in Barkédji, Sénégal. *Parasit. Vectors* 9, 111. <https://doi.org/10.1186/s13071-016-1399-3>.
- Tourre, Y.M., Lacaux, J.-P., Vignolles, C., Lafaye, M., 2009. Climate impacts on environmental risks evaluated from space: a conceptual approach to the case of Rift Valley fever in Senegal. *Glob. Health Action* 2 (1), 2053. <https://doi.org/10.3402/gha.v2i0.2053>.
- Tran, A., Trevennec, C., Lutwama, J., Sserugga, J., Gély, M., Pittiglio, C., Pinto, J., Chevalier, V., 2016. Development and assessment of a geographic knowledge-based model for mapping suitable areas for Rift Valley fever transmission in Eastern Africa. *PLoS Negl. Trop. Dis.* 10 (9) <https://doi.org/10.1371/journal.pntd.0004999> e0004999.
- Tran, A., Fall, A.G., Biteye, B., Ciss, M., Gimonneau, G., Castets, M., Seck, M.T., Chevalier, V., 2019. Spatial modeling of mosquito vectors for Rift Valley fever virus in northern Senegal: integrating satellite-derived meteorological estimates in population dynamics models. *Remote Sens. (Basel)* 11, 1024. <https://doi.org/10.3390/rs11091024>.
- Turner, J., Bowers, R.G., Baylis, M., 2013. Two-host, two-vector basic reproduction ratio (R0) for Bluetongue. *PLoS One* 8 (1), e53128. <https://doi.org/10.1371/journal.pone.0053128>.
- van den Driessche, P., Watmough, J., 2002. Reproduction numbers and sub-threshold endemic equilibria for compartmental models of disease transmission. *Math. Biosci.* 180 (1–), 29–48. [https://doi.org/10.1016/S0025-5564\(02\)00108-6](https://doi.org/10.1016/S0025-5564(02)00108-6), 2.
- Vignolles, C., Lacaux, J.-P., Tourre, Y.M., Bigeard, G., Ndione, J.-A., Lafaye, M., 2009. Rift Valley fever in a zone potentially occupied by *Aedes vexans* in Senegal: dynamics and risk mapping. *Geospat. Health* 3 (2), 211–220. <https://doi.org/10.4081/gh.2009.221>.
- Wonham, M.J., Lewis, M.A., Renclawowicz, J., van den Driessche, P., 2006. Transmission assumptions generate conflicting predictions in host-vector disease models: a case study in West Nile virus. *Ecol. Lett.* 9 (6), 706–725. <https://doi.org/10.1111/j.1461-0248.2006.00912.x>.
- World Health Organization (WHO), 2014. *A Global Brief on Vector-borne Diseases* [http://apps.who.int/iris/bitstream/10665/111008/1/WHO\\_DCO\\_WH-D\\_2014.1\\_eng.pdf](http://apps.who.int/iris/bitstream/10665/111008/1/WHO_DCO_WH-D_2014.1_eng.pdf). URL (Accessed 17 February 2020).
- Xue, L., Scoglio, C., 2013. The network level reproduction number for infectious diseases with both vertical and horizontal transmission. *Math. Biosci.* 243 (1), 67–80. <https://doi.org/10.1016/j.mbs.2013.02.004>.

# Supplementary Information

Cecilia H, Métras R, Fall AG, Lo MM, Lancelot R, Ezanno P

It's risky to wander in September: modelling the epidemic potential of Rift Valley fever in a Sahelian setting

## Contents

<b>1</b>	<b>The model</b>	<b>2</b>
1.1	Equations . . . . .	2
1.2	Parameterization . . . . .	3
<b>2</b>	<b>Basic reproduction number</b>	<b>6</b>
<b>3</b>	<b>Removing outliers</b>	<b>7</b>
<b>4</b>	<b>Spatio-temporal pattern of <math>R_0</math></b>	<b>11</b>
<b>5</b>	<b>Role of vector and host populations</b>	<b>12</b>
5.1	Relative vector abundances over the rainy season . . . . .	12
5.2	Effect of herd immunity . . . . .	13
<b>6</b>	<b>Sensitivity analysis</b>	<b>13</b>
6.1	Sensitivity of $R_0$ temporal pattern . . . . .	14
6.2	Sensitivity of $R_0$ spatial pattern . . . . .	16
<b>7</b>	<b>References</b>	<b>16</b>
<b>8</b>	<b>Credits</b>	<b>17</b>

# 1 The model

## 1.1 Equations

$$\left. \begin{aligned}
 &\text{Vector population: } Aedes vexans arabiensis \text{ (Ferlo) or } Culex tritaeniorhynchus \text{ (SRDV)} \\
 &\frac{dS_1}{dt} = b_1 N_1 - d_1 S_1 - a_1 \phi_{12} \frac{I_2}{N_2} \alpha_{21} S_1 - a_1 \phi_{13} \frac{I_3}{N_3} \alpha_{31} S_1 \\
 &\frac{dE_1}{dt} = -d_1 E_1 + a_1 \phi_{12} \frac{I_2}{N_2} \alpha_{21} S_1 + a_1 \phi_{13} \frac{I_3}{N_3} \alpha_{31} S_1 - \epsilon_1 E_1 \\
 &\frac{dI_1}{dt} = \epsilon_1 E_1 - d_1 I_1 \\
 &N_1 = S_1 + E_1 + I_1 \\
 \\
 &\text{Host population: Cattle} \\
 &\frac{dS_2}{dt} = b_2 N_2 - d_2 S_2 - a_1 \phi_{12} \frac{I_1}{N_2} \alpha_{12} S_2 - a_4 \phi_{42} \frac{I_4}{N_2} \alpha_{42} S_2 \\
 &\frac{dE_2}{dt} = -d_2 E_2 + a_1 \phi_{12} \frac{I_1}{N_2} \alpha_{12} S_2 + a_4 \phi_{42} \frac{I_4}{N_2} \alpha_{42} S_2 - \epsilon_2 E_2 \\
 &\frac{dI_2}{dt} = -d_2 I_2 + \epsilon_2 E_2 - \gamma_2 I_2 - \mu_2 I_2 \\
 &\frac{dR_2}{dt} = -d_2 R_2 + \gamma_2 I_2 \\
 &N_2 = S_2 + E_2 + I_2 + R_2 \\
 \\
 &\text{Host population: Small ruminants} \\
 &\frac{dS_3}{dt} = b_3 N_3 - d_3 S_3 - a_1 \phi_{13} \frac{I_1}{N_3} \alpha_{13} S_3 - a_4 \phi_{43} \frac{I_4}{N_3} \alpha_{43} S_3 \\
 &\frac{dE_3}{dt} = -d_3 E_3 + a_1 \phi_{13} \frac{I_1}{N_3} \alpha_{13} S_3 + a_4 \phi_{43} \frac{I_4}{N_3} \alpha_{43} S_3 - \epsilon_3 E_3 \\
 &\frac{dI_3}{dt} = -d_3 I_3 + \epsilon_3 E_3 - \gamma_3 I_3 - \mu_3 I_3 \\
 &\frac{dR_3}{dt} = -d_3 R_3 + \gamma_3 I_3 \\
 &N_3 = S_3 + E_3 + I_3 + R_3 \\
 \\
 &\text{Vector population: } Culex poicilipes \\
 &\frac{dS_4}{dt} = b_4 N_4 - d_4 S_4 - a_4 \phi_{42} \frac{I_2}{N_2} \alpha_{24} S_4 - a_4 \phi_{43} \frac{I_3}{N_3} \alpha_{34} S_4 \\
 &\frac{dE_4}{dt} = -d_4 E_4 + a_4 \phi_{42} \frac{I_2}{N_2} \alpha_{24} S_4 + a_4 \phi_{43} \frac{I_3}{N_3} \alpha_{34} S_4 - \epsilon_4 E_4 \\
 &\frac{dI_4}{dt} = \epsilon_4 E_4 - d_4 I_4 \\
 &N_4 = S_4 + E_4 + I_4
 \end{aligned} \right\} \tag{S.1}$$

$$a_i = \frac{1 + c_i}{g_i(T)} \quad i \in \{1, 4\} \tag{S.2}$$

$a_i$ : biting rate of vector population  $i$ .

$g_i(T)$ : lenght of the gonotrophic cycle of vector population  $i$ , function of temperature  $T$ .

$c_i$ : proportion of double blood meals;  $1 + c_i$  therefore being the feeding rate per gonotrophic cycle of vector population  $i$ .

$$\phi_{ij} = \frac{\pi_{ij} N_j}{\pi_{i2} N_2 + \pi_{i3} N_3} \quad i \in \{1, 4\}, j \in \{2, 3\} \tag{S.3}$$

$\phi_{ij}$  is the proportion of blood meals taken by vector population  $i$  on host population  $j$ .  $\pi_{ij}$  is the relative preference of vector population  $i$  for host population  $j$ . For each vector population  $i$ ,  $\pi_{i2} + \pi_{i3} = 1$ .

## 1.2 Parameterization

### Inclusion of input data from previous models

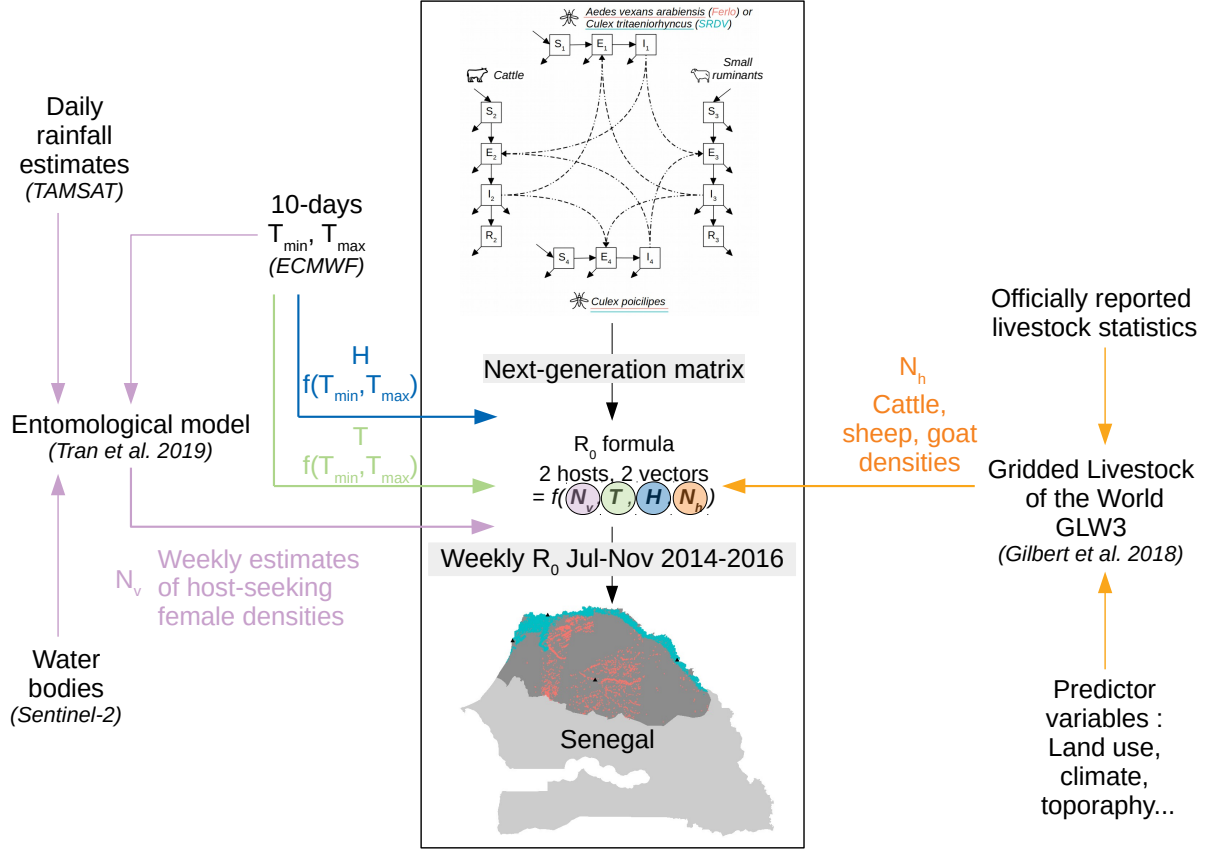


Figure S.1: Modelling framework of the study. We built a mechanistic model of Rift Valley fever virus transmission with 2 host and 2 vector populations in two study areas belonging to different ecosystems (Ferlo and Senegal River delta and valley, SRDV). We derived the basic reproduction number  $R_0$  using the next generation matrix approach (see Supplementary Information 2, Eq 1-5 in main text). We then used input data from various sources to compute  $R_0$  for weekly introduction dates, for each pixel containing both hosts and vectors, for three consecutive rainy seasons (July-November 2014, 2015, and 2016) in northern Senegal.

TAMSAT : Tropical Applications of Meteorology using SATellite. ECMWF: European Center for Medium Range Weather Forecasts.

In the entomological model by Tran et al. (2019), the rainfall from ground weather station, when available, or TAMSAT satellite-derived estimates otherwise, is used in a hydrological model to dynamically compute the surface of ponds. This surface is used for the transition rate from eggs to larvae for *Aedes* mosquitoes. In this sense, it acts as a trigger. The entomological model also uses pond surface to compute the carrying capacity and mortality rate of larvae and pupae for species in the Ferlo.

Minimum and maximum temperatures over 10-day periods,  $T_{min}$ ,  $T_{max}$  were retrieved from the European Centre for Medium Range Weather Forecasts (ECMWF). These temperatures were used to compute the relative humidity  $H$  as follows:

$$H = 100 \cdot \frac{\exp(\frac{17.27(T_{min}-2)}{(T_{min}-2)+237.3})}{\exp(\frac{17.27T_{max}}{T_{max}+237.3})} \quad (S.4)$$

The relative humidity was then used to compute mortality rates of *Culex* populations (see Table 1 in main text). Temperature-dependent functions related to vector parameters (mortality rate, biting rate

and extrinsic incubation period, see Table 1 in main text) were computed with:

$$T = (T_{min} + T_{max})/2 \quad (\text{S.5})$$

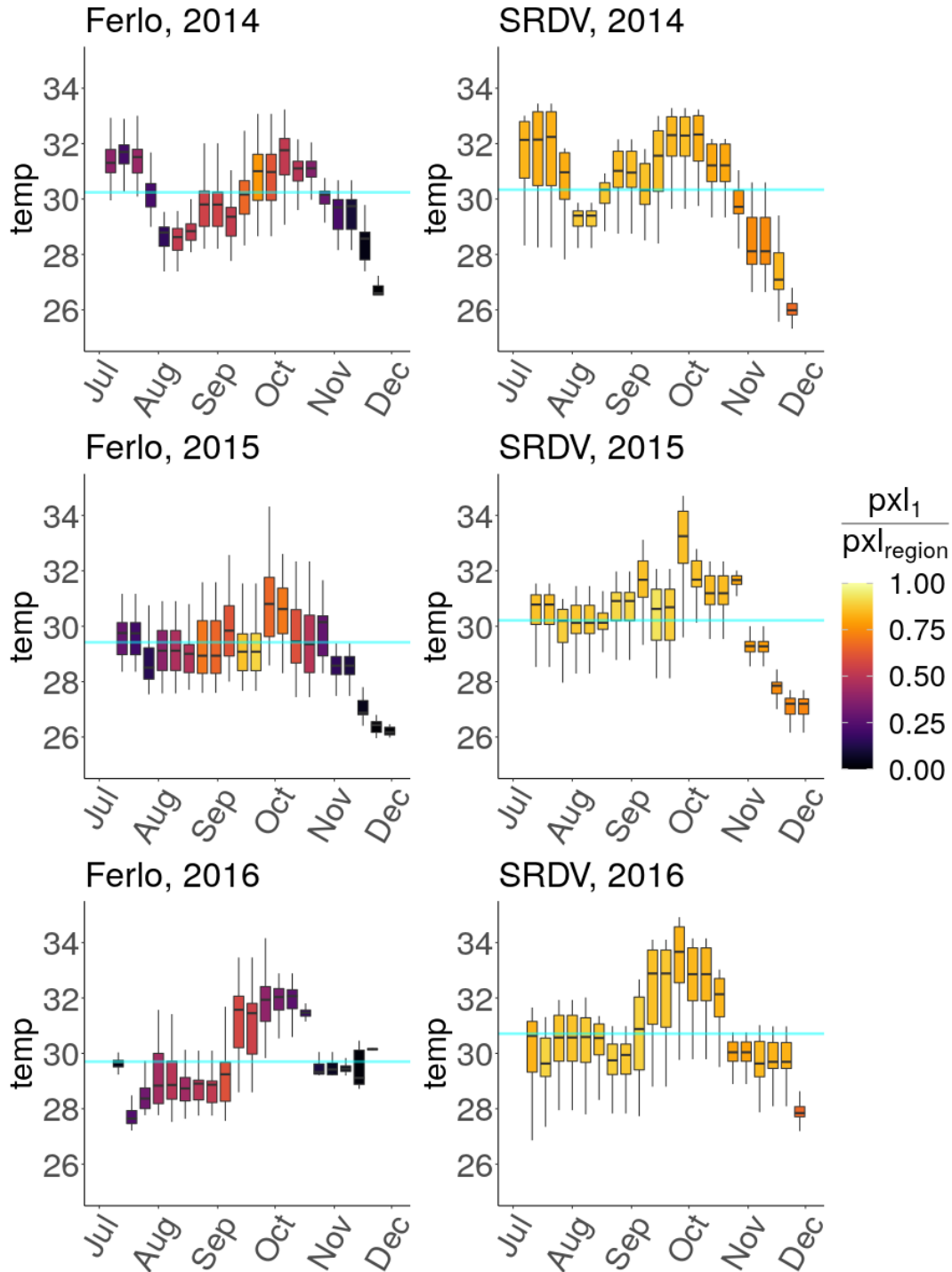


Figure S.2: Temperature distribution by virus introduction date for each rainy season, spatially aggregated by study area (left : Ferlo, right : SRDV). Boxplots are coloured by the number of pixels with  $R_0 > 1$  ( $pxl_1$ ) for each introduction date, normalized by the total number of pixels in the study area. The blue line indicates the mean temperature over the rainy season in a given study area.

## Vector parameters

- Gonotrophic cycle : this cycle consists in searching for a vertebrate host, blood feeding, blood meal digestion, egg maturation and oviposition. Mating only happens once for females. Here we used the ovarian development time as a proxy, which is the longest part of the gonotrophic cycle and is temperature-dependent. We used the same equation for every vector population, taken from Madder et al. 1983 for *Culex pipiens* in field conditions. Values are consistent with what was measured by Ndiaye et al. 2006 on *Ae. v. arabiensis* collected in Barkedji.
- Multiple blood meals : It is generally assumed that one blood meal takes place by gonotrophic cycle, but there are conditions where mosquitoes have to take multiple partial blood meals, because of host defense mechanisms for instance. This changes the contact rate between vectors and hosts and influences disease transmission. We decided to include it in our study, as it has been evidenced in several species in non-trivial proportions.  
Ba et al. 2006 showed 16.88% (n=693) of multiple blood meals in naturally fed *Aedes vexans* in the Ferlo region. Edman and Downe 1964 showed 18.5% (n=1417) of multiple blood meals for *Aedes vexans* in Kansas, USA.  
Multiple blood meals have also been evidenced in *C. poicilipes* in Muturi et al. 2008 (Kenya, 73.3%, n=11), Gordon et al. 1991 (Senegal, 2.2%, n=91) and Crabtree et al. 2013 (Uganda, 0.4%, n=40). These studies were sometimes able to detect more than two different origins in the blood meals, but we decided to limit our model complexity and consider these proportions as double bites only. We favoured values from studies on *Aedes vexans* because of their bigger sample sizes. We chose 17% as reference value, which was consistent with the two studies at our disposal, and applied it to every vector population. We considered *C. tritaeniorhynchus* to exhibit the same kind of behaviour.
- Extrinsic incubation period : We used an equation calibrated by Barker et al. 2013 including data from a study conducted on *Aedes fowleri* in Senegal (Turell 1989). We applied it to every vector population.

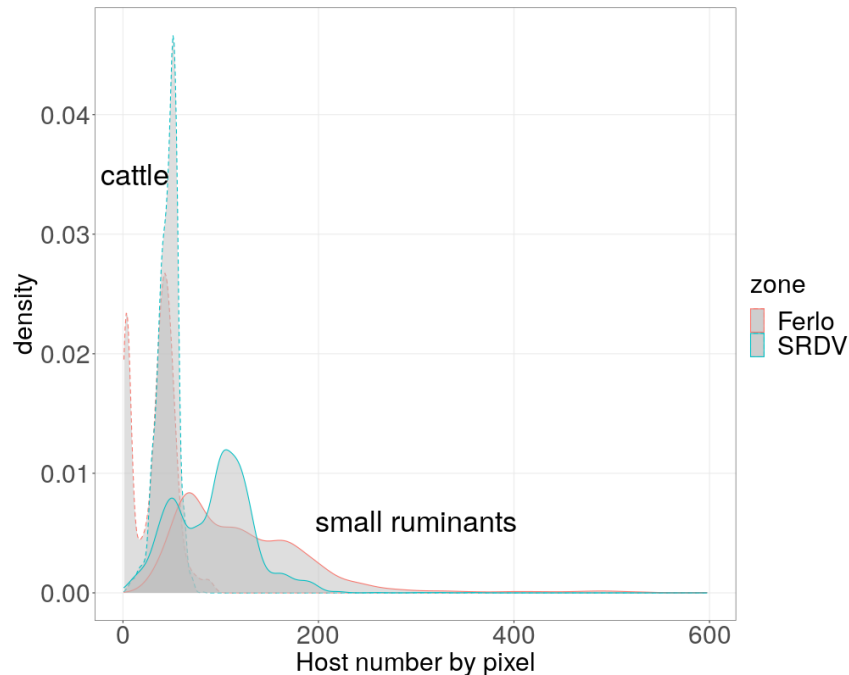


Figure S.3: Distribution of host densities within pixels, by population and study area. Dashed lines are for cattle, solid lines for small ruminants. Red lines for Ferlo, blue ones for SRDV.



## Host parameters

- Density downscaling : Gridded Livestock of the World (GLW3, Gilbert et al. 2018) pixel resolution is  $100\text{km}^2$ . Tran et al. 2019 pixels are hexagons of  $1\text{km}$  radius, which corresponds to  $\frac{6}{\sqrt{(3)}}\text{km}^2$ . GLW3 animal densities were therefore divided by  $\frac{100 \times \sqrt{(3)}}{6}$  and assigned to Tran et al. 2019 pixel centroids.
- Lifespan : Based on expert opinion, cattle (mostly Gobra Zebu) live 8 years on average in our study region. For small ruminants, Table S2 of Hammami et al. 2016 gives natural death rates of sheep in Ndiagne, northern Senegal.
- Disease-induced mortality rate : In our model, infectious hosts were not separated between symptomatic and asymptomatic animals. Therefore, the disease-induced mortality rate could not be directly equal to the case fatality rate observed on clinical cases. Gaff et al. 2007 used values of 0.0176 and 0.0312, corresponding to case fatality rates of 15% and 25% respectively, with approximately 12% of symptomatic hosts in both populations.

## Feeding preferences

Ba et al. (2006) did experiments with baited traps in the Ferlo region and provided monthly values of the percentage of mosquitoes found in each trap. They corrected the effect of host weight and  $\text{CO}_2$  production by putting different numbers of animals in the trap depending on the species (1 veal, 2 sheep). We computed weighted means from monthly values, because we did not consider preferences to vary over time. We normalized to account for cattle and small ruminants only, leaving aside other preys (Ba et al. 2006 also included human and chicken). Separate values for *Aedes vexans* and *C. poicilipes* were computed, the latter was also applied to *C. tritaeniorhynchus*. This species was also part of Ba et al. (2006) experiment but much less individuals were trapped so we favoured a bigger sample size for robustness.

## 2 Basic reproduction number

We used the next generation matrix method (van den Driessche and Watmough 2002) to determine the basic reproduction number  $R_0$  of our ODE compartmental model. Let us sort our compartments so that the first  $m$  compartments correspond to infected individuals. We then expressed our system equations in the form  $\frac{dx_i}{dt} = \mathcal{F}_i(x) - \mathcal{V}_i(x)$  for all compartments  $x_i, 1 \leq i \leq m$  containing infected individuals.  $\mathcal{F}_i(x)$  is the rate at which new infections arise and  $\mathcal{V}_i(x)$  reflects vital dynamics, i.e the rate at which individuals enter or leave the compartment due to completion of an infection stage or death.

$$\frac{d}{dt} \begin{bmatrix} E_1 \\ I_1 \\ E_2 \\ I_2 \\ E_3 \\ I_3 \\ E_4 \\ I_4 \end{bmatrix} = \mathcal{F} - \mathcal{V} = \begin{bmatrix} a_1\phi_{12}\frac{I_2}{N_2}\alpha_{21}S_1 + a_1\phi_{13}\frac{I_3}{N_3}\alpha_{31}S_1 \\ 0 \\ a_1\phi_{12}\frac{I_1}{N_2}\alpha_{12}S_2 + a_4\phi_{42}\frac{I_4}{N_2}\alpha_{42}S_2 \\ 0 \\ a_1\phi_{13}\frac{I_1}{N_3}\alpha_{13}S_3 + a_4\phi_{43}\frac{I_4}{N_3}\alpha_{43}S_3 \\ 0 \\ a_4\phi_{42}\frac{I_2}{N_2}\alpha_{24}S_4 + a_4\phi_{43}\frac{I_3}{N_3}\alpha_{34}S_4 \\ 0 \end{bmatrix} - \begin{bmatrix} d_1E_1 + \epsilon_1E_1 \\ d_1I_1 - \epsilon_1E_1 \\ d_2E_2 + \epsilon_2E_2 \\ d_2I_2 + \gamma_2I_2 + \mu_2I_2 - \epsilon_2E_2 \\ d_3E_3 + \epsilon_3E_3 \\ d_3I_3 + \gamma_3I_3 + \mu_3I_3 - \epsilon_3E_3 \\ d_4I_4 + \epsilon_4E_4 \\ d_4I_4 - \epsilon_4E_4 \end{bmatrix}$$

We then defined the Jacobian matrices at disease-free equilibrium (DFE)  $x_0$ ,  $F = \left[ \frac{\partial \mathcal{F}_i(x_0)}{\partial x_j} \right]$  and  $V = \left[ \frac{\partial \mathcal{V}_i(x_0)}{\partial x_j} \right], 1 \leq i, j \leq m$ . Thus  $FV^{-1}$  is the next generation matrix  $K$  and  $R_0 = \rho(K)$  where  $\rho$  denotes the spectral radius (largest eigenvalue).

Here, we considered the possibility for the DFE to incorporate a proportion of immune individuals. Thus, we had:

$S_i = N_i$  for vectors,  $i \in \{1, 4\}$ , and  $S_j = (1 - p_j) \times N_j$  for hosts,  $j \in \{2, 3\}$ ,  $p_j$  being the proportion of immune individuals among host population  $j$ .

$$F = \begin{pmatrix} 0 & 0 & 0 & a_1\phi_{12}\alpha_{21}\frac{N_1}{N_2} & 0 & a_1\phi_{13}\alpha_{31}\frac{N_1}{N_3} & 0 & 0 \\ 0 & 0 & 0 & 0 & 0 & 0 & 0 & 0 \\ 0 & a_1\phi_{12}\alpha_{12}(1 - p_2) & 0 & 0 & 0 & 0 & 0 & a_4\phi_{42}\alpha_{42}(1 - p_2) \\ 0 & 0 & 0 & 0 & 0 & 0 & 0 & 0 \\ 0 & a_1\phi_{13}\alpha_{13}(1 - p_3) & 0 & 0 & 0 & 0 & 0 & a_4\phi_{43}\alpha_{43}(1 - p_3) \\ 0 & 0 & 0 & 0 & 0 & 0 & 0 & 0 \\ 0 & 0 & 0 & a_4\phi_{42}\alpha_{24}\frac{N_4}{N_2} & 0 & a_4\phi_{43}\alpha_{34}\frac{N_4}{N_3} & 0 & 0 \\ 0 & 0 & 0 & 0 & 0 & 0 & 0 & 0 \end{pmatrix}$$

$$V = \begin{pmatrix} d_1 + \epsilon_1 & 0 & 0 & 0 & 0 & 0 & 0 & 0 & 0 \\ -\epsilon_1 & d_1 & 0 & 0 & 0 & 0 & 0 & 0 & 0 \\ 0 & 0 & d_2 + \epsilon_2 & 0 & 0 & 0 & 0 & 0 & 0 \\ 0 & 0 & -\epsilon_2 & d_2 + \gamma_2 + \mu_2 & 0 & 0 & 0 & 0 & 0 \\ 0 & 0 & 0 & 0 & d_3 + \epsilon_3 & 0 & 0 & 0 & 0 \\ 0 & 0 & 0 & 0 & -\epsilon_3 & d_3 + \gamma_3 + \mu_3 & 0 & 0 & 0 \\ 0 & 0 & 0 & 0 & 0 & 0 & 0 & d_4 + \epsilon_4 & 0 \\ 0 & 0 & 0 & 0 & 0 & 0 & 0 & -\epsilon_4 & d_4 \end{pmatrix}$$

$$K = F.V^{-1} = \begin{matrix} & E_2 & E_3 & I_2 & I_3 & E_1 & E_4 & I_1 & I_4 \\ E_2 & \begin{pmatrix} 0 & 0 & 0 & 0 & k_{21} & k_{24} & \tilde{k}_{21} & \tilde{k}_{24} \end{pmatrix} \\ E_3 & \begin{pmatrix} 0 & 0 & 0 & 0 & k_{31} & k_{34} & \tilde{k}_{31} & \tilde{k}_{34} \end{pmatrix} \\ I_2 & \begin{pmatrix} 0 & 0 & 0 & 0 & 0 & 0 & 0 & 0 \end{pmatrix} \\ I_3 & \begin{pmatrix} 0 & 0 & 0 & 0 & 0 & 0 & 0 & 0 \end{pmatrix} \\ E_1 & \begin{pmatrix} k_{12} & k_{13} & \tilde{k}_{12} & \tilde{k}_{13} & 0 & 0 & 0 & 0 \end{pmatrix} \\ E_4 & \begin{pmatrix} k_{42} & k_{43} & \tilde{k}_{42} & \tilde{k}_{43} & 0 & 0 & 0 & 0 \end{pmatrix} \\ I_1 & \begin{pmatrix} 0 & 0 & 0 & 0 & 0 & 0 & 0 & 0 \end{pmatrix} \\ I_4 & \begin{pmatrix} 0 & 0 & 0 & 0 & 0 & 0 & 0 & 0 \end{pmatrix} \end{matrix}$$

Where  $k_{ij}$  is the number of cases in compartment  $i$  produced by an infectious individual from compartment  $j$ .  $\tilde{k}_{ij}$  represent incomplete cycle of infections ( $I_j$  to  $E_i$ ).

$K = \begin{pmatrix} 0 & A \\ B & 0 \end{pmatrix}$  with  $A$  representing vector-to-host transmission and  $B$  host-to-vector transmission. Therefore,  $AB$  and  $BA$  products represent 2 generations “like to like” transmission. Interestingly,  $R_0^2$  is the dominant eigenvalue of both  $AB$  and  $BA$  (see Turner et al. 2013 Supporting Information for more details). We used the vector-to-host-to-vector generation matrix, which explains the presence of both vector populations in sub-parts of our  $R_0$  and the sum to account for both host populations (see Eq 1-5 in main text). As a reminder,  $R_0$  is a geometric mean, representing the average number of secondary cases arising from vector-to-host and host-to-vector transmission scenarios, as these were the only possible transmission routes in our system.

### 3 Removing outliers

Because we used a reservoir frequency-dependent transmission function (Wonham et al. 2006), we had to remove overestimations resulting from high vector-to-host ratios. We chose a threshold  $\frac{N_1+N_4}{N_2+N_3} > 1000$ , intended as a good compromise to significantly drop the highest values of  $R_0$  without removing too many points (Table S.1).

Most pixels remain in the analysis, even if they are removed for some introduction dates due to this criterion. However, 41 pixels are entirely removed from the study because their ratio never goes below the chosen threshold during the 3 rainy seasons. These pixels, located in SRDV, are characterized by very high vector densities year round (minimum 6394, median 80540 *vs* minimum 7, median 7211 for the ones kept in the analysis). Since host densities are constant in time in our model (variations in space in pixels removed: min 3, median 38, max 207), the vector-to-host ratio remains high at all time.

	Ferlo		SRDV	
Threshold (vector-to-host ratio)	Pixel-timestep under threshold (%)	Maximum $R_0$	Pixel-timestep under threshold (%)	Maximum $R_0$
None	64535 (100)	480	170914 (100)	773
20000	64520 (99.98)	314	170797 (99.93)	498
5000	64423 (99.82)	174	169753 (99.32)	254
1000	63966 (99.12)	84.7	162731 (95.21)	124
500	63566 (98.50)	62.5	152853 (89.43)	86.8
200	62660 (97.09)	49.4	127542 (74.62)	55.5
100	61314 (95.01)	35.3		
50	59332 (91.94)	25.8		
10	50986 (79.01)	11.3		

Table S.1: Number of pixel-timestep under different threshold of vector-to-host ratio ( $\frac{N_1+N_4}{N_2+N_3}$ ), and corresponding maximum  $R_0$  value, in each study area.

Intro. date	Nb pixels contain hosts and vectors	Nb pixels removed due to ratio threshold	Nb pixels r0 computed
2014-07-07	2663	83	2580
2014-07-14	2667	85	2582
2014-07-21	2670	91	2579
2014-07-28	2679	111	2568
2014-08-04	2691	156	2535
2014-08-11	2710	170	2540
2014-08-18	2716	171	2545
2014-08-25	2717	143	2574
2014-09-01	2717	131	2586
2014-09-08	2717	154	2563
2014-09-15	2717	174	2543
2014-09-22	2717	185	2532
2014-09-29	2717	121	2596
2014-10-06	2717	75	2642
2014-10-13	2717	70	2647
2014-10-20	2717	68	2649
2014-10-27	2717	62	2655
2014-11-03	2717	62	2655
2014-11-10	2717	60	2657
2014-11-17	2717	109	2608
2014-11-24	2717	70	2647

Table S.2: **Pixel count for SRDV, 2014.** Number of pixels containing both hosts and vectors and number of pixels removed for having  $(\frac{N_1+N_4}{N_2+N_3} > 1000)$ , giving the total number of pixels where  $R_0$  is computed, for each introduction week.

Intro. date	Nb pixels contain hosts and vectors	Nb pixels removed due to ratio threshold	Nb pixels r0 computed
2015-07-13	2692	105	2587
2015-07-20	2710	134	2576
2015-07-27	2716	164	2552
2015-08-03	2717	177	2540
2015-08-10	2717	181	2536
2015-08-17	2717	169	2548
2015-08-24	2717	173	2544
2015-08-31	2717	197	2520
2015-09-07	2717	145	2572
2015-09-14	2717	194	2523
2015-09-21	2717	316	2401
2015-09-28	2717	135	2582
2015-10-05	2717	121	2596
2015-10-12	2717	133	2584
2015-10-19	2717	120	2597
2015-10-26	2717	101	2616
2015-11-02	2717	92	2625
2015-11-09	2717	89	2628
2015-11-16	2717	84	2633
2015-11-23	2717	76	2641
2015-11-30	2717	72	2645

Table S.3: **Pixel count for SRDV, 2015.** Number of pixels containing both hosts and vectors and number of pixels removed for having  $(\frac{N_1+N_4}{N_2+N_3} > 1000)$ , giving the total number of pixels where  $R_0$  is computed, for each introduction week.

Intro. date	Nb pixels contain hosts and vectors	Nb pixels removed due to ratio threshold	Nb pixels r0 computed
2016-07-11	2716	155	2561
2016-07-18	2717	158	2559
2016-07-25	2717	164	2553
2016-08-01	2717	171	2546
2016-08-08	2717	169	2548
2016-08-15	2717	156	2561
2016-08-22	2717	167	2550
2016-08-29	2717	236	2481
2016-09-05	2717	230	2487
2016-09-12	2717	219	2498
2016-09-19	2717	157	2560
2016-09-26	2717	113	2604
2016-10-03	2717	94	2623
2016-10-10	2717	77	2640
2016-10-17	2717	96	2621
2016-10-24	2717	75	2642
2016-10-31	2717	69	2648
2016-11-07	2717	99	2618
2016-11-14	2717	103	2614
2016-11-21	2717	105	2612
2016-11-28	2717	41	2676

Table S.4: **Pixel count for SRDV, 2016.** Number of pixels containing both hosts and vectors and number of pixels removed for having ( $\frac{N_1+N_4}{N_2+N_3} > 1000$ ), giving the total number of pixels where  $R_0$  is computed, for each introduction week.

Intro. date	Nb pixels contain hosts and vectors	Nb pixels removed due to ratio threshold	Nb pixels r0 computed
2014-07-07	1058	0	1058
2014-07-14	1102	0	1102
2014-07-21	1276	0	1276
2014-07-28	943	0	943
2014-08-04	890	0	890
2014-08-11	1035	0	1035
2014-08-18	1119	0	1119
2014-08-25	1285	0	1285
2014-09-01	1233	0	1233
2014-09-08	1132	0	1132
2014-09-15	1642	3	1639
2014-09-22	1680	7	1673
2014-09-29	1634	16	1618
2014-10-06	1550	18	1532
2014-10-13	1391	16	1375
2014-10-20	990	6	984
2014-10-27	720	2	718
2014-11-03	608	1	607
2014-11-10	502	1	501
2014-11-17	445	0	445
2014-11-24	54	0	54

Table S.5: **Pixel count for Ferlo, 2014.** Number of pixels containing both hosts and vectors and number of pixels removed for having ( $\frac{N_1+N_4}{N_2+N_3} > 1000$ ), giving the total number of pixels where  $R_0$  is computed, for each introduction week.

Intro. date	Nb pixels contain hosts and vectors	Nb pixels removed due to ratio threshold	Nb pixels r0 computed
2015-07-13	1140	0	1140
2015-07-20	1100	0	1100
2015-07-27	877	0	877
2015-08-03	1630	0	1630
2015-08-10	1632	0	1632
2015-08-17	1628	0	1628
2015-08-24	1702	0	1702
2015-08-31	1691	2	1689
2015-09-07	1603	9	1594
2015-09-14	1700	26	1674
2015-09-21	1695	48	1647
2015-09-28	1681	45	1636
2015-10-05	1702	41	1661
2015-10-12	1646	36	1610
2015-10-19	1305	29	1276
2015-10-26	846	18	828
2015-11-02	592	10	582
2015-11-09	498	2	496
2015-11-16	318	1	317
2015-11-23	60	0	60
2015-11-30	7	0	7

Table S.6: **Pixel count for Ferlo, 2015.** Number of pixels containing both hosts and vectors and number of pixels removed for having ( $\frac{N_1+N_4}{N_2+N_3} > 1000$ ), giving the total number of pixels where  $R_0$  is computed, for each introduction week.

Intro. date	Nb pixels contain hosts and vectors	Nb pixels removed due to ratio threshold	Nb pixels r0 computed
2016-07-11	296	0	296
2016-07-18	912	0	912
2016-07-25	1057	0	1057
2016-08-01	1678	0	1678
2016-08-08	1622	0	1622
2016-08-15	1231	0	1231
2016-08-22	1293	0	1293
2016-08-29	1176	4	1172
2016-09-05	1332	21	1311
2016-09-12	1528	42	1486
2016-09-19	1273	45	1228
2016-09-26	987	37	950
2016-10-03	852	28	824
2016-10-10	690	25	665
2016-10-17	507	17	490
2016-10-24	375	6	369
2016-10-31	216	3	213
2016-11-07	125	3	122
2016-11-14	41	1	40
2016-11-21	2	0	2
2016-11-28	0	0	0

Table S.7: **Pixel count for Ferlo, 2016.** Number of pixels containing both hosts and vectors and number of pixels removed for having ( $\frac{N_1+N_4}{N_2+N_3} > 1000$ ), giving the total number of pixels where  $R_0$  is computed, for each introduction week.

## 4 Spatio-temporal pattern of $R_0$

	2014		2015		2016	
Region	<b>Ferlo</b>	<b>SRDV</b>	<b>Ferlo</b>	<b>SRDV</b>	<b>Ferlo</b>	<b>SRDV</b>
Nb pixels $R_0 > Q_{3,year}$	562	1588	436	2040	280	1841
mean nb events (weeks)	7.36	9.47	4.87	8.62	4.32	9.01
standard deviation nb events	3.37	5.06	2.99	5.02	2.38	5.67
	Total					
Nb pixels $R_0 > Q_{3,year}$	2150		2476		2121	
mean nb events (weeks)	8.92		7.96		8.39	
standard deviation nb events	4.77		4.93		5.58	

Table S.8: **Quantitative results to complete Figure 3 of main text.** Detailed number of pixels reaching  $R_0 > Q_{3,year}$  by study area. Mean and standard deviation of the number of weeks spent above this threshold.  $Q_{3,year}$  is the third quartile of  $R_0$  values, computed by season, independently of the study area and date of virus introduction.

## 5 Role of vector and host populations

### 5.1 Relative vector abundances over the rainy season

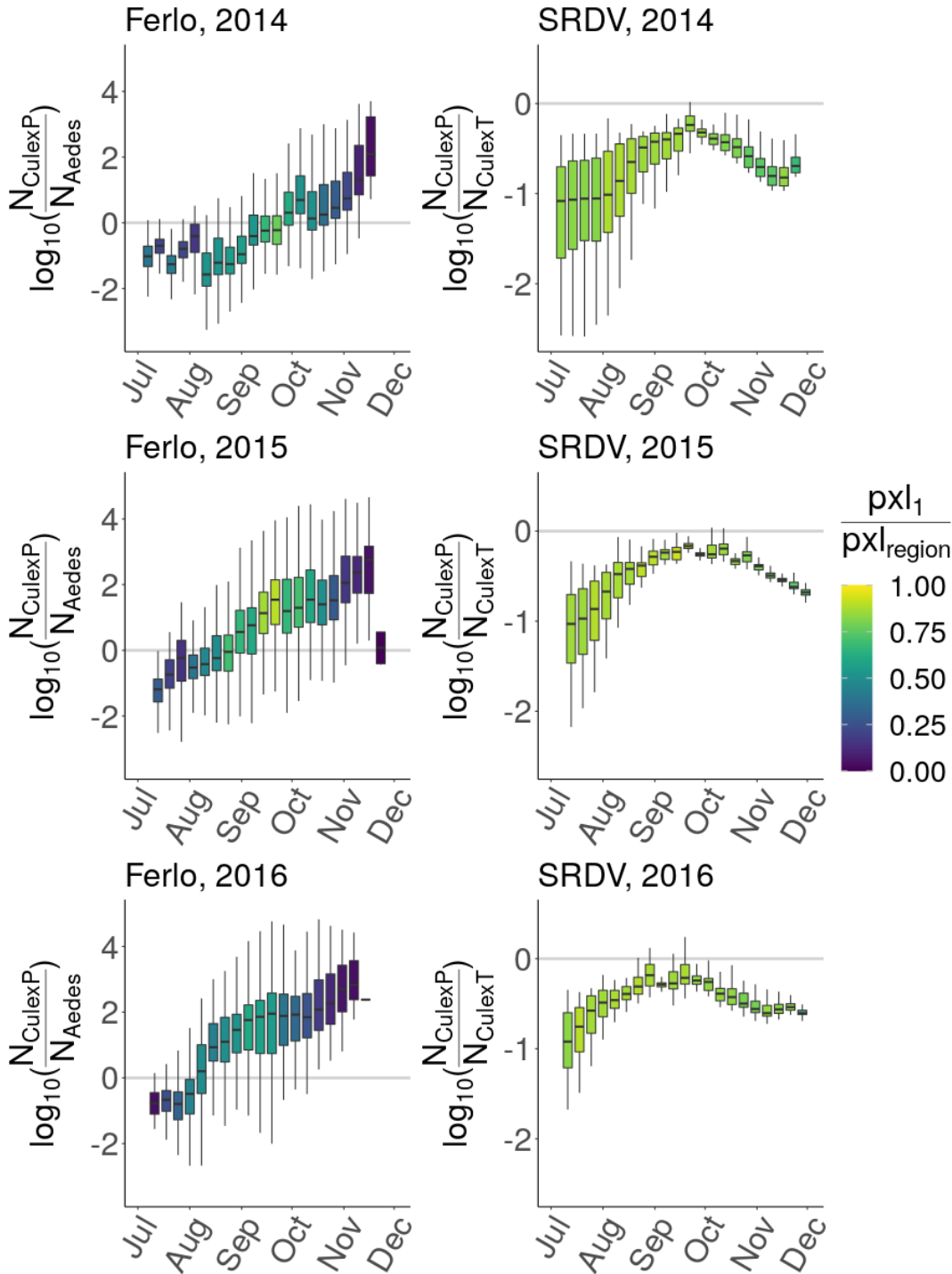


Figure S.4: Distribution of vector relative abundances within pixels having  $R_0 > 1$ . The metric is  $\log_{10}\left(\frac{N_{C. poicilipes}}{N_{Ae. v. arabiensis}}\right)$  in the Ferlo, on the right, and  $\log_{10}\left(\frac{N_{C. poicilipes}}{N_{C. tritaeniorhynchus}}\right)$  in SRDV, on the left. From top to bottom, 2014 to 2016. Boxplots are coloured by the number of pixels with  $R_0 > 1$  ( $pxl_1$ ) within the study area at each introduction date, normalized by the total number of pixels in the study area. In SRDV, *C. tritaeniorhynchus* is always more abundant than *C. poicilipes*. In the Ferlo, there is a time during each season where pixels with  $R_0 > 1$  go from having on average more *Ae. v. arabiensis* than *C. poicilipes* to the opposite. This switch happens a bit earlier each year from 2014 to 2016. The variability between pixels is important, for most virus introduction dates, there are pixels with both positive and negative  $\log_{10}$  ratios among those with  $R_0 > 1$ .

## 5.2 Effect of herd immunity

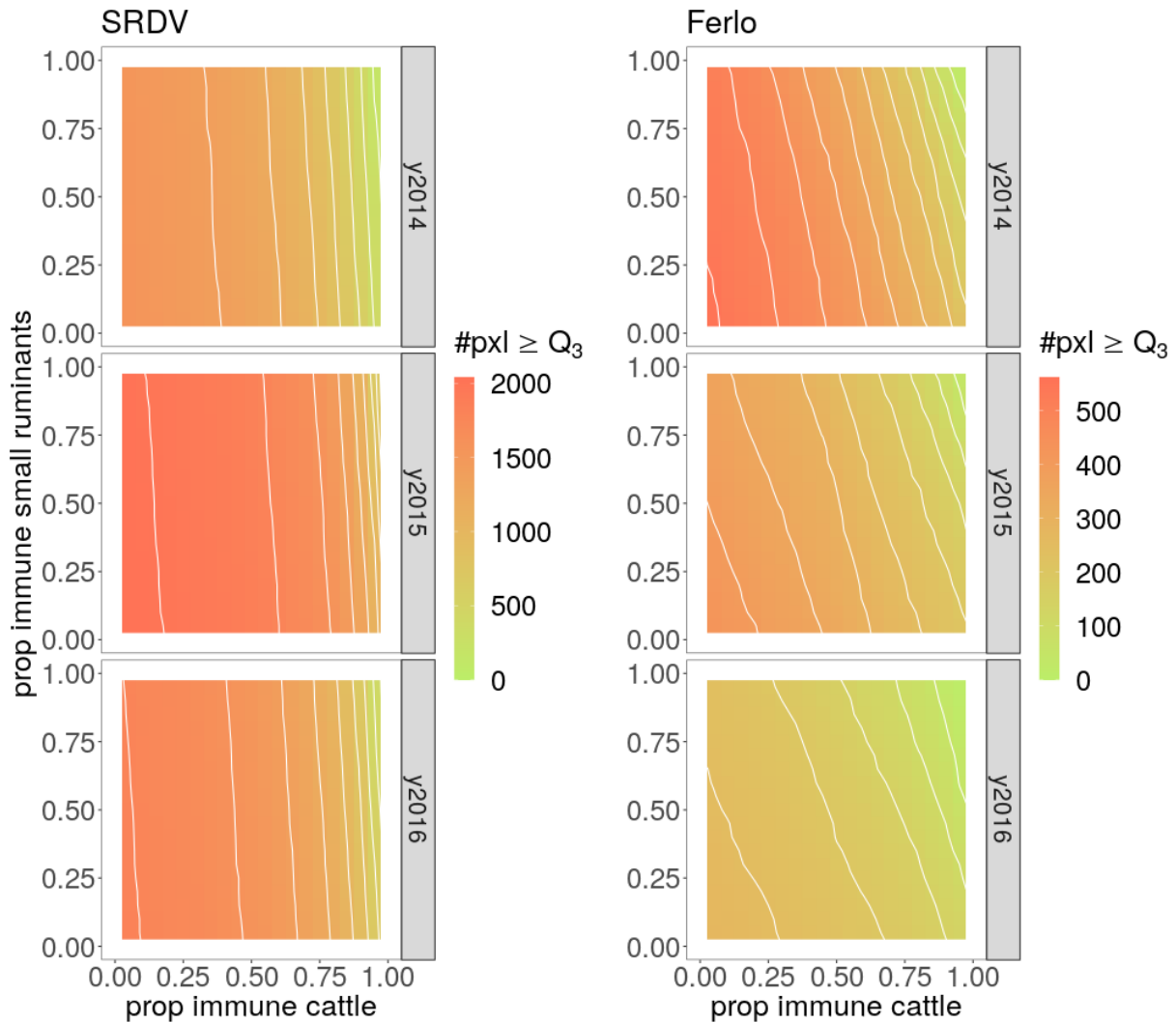


Figure S.5: Effect of increasing the immunity of the cattle population (x-axis) or small ruminant population (y-axis) on the number of pixels with  $R_0 > Q_{3,year}$  (third quartile of  $R_0$  values), by study area and season.

## 6 Sensitivity analysis

We performed a variance-based global sensitivity analysis using a Fourier Amplitude Sensitivity Testing (FAST, Saltelli et al. 2008). Parameters were varied within a 10% range using scaling factors (reference value of 1). A given set (scenario) of scaling factors was applied to all  $R_0$  computations of a given study area and rainy season, to maintain the spatial heterogeneity as well as the relative temporal dynamics of vector densities and temperature-dependent parameters. Temperature-dependent function formulas were kept, and temperature was not varied. We sampled 10,000 values per parameter. We tested whether our results on introduction dates and locations with high epidemic potential were robust to these parameter variations.



## 6.1 Sensitivity of $R_0$ temporal pattern

	2014		2015		2016	
SRDV	<b>08-11</b> (292,134)	08-04 (7,866)	09-14 (300,000)		<b>07-18</b> (256,762)	08-22 (4,156) 09-05 (39082)
Ferlo	09-22 (300,000)		<b>09-21</b> (299,999)	09-14 (1)	<b>09-05</b> (293,789)	09-12 (6,211)
Global (SRDV + Ferlo)	<b>2014-09-22 / 2015-09-14 / 2016-09-05</b> (291382) 2014-09-22 / 2015-09-21 / 2016-09-05 (8618)					

Table S.9: Introduction date inducing the highest number of pixels with  $R_0 > 1$  for the different scenarios tested in the sensitivity analysis, by study area and rainy season. 30 parameters are varied within a 10% range, with 10,000 values sampled per parameter, which gives 300,000 scenarios. Number of scenarios giving the same introduction date is given in parenthesis. When two different dates are possible, the one given by the reference scenario is in bold.

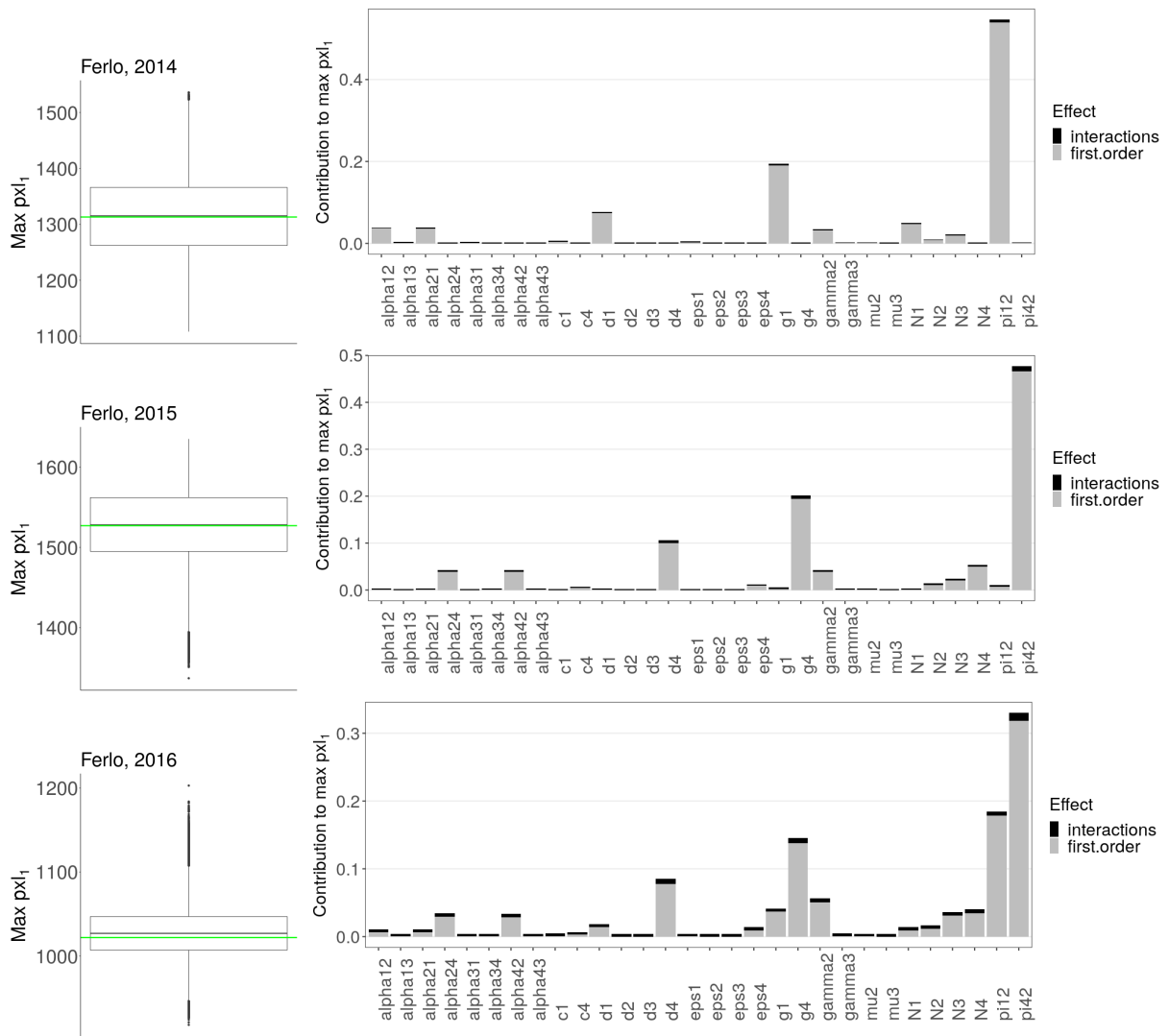


Figure S.6: **Sensitivity of  $R_0$  temporal pattern Ferlo** Left : Distribution of  $\text{max}(pxl_1)_{year}$  among scenarios tested in the sensitivity analysis. Green line shows the value with reference parameters. Right : Contribution of model parameteres to  $\text{max}(pxl_1)_{year}$ , introduction weeks when  $\text{max}(pxl_1)$  is reached might vary between scenarios (see Table S.9). Results for the Ferlo, 2014 to 2016 (top to bottom). In the box plots, the boundaries of the box indicate the 25<sup>th</sup> (bottom) and 75<sup>th</sup> (top) percentile. The black line within the box (often masked by the green line) marks the median. Whiskers above and below the box indicate the 10<sup>th</sup> and 90<sup>th</sup> percentiles. Points above and below the whiskers indicate outliers outside the 10<sup>th</sup> and 90<sup>th</sup> percentiles.

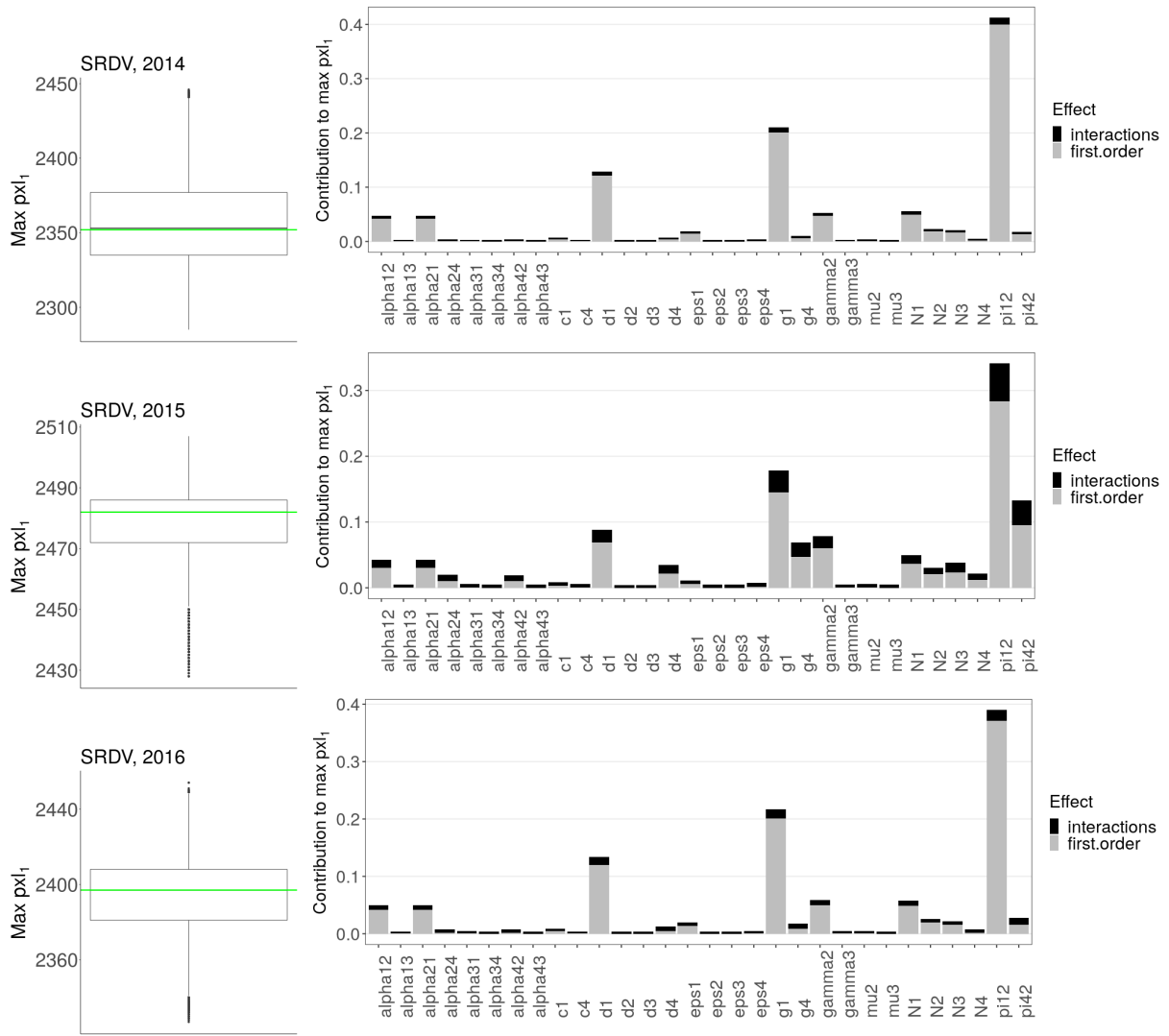


Figure S.7: **Sensitivity of  $R_0$  temporal pattern SRDV** Left : Distribution of  $\max(px1)_{year}$  among scenarios tested in the sensitivity analysis. Green line shows the value with reference parameters. Right : Contribution of model parameteres to  $\max(px1)_{year}$ , introduction weeks when  $\max(px1)$  is reached might vary between scenarios (see Table S.9). Results for the Ferlo, 2014 to 2016 (top to bottom). In the box plots, the boundaries of the box indicate the 25<sup>th</sup> (bottom) and 75<sup>th</sup> (top) percentile. The black line within the box (often masked by the green line) marks the median. Whiskers above and below the box indicate the 10<sup>th</sup> and 90<sup>th</sup> percentiles. Points above and below the whiskers indicate outliers outside the 10<sup>th</sup> and 90<sup>th</sup> percentiles.

## 6.2 Sensitivity of $R_0$ spatial pattern

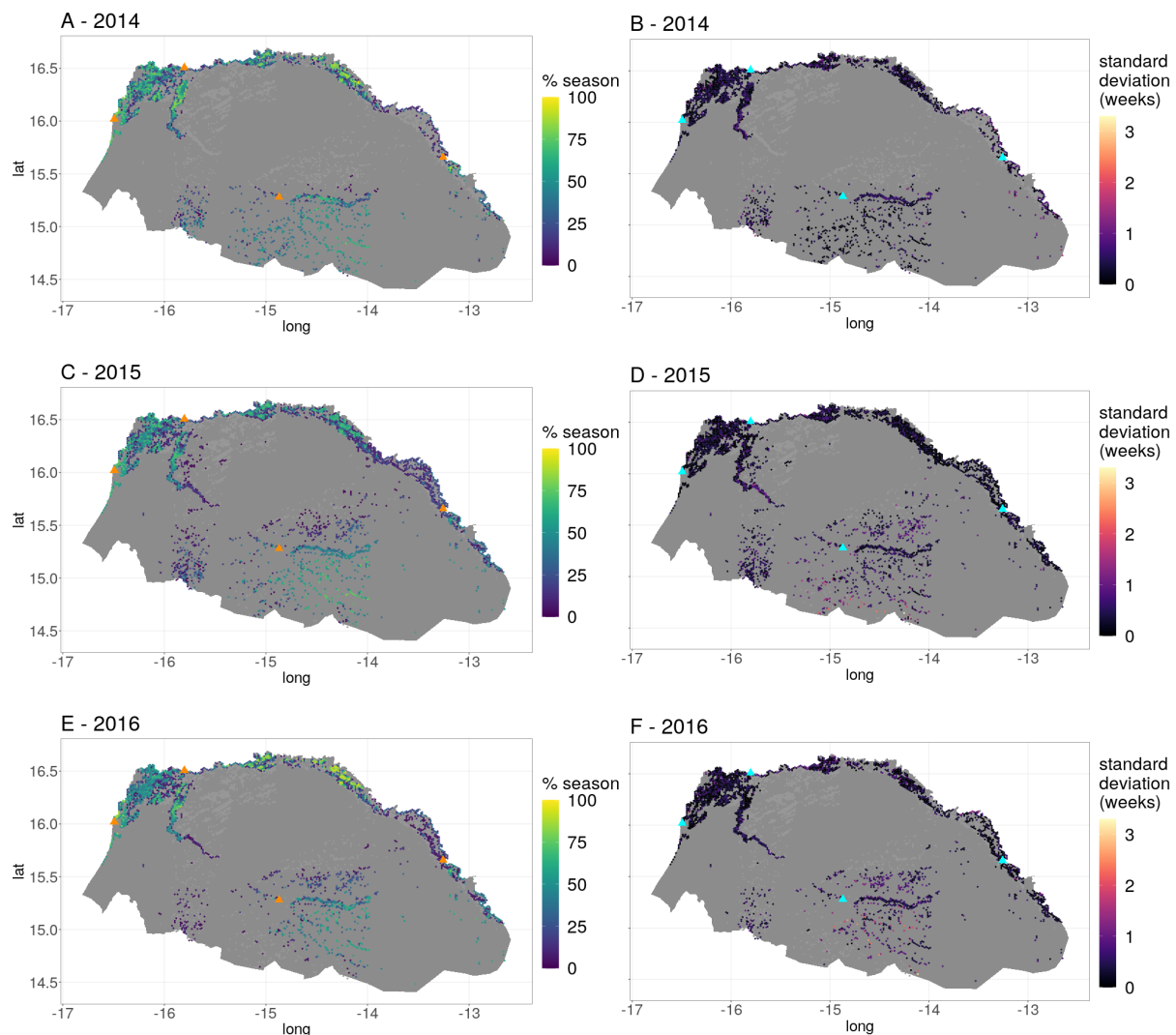


Figure S.8: Map of northern Senegal showing pixels with  $R_0 \geq Q_{3,region,year}$  at least once in the season. Coloured pixels fill this criteria in at least one of the 300,000 scenarios tested in the sensitivity analysis, grey pixels do not.  $Q_{3,region,year}$  is the third quartile of  $R_0$  values, computed by study area and season. Left: Pixels are coloured by the average % of the season spent above the threshold (1 to 21 weeks) over all the scenarios. Right: Pixels are coloured by the standard deviation of the time spent above the threshold (1 to 21 weeks) over all the scenarios. Triangles are important locations to ease figure reading (left to right, top to bottom : Rosso, Saint-Louis, Matam, Barkedji).

## 7 References

Ba Y, Diallo D, Dia I, Diallo, M. Comportement trophique des vecteurs du virus de la fièvre de la vallée du Rift au Sénégal: implications dans l'épidémiologie de la maladie. Bull Soc Pathol Exot. 2006;7.

Barker CM, Niu T, Reisen WK, Hartley DM. Data-Driven Modeling to Assess Receptivity for Rift Valley Fever Virus. Turell MJ, editor. PLoS Neglected Tropical Diseases. 2013 Nov 14;7(11):e2515.

Crabtree MB, Kading RC, Mutebi J-P, Lutwama JJ, Miller BR. Identification of host blood from engorged mosquitoes collected in western Uganda using cytochrome oxidase I gene sequences. Journal of Wildlife Diseases. 2013 Jul;49(3):611–26.

van den Driessche P, Watmough J. Reproduction numbers and sub-threshold endemic equilibria for compartmental models of disease transmission. Mathematical Biosciences. 2002 Nov;180(1–2):29–48.

- Edman JD, Downe AER. Host-blood sources and multiple-feeding habits of mosquitoes in Kansas. 1964;24(2):154-60.
- Gaff HD, Hartley DM, Leahy NP. An epidemiological model of Rift Valley fever. 2007;12.
- Gilbert M, Nicolas G, Cinardi G, Van Boeckel TP, Vanwambeke SO, Wint GRW, et al. Global distribution data for cattle, buffaloes, horses, sheep, goats, pigs, chickens and ducks in 2010. Scientific Data. 2018 Oct 30;5:180227.
- Gordon SW, Tammariello RF, Linthicum KJ, Wirtz' RA, Digoutte JP. Feeding patterns of mosquitoes collected in the Senegal River basin. Journal of the american mosquito control association. 1991;7(3):424-32.
- Hammami P, Lancelot R, Lesnoff M. Modelling the Dynamics of Post-Vaccination Immunity Rate in a Population of Sahelian Sheep after a Vaccination Campaign against Peste des Petits Ruminants Virus. Munderloh UG, editor. PLOS ONE. 2016 Sep 7;11(9):e0161769.
- Madder DJ, Surgeoner GA, Helson BV. Number of Generations, Egg Production, and Developmental Time of Culex Pipiens and Culex Restuans (Diptera: Culicidae) in Southern Ontario1. Journal of Medical Entomology. 1983 May 26;20(3):275-87.
- Muturi EJ, Muriu S, Shililu J, Mwangangi JM, Jacob BG, Mbogo C, et al. Blood-feeding patterns of Culex quinquefasciatus and other culicines and implications for disease transmission in Mwea rice scheme, Kenya. Parasitology Research. 2008 May;102(6):1329-35.
- Ndiaye PI, Bicout DJ, Mondet B, Sabatier P. Rainfall triggered dynamics of Aedes mosquito aggressiveness. Journal of Theoretical Biology. 2006 Nov;243(2):222-9.
- Saltelli, A, Chan, R, Scott, FM. Sensitivity analysis. Wiley. 2008. 494 p. ISBN: 978-0-470-74382-9.
- Tran A, Fall AG, Biteye B, Ciss M, Gimonneau G, Castets M, et al. Spatial Modeling of Mosquito Vectors for Rift Valley Fever Virus in Northern Senegal: Integrating Satellite-Derived Meteorological Estimates in Population Dynamics Models. Remote Sensing. 2019 Apr 30;11(9):1024.
- Turell MJ. Effect of environmental temperature on the vector competence of Aedes fowleri for rift valley fever virus. Research in Virology. 1989 Jan;140:147-54.
- Turner J, Bowers RG, Baylis M. Two-Host, Two-Vector Basic Reproduction Ratio (R0) for Bluetongue. Gomez-Gardenes J, editor. PLoS ONE. 2013 Jan 8;8(1):e53128.
- Wonham MJ, Lewis MA, Renclawowicz J, van den Driessche P. Transmission assumptions generate conflicting predictions in host-vector disease models: a case study in West Nile virus. Ecology Letters. 2006 Jun;9(6):706-25.

## 8 Credits

Regarding icons used in Figures 1, S.1, and the graphical abstract.

Droplets: made by Good Ware (<https://www.flaticon.com/authors/good-ware>), from Flaticon.

Sheep: made by Turkukub (<https://www.flaticon.com/authors/turkkub>), from Flaticon.

Temperature: made by Prosymbols (<https://www.flaticon.com/authors/prosymbols>), from Flaticon.

Cow: made by Freepik (<https://www.flaticon.com/authors/freepik>), from Flaticon.

Mosquito (Figures 1, S.1): made by Freepik, from Flaticon.

Mosquito (graphical abstract): made by Monkik (<https://www.flaticon.com/authors/monkik>), from Flaticon.

# 4

## Transmission potential of RVFV livestock hosts

The preprint in Section 4.2 is under revision at Plos Computational Biology.

### 4.1 [In French] Résumé grand public

*Préambule: Le travail présenté ici est le fruit de ma collaboration avec l'université de Wageningen aux Pays-Bas, et plus particulièrement avec Dr Quirine ten Bosch. Le contexte de cette collaboration est présenté plus en détails dans l'annexe C. Il s'agit du rapport de mobilité envoyé à l'école doctorale EGAAL le 23 mars 2020. Il vous permettra également de réaliser le changement de question de recherche que nous avons opéré depuis cette date, et l'état d'esprit dans lequel je me trouvais au début de la pandémie de Covid-19 !*

Dans le résumé du chapitre 3 (3.1), j'ai évoqué les différents facteurs qui pouvaient contribuer à l'apparition d'une épidémie. L'un d'eux était la nécessité que le virus se multiplie efficacement dans l'individu qu'il infecte, jusqu'à le rendre contagieux, c'est-à-dire capable de transmettre le virus à son tour. Dans le présent chapitre, nous allons étudier la contagiosité des 3 principaux animaux d'élevage sujets à l'infection par le virus de la FVR: les chèvres, les bovins, et les moutons.

*Pour déterminer quelle espèce contribue le plus à la transmission du virus de la FVR dans une population, il manque une estimation de leur contagiosité individuelle*

Ces 3 espèces<sup>1</sup> sont touchées différemment par la FVR. En terme de signes cliniques, les petits ruminants sont généralement plus sévèrement touchés (avortement, mort) que les bovins. Par ailleurs, bien que les bovins constituent souvent une cible privilégiée pour les moustiques, ils peuvent ne représenter qu'une petite partie de l'effectif total des troupeaux. Ces éléments sont importants à prendre en compte, mais pour déterminer précisément quelle(s) espèce(s) contribuent le plus à la transmission du virus de la FVR dans une population, il manque justement une estimation de leur contagiosité individuelle. Pour quantifier plus précisément cette contagiosité, une manière de procéder est d'observer la quantité de virus produite par les animaux durant leur infection, et de déterminer le lien entre cette quantité de virus et la probabilité d'infecter les moustiques qui viendraient les piquer. C'est cela que nous avons modélisé dans ce chapitre, en nous appuyant sur des données produites en laboratoire.

*Pour quantifier la contagiosité d'un animal, on peut mesurer la quantité de virus produite pendant son infection, et déterminer le lien entre cette quantité de virus et la probabilité d'infecter les moustiques qui viendraient le piquer*

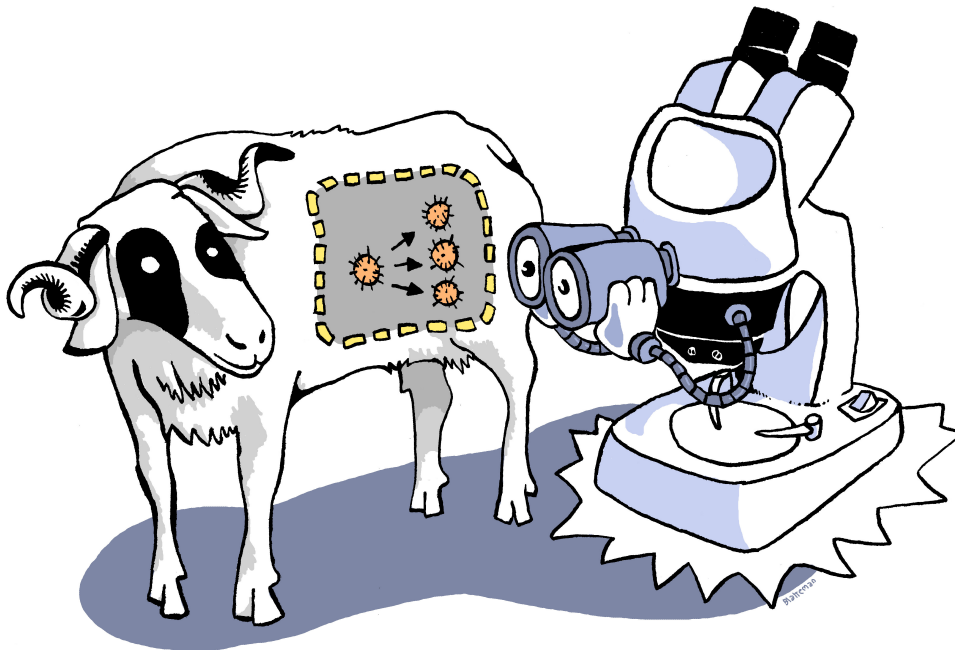
#### 4.1.1 La multiplication du virus dans un hôte : comment ça marche ?

L'appartenance des virus au règne du vivant fait débat. En effet, pour beaucoup, la capacité à se reproduire de manière autonome est une condition sine qua non à l'appartenance au monde vivant. Or, les virus en sont incapables. Pour reproduire leur matériel génétique, ils ont besoin d'infecter un hôte<sup>2</sup>, de pénétrer dans ses cellules et de les hacker pour les obliger à produire de nouveaux virus. Récemment, la reconstruction de "l'arbre généalogique" des virus semble montrer qu'ils descendent de cellules anciennes, capables à l'époque de se reproduire toutes seules<sup>3</sup>! La pression évolutive, poussant à la réduction de la taille des génomes, aurait fait perdre aux virus cette propriété clé des êtres vivants. Une question se pose alors : peut-on être exclu du règne vivant si l'on descend directement d'un être vivant? Pour ma part, je n'ai pas l'expertise nécessaire pour répondre à cette question...

<sup>1</sup> J'utilise ici ce terme de manière abusive dans un souci de vulgarisation. Les catégories mentionnées, si on s'en réfère à la classification scientifique des espèces, renvoient plutôt à des genres (*Ovis*, *Capra*) ou sous-familles (*Bovinae*).

<sup>2</sup> Ces hôtes peuvent être de toutes sortes : animaux, végétaux, ou même bactéries! On parle dans ce dernier cas de virus bactériophage.

<sup>3</sup> Attention, ceci est un article scientifique, en anglais, non vulgarisé ;) A.Nasir and G. Caetano-Anollés (2015) A phylogenomic data-driven exploration of viral origins and evolution. *Science Advances*, Vol. 1, no. 8, e1500527 <https://advances.sciencemag.org/content/1/8/e1500527>



Bon, revenons-en à nos moutons<sup>4</sup> (et chèvres, et bovins)! Dans notre projet, nous disposons de données expérimentales générées par l'université de Wageningen (Pays-Bas). Dans ces expériences, des veaux, chevreaux et agneaux ont été infectés par le virus de la FVR, selon un protocole respectant les directives européennes<sup>5,6</sup>. Des prélèvements sanguins ont ensuite été effectués chaque jour pour mesurer la quantité de virus circulant dans les hôtes. Cette quantité de virus, aussi appelée charge virale, ou virémie, a été mesurée de deux manières. Comme je ne suis pas virologue, j'ai moi-même eu du mal à bien comprendre les types de protocoles utilisés et comment cela allait impacter la construction de mon modèle mathématique. Maintenant que j'y vois plus clair, je vais tenter de vous expliquer ça simplement. Je m'essaie donc aujourd'hui à l'exercice de la métaphore filée : je vous emmène dans une usine de t-shirt !

<sup>4</sup> Vous aussi vous vous demandez d'où vient cette drôle d'expression? D'après <http://www.linternaute.fr/expression/langue-francaise/844/revenons-en-a-nos-moutons/>, c'est la comédie "La Farce du Maître Pathelin" (XVe siècle), dont l'auteur reste inconnu, qui est à l'origine de cette expression. Le héros, Pathelin trompe le marchand Guillaume pour lui acheter à bas prix un drap. Au moment de payer, Pathelin feint d'être mourant et de délirer. Guillaume se demande alors si lui-même ne délire pas et si la transaction a réellement eu lieu. Guillaume va ensuite être trompé à nouveau par le berger Thibault, qui lui vole tous ses moutons. Il décide de porter ces deux affaires devant le juge mais finit par confondre les draps et les moutons, tant et si bien que le juge, agacé, lui demande fermement de "revenir à ses moutons". Depuis, l'expression a subsisté et a conservé son sens originel.

<sup>5</sup> En accord avec la directive européenne 2010/63/EU et la loi néerlandaise sur l'expérimentation animale BWBR0003081. Procédure ayant nécessité l'accord du Comité d'éthique animale de l'université de Wageningen. Permis AVD401002017816 et AVD4010020187168 accordés par l'autorité centrale néerlandaise.

<sup>6</sup> Précisons également que cette expérience faisait partie d'essais vaccinaux. En fait, pour ce projet, nous avons utilisé les données du "groupe témoin" qui n'avait pas été vacciné et a donc développé la maladie. Mais l'objectif de l'étude était de montrer l'efficacité du vaccin actuellement développé pour la FVR par l'université de Wageningen (spoiler : le groupe vacciné, une fois la FVR injectée, ne développe pas de charge virale car immunisé).

Le génome du virus de la FVR est composé de 3 segments distincts, appelés S, M, L, en rapport avec leur taille, comme des t-shirt! Lorsque le virus infecte les cellules d'un hôte, il les transforme en petites usines Amaron<sup>7</sup>. Ces usines commencent alors à produire des colis de t-shirt à foison et à les envoyer un peu partout dans l'hôte. Théoriquement, ces usines sont programmées pour préparer un seul et unique type de commande : des colis (= virus) comportant un t-shirt de chaque taille (un S, un M, un L), tous en bon état. Mais les usines ne sont pas infaillibles, alors il existe des erreurs de packaging: une ou plusieurs tailles manquantes, ou en plusieurs exemplaires, dans le colis. Il existe également des erreurs de fabrication: des t-shirt distendus, avec un trou, une manche en trop ou en moins, vous voyez l'idée. La particularité du système décrit ici est qu'il s'auto-alimente : les usines produisent des colis, et ces mêmes colis sont capables d'aller créer de nouvelles usines (= infecter des cellules)! Cependant, on sait que parmi tous les colis produits (charge virale totale), seule une partie est capable de rentrer dans les cellules pour les pirater et en faire de nouvelles usines (charge virale infectieuse). Mais nous ne savons pas exactement quel types de colis sont infectieux. Il y a fort à parier que les colis "idéaux" que j'évoquais précédemment (un S, un M, un L, tous en bon état), sont les principaux colis infectieux, mais il existe peut-être certains mécanismes permettant à des colis imparfaits de créer de nouvelles usines<sup>8</sup>. Ces mécanismes sont difficiles à étudier et n'ont pas été explorés dans ce chapitre. Nous avons cependant pu, grâce aux méthodes de comptage que je vais vous présenter, caractériser un peu mieux le rendement et l'efficacité des usines (charge virale totale et infectieuse) dans chaque type d'hôte.

La première méthode, nommée RT-qPCR, permet de dénombrer tous les t-shirt d'une certaine taille (par exemple M), sans savoir dans quel type de colis ils se trouvent (complet, incomplet, défectueux). Cette méthode est considérée comme une bonne approximation de la charge virale totale. La deuxième méthode, appelée TCID<sub>50</sub>, consiste à créer une nouvelle unité de mesure, puisque l'identification et le dénombrement des colis infectieux ne peut pas se faire directement. En fait, le protocole consiste à récupérer des containers de colis, sans savoir ce que ces colis contiennent. Lorsque le contenu de ce container, une fois mis en contact avec 100 cellules saines, permet la création de 50 nouvelles usines Amaron (50%), alors le container devient la dose référence, et la charge virale infectieuse est ensuite exprimée en multiple de cette nouvelle unité. Elle reflète donc la capacité des colis à créer de nouvelles usines, mais pas la quantité exacte de t-shirt ou type de colis présente à l'intérieur. Ces deux mesures sont

---

<sup>7</sup> Toute ressemblance avec un nom de produit, d'organisation ou de personne existant serait purement fortuite.

<sup>8</sup> Un des mécanismes soupçonnés est la complémentation : un colis [S,M] et un colis [L] (par exemple) arrivent séparément dans une cellule, leurs contenus se complètent alors et permettent l'infection.



complémentaires et nous ont permis de construire un modèle plus réaliste de ce qui se passe dans l'animal lorsqu'il est infecté.

Ainsi, dans le modèle mathématique développé, présenté Figure 4.1, les particules virales infectieuses  $V_{inf}$ , pénètrent dans les cellules de l'hôte  $T$  (pour "target cell", cellule cible, car les virus ne peuvent pas infecter tous les types de cellules présents dans l'animal). Une fois le virus internalisé, les cellules passent d'abord par une phase d'éclipse (latente)  $L$ , c'est à dire qu'elles ne produisent pas tout de suite de nouveaux virus. Une fois dans le stade infecté  $I$ , les cellules produisent de nouvelles particules virales, qui peuvent être infectieuses ou pas. Nous représentons ainsi la quantité totale de virus produite ( $V_{tot}$ ), qui doit correspondre au mieux à la mesure de la charge virale totale (RT-qPCR) présentée précédemment ; et la charge virale infectieuse ( $V_{inf}$ ), qui doit correspondre au mieux à la mesure TCID<sub>50</sub>, et qui est une sous-partie de  $V_{tot}$ . D'autres mécanismes sont intégrés dans ce modèle, à savoir :

- la mort des cellules infectées, qui cessent alors de produire de nouveaux virus
- la possible dégradation de virus infectieux en virus non-infectieux : une fois sorti de l'usine, l'état et le contenu du colis peut donc potentiellement évoluer, si le livreur n'est pas très précautionneux par exemple ;-)
- l'élimination des particules virales, infectieuses ou non, par l'hôte

Vous avez peut-être remarqué que la réponse immunitaire, dont on nous parle souvent lorsqu'on est malade, n'apparaît pas explicitement ici : pas de compartiment "anticorps" ou "lymphocytes" pour ne citer qu'eux. Cela ne veut pas dire que la réponse immunitaire ne joue pas de rôle dans notre cas, mais plutôt que nous avons pris son action en compte de manière indirecte, dans les paramètres du modèle. En effet, la réponse immunitaire peut influencer sur la capacité du virus à pénétrer dans les cellules, sur la durée de vie des cellules une fois infectée, ou encore la durée de vie des particules virales dans l'hôte. Ces processus sont tous pris en compte dans le modèle, via les paramètres (symboles au niveau des flèches Figure 4.1), mais ne sont pas assignés à un acteur (boîte de couleur Figure 4.1) donné. Enfin, il est important de noter que nous avons à disposition des données sur la charge virale dans l'animal au cours de son infection, mais pas de suivi de l'état des cellules de l'hôte, qu'il n'est en pratique pas possible de surveiller en temps réel et in vivo (dans l'animal vivant). Nous avons fait l'hypothèse que les cellules cibles majoritairement responsables de la charge virale de l'animal étaient les cellules du foie (hépatocytes), car c'est l'organe touché en premier et le plus sévèrement lors

d'une infection par le virus de la FVR.

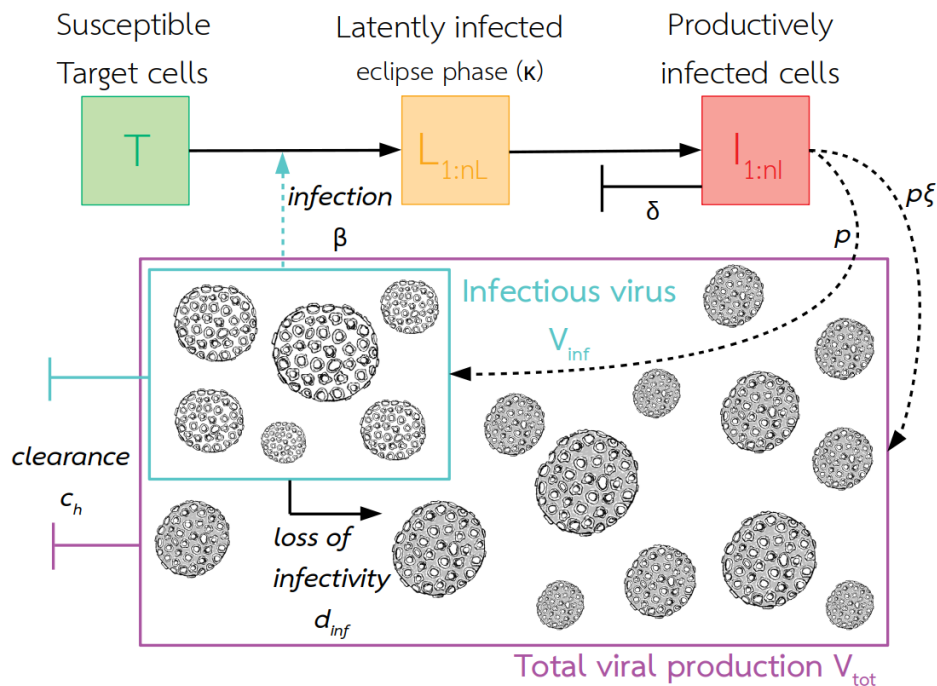


**Figure 4.1** – Schéma du modèle intra-hôte (idem Figure 4.6).

Susceptible target cells : cellules cibles sensibles

Latently infected : infection latente

Productively infected cells : cellules infectées productrices de particules virales

Infectious virus : particule virale infectieuse

Clearance : clairance (élimination)

Loss of infectivity : perte d'infectiosité

Total viral production : Charge virale totale

Une fois la structure du modèle arrêtée, la prochaine étape consiste à trouver les valeurs de paramètres permettant de reproduire au mieux les charges virales observées chez les différentes espèces d'hôte.

#### 4.1.2 Comment faire pour qu'un modèle mathématique reproduise fidèlement les données réelles ?

J'ai expliqué en introduction que le but de ce chapitre était d'étudier la contagiosité des différentes espèces d'hôtes, et que pour cela il nous fallait faire le lien entre virus produit par l'hôte et probabilité d'infecter un moustique. J'ai ensuite expliqué que nous disposions de données sur les quantités de virus produites par les hôtes, mesurées quotidiennement dans leur plasma. D'ailleurs, si on regarde ces données brutes (Figure 4.2), on peut déjà remarquer des différences entre espèces :

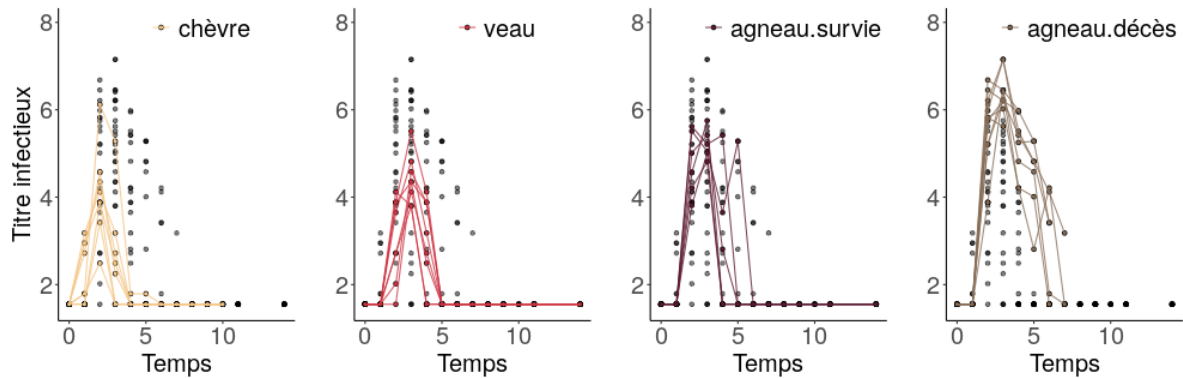


**Figure 4.2** – Titre infectieux au cours du temps mesuré chez les animaux à la suite de leur infection par le virus de la FVR. Toutes les données (points) sont représentées dans chaque case, avec le groupe d'intérêt en couleur. Les lignes regroupent les mesures effectuées sur un même individu.

Si on se concentre sur la charge virale infectieuse par exemple, on voit que celle des chèvres démarre plus tôt que tout le monde, mais qu'elle n'atteint pas des niveaux aussi élevés que les autres espèces. On voit que ce sont les moutons qui atteignent les charges virales infectieuses les plus élevées, et que parmi eux, les individus ayant succombé à l'infection ont des charges virales plus élevées que ceux ayant survécu.

Super! On a déjà caractérisé plein de choses. Mais alors... pourquoi je suis venue vous embrouiller tout à l'heure avec un modèle mathématique visant à reproduire les données observées? Pourquoi ne pas directement utiliser ces données et s'atteler à faire le lien avec la transmission aux moustiques? Parce qu'en tant que chercheuse, ce qui m'anime est de comprendre ce que j'observe! Qu'est-ce qui explique ces différences entre espèces, quels mécanismes? Loin de pouvoir répondre très précisément à cette question, la modélisation offre un moyen de soulever des pistes.

### *Un modèle mécaniste peut permettre d'identifier des processus biologiques responsables des différences entre les espèces*

Comme nous avons développé un modèle dit mécaniste, les paramètres présents dans les équations du modèle correspondent à des mécanismes précis, ils ont une signification biologique. Dès lors, si on arrive à déterminer quelles valeurs de paramètres, pour chaque espèce, permet de ressembler le plus aux données observées, alors on pourra potentiellement identifier les mécanismes qui diffèrent le plus entre les espèces, et surtout, quantifier cette différence. Mais comme le système est complexe, les paramètres sont nombreux et influent sur des caractéristiques fines de la courbe (Figure 4.3). Il n'est donc pas possible de trouver "à la main" le meilleur jeu de

paramètres. C'est pourquoi on fait appel à un algorithme pour leur estimation.

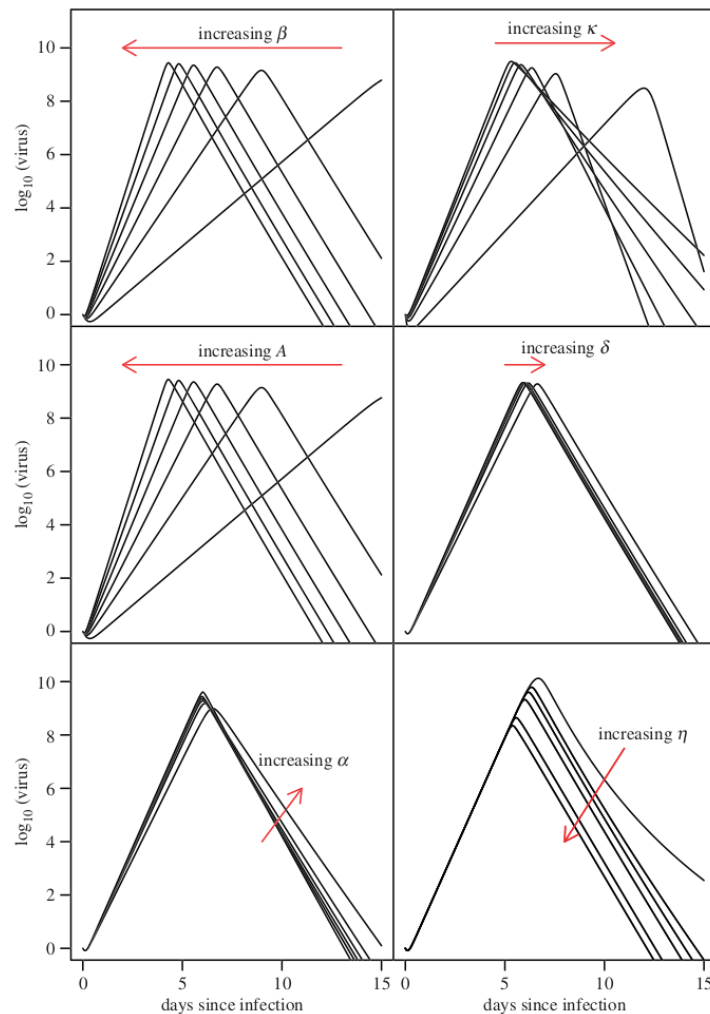


**Figure 4.3** – Sensibilité du modèle au changement de valeurs des paramètres. Il s’agit ici de montrer comment l’augmentation (sens de la flèche) de différents paramètres (cases) d’un modèle très similaire au notre, change l’allure de la charge virale (ordonnée) au cours du temps (abscisse). Extraite de Clapham et al., 2014.

L’idée globale de cet algorithme peut être décrite en plusieurs étapes successives:

1. Pour faire tourner notre modèle, il faut lui fournir

- Des paramètres, à titre d’exemple : mortalité des cellules infectées, vitesse d’élimination des particules virales etc. Dans notre modèle, il y en a 10.
- Des conditions initiales, soit l’état du système au début de la simulation. Dans notre modèle, il y en a 3 principales : le nombre de cellules susceptibles ( $T$ ) de l’hôte au moment de l’infection et le nombre de particules virales, infectieuses ( $V_{inf}$ ) et totales ( $V_{tot}$ ), que l’hôte reçoit au départ, ce qu’on peut appeler inoculum. Logiquement, on commence avec 0 cellules dans l’état latent ( $L$ ) et 0 dans l’état infecté ( $I$ ).

2. Tous les paramètres ne peuvent pas être estimés par l'algorithme. En effet, certains ont des effets très similaires sur la dynamique virale (cf par exemple  $A$  et  $\beta$  dans la Figure 4.3), donc on ne peut pas savoir qui de l'un ou de l'autre doit être modifié le cas échéant. Ces paramètres ont peut-être un effet différent sur d'autres compartiments du modèle, par exemple le nombre de cellules infectées au cours du temps. Mais comme cela ne fait pas partie des données mesurées expérimentalement, nous ne pouvons pas les discriminer sur cette base.

Il faut alors fixer certains paramètres, en fonction de ce qu'on connaît du système. Par exemple on sait quelle quantité de virus a été injectée à chaque animal, et on connaît grâce à d'autres expériences réalisées *in vitro* la durée approximative de la phase latente, à savoir 8h.

Pour les paramètres restant à estimer, il faut aider l'algorithme à explorer l'espace des paramètres, en le restreignant à des valeurs biologiquement réalistes. C'est une manière d'aider l'algorithme grâce à notre connaissance a priori du système. Par exemple, une cellule infectée pourrait raisonnablement survivre de quelques heures à quelques jours, mais pas des mois ou années. L'algorithme ne sait pas ça au départ donc si on ne lui précise pas, il va tester toutes les valeurs possibles et imaginables et vous n'êtes pas prêt d'avoir votre résultat. Une fois qu'on a fait ça, on est paré pour la suite!

3. Un premier jeu de paramètres et conditions initiales est défini, dont certains resteront fixes pendant tout le processus d'estimation, comme je viens de l'expliquer. La dynamique virale est simulée par le modèle. On la compare avec les données expérimentales, à l'aide d'un score qui quantifie à quel point notre courbe passe près des données.
4. Une fois ce score obtenu, on le garde en mémoire, et on fait tourner une nouvelle fois le modèle avec un autre jeu de paramètres tiré aléatoirement. On compare ensuite les scores des deux simulations, pour savoir laquelle des deux reproduit le mieux les données. L'algorithme se sert de ces comparaisons de scores pour naviguer dans l'espace des paramètres. Les tirages "aléatoires" de paramètres favorisent en fait ceux qui produisent de meilleurs scores.
5. Une fois ce processus réitéré plusieurs dizaines de milliers de fois, on obtient une estimation des différents paramètres de notre modèle. L'algorithme ne nous donne pas une valeur unique pour chaque paramètre, mais une densité de probabilité : c'est à dire un ensemble de valeurs, auxquelles sont assignées des probabilités d'être celles qui aurait pu

générer les données observées. La notion d'incertitude est donc directement intégrée dans le processus d'estimation.

Voilà, vous avez les bases de l'algorithme Metropolis Hastings<sup>9</sup> Monte Carlo Markov Chain et de l'inférence bayésienne<sup>10</sup>, rien que ça<sup>11</sup>! Je vous laisse digérer cette information, prendre un verre d'eau, un carré de chocolat. Je vais maintenant vous expliquer ce qui se passe quand le moustique vient se nourrir sur un hôte avec une charge virale plus ou moins élevée.

### 4.1.3 *Le voyage du virus dans un moustique*

Une femelle moustique ne s'accouple qu'une seule fois. Lors de cet évènement, elle stocke les spermatozoïdes du mâle dans sa spermathèque, et les utilisera à intervalles réguliers pour féconder les œufs qu'elle produit avant de les pondre. C'est pour obtenir les protéines nécessaires à la maturation des oeufs que la femelle doit se nourrir de sang et donc, piquer un hôte vertébré<sup>12</sup>.

Pour piquer, la femelle se sert de sa trompe (ou proboscis). C'est un organe complexe<sup>13</sup> qui lui permet notamment de détecter les vaisseaux sanguins et récolter du sang. Pour éviter qu'il ne coagule dans sa trompe, elle nous injecte simultanément un peu de salive, qui contient des molécules anticoagulantes. C'est cette salive qui est responsable de la démangeaison que l'on ressent, mais c'est surtout par elle que transitent les virus que les moustiques peuvent transmettre à leurs hôtes ! En résumé, c'est par le sang qu'il ingère qu'un moustique devient porteur, et donc vecteur, d'un virus, mais c'est par la salive qu'il le transmet à son tour. Ce passage du sang d'un hôte aux glandes salivaires du moustique n'est pas systématique ni anodin, et la recherche est loin d'avoir résolu tous les mystères de ce voyage.

---

<sup>9</sup> C'est le nom communément employé, mais il laisse de côté une des contributrices majeures à son développement, Arianna Rosenbluth <https://www.nytimes.com/2021/02/09/science/arianna-wright-dead.html> (en anglais)

<sup>10</sup> Une autre ressource l'explique bien, avec des cookies et des dinosaures (en anglais simple et avec des dessins) ! <https://psyarxiv.com/w5vbp/>

<sup>11</sup> Je vous avoue que ça me fait un peu mal de voir résumé en une page un processus que j'ai mis près d'un an à maîtriser et coder correctement... Les joies de la vulgarisation!

<sup>12</sup> Pour son alimentation, le moustique se nourrit autrement du nectar des fleurs. Voilà donc une partie de la réponse à la question qu'on me pose souvent "A quoi servent les moustiques?" Ce sont des pollinisateurs! Pour aller plus loin : <https://theconversation.com/la-vie-etrange-secrete-et-tres-ecolos-des-moustiques-devoilee-128451>

<sup>13</sup> Il y a 6 "aiguilles" différentes dans sa trompe, chacune avec une fonction ! Pour visualiser ça plus en détails, je vous suggère cette vidéo : <https://youtu.be/rD8SmacBUcU>

Une fois absorbé, le sang et les particules virales qu'il contient se retrouvent dans l'estomac du moustique (Figure 4.4, étape 2). Là, si l'environnement y est propice<sup>14</sup>, le virus s'y multiplie, on dit alors que le moustique est *infecté*. Le succès de cette étape dépend notamment de la dose de virus ingérée initialement. On comprend donc le lien avec ce qu'on a vu précédemment sur la virémie des hôtes au cours du temps. Ensuite, le virus doit franchir une première barrière pour atteindre le système circulatoire du moustique, dans lequel circule non pas du sang mais ce qu'on appelle l'hémolymphe (Figure 4.4, étape 3). On dit alors que l'infection est *disséminée*. Enfin, si le virus franchit la deuxième barrière et pénètre dans les glandes salivaires (Figure 4.4, étape 4), alors le moustique sera capable de *transmettre* le virus au prochain hôte qu'il piquera.

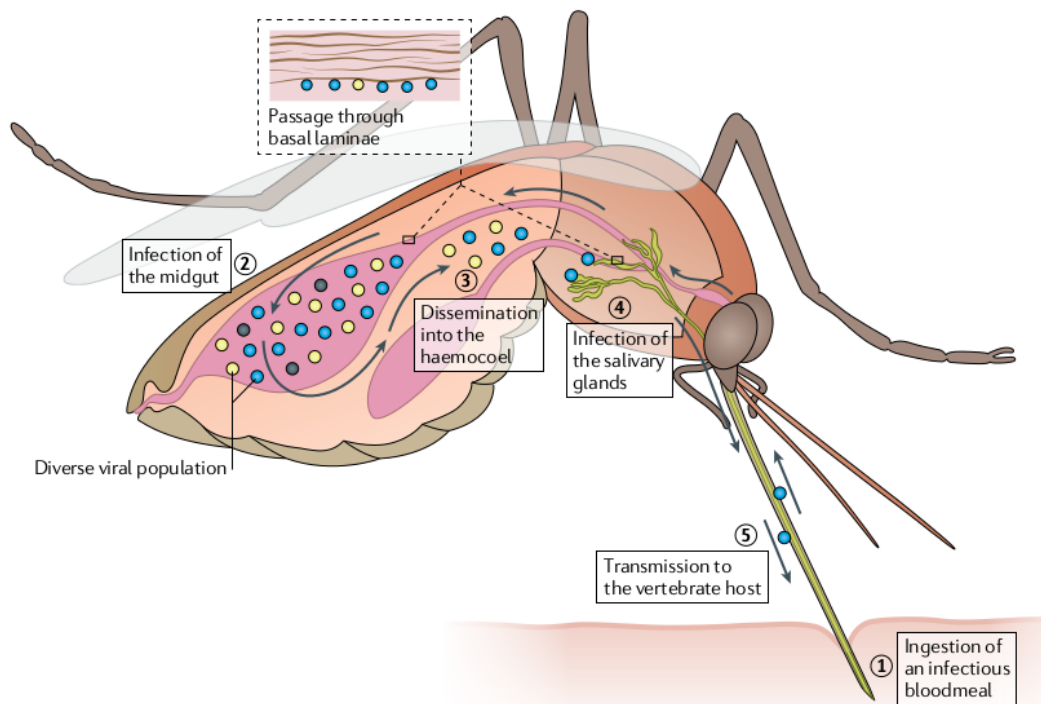
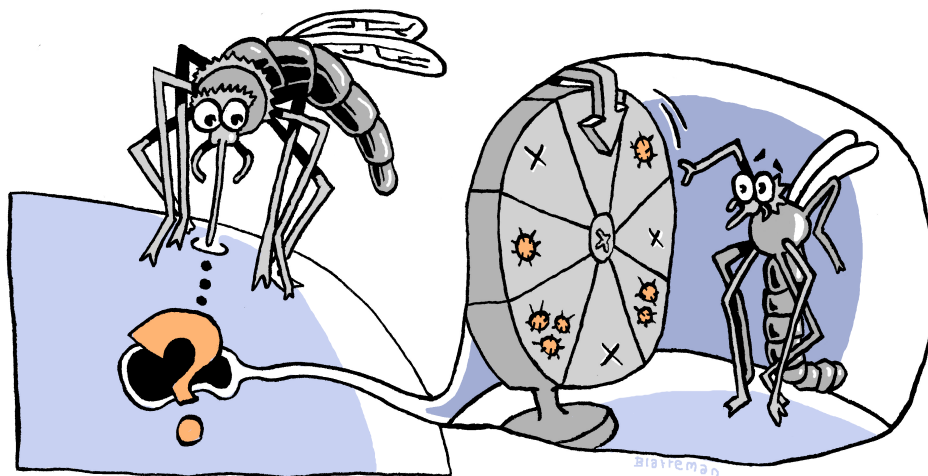


**Figure 4.4** – Représentation schématique des événements se déroulant dans le moustique de l'ingestion d'un repas de sang infecté à la retransmission du virus à un nouvel hôte. Les petits rectangles représentent de possibles goulots d'étranglement (passages délicats où la chaîne d'infection-transmission peut potentiellement être rompue). Extraite de Weaver et al., 2021.

<sup>14</sup> Plusieurs facteurs peuvent jouer, et notamment la composition du microbiote du moustique, plus ou moins favorable à la multiplication du virus. Ce sujet est abordé dans la vidéo suivante : <https://youtu.be/MoGpMOz8nPc>



Pour faire suite à la première étape de notre étude dans laquelle nous avons pu caractériser l'évolution de la charge virale au cours du temps, nous avons besoin d'estimer, pour une charge virale donnée, la probabilité d'infecter un moustique qui viendrait se nourrir sur l'hôte. Pour cela, je n'ai pas directement mené des expériences et fait des mesures<sup>15</sup>. J'ai préféré capitaliser sur les expériences qui avaient déjà été faites pas d'autres équipes, et j'ai donc entamé une revue de la littérature. Après avoir recensé<sup>16</sup> tous les articles dont nous pouvions extraire des données du type "X moustiques infectés parmi Y s'étant nourris sur un animal dont le titre infectieux était Z"<sup>17</sup>, j'ai estimé la relation dose-réponse correspondante, pour les *Aedes* et les *Culex* séparément (Figure 4.5). Ce qu'il faut y voir, c'est que pour une même dose de virus ingérée (si vous tracez une droite verticale qui coupe l'axe des abscisses à 5 par exemple), il y a une plus grande probabilité d'infecter un moustique *Aedes* qu'un *Culex* (25% vs 11% de chance pour l'exemple en question). C'est une différence significative au sens statistique du terme, et cela montre que **selon les critères pris en compte ici (la dose de virus et l'infection du moustique, donc la présence du virus dans son estomac), les *Aedes* sont plus vulnérables que les *Culex* face au virus de la FVR.**

<sup>15</sup> non seulement parce que ça aurait demandé beaucoup de temps, d'argent, des agréments pour avoir le droit de manipuler le virus, élever des colonies de moustiques etc. mais "accessoirement" parce que je suis incapable de disséquer un moustique!

<sup>16</sup> Ce travail a été réalisé par Roosmarie Vriens, une stagiaire de l'université de Wageningen, merci à elle!

<sup>17</sup> Nous avons restreint aux expériences faites avec des moustiques *Aedes* ou *Culex*<sup>18</sup>, nourris sur des hamsters qui avaient été infectés par un certain variant du virus de la FVR.



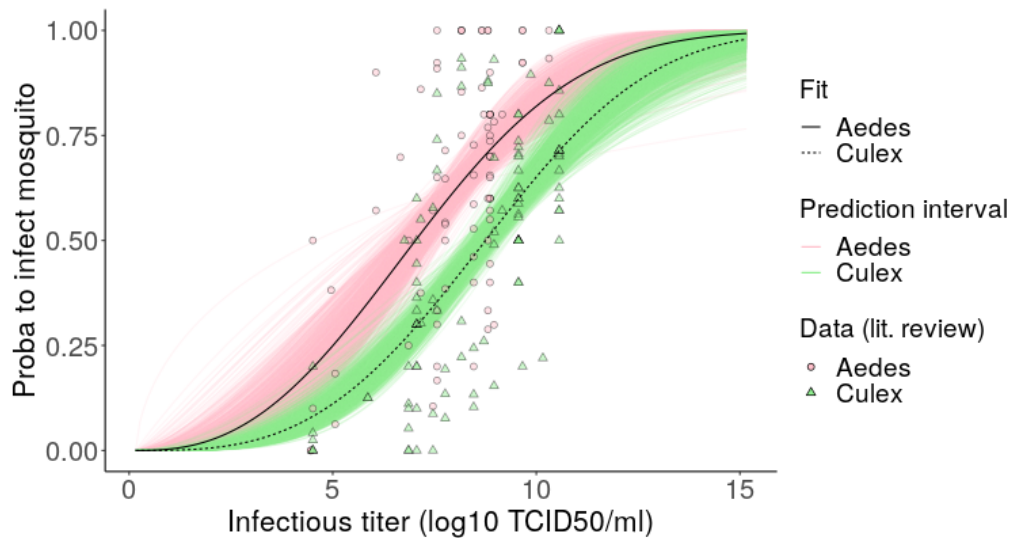


**Figure 4.5** – Relation entre le titre infectieux de l’animal (abscisse) et la probabilité d’infecter un moustique qui viendrait le piquer (ordonnée). Les points et triangles sont des données expérimentales issues de la littérature, et les courbes représentent la relation statistique estimée (le halo de couleur représente l’incertitude autour de cette estimation).

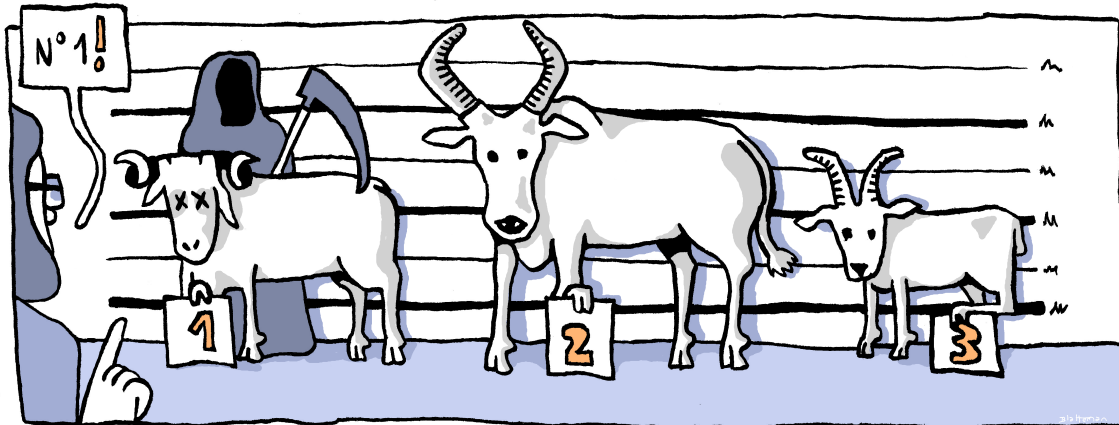
Nous avons désormais tous les éléments pour conclure sur la contagiosité des différentes espèces animales vis-à-vis du virus de la FVR!

#### 4.1.4 Notre étude: les différentes espèces animales sont-elles toutes logées à la même enseigne pour transmettre la fièvre de la Vallée du Rift ?

L’estimation des paramètres du modèle nous a permis de mettre en exergue d’importantes différences entre groupe d’hôtes, qui une fois combinées à la réponse du vecteur, permettent de conclure à une différence de contagiosité entre les espèces, et entre infection modérée et fatale chez les moutons:

- **Le processus de réplication virale semble moins efficace chez les chèvres, qui pour toute particule virale infectieuse produite, produisent bien plus de particules virales non infectieuses que les deux autres espèces.**
- **Au sein des moutons, ceux qui succombent à l’infection montrent une survie plus longue de leur cellules infectées, ainsi que de leurs particules virales infectieuses, que les moutons ayant survécu.** L’étude de la réponse immunitaire chez ces deux groupes semble nécessaire pour comprendre d’où vient cette différence.
- **Les chèvres sont les animaux les moins contagieux, et les moutons les plus contagieux.** L’écart entre espèces est plus important lorsque l’on compare la transmission aux *Culex* qu’aux *Aedes*.

- **En moyenne, un mouton qui succombent à l'infection sera plus contagieux qu'un mouton ayant survécu.** Cela est dû au fait que la plupart des moutons survivent une semaine avant de mourir, et que leur charge virale est très importante pendant tout ce temps, tandis que les moutons moins sévèrement affectés ont une charge virale plus modérée et cessent d'être infectieux au bout de 5 jours.



#### A garder en tête

- Les infections expérimentales peuvent sembler différentes de celles ayant lieu en condition réelles, mais elles apportent de précieuses informations sur la manière dont les hôtes réagissent à l'infection, que l'on ne pourrait pas suivre avec autant de précision sur le terrain.
- La modélisation mécaniste permet de soulever des pistes sur les processus biologiques régissant la réponse de l'hôte à l'infection. Ces hypothèses peuvent ensuite être vérifiées par des expériences dédiées.
- Le potentiel de transmission peut dépendre de l'hôte mais également du vecteur concerné. Une fois de plus, les estimations uniques risquent de cacher une réelle hétérogénéité.
- L'étude des maladies vectorielles multi-hôtes et multi-vecteurs nécessitent de bien comprendre le rôle joué par chaque espèce, pour pouvoir mettre en place des stratégies de maîtrise efficaces.

# Heterogeneity of Rift Valley fever virus transmission potential across livestock hosts, quantified through a model-based analysis of host viral load and vector infection

Hélène Cecilia<sup>1\*</sup>, Roosmarie Vriens<sup>2</sup>, Jeroen Kortekaas<sup>3,4</sup>,

Paul J. Wichgers Schreur<sup>3</sup>, Mariken de Wit<sup>2</sup>, Raphaëlle Métras<sup>5</sup>,

Pauline Ezanno<sup>1</sup>, Quirine A. ten Bosch<sup>2\*</sup>

<sup>1</sup> INRAE, Oniris, BIOEPAR, 44300, Nantes, France

<sup>2</sup> Quantitative Veterinary Epidemiology, Wageningen University and Research, Wageningen, The Netherlands

<sup>3</sup> Wageningen Bioveterinary Research, Lelystad, The Netherlands

<sup>4</sup> Laboratory of Virology, Wageningen University & Research, Wageningen, The Netherlands

<sup>5</sup> Sorbonne Université, INSERM, Institut Pierre Louis d'Epidémiologie et de Santé Publique (IPLESP), F-75012, Paris, France

\* corresponding authors

## Abstract

Rift Valley fever (RVF) is a viral, vector-borne, zoonotic disease. The relative contributions of livestock species to RVFV transmission has not been previously quantified. To estimate their potential to transmit the virus over the course of their infection, we 1) fitted a within-host model to viral RNA and infectious virus measures, obtained daily from infected lambs, calves, and young goats, 2) estimated the relationship between vertebrate host infectious titers and probability to infect mosquitoes, and 3) estimated the net infectiousness of each host species over the duration of their infectious periods, taking into account different survival outcomes for lambs. Our results indicate that the efficiency of viral replication, along with the lifespan of infectious particles, could be sources of heterogeneity between hosts. For similar infectious titers, we found that infection rates in *Aedes* spp. vectors were significantly higher than in *Culex* spp. vectors. Consequently, for *Aedes* infections, we estimated the net infectiousness of lambs to be 2.93 (median) and 3.65 times higher than that of calves and goats, respectively. Among lambs, individuals which eventually died from the infection were 1.93 times more infectious than lambs recovering. Beyond infectiousness, the relative contributions of host species to transmission depend on local ecological factors, including relative abundances and vector host-feeding preferences. Quantifying these contributions will ultimately help design

efficient, targeted, surveillance and vaccination strategies.

## 1 Introduction

At the beginning of this century, 75% of emerging pathogens in humans were estimated to be zoonotic (Taylor et al., 2001) and 77% of livestock pathogens could be transmitted between different host species (Cleaveland et al., 2001). Estimating the relative role different species play in sustaining or amplifying pathogen spread is fundamental for designing control strategies (Hollingsworth et al., 2015; Buhnerkempe et al., 2015; Lloyd-Smith et al., 2015; Webster et al., 2017), yet is hampered by an incomplete understanding of the host(-vector)-pathogen interactions that underlie the spread of these pathogens (Roche et al., 2013; Vazquez-Prokopec et al., 2016; Fenton et al., 2015; Martin et al., 2019).

The potential of a host to contribute to virus transmission is determined by the complex interplay of different factors. For viruses transmitted by arthropod vectors (i.e., arboviruses) these epidemiological interactions are driven both by ecological, population-level factors (i.e., the presence of specific host and vector species and their respective interactions) and the individual-level interactions of the virus with its hosts and vectors. The ability of a host species to infect a susceptible vector upon a potentially infectious contact is determined by the latter. Namely, it derives from i) the viral replication in the host and ii) the ability of a vector to pick up the virus upon blood feeding and subsequently become infected and infectious. While these processes can and have been studied in experimental settings, combining these findings into epidemiologically meaningful parameters is challenging (Althouse and Hanley, 2015; Bosch et al., 2018; Kain and Bolker, 2019).

Within-host mathematical models and accompanying inference frameworks have been developed to aid the analysis and interpretation of viral load patterns obtained in controlled infection experiments. Such models provide insights into the biological mechanisms underlying observed patterns (Clapham et al., 2014; Ben-Shachar and Koelle, 2015; Ben-Shachar et al., 2016; Clapham et al., 2016; Koelle et al., 2019) and how those patterns relate to the clinical expression of the disease (Bosch et al., 2018). The majority of these modelling efforts are based on viral RNA (or DNA) data, which are indirect measures of infectious virus. Efforts to combine these with infectious virus data (e.g., median tissue culture infectious dose, TCID<sub>50</sub> or plaque forming units, PFU) have recently emerged for influenza viruses and provide better mechanistic insights into the proportion of particles that are infectious and could contribute to onward transmission (Schulze-Horsel et al., 2009; Pinilla et al., 2012; Petrie et al., 2013, 2015; Simon et al., 2016; Yan et al., 2020).

Rift Valley fever virus (RVFV) exemplifies the challenges inherent to battling multi-host arboviruses. It was first identified in Kenya, in 1930, after description of an enzootic hepatitis in sheep (Daubney et al., 1931). The

virus has since caused outbreaks throughout the African continent as well as in the Southwest Indian ocean islands (Comoros archipelago, Madagascar) and the Arabian Peninsula (Nanyingi et al., 2015). RVFV mainly affects sheep, goats, and cattle, in which it causes abortion storms and sudden death of newborns (Al-Afalet and Hussein, 2011; El Mamy et al., 2011). Spillover to humans happens through the handling of infectious animal tissue or by vectorial transmission. While most human infections remain asymptomatic or manifest as a mild illness, symptoms can range from flu-like to hepatitis, retinitis and in the most severe cases, haemorrhagic disease (LaBeaud et al., 2010). RVFV vector-borne transmission is mainly mediated by *Aedes* and *Culex* spp. mosquitoes, making its establishment possible in a wide range of ecosystems (Linthicum et al., 2016). While sheep are generally believed to be the most important host species (Bird et al., 2009; Clark et al., 2018; Bron et al., 2021), efforts fall short of quantifying livestock hosts relative contribution to RVFV transmission.

Here, we aim to gain more insight into the relative importance of livestock species in RVFV transmission. Using experimental data and mathematical modeling, we derive estimates of hosts' individual potential to transmit RVFV to vectors during their infection.

## 2 Results

### 2.1 Overall approach

We developed a mechanistic compartmental within-host model, representing the infection of target cells and the subsequent production of viral particles, not all of which are infectious (Figure 1). We distinguish the total amount of viral particles produced by infected cells,  $V_{tot}$ , and the subpart capable of infecting new cells,  $V_{inf}$ . We fitted this model to time-series of viral RNA (RT-qPCR) and infectious virus (TCID<sub>50</sub>), measured in experimentally infected calves, lambs, and young goats. We compared the cell-level basic reproduction number  $R_0$  and mean generation time  $T_g$ , between groups. We quantified the relationship between vertebrate hosts' infectious titers and transmission to mosquitoes using data extracted from a literature review. Finally, we estimated the net infectiousness of livestock species, a metric proportional to the number of mosquitoes a host would infect over the entire course of its infection.

### 2.2 Data

Data on viral RNA and infectious virus were obtained from a published study on a candidate RVFV vaccine (Wichgers Schreur et al., 2020a) (Section 4). Mock vaccinated animals were infected with a virulent RVFV strain. Eight animals were exposed per species (lambs, calves, young goats), all animals became viraemic. An additional dataset obtained from 8 lambs, following the same protocol, was added. In total, 10/16 lambs succumbed to the infection or were euthanized, 3 to 7 days after RVFV inoculation, while others survived until the end of the experiment (2 weeks). All calves and young goats survived until the end of the experiment.

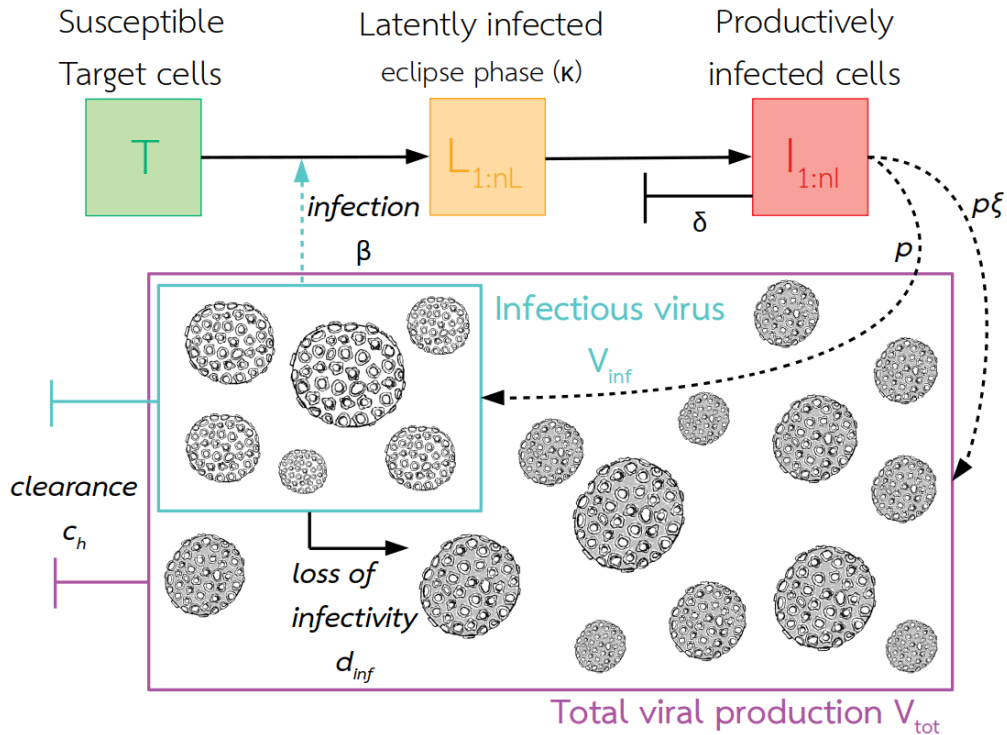


Figure 1: Graphical representation of the within-host model. Infectious viruses  $V_{inf}$  were fitted to TCID<sub>50</sub> measures, and total viral production  $V_{tot}$  to RT-qPCR measures. The eclipse phase (state  $L$ ) is the period between the infection of a cell by a virus and the appearance of mature virus within the cell. Productively infected cells  $I$  are the only ones producing progeny virions. Subscripts in  $L$  and  $I$  indicate the use of Erlang distributions for the time spent in those states. Target cells are not replenished and only productively infected cells die. Model assumptions, equations and parameter definitions can be found in Section 4, Eq. 1, and Table 2.

### 2.3 Within-host model of RVFV infection

We fitted a within-host model to four datasets, measuring viral RNA and infectious virus in RVFV-infected lambs (surviving ; dying), calves, and young goats, using a Bayesian framework (Section 4). The model consisted of 10 parameters, 5 of which were held constant (Table 2). We estimated the death rate  $\delta$  of infected cells, their total daily production of viral particles  $\xi p$ , among which  $p$  are infectious, the degradation rate  $d_{inf}$  of infectious viruses into non-infectious viruses, and the clearance rate  $c_h$  of viral particles. Parameter values were then used to calculate the cell-level basic reproduction number  $R_0$  and mean generation time  $T_g$ . Initial conditions were set using elements of the experimental protocol along with a sensitivity analysis (Section 4, Table 2). Outputs from the Markov Chain Monte Carlo (MCMC) procedure can be found in Supplementary Information S.1. The fits satisfyingly capture the dynamics present in the data (Figure 2).

The model selection performed highlights different viral load dynamics between livestock species (Deviance Information Criterion (DIC) 1307 *vs* 1186, comparison based on surviving animals as calves and young goats all survived, Figure 2). In particular, the ratio of daily viral RNA over infectious viruses produced ( $\xi$ ) is the highest in the goat group, meaning that the replication process might be less efficient in this species (Table 1). The

highest density intervals (HDIs) for this parameter are wide (Table 1), but the posterior distributions remain informative (Figure S.4). In addition, among surviving hosts, the lifespan of infectious particles  $(d_{inf} + c_h)^{-1}$  is estimated to be the longest in goats (Table 1). The resulting dynamics show viremia in goats peaks sooner than in calves and in lambs, but with a lower peak value for infectious viruses (Figure 2). Lambs have on average the most infectious viral particles. Model results indicate this could be a result of a slightly higher daily production rate  $p$  (Table 1), as well as their initial susceptible cell population, which we estimated to be higher than in other species (Figure S.1). Characterizing the infectious replication process through the basic reproduction number  $R_0$  and generation time  $T_g$  (Section 4, Eq. 2-3) shows no strong differences between species when comparing surviving individuals (Figure 3).  $R_0$  ranges from 8.51 (median; 95% HDI 5.69 - 14.53) for calves, to 11.47 (median; 95% HDI 7.73 - 17.68) for lambs.  $T_g$  (i.e., the time between infection of a cell and infection of a secondary cell) ranges from 13.48h (median; 95% HDI 12.84h - 15.23h) in goats to 14.43h (median; 95% HDI 12.82h - 18.31h) in calves.

Among lambs, individuals succumbing to RVF are characterized by higher viral loads, both total and infectious, and a slower decay after the peak is reached (Figure 2). The best model fit is achieved when allowing parameters to vary depending on the survival of the individuals (Figure 2, DIC 928 vs 745), indicating significantly different within-host dynamics depending on clinical outcome. In particular, we estimated that both infected cells and infectious viral particles have prolonged lifespans in dying lambs ( $\delta^{-1}$  and  $(d_{inf} + c_h)^{-1}$  respectively, Table 1). This impacts  $R_0$  which is 1.88 times higher (median ratio; 95% HDI 0.84 ; 3.51) in dying individuals than surviving ones, and  $T_g$ , which is 1.19 times longer (median ratio; 95% HDI 0.91 ; 1.65) in dying individuals than surviving ones. Besides, the ratio of daily viral RNA over infectious viruses produced ( $\xi$ ), which does not influence  $R_0$ , is higher in dying lambs than surviving ones (Table 1).

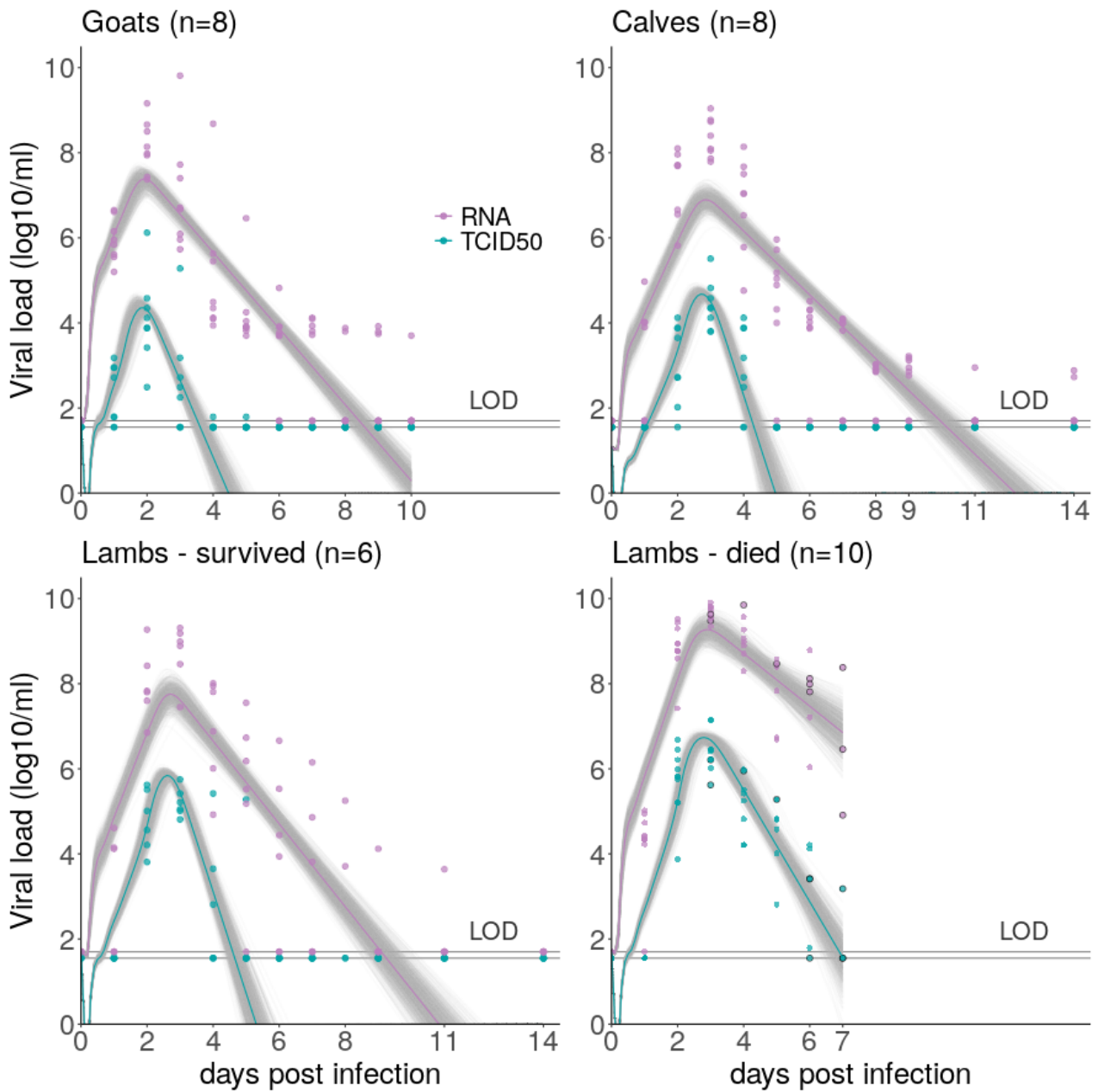


Figure 2: Data on viral RNA (RT-qPCR) and infectious virus (TCID<sub>50</sub>), in log<sub>10</sub>/ml of plasma, and model fits, for host groups showing significantly different viral dynamics. Circles are data points. Solid colored lines show predicted median. Grey lines represent model trajectories resulting from 1000 parameter sets sampled in posterior distributions. Purple is for viral RNA and blue for infectious viruses. For lambs which died from RVF, circled points represent individuals' time of death. LOD = limit of detection, 1.55 for TCID<sub>50</sub>, 1.7 for viral RNA (log<sub>10</sub>)



Parameter		Estimate : median [HDI]			
		Goat	Calf	Lamb surv.	Lamb dead
$\delta$	$I$ death rate	2.61 [1.91 ; 3.0]	2.17 [1.30 ; 3.0]	2.34 [1.60 ; 3.0]	1.52 [0.85 ; 2.44]
$p$	production of $V_{inf}$	20.14 [13.33 ; 29.40]	14.98 [12.31 ; 17.89]	21.53 [17.09 ; 26.50]	25.27 [19.72 ; 31.00]
$\xi$	ratio $\frac{V_{tot}}{V_{inf}}$ produced	672.76 [333.96 ; 999.56]	75.16 [20.60 ; 161.05]	44.33 [9.66 ; 104.48]	221.15 [50.57 ; 510.97]
$d_{inf}$	degradation $V_{inf} \rightarrow V_{tot}$	2.10 [1.36 ; 2.92]	3.77 [2.17 ; 6.63]	3.26 [2.19 ; 4.48]	1.60 [0.90 ; 2.31]
$c_h$	clearance of $V_{inf}$ and $V_{tot}$	2.06 [1.88 ; 2.24]	1.72 [1.53 ; 1.92]	2.24 [1.94 ; 2.53]	1.43 [0.87 ; 2.01]

Table 1: Parameter estimates per host group. Median of joint posterior distributions (3 chains) and HDI = highest density interval (95%). All parameters are in unit  $\text{day}^{-1}$ , see Section 4 for detailed definitions. The HDI is built such as every point inside the interval has higher credibility than any point outside the interval (Kruschke, 2015).

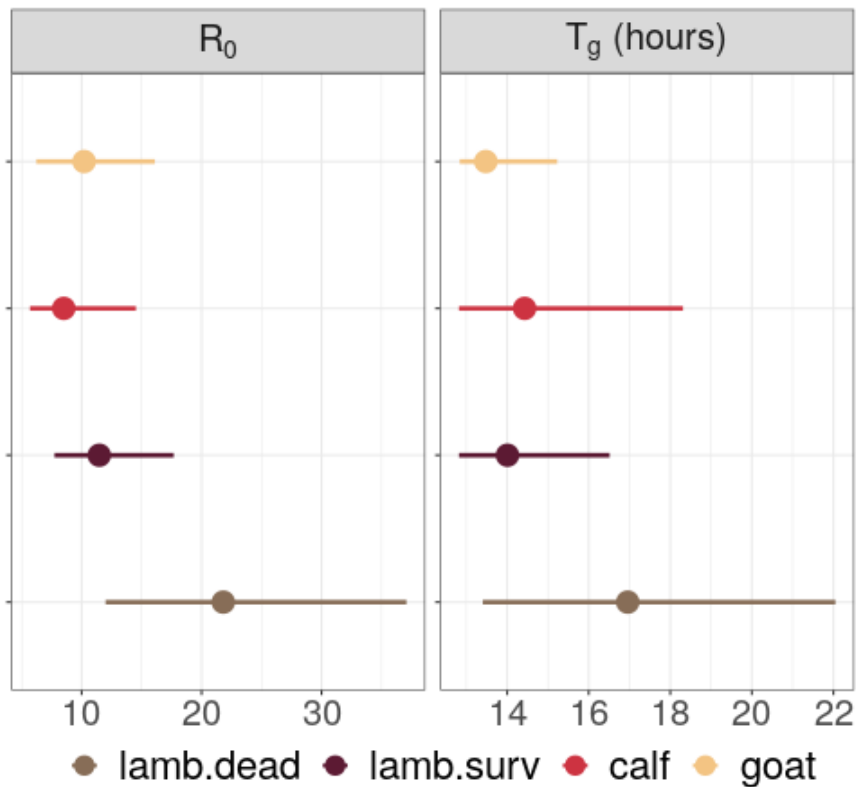


Figure 3: Outcome measures per host group. Points are median estimates, lines show highest density intervals, computed from joint posterior distributions (3 chains). Basic reproduction number  $R_0$  is computed with Eq. 2 and generation time  $T_g$  with Eq. 3. Note that generation times are constrained in their lower values due to the eclipse phase duration ( $\kappa^{-1}$ ) and rate of virus entry into cells ( $\beta$ ) being fixed (Table 2).

## 2.4 Dose-response relationship in RVFV mosquito vectors

Through a systematic review, we identified 9 papers from which data could be extracted to estimate the relationship between vertebrate host infectious titers and associated infection rates in vectors (Section 4, Supplementary Information S.2.1). Selected experiments were performed with hamster hosts, *Aedes* or *Culex* spp. vectors, using RVFV strain ZH501.

Dose-response curves differ significantly between *Aedes* and *Culex* spp. (Figure 4, Supplementary Information S.2). At  $5 \log_{10}$  TCID<sub>50</sub>/ml for instance, which most animals could reach or exceed (Figure 2), there is 25% [15 ; 38] probability to infect an *Aedes* spp. vector and 11% [7 ; 18] probability to infect a *Culex* spp. vector (Figure 4). We did not find a significant effect of temperature and number of days post exposure on infection rates (Supplementary Information S.2.2, S.2.3). The effect of dose is best captured by Eq. S.6, used by Ferguson et al., 2015, fitted with a betabinomial likelihood accounting for overdispersal in the data (Supplementary Information S.2.3). Species-specific curves were estimated for *Aedes vexans*, *Aedes japonicus*, *Culex nigripalpus*, and *Culex tarsalis* (Supplementary Information S.2.3, Figure S.6). While there is intra-genus variability, infection rates in *Aedes vexans* and *Aedes japonicus* are on average higher than in *Culex nigripalpus*, and *Culex tarsalis* at similar host infectious titers (Figure S.6).

## 2.5 Net infectiousness of RVFV livestock hosts

Net infectiousness (NI, Eq. 4) varies with both host species and mosquito genus involved (Section 4, Figure 5). NI is lowest for goats and highest for lambs. The relative differences in NI between host species is stronger when comparing transmission to *Culex* (median ratio lamb:goat 4.79 ; median ratio lamb:calf 3.75) than to *Aedes* mosquitoes (median ratio lamb:goat 3.65 ; median ratio lamb:calf 2.93). Every host type studied has the highest NI when bitten by an *Aedes* spp. vector, but the uncertainty around NI estimates decreases when considering *Culex* bites (Figure 5).

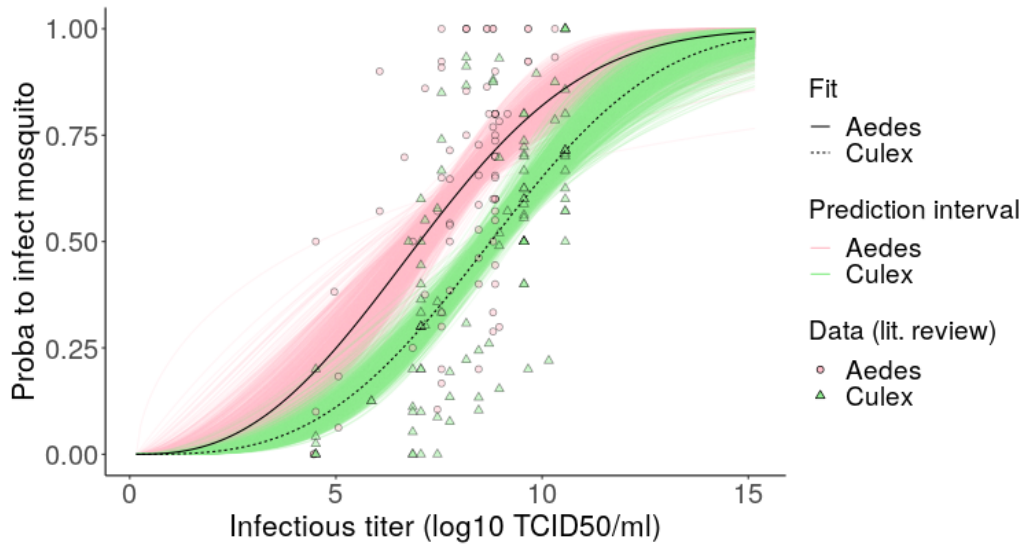


Figure 4: Dose-response relationships linking host infectious titers to the probability to infect mosquito vectors. Data retrieved from a systematic review (Section 4, Supplementary Information S.2). Points and triangles show infection rates (presence of RVFV in mosquito bodies, legs excluded) from experiments performed with hamsters with RVFV strain ZH501. Fits were obtained with Eq. S.6 using a betabinomial likelihood to account for overdispersal in the data. Prediction intervals correspond to trajectories resulting from 1000 parameter sets sampled in posterior distributions. Note that infectious titers  $>10 \log_{10}$  are not to be expected in hosts, but were included to show the full curve.

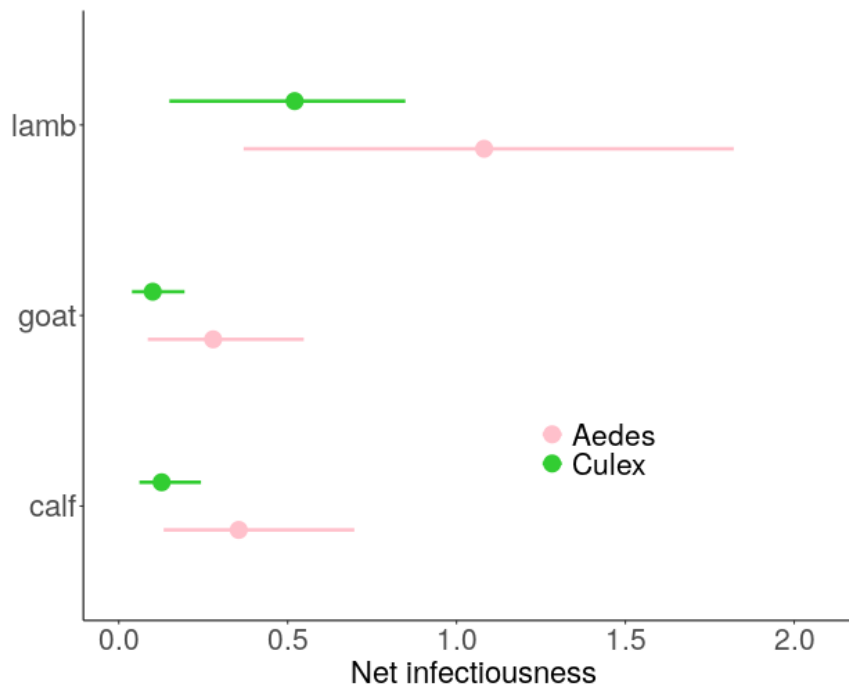


Figure 5: Net infectiousness of RVFV livestock host species, function of the mosquito genus involved in transmission. Points are median estimates, lines show highest density intervals, computed using 1000 parameter sets sampled in joint posterior distributions (3 chains). For lambs, parameters were sampled in the posteriors of both surviving and dying groups, according to the survival rate observed in the original dataset (6/16, Figure S.7). Time of death also varied according to a Weibull survival model (Section 4).

Lambs' NI varies with the expected death rate among lambs (Section 4, Figure S.7). Lambs dying from RVF have a higher NI than lambs surviving (Figure S.7). Indeed, dying lambs are more infectious than their surviving

counterparts during their whole viremic period, which in 60% of cases can last longer (day 7) than the infectious period of surviving individuals (probability  $< 1\%$  to infect an *Aedes* or a *Culex* past day 5 post inoculation). When bitten by an *Aedes* spp. vector, lambs NI ranges from 0.24 to 2.54, increasing by a factor 1.93 (median ratio) from surviving to succumbing individuals. When bitten by a *Culex* spp. vector, lambs NI ranges from 0.12 to 1.36, increasing by a factor 2.22 (median ratio) from surviving to succumbing individuals.

### 3 Discussion

We have presented the results of a data-driven estimation of livestock hosts RVFV transmission potential, providing mechanistic insights into potential sources of heterogeneity between species. Our results demonstrate that sheep are the most infectious livestock hosts, and that virulent infection leading to death reinforces the infectiousness of this species. We also showed that lower infectious doses are needed to infect *Aedes* spp. vectors than *Culex* spp.. The framework presented here can be applied to other multi-host arboviruses to estimate transmission potential, a key component of hosts contribution to transmission at large scale.

The suite of experimental data used in our study incorporated the major elements needed for an epidemiologically relevant estimation of hosts transmission potential. We included both viral RNA and infectious viruses, measured *in vivo*, in natural RVFV hosts. Similar existing models used data coming either from *in vitro* experiments (Schulze-Horsel et al., 2009; Iwami et al., 2012; Pinilla et al., 2012; Simon et al., 2016; Yan et al., 2020), or from model hosts, such as ferrets for influenza (Petrie et al., 2013, 2015). The breeds infected in our dataset make our estimates directly relevant for scenarios of RVFV emergence in Europe, and a comparison with African breeds would be an appropriate next step, along with the comparison of several RVFV strains (Vloet et al., 2017; Fontaine et al., 2018). Performing infection through mosquito bites rather than intravenous injection would ensure a natural course of infection, although the protocol presently used was shown to yield similar viral load dynamics as mosquito-mediated infection (Wichgers Schreur et al., 2021). This would further allow for the exploration of the impact of heterogeneity of exposure (i.e., number of infectious bites or infectious titers in vector saliva) on infectiousness. Finally, data on adult livestock as well as human viremia levels will be key to complete our understanding of hosts contribution to RVFV transmission.

Our within-host model is the second developed for RVFV (Tuncer et al., 2016), but the first to mechanistically represent the process of viral production from host cells. This enabled an identification of processes driving differences between groups and an increased understanding of the cell-level viral replication process. First, we estimated a less efficient replication in goats, further advocating for the use of infectious virus measures in order not to overestimate transmission potential (Tesla et al., 2018). Besides, we estimated the lifetime of infectious viral particles and infected cells to be longer in dying lambs than their surviving counterparts, which calls for an

exploration of corresponding (immune) mechanisms in future experiments. The uncertainty around parameter estimates remains important, and summarizing parameter estimates into aggregated outcome measures  $R_0$  and  $T_g$  put those mechanistic differences into perspective. Indeed, once correlation between parameters are taken into account, the replication process is most different between severe and moderate infection within sheep and less so between host species. The model could be refined by incorporating an explicit immune response (Elliott and Weber, 2009; Mapder et al., 2019) or taking into account the genomic composition of viral particles (Jacobs et al., 2019; Bermúdez-Méndez et al., 2021), but the quantity of information needed (number of timesteps and replicates, inclusion of data on immune responses ) could hamper this costly data collection.

By gathering relevant competence studies into a meta-analysis, we quantified the relationship between infectious titers and mosquito RVFV infections. To our knowledge, such dose-response relationship had not been quantified for RVFV. This results in a lack of precision in between-host RVFV transmission models which usually assume constant infectiousness of hosts over their infectious period. Quantifying how the probability to infect a vector increases with dose will also affect the stochasticity of transmission in small populations (be it emergence or extinction). Dose-response curves have been important for the study of other arboviruses, e.g., for exploring the role of asymptomatic dengue infections (Bosch et al., 2018) or the epidemic potential of *Aedes albopictus* for Zika virus (Lequime et al., 2020). One important originality of our work was to highlight a higher susceptibility of *Aedes* spp. vectors to RVFV infection compared to *Culex* spp. vectors, at similar infectious titers. Further studies are needed to confirm whether this higher probability of infection is also accompanied by a higher probability of the mosquito becoming infectious itself. This would require the detection of infectious particles in mosquitoes' saliva, which was only performed in 23 out of 185 data points in the present systematic review.

A lot remains unknown about the bottlenecks of arboviruses propagation in mosquitoes (Weaver et al., 2021). It can depend on species within each genus (Bustamante and Lord, 2010; Golnar et al., 2014) or even mosquito provenance (field *vs* laboratory-reared, Turell et al., 2008, 2010, 2013), in part because of the role of temperature (Turell et al., 2020). Further experiments are needed to know whether a given infectious titer sampled during the increasing or the decreasing phase of viral dynamics would yield the same probability to infect vectors. This comes down to defining what makes a viral particle infectious to host cells *vs* vector cells, and might relate to the efficiency of genome packaging by those cells (Bermúdez-Méndez et al., 2021). Mechanistic modeling will help grasp the complexity of involved processes.

Our study provided key estimates of RVFV livestock hosts' transmission potential. It quantified for the first time the prominent role of sheep, which are 3 to 4 times more infectious than cattle and goats, due to more infectious viruses and a longer infectious period. In addition, fatal infection in sheep does not diminish trans-

mission potential but could rather increase it, based on time of deaths observed in our dataset. This entails that most vulnerable populations, in addition to suffering more deaths, will likely experience larger outbreaks.

Understanding the relationship between infectiousness and pathogen load represents a key challenge to connect modeling scales (Gog et al., 2015). We have importantly contributed to deciphering this relationship for Rift Valley fever virus. Combining these results with ecological factors such as vector presence, population dynamics, and trophic preference, as well as human factors which define the presence of livestock hosts and their mobility, will increase our understanding of RVFV transmission dynamics at large scale. These interacting scales might yield unexpected patterns and reshape the way we design surveillance and control strategies for multi-host arboviruses in general.

## 4 Materials and Methods

### 4.1 Data

Animals (16 lambs, 8 calves, 8 young goats) were inoculated intravenously with  $5 \log_{10}$  TCID<sub>50</sub> of strain rRVFV 35/74. Animals' age was 2-3 weeks for calves, 8-10 weeks for lambs and goats. The average body weight of animals, used further to calibrate the inoculum per ml of plasma, was 45 kg for lambs, 30 kg for goats, and 80 kg for calves. Animals were purchased from conventional Dutch farms, and the breed was Texel cross for sheep, Saanen for goats, and Holstein-Friesian for cattle (Wichgers Schreur et al., 2020b).

### 4.2 Within-host model of RVFV infection

Our mechanistic model (Figure 1) is formulated as a set of ordinary differential equations, and is similar to existing within-host models developed for influenza (Petrie et al., 2013; Yan et al., 2020):

$$\begin{aligned}
 \frac{dT}{dt} &= -\beta TV_{inf} \\
 \frac{dL_1}{dt} &= \beta TV_{inf} - n_L \kappa L_1 \\
 \frac{dL_i}{dt} &= n_L \kappa (L_{i-1} - L_i), & i = 2, \dots, n_L \\
 \frac{dI_1}{dt} &= n_L \kappa L_{n_L} - n_I \delta I_1 \\
 \frac{dI_j}{dt} &= n_I \delta (I_{j-1} - I_j), & j = 2, \dots, n_I \\
 \frac{dV_{inf}}{dt} &= p \sum_{j=1}^{n_I} I_j - d_{inf} V_{inf} - c_h V_{inf} - \sigma \beta TV_{inf} \\
 \frac{dV_{tot}}{dt} &= \xi p \sum_{j=1}^{n_I} I_j - c_h V_{tot}
 \end{aligned} \tag{1}$$

In this model, infectious viruses  $V_{inf}$  infect susceptible target cells  $T$  at rate  $\beta$ . Infected cells first go through a latent state,  $L$  (eclipse phase). Then, they become productively infected cells,  $I$ . These cells produce viral particles  $V_{tot}$  at rate  $\xi p$ , not all of which are infectious ( $V_{inf}$  produced at rate  $p$ ). Infectious viruses degrade into non-infectious viruses at rate  $d_{inf}$ , which does not impact total viral production  $V_{tot}$ . A similar host clearance rate  $c_h$  is applied to both non-infectious and infectious particles.

To achieve realistic distributions of time spent in  $L$  and  $I$  states, we used Erlang distributions. This means that infected cells go through  $n_L$  latent stages and  $n_I$  infectious stages, where the time spent in each stage is exponentially distributed. We used  $n_L = n_I = 20$ , sufficient for the resulting latent and infectious periods to be almost normally or lognormally distributed (Krylova and Earn, 2013; Lloyd, 2001). The mean of these Erlang distributions are  $\kappa^{-1}$  and  $\delta^{-1}$ , and their variance  $\frac{1}{n_L \kappa^2}$  and  $\frac{1}{n_I \delta^2}$ .

We used a target-cell limited model, meaning that the depletion of target cells is what triggers the viral load peak and subsequent decline. We did not incorporate an explicit immune response. However, as explained by Beauchemin and Handel, 2011, this type of model can be seen as equivalent to assuming a constant effect of the immune response (IR). This IR can act implicitly by limiting the number of cells susceptible to the infection, removing infected cells or viral particles.

We fitted  $V_{inf}$  to TCID<sub>50</sub> measures and  $V_{tot}$  to RT-qPCR measures. As TCID<sub>50</sub> measures the dose needed to induce a cytopathic effect in 50% of the cells, a conversion factor  $\sigma$  is needed to express it as a quantity of infectious viruses, usually measured in plaque forming units (PFUs). Here, we set  $\sigma = 0.69$  TCID<sub>50</sub>/ml, consistent with 1 ml virus stock having half the number of (PFUs) as TCID<sub>50</sub> using Poisson sampling (Canini et al., 2016).

We used a Metropolis Rosenbluth Monte Carlo Markov Chain (MCMC) algorithm to fit our model, implemented in R, using the *odin* package (<https://github.com/mrc-ide/odin>) to speed up simulations. The composite log-likelihood, applied to log<sub>10</sub> measures, was similar to Clapham et al., 2014 (errors normally distributed, limit of detection accounted for). Log-likelihoods for total and infectious viruses were summed, as well as across individuals. The score obtained was used by the algorithm to determine if a parameter set should be accepted. At each iteration, parameters were simultaneously sampled using normal distributions centered around their last accepted value, with a standard deviation specific to each parameter. To obtain acceptance rates between 10% and 45% (the optimal acceptance rate being 23.4% as shown by Roberts et al., 1997) for each parameter, we used a custom function which determines appropriate standard deviations for their sampling. Fixed and estimated parameters can be found in Table 2, chosen in agreement with identifiability analyses of similar models (Miao et al., 2011; Beauchemin and Handel, 2011). Priors represent the probability distribution of possible parameter values, based on prior knowledge. We used uniform distributions, with bounds intended to allow a

wide exploration of parameter values while being biologically realistic.

Our fitting procedure worked as follows : for each dataset to fit, we ran small chains (10,000 iterations, 5,000 burn-in period) fixing  $T_0$  at different values spread across [3;6.5]  $\log_{10}/\text{ml}$  plasma. The best  $T_0$  value was then assessed through maximum log-likelihood profiles (Figure S.1) and kept for longer chains. Three long chains were run (100,000 iterations, 20,000 burn-in) for each dataset. The Gelman Rubin diagnostic test was used to assess common convergence of the chains (Supplementary Information S.1).

To determine whether viral load dynamics  $V(t)$  differ between livestock host groups, we ran the inference procedure in two distinct ways : treating these groups as equal (aggregating datasets) or different (fitting done for each dataset separately, Supplementary Information S.1). The resulting joint posterior distributions was used to compute the Deviance Information Criterion (DIC) of these models and select those with the smallest DIC (Supplementary Information S.1). We did not attempt to find differences between individuals of a given group.

To characterize the replication process at the beginning of the infection, we computed two outcome measures from the parameters of our model. The basic reproduction number  $R_0$  (Eq. 2, Beauchemin et al., 2008; Yan et al., 2020) is defined as the average number of new infected cells produced by one infected cell introduced into an entirely susceptible target-cell population. The generation time  $T_g$  (Eq. 3, Wallinga and Lipsitch, 2007; Svensson, 2007; Yan et al., 2020) is the average time between the infection of a cell and the infection of a secondary cell, again in an entirely susceptible target cell population. The formula for  $T_g$  was adapted to a model using Erlang distributions (for time spent in  $L$  and  $I$  states). How it changes compared to  $T_g$  computed for models with exponential distributions is explained in Supplementary Information S.1.

$$R_0 = \frac{\beta T_0 p}{\delta(c_h + d_{inf} + \sigma \beta T_0)} \quad (2)$$

$$T_g = \frac{1}{\kappa} + \frac{n_I + 1}{2n_I} \cdot \frac{1}{\delta} + \frac{1}{c_h + d_{inf} + \sigma \beta T_0} \quad (3)$$



Name	Meaning	Value/Estimated	Reference/Prior
$T_0$	initial number of susceptible target cells	Fixed within MCMC, estimated <i>a priori</i> through likelihood profiles	see Figure S.1
$L_0$	initial number of latently infected cells	0	
$I_0$	initial number of productively infected cells	0	
$V_{inf,0}$	initial number of infectious virions	12.5 for calves, 62.5 for goats, 52.6 for lambs (per ml of plasma, total inoculum per animal being $10^5$ )	References for plasma:body weight ratios Quigley et al., 1998; Courtice, 1943; Coghlan et al., 1977
$\beta$	rate governing infection of target cells by infectious virions	set such as $\beta T_0 = 48 \text{ day}^{-1}$	assumed
$n_L, n_I$	number of $L$ and $I$ states for the Erlang distributions	20	Krylova and Earn, 2013; Lloyd, 2001
$\kappa^{-1}$	eclipse phase duration	1/3 day (8 hours)	P. Wichgers-Schreur personal communication, observed <i>in vitro</i>
$\delta$	death rate of productively infected cells	Estimated	$[0.1 ; 10]^\circ \text{ day}^{-1}$
$p$	rate of production of infectious virions	Estimated	$[0.2 ; 3 \cdot 10^4]^\dagger \text{ day}^{-1}$
$d_{inf}$	rate of degradation of infectious virions into non-infectious viral particles	Estimated	$[0.1 ; 10] \text{ day}^{-1}$
$c_h$	host-driven clearance rate	Estimated	$[0.1 ; 10] \text{ day}^{-1}$
$\sigma$	correction factor to convert from infectious virions to TCID <sub>50</sub>	0.69	Canini et al., 2016
$\xi$	ratio of total viral particles to infectious virions, as produced by infected cells	Estimated	$[1 ; 1000]^\dagger \text{ day}^{-1}$

Table 2: Parameters of the within-host model. Values if fixed, prior range (uniform distribution) if estimated.

$\dagger$  : these values were applied for each  $L$  (respectively  $I$ ) states, so a daily rate per  $L$  ( $I$ ) cell (not state) can be obtained by multiplying by  $n_L$  ( $n_I$ )

$^\circ$  :  $\delta$  was constrained to be inferior to  $\kappa$  and  $(c_h + d_{inf})$ , as advised by Smith et al., 2010.

### 4.3 Dose-response relationship in RVFV mosquito vectors

A systematic review of the literature was performed to study  $F(V)$ , the relationship between a vertebrate host RVFV infectious titer and the associated probability to infect a mosquito upon its bite (Supplementary Information S.2.1). We limited our quantitative analysis to experiments performed with *Aedes* and *Culex* spp., with strain ZH501, on hamsters (Supplementary Information S.2.1). This corresponded to 185 data points from 9 papers.

To assess the impact of the diversity of protocols from which the data originated, we tested the effect of temperature, and number of days between mosquito feeding and dissection, in addition to dose (infectious titer) on infection rates (presence of RVFV in the body of mosquitoes, legs excluded, Supplementary Information S.2.2, S.2.3). For that we used a logistic function (Eq. S.5), fitted with a binomial and a beta-binomial likelihood, the latter to account for overdispersal in the data (Supplementary Information S.2.3).

We used Akaike Information Criterion (AIC) to compare model fit of different functional forms (Supplementary Information S.2.3). Best fitting functions were then used to explore differences between and within genera (Table S.1, Figure S.6).

### 4.4 Net infectiousness of RVFV livestock hosts

We define net infectiousness (NI) as the integral of an infectiousness curve over time (Eq. 4)

$$NI_{vect,host} = \int F_{vect}(V_{host}(t))dt \quad (4)$$

NI combines the dose-response relationship in vectors  $F_{vect}(V)$  with infectious virus dynamics in hosts  $V_{host}(t)$ . As such, it must incorporate the uncertainty from both estimations. This was done by sampling 1000 parameter sets in  $F_{vect}(V)$  and  $V_{host}(t)$  posteriors. For lambs, a draw in a Bernoulli distribution first determined whether the viral load dynamics should be of a surviving or dying type. In the latter case, a time of death was sampled in a Weibull survival model fitted to death times present in our dataset, and determined the end of the viral load curve. Finally, a sensitivity analysis explored how the survival rate in the lamb population impacts the average NI of lambs.

This quantity NI is proportional to the expected number of mosquitoes infected by a host over the entire course of its infection, assuming that biting occurs at a constant rate over this period. By extension, the NI ratio of two host categories is identical to the ratio of the expected number of mosquitoes infected by those two types of hosts, assuming bites to be equally distributed over both species. In the present study, NI was also vector-specific.

## 5 Acknowledgments

We thank Hannah Clapham, Sander Koenraadt, Vincent Raquin, and Maxime Ratinier for fruitful discussions.

## 6 Funding

This work was part of the FORESEE project funded by INRAE metaprogram GISA (Integrated Management of Animal Health). HC was funded by INRAE, Région Pays de la Loire, CIRAD. MdW is part of the research programme One Health PACT with project number 109986, which is (partly) financed by the Dutch Research Council (NWO).

## References

- Al-Afaleq, A. I. and M. F. Hussein (2011). “The Status of Rift Valley Fever in Animals in Saudi Arabia: A Mini Review”. en. In: *Vector-Borne and Zoonotic Diseases* 11.12, pp. 1513–1520. DOI: 10.1089/vbz.2010.0245.
- Althouse, B. M. and K. A. Hanley (2015). “The tortoise or the hare? Impacts of within-host dynamics on transmission success of arthropod-borne viruses”. en. In: *Philosophical Transactions of the Royal Society B: Biological Sciences* 370.1675, p. 20140299. DOI: 10.1098/rstb.2014.0299.
- Beauchemin, C. A. and A. Handel (2011). “A review of mathematical models of influenza A infections within a host or cell culture: lessons learned and challenges ahead”. en. In: *BMC Public Health* 11.Suppl 1, S7. DOI: 10.1186/1471-2458-11-S1-S7.
- Beauchemin, C. A., J. J. McSharry, G. L. Drusano, J. T. Nguyen, G. T. Went, R. M. Ribeiro, and A. S. Perelson (2008). “Modeling amantadine treatment of influenza A virus in vitro”. en. In: *Journal of Theoretical Biology* 254.2, pp. 439–451. DOI: 10.1016/j.jtbi.2008.05.031.
- Ben-Shachar, R. and K. Koelle (2015). “Minimal within-host dengue models highlight the specific roles of the immune response in primary and secondary dengue infections”. en. In: *Journal of The Royal Society Interface* 12.103, p. 20140886. DOI: 10.1098/rsif.2014.0886.
- Ben-Shachar, R., S. Schmidler, and K. Koelle (2016). “Drivers of Inter-individual Variation in Dengue Viral Load Dynamics”. en. In: *PLOS Computational Biology* 12.11. Ed. by N. M. Ferguson, e1005194. DOI: 10.1371/journal.pcbi.1005194.
- Bermúdez-Méndez, E., E. A. Katrukha, C. M. Spruit, J. Kortekaas, and P. J. Wichgers Schreur (2021). “Visualizing the ribonucleoprotein content of single bunyavirus virions reveals more efficient genome packaging in the arthropod host”. en. In: *Commun Biol* 4.1, p. 345. DOI: 10.1038/s42003-021-01821-y.
- Bird, B. H., T. G. Ksiazek, S. T. Nichol, and N. J. MacLachlan (2009). “Rift Valley fever virus”. en. In: 234.7, p. 11.

- Bosch, Q. A. ten et al. (2018). “Contributions from the silent majority dominate dengue virus transmission”. en. In: *PLOS Pathogens* 14.5. Ed. by N. M. Ferguson, e1006965. DOI: 10.1371/journal.ppat.1006965.
- Bron, G. M., K. Strimbu, H. Cecilia, A. Lerch, S. Moore, Q. Tran, T. A. Perkins, and Q. A. ten Bosch (2021). “Over 100 years of Rift Valley Fever: a patchwork of data on pathogen spread and spillover”. en. In: *Pathogens* 10.708. DOI: 10.3390/pathogens10060708.
- Buhnerkempe, M. G., M. G. Roberts, A. P. Dobson, H. Heesterbeek, P. J. Hudson, and J. O. Lloyd-Smith (2015). “Eight challenges in modelling disease ecology in multi-host, multi-agent systems”. en. In: *Epidemics* 10, pp. 26–30. DOI: 10.1016/j.epidem.2014.10.001.
- Bustamante, D. M. and C. C. Lord (2010). “Sources of Error in the Estimation of Mosquito Infection Rates Used to Assess Risk of Arbovirus Transmission”. en. In: *American Journal of Tropical Medicine and Hygiene* 82.6, pp. 1172–1184.
- Canini, L., M. E. J. Woolhouse, T. R. Maines, and F. Carrat (2016). “Heterogeneous shedding of influenza by human subjects and its implications for epidemiology and control”. en. In: *Scientific Reports* 6.1. DOI: 10.1038/srep38749.
- Clapham, H. E., V. Tricou, N. Van Vinh Chau, C. P. Simmons, and N. M. Ferguson (2014). “Within-host viral dynamics of dengue serotype 1 infection”. en. In: *Journal of The Royal Society Interface* 11.96, p. 20140094. DOI: 10.1098/rsif.2014.0094.
- Clapham, H. E., T. H. Quyen, D. T. H. Kien, I. Dorigatti, C. P. Simmons, and N. M. Ferguson (2016). “Modelling Virus and Antibody Dynamics during Dengue Virus Infection Suggests a Role for Antibody in Virus Clearance”. en. In: *PLOS Computational Biology* 12.5. Ed. by R. Antia, e1004951. DOI: 10.1371/journal.pcbi.1004951.
- Clark, M. H. A., G. M. Warimwe, A. Di Nardo, N. A. Lyons, and S. Gubbins (2018). “Systematic literature review of Rift Valley fever virus seroprevalence in livestock, wildlife and humans in Africa from 1968 to 2016”. en. In: *PLOS Neglected Tropical Diseases* 12.7. Ed. by C. M. Barker, e0006627. DOI: 10.1371/journal.pntd.0006627.
- Cleaveland, S., M. Laurenson, and L. Taylor (2001). “Diseases of humans and their domestic mammals: pathogen characteristics, host range and the risk of emergence”. en. In: *Phil. Trans. R. Soc. Lond. B* 356.1411. Ed. by M. E. J. Woolhouse and C. Dye, pp. 991–999. DOI: 10.1098/rstb.2001.0889.
- Coghlan, J. P., J. S. Fan, B. A. Scoggins, and A. A. Shulkes (1977). “Measurement of extracellular fluid volume and blood volume in sheep”. In: *Aust J Biol Sci.* 30.1-2, pp. 71–84.
- Courtice, F. C. (1943). “The blood volume of normal animals”. en. In: *The Journal of Physiology* 102.3, pp. 290–305. DOI: 10.1113/jphysiol.1943.sp004035.
- Daubney, R., J. R. Hudson, and P. C. Garnham (1931). “Enzootic hepatitis or rift valley fever. An undescribed virus disease of sheep cattle and man from east africa”. en. In: *The Journal of Pathology and Bacteriology* 34.4, pp. 545–579. DOI: 10.1002/path.1700340418.

- El Mamy, A. B. O. et al. (2011). “Unexpected Rift Valley Fever Outbreak, Northern Mauritania”. en. In: *Emerging Infectious Diseases* 17.10, pp. 1894–1896. DOI: 10.3201/eid1710.110397.
- Elliott, R. and F. Weber (2009). “Bunyaviruses and the Type I Interferon System”. en. In: *Viruses* 1.3, pp. 1003–1021. DOI: 10.3390/v1031003.
- Fenton, A., D. G. Streicker, O. L. Petchey, and A. B. Pedersen (2015). “Are All Hosts Created Equal? Partitioning Host Species Contributions to Parasite Persistence in Multihost Communities”. en. In: *The American Naturalist* 186.5, pp. 610–622. DOI: 10.1086/683173.
- Ferguson, N. M. et al. (2015). “Modeling the impact on virus transmission of *Wolbachia* -mediated blocking of dengue virus infection of *Aedes aegypti*”. en. In: *Sci. Transl. Med.* 7.279, 279ra37–279ra37. DOI: 10.1126/scitranslmed.3010370.
- Fontaine, A., S. Lequime, I. Moltini-Conclois, D. Jiolle, I. Leparç-Goffart, R. C. Reiner, and L. Lambrechts (2018). “Epidemiological significance of dengue virus genetic variation in mosquito infection dynamics”. en. In: *PLOS Pathogens* 14.7. Ed. by N. M. Ferguson, e1007187. DOI: 10.1371/journal.ppat.1007187.
- Gog, J. R., L. Pellis, J. L. Wood, A. R. McLean, N. Arinaminpathy, and J. O. Lloyd-Smith (2015). “Seven challenges in modeling pathogen dynamics within-host and across scales”. en. In: *Epidemics* 10, pp. 45–48. DOI: 10.1016/j.epidem.2014.09.009.
- Golnar, A. J., M. J. Turell, A. D. LaBeaud, R. C. Kading, and G. L. Hamer (2014). “Predicting the Mosquito Species and Vertebrate Species Involved in the Theoretical Transmission of Rift Valley Fever Virus in the United States”. en. In: *PLoS Neglected Tropical Diseases* 8.9. Ed. by C. M. Barker, e3163. DOI: 10.1371/journal.pntd.0003163.
- Hollingsworth, T. D., J. R. Pulliam, S. Funk, J. E. Truscott, V. Isham, and A. L. Lloyd (2015). “Seven challenges for modelling indirect transmission: Vector-borne diseases, macroparasites and neglected tropical diseases”. en. In: *Epidemics* 10, pp. 16–20. DOI: 10.1016/j.epidem.2014.08.007.
- Iwami, S., B. P. Holder, C. A. Beauchemin, S. Morita, T. Tada, K. Sato, T. Igarashi, and T. Miura (2012). “Quantification system for the viral dynamics of a highly pathogenic simian/human immunodeficiency virus based on an in vitro experiment and a mathematical model”. en. In: p. 12.
- Jacobs, N. T., N. O. Onuoha, A. Antia, J. Steel, R. Antia, and A. C. Lowen (2019). “Incomplete influenza A virus genomes occur frequently but are readily complemented during localized viral spread”. en. In: *Nature Communications* 10.1. DOI: 10.1038/s41467-019-11428-x.
- Kain, M. P. and B. M. Bolker (2019). “Predicting West Nile virus transmission in North American bird communities using phylogenetic mixed effects models and eBird citizen science data”. en. In: *Parasites Vectors* 12.1, p. 395. DOI: 10.1186/s13071-019-3656-8.
- Koelle, K., A. P. Farrell, C. B. Brooke, and R. Ke (2019). “Within-host infectious disease models accommodating cellular coinfection, with an application to influenza†”. en. In: *Virus Evolution* 5.2. DOI: 10.1093/ve/vez018.

- Kruschke, J. (2015). “Doing Bayesian Data Analysis: A tutorial with R and Bugs”. en. In: *Doing Bayesian Data Analysis*. Elsevier, pp. i–ii. DOI: 10.1016/B978-0-12-405888-0.09999-2.
- Krylova, O. and D. J. D. Earn (2013). “Effects of the infectious period distribution on predicted transitions in childhood disease dynamics”. en. In: *Journal of The Royal Society Interface* 10.84, p. 20130098. DOI: 10.1098/rsif.2013.0098.
- LaBeaud, A. D., J. W. Kazura, and C. H. King (2010). “Advances in Rift Valley fever research: insights for disease prevention.” en. In: *Current Opinion in Infectious Diseases* 23.5, pp. 403–408. DOI: 10.1097/QCO.0b013e32833c3da6.
- Lequime, S., J.-S. Dehecq, S. Matheus, F. de Laval, L. Almeras, S. Briolant, and A. Fontaine (2020). “Modeling intra-mosquito dynamics of Zika virus and its dose-dependence confirms the low epidemic potential of *Aedes albopictus*”. en. In: *PLOS Pathogens* 16.12. Ed. by E. A. McGraw, e1009068. DOI: 10.1371/journal.ppat.1009068.
- Linthicum, K. J., S. C. Britch, and A. Anyamba (2016). “Rift Valley Fever: An Emerging Mosquito-Borne Disease”. In: *Annual Review of Entomology* 61.1, pp. 395–415. DOI: 10.1146/annurev-ento-010715-023819.
- Lloyd, A. L. (2001). “Realistic Distributions of Infectious Periods in Epidemic Models: Changing Patterns of Persistence and Dynamics”. en. In: *Theoretical Population Biology* 60.1, pp. 59–71. DOI: 10.1006/tpbi.2001.1525.
- Lloyd-Smith, J. O., S. Funk, A. R. McLean, S. Riley, and J. L. Wood (2015). “Nine challenges in modelling the emergence of novel pathogens”. en. In: *Epidemics* 10, pp. 35–39. DOI: 10.1016/j.epidem.2014.09.002.
- Mapder, T., S. Clifford, J. Aaskov, and K. Burrage (2019). “A population of bang-bang switches of defective interfering particles makes within-host dynamics of dengue virus controllable”. en. In: *PLOS Computational Biology* 15.11. Ed. by J. A. Papin, e1006668. DOI: 10.1371/journal.pcbi.1006668.
- Martin, L. B. et al. (2019). “Extreme Competence: Keystone Hosts of Infections”. en. In: *Trends in Ecology & Evolution* 34.4, pp. 303–314. DOI: 10.1016/j.tree.2018.12.009.
- Meegan, J. M. (1979). “The Rift Valley fever epizootic in Egypt 1977–1978 1. Description of the epizootic and virological studies”. en. In: *Transactions of the Royal Society of Tropical Medicine and Hygiene* 73.6, pp. 618–623. DOI: 10.1016/0035-9203(79)90004-X.
- Miao, H., X. Xia, A. S. Perelson, and H. Wu (2011). “On Identifiability of Nonlinear ODE Models and Applications in Viral Dynamics”. en. In: *SIAM Review* 53.1, pp. 3–39. DOI: 10.1137/090757009.
- Nanyingi, M. O., P. Munyua, S. G. Kiama, G. M. Muchemi, S. M. Thumbi, A. O. Bitek, B. Bett, R. M. Muriithi, and M. K. Njenga (2015). “A systematic review of Rift Valley Fever epidemiology 1931–2014”. en. In: *Infection Ecology & Epidemiology* 5.1, p. 28024. DOI: 10.3402/iee.v5.28024.
- Petrie, S. M., T. Guarnaccia, K. L. Laurie, A. C. Hurt, J. McVernon, and J. M. McCaw (2013). “Reducing Uncertainty in Within-Host Parameter Estimates of Influenza Infection by Measuring Both Infectious and

- Total Viral Load”. en. In: *PLoS ONE* 8.5. Ed. by J. D. Brown, e64098. DOI: 10.1371/journal.pone.0064098.
- Petrie, S. M., J. Butler, I. G. Barr, J. McVernon, A. C. Hurt, and J. M. McCaw (2015). “Quantifying relative within-host replication fitness in influenza virus competition experiments”. en. In: *Journal of Theoretical Biology* 382, pp. 259–271. DOI: 10.1016/j.jtbi.2015.07.003.
- Pinilla, L. T., B. P. Holder, Y. Abed, G. Boivin, and C. A. A. Beauchemin (2012). “The H275Y Neuraminidase Mutation of the Pandemic A/H1N1 Influenza Virus Lengthens the Eclipse Phase and Reduces Viral Output of Infected Cells, Potentially Compromising Fitness in Ferrets”. en. In: *Journal of Virology* 86.19, pp. 10651–10660. DOI: 10.1128/JVI.07244-11.
- Quigley, J., J. Drewry, and K. Martin (1998). “Estimation of Plasma Volume in Holstein and Jersey Calves”. en. In: *Journal of Dairy Science* 81.5, pp. 1308–1312. DOI: 10.3168/jds.S0022-0302(98)75693-0.
- Roberts, G. O., A. Gelman, and W. R. Gilks (1997). “Weak convergence and optimal scaling of random walk Metropolis algorithms”. en. In: *The Annals of Applied Probability* 7.1, pp. 110–120. DOI: 10.1214/aoap/1034625254.
- Roche, B., M Eric Benbow, R. Merritt, R. Kimbirauskas, M. McIntosh, P. L. C. Small, H. Williamson, and J.-F. Guégan (2013). “Identifying the Achilles heel of multi-host pathogens: the concept of keystone ‘host’ species illustrated by *Mycobacterium ulcerans* transmission”. en. In: *Environ. Res. Lett.* 8.4, p. 045009. DOI: 10.1088/1748-9326/8/4/045009.
- Scharton, D., A. J. Van Wettere, K. W. Bailey, Z. Vest, J. B. Westover, V. Siddharthan, and B. B. Gowen (2015). “Rift Valley Fever Virus Infection in Golden Syrian Hamsters”. en. In: *PLoS ONE* 10.1. Ed. by K. Kehm-Hall, e0116722. DOI: 10.1371/journal.pone.0116722.
- Schulze-Horsel, J., M. Schulze, G. Agalaridis, Y. Genzel, and U. Reichl (2009). “Infection dynamics and virus-induced apoptosis in cell culture-based influenza vaccine production—Flow cytometry and mathematical modeling”. en. In: *Vaccine* 27.20, pp. 2712–2722. DOI: 10.1016/j.vaccine.2009.02.027.
- Simon, P. F., M.-A. de La Vega, E. Paradis, E. Mendoza, K. M. Coombs, D. Kobasa, and C. A. A. Beauchemin (2016). “Avian influenza viruses that cause highly virulent infections in humans exhibit distinct replicative properties in contrast to human H1N1 viruses”. en. In: *Scientific Reports* 6.1. DOI: 10.1038/srep24154.
- Smith, A. M., F. R. Adler, and A. S. Perelson (2010). “An accurate two-phase approximate solution to an acute viral infection model”. en. In: *Journal of Mathematical Biology* 60.5, pp. 711–726. DOI: 10.1007/s00285-009-0281-8.
- Somvanshi, P. R. and K. V. Venkatesh (2013). “Hill Equation”. In: *Encyclopedia of Systems Biology*. Ed. by W. Dubitzky, O. Wolkenhauer, K.-H. Cho, and H. Yokota. New York, NY: Springer New York, pp. 892–895. DOI: 10.1007/978-1-4419-9863-7\_946.
- Svensson, A. (2007). “A note on generation times in epidemic models”. en. In: *Mathematical Biosciences* 208.1, pp. 300–311. DOI: 10.1016/j.mbs.2006.10.010.

- Taylor, L. H., S. M. Latham, and M. E. Woolhouse (2001). “Risk factors for human disease emergence”. en. In: *Phil. Trans. R. Soc. Lond. B* 356.1411. Ed. by M. E. J. Woolhouse and C. Dye, pp. 983–989. DOI: 10.1098/rstb.2001.0888.
- Tesla, B., L. R. Demakovskiy, H. S. Packiam, and E. A. Mordecai (2018). “Estimating the effects of variation in viremia on mosquito susceptibility, infectiousness, and R0 of Zika in *Aedes aegypti*”. en. In: *PLOS Neglected Tropical Diseases* 12.8, p. 19.
- Tuncer, N., H. Gulbudak, V. L. Cannataro, and M. Martcheva (2016). “Structural and Practical Identifiability Issues of Immuno-Epidemiological Vector–Host Models with Application to Rift Valley Fever”. en. In: *Bulletin of Mathematical Biology* 78.9, pp. 1796–1827. DOI: 10.1007/s11538-016-0200-2.
- Turell, M. J., D. J. Dohm, C. N. Mores, L. Terracina, D. L. Wallete, L. J. Hribar, J. E. Pecor, and J. A. Blow (2008). “Potential for North American Mosquitoes to Transmit Rift Valley Fever Virus<sup>1</sup>”. en. In: *Journal of the American Mosquito Control Association* 24.4, pp. 502–507. DOI: 10.2987/08-5791.1.
- Turell, M. J., W. C. Wilson, and K. E. Bennett (2010). “Potential for North American Mosquitoes (Diptera: Culicidae) to Transmit Rift Valley Fever Virus”. en. In: *J Med Entomol* 47.5, pp. 884–889. DOI: 10.1093/jmedent/47.5.884.
- Turell, M. J., S. C. Britch, R. L. Aldridge, D. L. Kline, C. Boohene, and K. J. Linthicum (2013). “Potential for Mosquitoes (Diptera: Culicidae) From Florida to Transmit Rift Valley Fever Virus”. en. In: *J Med Entomol* 50.5, pp. 1111–1117. DOI: 10.1603/ME13049.
- Turell, M. J., L. W. Cohnstaedt, and W. C. Wilson (2020). “Effect of Environmental Temperature on the Ability of *Culex tarsalis* and *Aedes taeniorhynchus* (Diptera: Culicidae) to Transmit Rift Valley Fever Virus”. en. In: *Vector-Borne and Zoonotic Diseases* 20.6, pp. 454–460. DOI: 10.1089/vbz.2019.2554.
- Vazquez-Prokopec, G. M., T. A. Perkins, L. A. Waller, A. L. Lloyd, R. C. Reiner, T. W. Scott, and U. Kitron (2016). “Coupled Heterogeneities and Their Impact on Parasite Transmission and Control”. en. In: *Trends in Parasitology* 32.5, pp. 356–367. DOI: 10.1016/j.pt.2016.01.001.
- Vloet, R. P. M., C. B. F. Vogels, C. J. M. Koenraadt, G. P. Pijlman, M. Eiden, J. L. Gonzales, L. J. M. van Keulen, P. J. Wichgers Schreur, and J. Kortekaas (2017). “Transmission of Rift Valley fever virus from European-breed lambs to *Culex pipiens* mosquitoes”. en. In: *PLOS Neglected Tropical Diseases* 11.12. Ed. by M. J. Turell, e0006145. DOI: 10.1371/journal.pntd.0006145.
- Wallinga, J and M Lipsitch (2007). “How generation intervals shape the relationship between growth rates and reproductive numbers”. en. In: *Proc. R. Soc. B* 274.1609, pp. 599–604. DOI: 10.1098/rspb.2006.3754.
- Weaver, S. C., N. L. Forrester, J. Liu, and N. Vasilakis (2021). “Population bottlenecks and founder effects: implications for mosquito-borne arboviral emergence”. en. In: *Nat Rev Microbiol* 19.3, pp. 184–195. DOI: 10.1038/s41579-020-00482-8.



- Webster, J. P., A. Borlase, and J. W. Rudge (2017). “Who acquires infection from whom and how? Disentangling multi-host and multi-mode transmission dynamics in the ‘elimination’ era”. en. In: *Phil. Trans. R. Soc. B* 372.1719, p. 20160091. DOI: 10.1098/rstb.2016.0091.
- Wichgers Schreur, P. J. et al. (2020a). “Safety and efficacy of four-segmented Rift Valley fever virus in young sheep, goats and cattle”. en. In: *npj Vaccines* 5.1. DOI: 10.1038/s41541-020-00212-4.
- (2020b). “Safety and efficacy of four-segmented Rift Valley fever virus in young sheep, goats and cattle”. en. In: *npj Vaccines* 5.1. DOI: 10.1038/s41541-020-00212-4.
- Wichgers Schreur, P. J., R. P. M. Vloet, J. Kant, L. van Keulen, J. L. Gonzales, T. M. Visser, C. J. M. Koenraadt, C. B. F. Vogels, and J. Kortekaas (2021). “Reproducing the Rift Valley fever virus mosquito-lamb-mosquito transmission cycle”. en. In: *Sci Rep* 11.1, p. 1477. DOI: 10.1038/s41598-020-79267-1.
- Yan, A. W., J. Zhou, C. A. Beauchemin, C. A. Russell, W. S. Barclay, and S. Riley (2020). “Quantifying mechanistic traits of influenza viral dynamics using in vitro data”. en. In: *Epidemics* 33, p. 100406. DOI: 10.1016/j.epidem.2020.100406.

# Supplementary Information

## Heterogeneity of Rift Valley fever virus transmission potential across livestock hosts, quantified through a model-based analysis of host viral load and vector infection

Hélène Cecilia, Roosmarie Vriens, Jeroen Kortekaas, Paul J. Wichgers Schreur, Mariken de Wit, Raphaëlle Métras, Pauline Ezanno, Quirine A. ten Bosch

### S.1 Within-host model of RVFV infection

#### S.1.1 Parameter estimation

The Deviance Information Criterion (DIC) is calculated as:

$$DIC = p_D + \overline{D(\theta)} \quad (\text{S.1})$$

$$D(\theta) = -2 \cdot \log(p(y|\theta)) + C \quad (\text{S.2})$$

$$p_D = \overline{D(\hat{\theta})} - D(\hat{\theta}) \quad (\text{S.3})$$

where  $\theta$  is the vector of unknown parameters sampled,  $p$  is the likelihood function and  $y$  the data. We compute this DIC on the joint posterior distribution of 3 chains, each with the burn-in period removed.

For species heterogeneity, as no cattle nor goats died during the experiment, we based our comparison on surviving individuals. Therefore, we compute the DIC of a model fitted to the dataset comprising all surviving individuals, and compare it to the sum of DICs of models fitted to each species dataset separately. Similarly, for lambs, we compute the DIC of a model fitted to the whole lamb dataset, and compare it to the sum of DICs of models fitted to surviving and dying lambs separately.

Due to correlation between parameters, the value of  $T_0$  could not be estimated within the MCMC procedure. Instead, we produced likelihood profiles by running the MCMC procedure for different values of  $T_0$ , for each animal group, and recorded the maximum log-likelihood (Figure S.1).

We then performed the Gelman-Rubin diagnostic to check for the common convergence of multiple chains (Figure S.2 for models selected by DIC). All multivariate potential scale reduction factors were  $<1.01$  (Figure S.3). The joint posterior distributions are shown in Figure S.4.

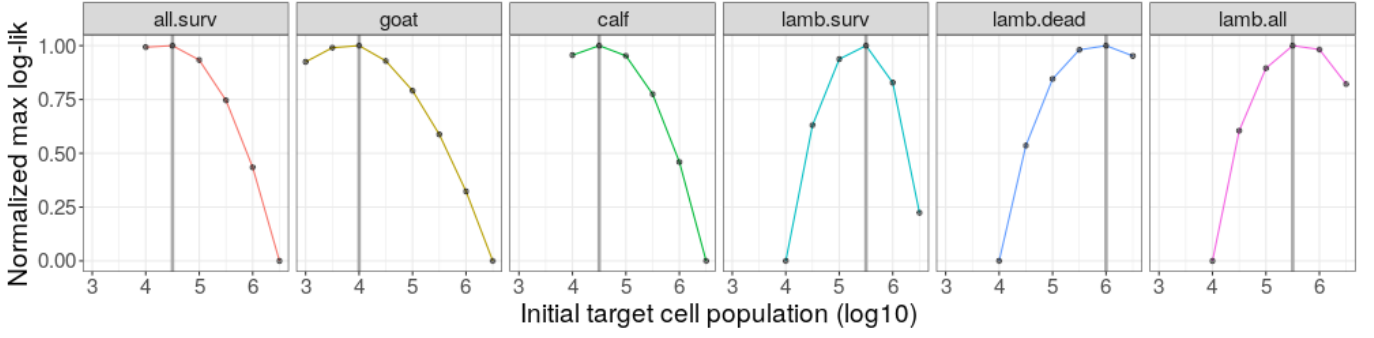


Figure S.1: Likelihood profiles to estimate  $T_0$ . Each point corresponds to the (normalized) maximum log-likelihood of an MCMC procedure run with a given  $T_0$  value, for a given animal group (facet title). Vertical lines show the  $T_0$  retained for further parameter estimation (chains of 100,000 iterations). Note that for lambs, assigning a common  $T_0$  to individuals surviving and succumbing to the infection does not give the best fits so these groups were assigned different values.

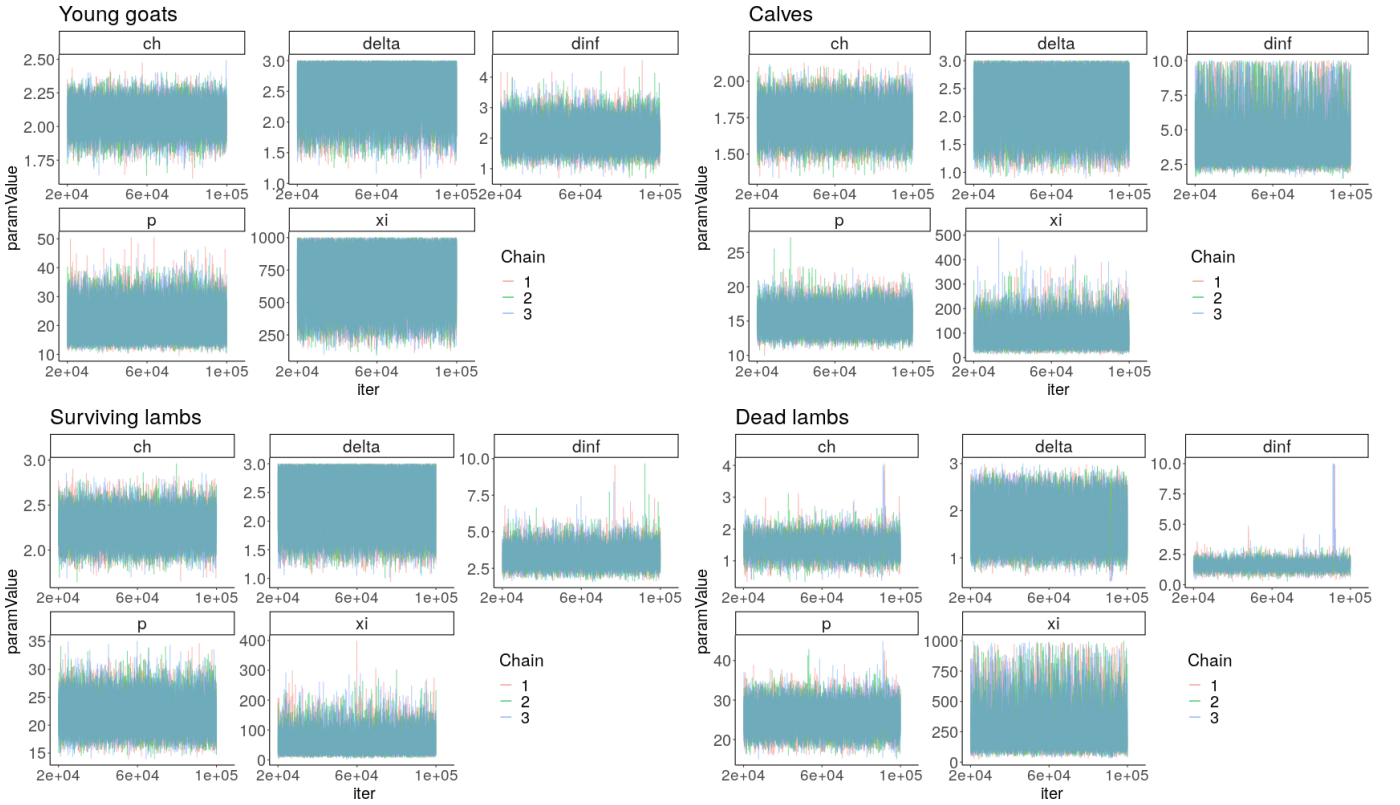


Figure S.2: Trace plots of selected models. Three chains, 100,000 iterations, 20,000 burn-in.

### S.1.2 Outcome measures

According to Svensson, 2007:

For a population model, the expected time between a primary case and a secondary case is :

$$E[T_g] = E[L] + \frac{E[I^2]}{2E[I]}$$

For our within-host model,  $I$  and  $L$  now refer to the state of the cells instead of individuals, and we add  $E[V_{inf}]$ .

A property of the expected value is :  $V[I] = E[I^2] - E[I]^2$

$$E[T_g] = E[L] + \frac{V[I] + E[I]^2}{2E[I]} + E[V_{inf}]$$

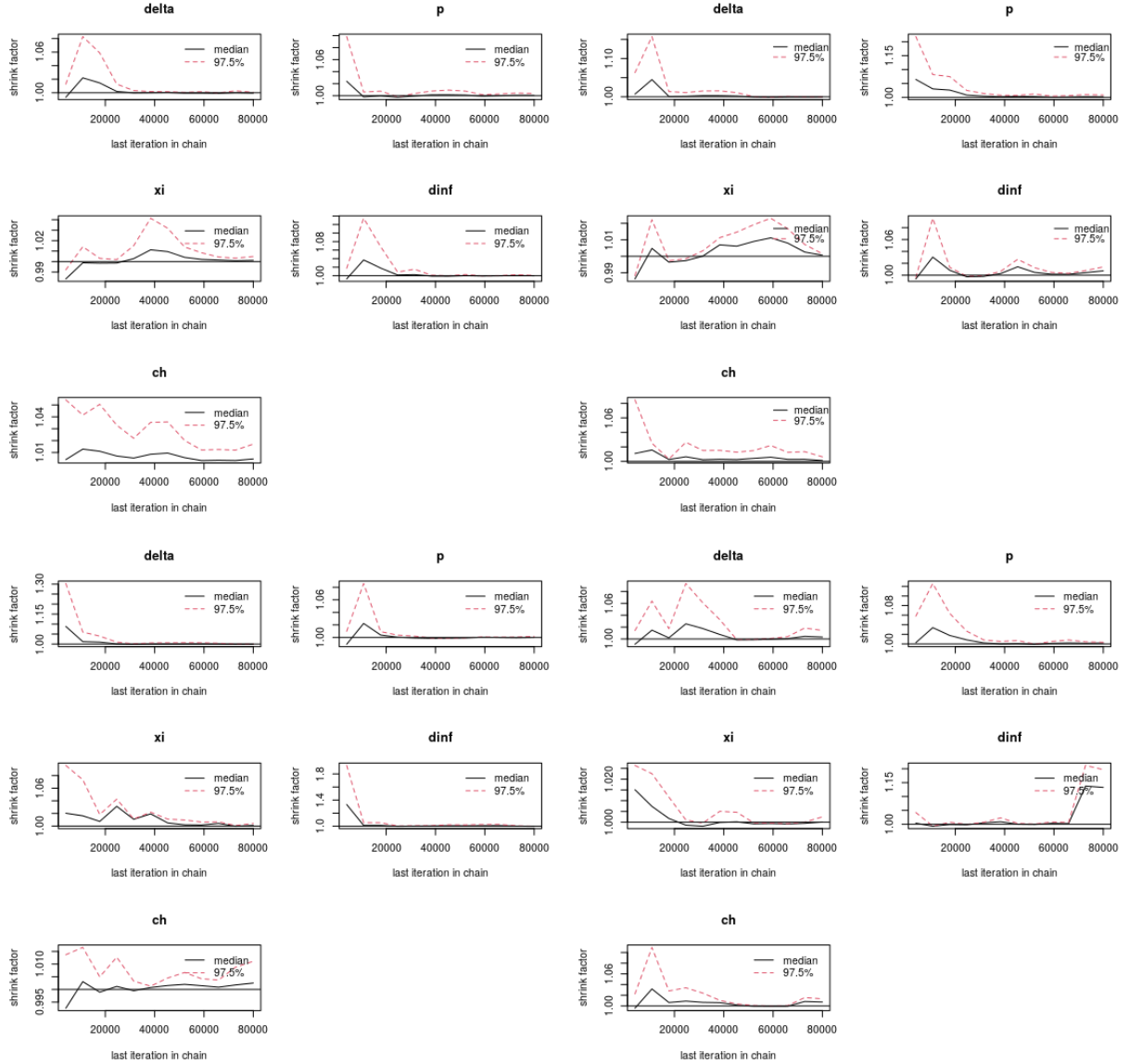


Figure S.3: Gelman diagnostic plots, per parameter for selected models. Top left : goats, top right : calves, bottom left : lambs which survived, bottom right : lambs which died.

for Erlang distributions,  $V[I] = \frac{E[I]^2}{n}$ ,  $n$  : shape parameter

$$\frac{V[I] + E[I]^2}{2E[I]} = \frac{\frac{E[I]^2}{n} + E[I]^2}{2E[I]} = \frac{\frac{n+1}{n}E[I]^2}{2E[I]} = \frac{n+1}{2n}E[I]$$

$$E[T_g] = E[L] + \frac{V[I] + E[I]^2}{2E[I]} + E[Vinf] = \kappa^{-1} + \frac{n+1}{2n}\delta^{-1} + (c_h + d_{inf} + \sigma\beta T_0)^{-1}$$

## S.2 Dose-response relationship in RVFV mosquito vectors

### S.2.1 Systematic review

A systematic review of the literature was performed in order to investigate the relationship between vertebrate host infectious titer at the moment of blood-feeding and infection of a vector. PubMed and Scopus were searched

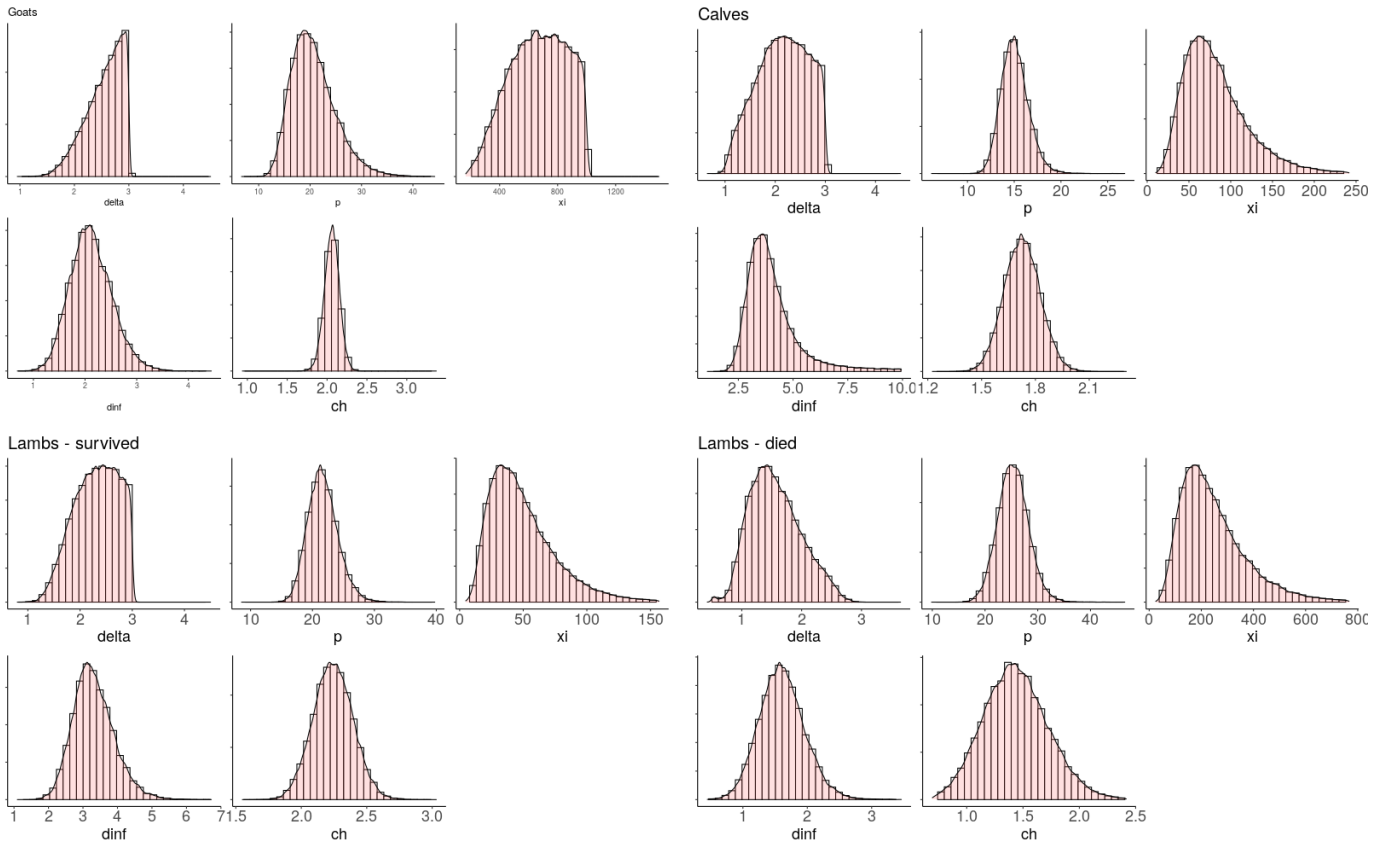


Figure S.4: Joint posterior distributions of parameters per selected model. Priors can be found in Table 2.  $\delta$  is constrained to be inferior to  $\kappa$  (fixed, = 3), and  $c_h + d_{inf}$ , as advised by Smith et al., 2010

on 27<sup>th</sup> september 2021 with the following query:

```
((Vector*) OR (Mosquit*) OR (Aedes) OR (Culex) OR (Anopheles))
AND
((Transm*) OR ("vector competence") OR (Infect*))
AND
(("rift valley fever"))
AND
((Virol*) OR ("virus level") OR ("viral level") OR ("virus load") OR ("Viral load"))
OR (Virem*) OR (Viraem*))
AND
((Host*) OR (Ruminant*) OR (Sheep*) OR (Goat*) OR (Cow) OR (Lamb*) OR (Calve*) OR (Ewe)
OR (Ewes) OR (Cows) OR (Buffalo*) OR (Camel*) OR (cattle) OR (rodent*) OR (hamster*))
```

This search provided 315 results in PubMed and 253 from Scopus, 357 of which were unique results. 316 articles were excluded at the title and abstract level, 23 at the full text level. The exclusion criteria (not mutually exclusive) for these steps were :

- no mention of RVFV (n = 26)
- no viral load values given (n = 215)
- no use of mosquito (n = 116)
- not written in English (n = 11)
- no presence of primary data (e.g number of mosquitoes, n = 51)
- full text not available (n = 9)
- review (n = 5)

Eventually, data from 18 articles was retrieved for further inspection. A descriptive analyses was performed to assess the diversity of protocols used. The 16 papers corresponded to 341 data points. Regarding hosts, 75% (n = 256) were hamster, 23% artificial feeding, and 2% lamb. Regarding mosquito vector used, 45% (n = 154) were *Culex* spp., 41% *Aedes* spp.. The rest was a mix of *Anopheles*, *Coquilleltidia*, *Mansionia*, *Culiseta*, and *Psophora* spp.. Regarding RVFV strains, 73% were ZH501 (n = 250). The detail of other strains will be spared here, but none was used in more than 20 experiments.

We limited our quantitative analysis to experiments performed with *Aedes* and *Culex* spp., with strain ZH501, on hamsters. This was done because the number of experiments performed with other hosts and strains was too small to properly test for the effect of these variables. Hamsters have been shown to be good model hosts for RVFV infection (Scharton et al., 2015). ZH501 is a wild strain originally isolated from a human patient during the outbreak of 1977 in Egypt (Meegan, 1979).

## S.2.2 Data description

Nine papers remained, corresponding to 185 data points (81 *Aedes*, 104 *Culex*). We first examined the distribution of timing of dissection, temperature and infectious titers in our dataset. The reporting of the duration between mosquito feeding and determination of its infection status was not always very precise. When a range was given, we used the middle point value ; when a lower limit was given, we used the limit plus 1 day. We applied the same rule for temperature and infectious titers, although the precision was usually better. The distribution of these 3 variables across experiments and for each genus is shown in Figure S.5. A Wilcox-test concluded that there was no significant difference between genus for these 3 variables.

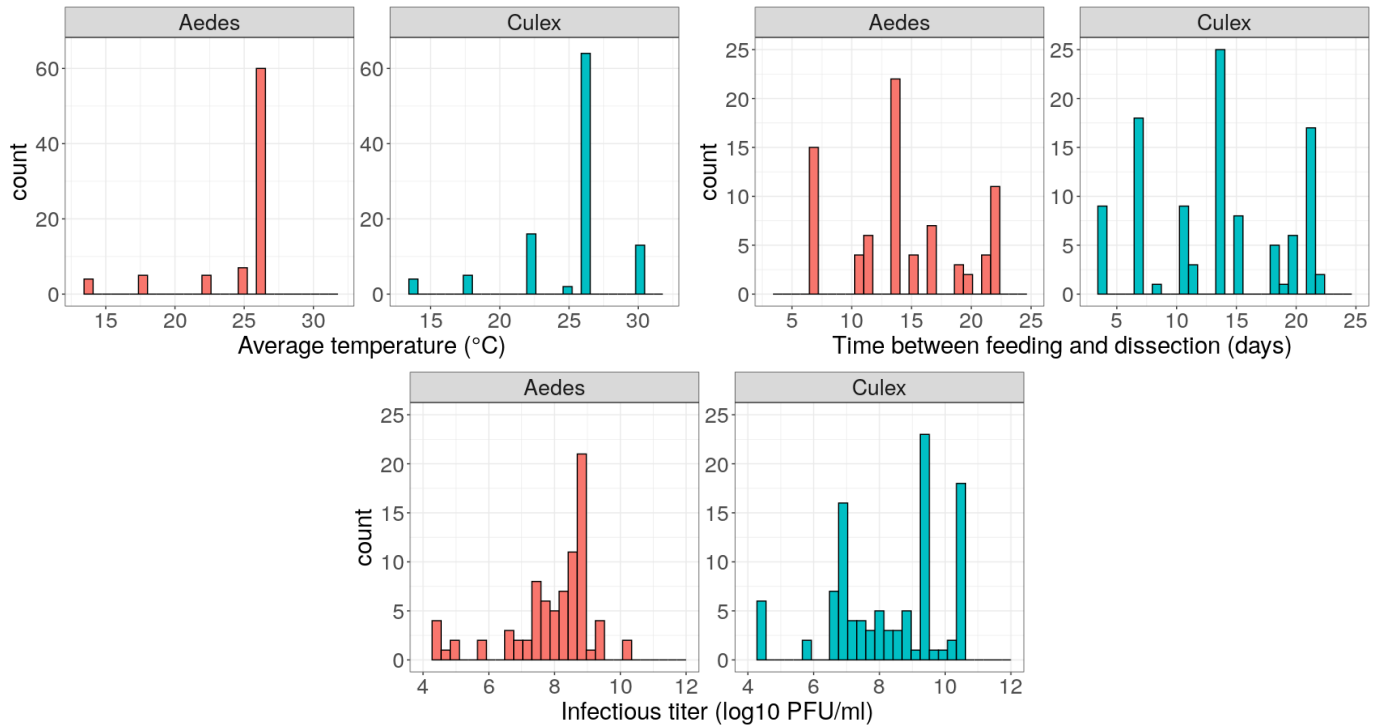


Figure S.5: Distribution of temperature, days post-exposure, and infectious titers, in experimental data retrieved from the systematic review, for *Aedes* and *Culex* spp. vectors.

Wilcoxon rank sum test with continuity correction

data: temp.aedes and temp.culex

W = 3847.5, p-value = 0.2275

alternative hypothesis: true location shift is not equal to 0

###

Wilcoxon rank sum test with continuity correction

data: dpf.aedes and dpf.culex

W = 4758, p-value = 0.1285

alternative hypothesis: true location shift is not equal to 0

###

Wilcoxon rank sum test with continuity correction

data: dose.aedes and dose.culex

W = 3536, p-value = 0.06089

alternative hypothesis: true location shift is not equal to 0

Note on units for infectious titers : In all experimental data retained for analysis, infectious titers were measured

using plaque forming units (PFUs). This unit was kept for the fitting of dose-response equations. However, for the computation of livestock infectiousness, we converted PFUs into TCID<sub>50</sub> to be compatible with our time series of viral load. We used  $V_{TCID_{50}} = V_{PFU} \times \frac{1}{0.69}$  which is consistent with 1 ml virus stock having half the number of PFUs as the TCID<sub>50</sub> (Canini et al. 2016).

### S.2.3 Functional forms

We used a logistic regression model (Eq. S.4) to study the effect of temperature ( $T$ ), duration between feeding of the mosquito and determination of its infection status ( $dpf$ ) and infectious titer of the host it fed on ( $dose$ ), on the probability to infect a mosquito. In our dataset, this probability is defined as the infection rate, i.e., the percentage of orally exposed mosquitoes that contained virus in their bodies (legs excluded). Indeed, dissemination rates (presence of virus in the head) showed strong variations, were measured on small sample sizes, and are likely to be influenced by other factors than infectious titers, out of the scope of this study. Transmission rates (presence of virus in the saliva) was only measured in 13% of our dataset.

$$F(T, dpf, dose) = \frac{1}{1 + e^{-(\beta_0 + \beta_1 \cdot T + \beta_2 \cdot dpf + \beta_3 \cdot dose)}} \quad (S.4)$$

We explored whether the infection data were over-dispersed using beta-binomial logistic regression. Based on AIC of models with or without overdispersal, we found that accounting for overdispersal was necessary (AIC for binomial model: 1509; AIC for beta-binomial model: 923). The beta-binomial model did not point towards a significant effect of temperature and number of days after feeding on infection rates. Dissection happened at least 4 days after blood feeding, which intuitively seems sufficient to infect a mosquito (before midgut barrier crossing).

	Estimate	Std. Error	z value	Pr(z)		
beta0	-4.54506155	0.90396837	-5.0279	4.959e-07 ***		
beta1	0.02605400	0.02419026	1.0770	0.2815		
beta2	-0.00097779	0.01451044	-0.0674	0.9463		
beta3	0.49687416	0.05892514	8.4323	< 2.2e-16 ***		
overdispersion	4.14372201	0.56620726	7.3184	2.510e-13 ***		
---						
Signif. codes:	0 '***'	0.001 '**'	0.01 '*'	0.05 '.'	0.1 ' '	1

We then compared three functional forms (Eq. S.5-Eq. S.7) for the dose-response relationship, again using both a binomial and a beta-binomial likelihood for each. This was done on the whole dataset, *Aedes* and *Culex* spp. aggregated. Eq. S.5 is the logistic function, with the curve's maximum value fixed at 1 since we are dealing with probabilities. Eq. S.6 (Ferguson et al., 2015) was used to study vector competence for dengue when carrying *Wolbachia*. Eq. S.7 (Somvanshi and Venkatesh, 2013) is often used to model biological interactions that



demonstrate sigmoidal response, in particular to capture the biomolecular interaction exhibiting cooperativity among two binding molecules.

$$\text{Logistic}(\text{dose}) = \frac{1}{1 + \exp(-(\beta_0 + \beta_1 \cdot \text{dose}))} \quad (\text{S.5})$$

$$\text{Ferguson}(\text{dose}) = 1 - \exp\left(\frac{-\text{dose}}{\beta_0} + \text{dose}\right)^{\beta_1} \quad (\text{S.6})$$

$$\text{Hill}(\text{dose}) = \frac{\text{dose}^{\beta_0}}{\beta_1} + \text{dose}^{\beta_0} \quad (\text{S.7})$$

Based on AIC, the Ferguson model best fitted the data. The AICs of all three functional forms supported the assumption that the data were betabinomially distributed.

	AIC	df
binom_Log	1532.8243	2
betabinom_Log	919.7607	3
binom_Ferg	1524.8107	2
betabinom_Ferg	918.8410	3
binom_Hill	1519.1427	2
betabinom_Hill	918.8682	3

We then fitted *Aedes* (n = 81) and *Culex* (n = 104) observations separately with Eq. S.6. The likelihood ratio test showed that the dose-response relationships associated with these two categories were significantly different ( Figure 4 in main text ).

```
> lrt(LL0 = betabinom_Ferg_CuAe@details$value,
+     LL1 = sum(betabinom_Ferg_Culex@details$value, betabinom_Ferg_Aedes@details$value),
+     df0 = 3, df1 = 6)
$L01
[1] 31.13315
$df
[1] 3
$`p-value`
[1] 7.969038e-07
```

Table S.1 shows the different species included in our dataset, with the associated number of observations. We explored species-specific curves for species that had sufficient data available at a large enough range of dosages. We ended up fitting a curve for *Cx. tarsalis*, *Cx. nigripalpus*, *Ae. vexans*, and *Ae. j. japonicus* (Figure S.6).

<i>Aedes</i> spp.		<i>Culex</i> spp.	
Species	n	Species	n
<i>Ae. taeniorhynchus</i>	21	<b><i>Cx. tarsalis</i></b>	57
<b><i>Ae. vexans</i></b>	13	<b><i>Cx. nigripalpus</i></b>	15
<b><i>Ae. j. japonicus</i></b>	8	<i>Cx. quinquefasciatus</i>	10
<i>Ae. infirmatus</i>	8	<i>Cx. pipiens</i>	7
<i>Ae. calceatus</i>	6	<i>Cx. salinarius</i>	6
<i>Ae. aegypti</i>	4	<i>Cx. erraticus</i>	5
<i>Ae. atlanticus</i>	4	<i>Cx. zombaensis</i>	2
<i>Ae. circumluteolus</i>	3	<i>Cx. annulirostris</i>	1
<i>Ae. dorsalis</i>	3	<i>Cx. erythrothoras</i>	1
<i>Ae. notoscriptus</i>	3		
<i>Ae. vigilax</i>	3		
<i>Ae. communis</i>	1		
<i>Ae. fitchii</i>	1		
<i>Ae. implicatus</i>	1		
<i>Ae. sticticus</i>	1		
<i>Ae. stimulans</i>	1		

Table S.1: Number of datapoints available per vector species, retrieved from the systematic review. *Ae. taeniorhynchus* was not selected as experiments performed on this species only included two distinct dosages.

### S.3 Net infectiousness of RVFV livestock hosts

Figure S.7 shows the sensitivity of lambs' net infectiousness (NI) to the survival rate in the population. Indeed, NI is computed from 1000 dose-response curves combined with 1000 viral load curves, each of which is assigned to be of a surviving or dying type depending on the survival rate in the population. For viral load curves of dying individuals, we then apply a Weibull survival model directly computed from experimental times of death to truncate the viral load dynamics at the relevant timestep. We do not test the sensitivity of NI to those death times.

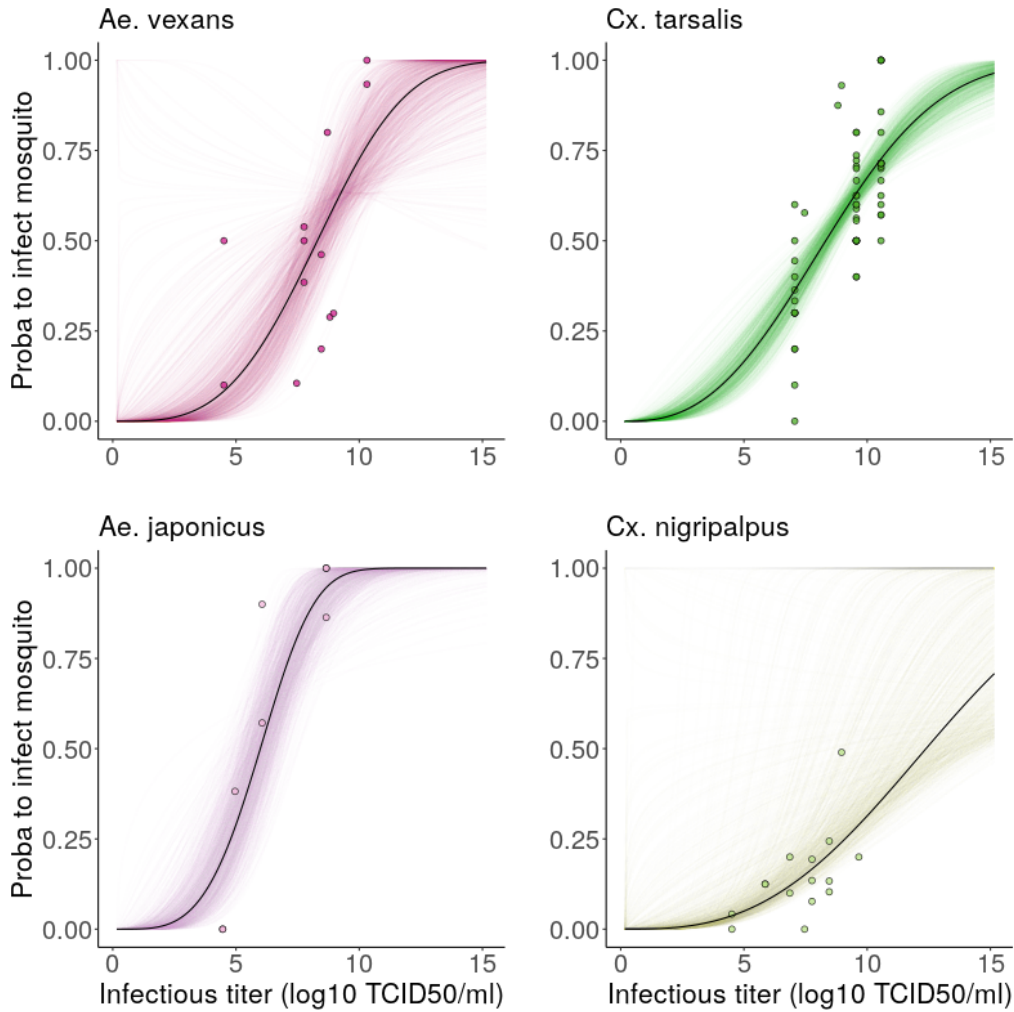


Figure S.6: **Species-specific dose-response curves.** Probability to infect a mosquito (y-axis) given feeding on a host with a certain infectious titer (x-axis). Points represent data gathered from literature review, where the probability is computed as the proportion of mosquitoes containing RVFV in their bodies (legs excluded), in a pool of fed mosquitoes (sample size not shown on plot for readability). Black lines show the dose-response relationship obtained by fitting Eq. S.6 with a betabinomial likelihood accounting for overdispersal in the data. Colored lines show the uncertainty around the fit : 1000 trajectories obtained by sampling in the variance-covariance matrix of the fitted model.

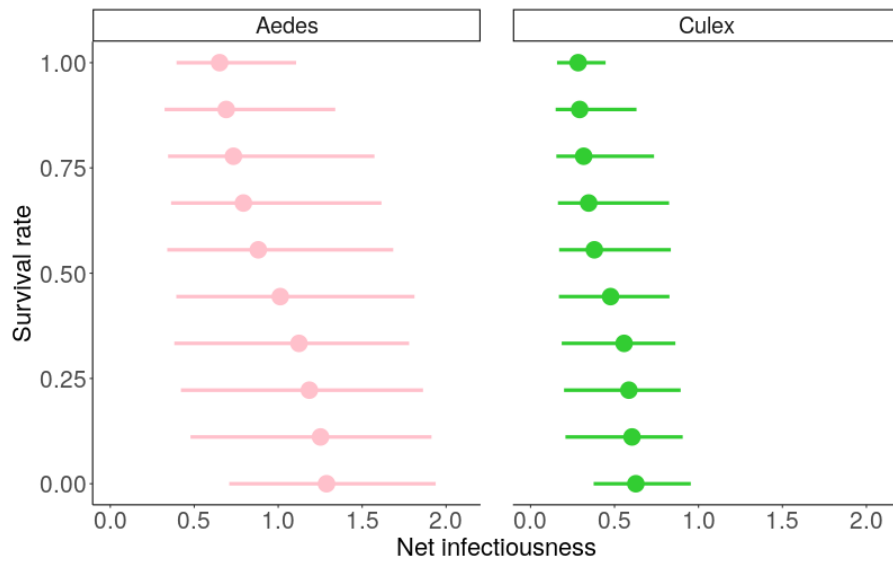


Figure S.7: Net infectiousness of an average lamb in relation with the expected survival rate in the population, for transmission to *Aedes* and *Culex* spp. vectors. Points show median, lines show highest density interval, computed from 1000 estimates.

# 5

## Metapopulation model of RVFV transmission dynamics in northern Senegal : the role of seasonal herd movements

### 5.1 Introduction

Metapopulation models are a type of spatial model, suited for cases where hosts can easily be partitioned into subunits (here called patches) (Keeling and Rohani, 2008). The subpopulations have independent dynamics and limited interactions between each other (Keeling and Rohani, 2008). Metapopulation models have been seen by ecologists as a compromise between theoretical ecology where the space is considered homogeneous, whether continuous or discrete (lattice), and landscape ecology, dealing with highly complex structures (Hanski, 1998; Lambin et al., 2010). An interesting property of these models, both for ecologists and epidemiologists, is the potential source-sink dynamics taking place, leading to extinctions and recolonizations (Grenfell and Harwood, 1997). Indeed, the level of local (within-patch) and global (metapopulation-wide) extinctions, and the possibility of a rescue effect, are emergent properties of the system, not easily predicted from model parameters (Keeling and Rohani, 2008; Eriksson et al., 2014).

In epidemiological applications, the strength of spatial interactions, called coupling, as well as its functional form, are usually dependent on the nature of the pathogen, its transmission routes, and its hosts (Keeling and Rohani, 2008). For animal and human diseases, the explicit representation of host movements can bring new insights into transmission dynamics. It has been shown that movement rates and distance can impact pathogen persistence (Jesse et al., 2008; Jesse and Heesterbeek, 2011). As a consequence, limiting or rewiring animal mobility networks are seen as useful strategies to control infectious diseases spread (Gates and Wool-

house, 2015; Hidano et al., 2016; Morel-Journal et al., 2021).

In metapopulation models of mosquito-borne diseases transmission dynamics, vectors are usually static while hosts link subpopulations. Models focusing on human hosts investigated rapid commuter movements, with residence and destination patches, which can vary in mosquito densities (Adams and Kapan, 2009; Moulay and Pigné, 2013; Manore et al., 2015; Anzo-Hernández et al., 2019). Metapopulation models have been developed to study Rift Valley fever virus (RVFV) transmission dynamics. They have been used to assess the role of intense animal mobility on RVFV spread around the time of religious festivals in Egypt (Xiao et al., 2015), or the role of cattle trade between different ecological zones (floodplain, residential, forest) in sustaining transmission in Madagascar and Tanzania (Nicolas et al., 2014; Sumaye et al., 2019).

The role of animal mobility on RVFV transmission dynamics in Senegal is established but hardly quantified (Belkhiria et al., 2019; Jahel et al., 2020). Two agent-based models (ABM) were developed to study its influence. The first, by Paul et al., 2014, focused on daily short-scale movements of animals, searching for water or pasture, around Barkedji. The second, by Paul et al., 2020, modeled animal migrations between cities, by truck. Besides, another ABM focused on an adjacent issue which is the multiple uses of land and resources around drillings in the Sahel (Bah et al., 2006). However, transhumance, in the sense of seasonal, pendular movements, constrained by environmental conditions and following similar itineraries every year (Gomez, 1979), have not yet been studied in a mechanistic model of RVFV transmission dynamics, in Senegal or elsewhere.

In northern Senegal, RVFV epidemic potential is heterogeneous across space and time (Cecilia et al., 2020). In the Senegal river delta and valley (SRDV), conditions are suitable for RVFV amplification year round (Cecilia et al., 2020). In the Ferlo region, the risk is strongly seasonal and is highest around temporary ponds which fill up during the wet season (Pin-Diop, 2006). In the Ferlo, the *peul* (fulani in english) are the most numerous pastoralist ethnicity (Pin-Diop, 2006). The *peul* can be sedentary, in which case their stay in the region during the dry season is made possible by permanent water points (Pin-Diop, 2006). The access to such water points is charged. During the wet season, they gather around ponds with nomadic herders, because the access to water there is free (Pin-Diop, 2006). Nomadic *peul* move their herds continuously, traveling long distances to search for water and pasture. Their mobility is

therefore strongly related to meteorologic conditions.

During the dry season, nomadic *peul* mostly stay southern of the Ferlo, where their herds do not disturb flood recession agriculture and can find some pasture. At that time, their camps are also free of mosquitoes. When the wet season starts, they start their transhumance towards the Ferlo, and their herds are expected to be mostly free from RVFV. After crossing the Ferlo a first time, they settle in their native village in SRDV for a while, when their animals are needed for harvesting. They are possibly exposed to RVFV during this period because this region is endemic. During the second half of the wet season, they start again their journey towards the south, possibly carrying RVFV, and crossing the Ferlo a second time. Besides this large-scale transhumance, short-range movements also exist, with herds navigating strictly between ponds of the Ferlo region.

In this chapter, we aim to develop a mechanistic metapopulation model to understand the role of seasonal herd movements in RVFV transmission dynamics in northern Senegal. The choice of locations composing our metapopulation is informed by field surveys of transhumance itineraries, along with the remotely-sensed detection of temporary ponds (5.2.1.1). The composition of local host and vector populations is based on field surveys as well as published models (5.2.1.3, 5.2.1.2). Animal movement scenarios are either i) directly extracted from field data, with the expected downside of not comprehensively representing herd movements in northern Senegal, or ii) synthetically generated, using rules to reproduce aforescribed patterns. We investigate the influence of spatio-temporal parameters shaping transhumance on RVFV transmission dynamics.

## 5.2 Material and Methods

### 5.2.1 Input data

#### 5.2.1.1 Patch selection

Two types of input data, reflecting pastoral dynamics as well as environmental suitability, are used to build the structure of our metapopulation. First, we use the study by Belkhiria et al., 2019, which provides a survey of 132 nomadic herders, interviewed in Younoufere, who described the main locations (nodes, dataset N) they visited during their transhumance journey. Second, through the entomological model developed by Tran et al., 2019, we have access to water-positive pixels (dataset P) detected through remote-sensing in northern Senegal. Such pixels can contain one or several ponds, corresponding to a given surface covered in water. To select

the most relevant locations to include in our RVFV metapopulation transmission model, we create patches by intersecting datasets N and P. Precisely, we define a buffer around each node of N and keep only those containing at least one pixel of P. When buffers themselves intersect, we merge them into a single patch for our metapopulation. Table S.1 shows, for different buffer sizes, the number of nodes from N close to at least one pixel from P, and the final number of patches retained after accounting for intersecting buffers. We exclude nodes close to water bodies present in Senegal river delta and valley (SRDV, as defined by Tran et al., 2019; Cecilia et al., 2020). Such nodes are too close to the endemic zone and are therefore better suited as external to the system we are modeling. Figure 5.1 shows the final set of patches retained in our metapopulation with the corresponding density of water-positive pixels. We chose a buffer of 6 km radius, corresponding to the maximum inclusion of patches in our metapopulation. One patch, corresponding to the merge of 5 nodes with intersecting buffers (including Younoufere) is larger. Indeed, out of the 48 water-positive pixels detected independently within these 5 buffers, 39 are unique. In other words, around 20% are redundant. We therefore consider that the buffers share 20% of their surface. The surface  $S$  and radius  $r$  of the resulting patch can then be obtained:

$$S = (1 - 0.2) \times (5 \times \text{buffer\_surface})$$

$$S = 0.8 \times 5 \times \pi \times 6^2$$

$$\pi r^2 = 144\pi$$

$$r = \sqrt{144} = 12$$

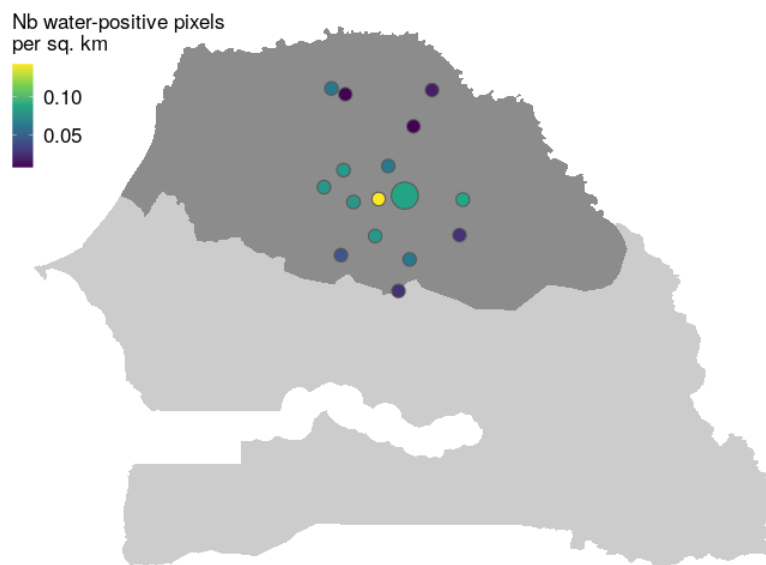


**Figure 5.1** – Selected patches for the metapopulation model. Color corresponds to the density of water-positive pixels within each patch, which determines vector and host densities. All patches have a radius of 6 km except one which has a radius of 12 km (see text).



### 5.2.1.2 Vector populations

Vector densities are extracted from the entomological model developed by Tran et al., 2019, also used in Chapter 3. We use the total number of *Aedes vexans* and *Culex poicilipes* adult females, which are provided weekly. The vector population dynamics of water-positive pixels assigned to a common patch are aggregated, as each patch is considered to be homogeneously mixed.

### 5.2.1.3 Host populations

The number and species composition of hosts within each patch is based on previous observations and models. We define two kinds of host populations : sedentary and nomadic. Durand et al., 2020 developed a model at the pond level and estimated that near Younoufere, there were 23 cattle and 117 small ruminants per pond for the resident population, which is constant year round. For nomadic breeders, they estimated 6 cattle and 29 small ruminants per pond in the dry season, and 382 cattle and 1273 small ruminants in the wet season. In a 86 sq. km area around Younoufere, they reported the existence of 25 ponds, corresponding to a density of 0.29 pond/sq.km. In the analysis described in section 5.2.1.1, 16 water-positive pixels were detected in the buffer centered around Younoufere (before merge with intersecting buffers). Assuming 16 water-positive pixels correspond to a density of 0.29 pond/sq.km, we compute the pond density within each patch of our metapopulation. In the absence of more precise knowledge, we then assume that the number of hosts per pond estimated by Durand et al., 2020 is generalizable to our whole study area and compute the corresponding number of hosts per patch, according to the patch surface. Therefore, absolute number of hosts vary in space, but the ratio resident/nomadic is 8% in the wet season and 400% in the dry season, everywhere. To distinguish between sheep and goats among small ruminants, we apply proportions according to what is found in Gridded Livestock of the World (Gilbert et al., 2018). This model computes animal densities based on official census and distributes them in 10×10km units based on spatial covariates (climate, land use, topography, human presence, vegetation). Figure 5.2 shows the density of livestock hosts per patch in our metapopulation, for the nomadic population during the wet season.

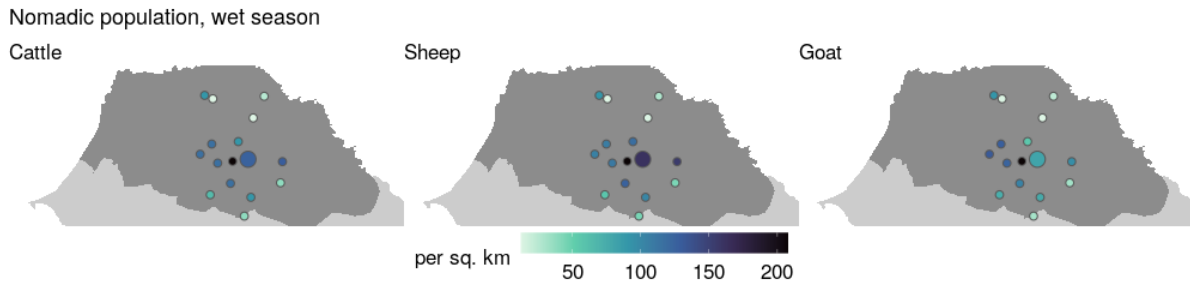


**Figure 5.2** – Density of nomadic individuals per patch, per species, during the wet season.

#### 5.2.1.4 Hosts movements

The movement dataset by Belkhiria et al., 2019 describes 623 movements from 132 nomadic herds (33292 animals), among 50 nodes, 29 of which are external to the modeled metapopulation. When keeping movements involving only retained patches, either as source, destination, or both, and neglecting movements performed between nodes merged together to form patches, the dataset comprises 551 movements. Figure 5.3a shows the distance between patches retained in our metapopulation. Figure 5.3b shows the total number of movements (undirected) between patches retained in our metapopulation. This is done using the full dataset, which includes movements taking place from september 2014 to december 2015 as well movements without dates (346 movements). Figure 5.3c shows the population dynamics per patch when applying the dataset for 2015 (370 movements, including movements from/to outside the metapopulation).

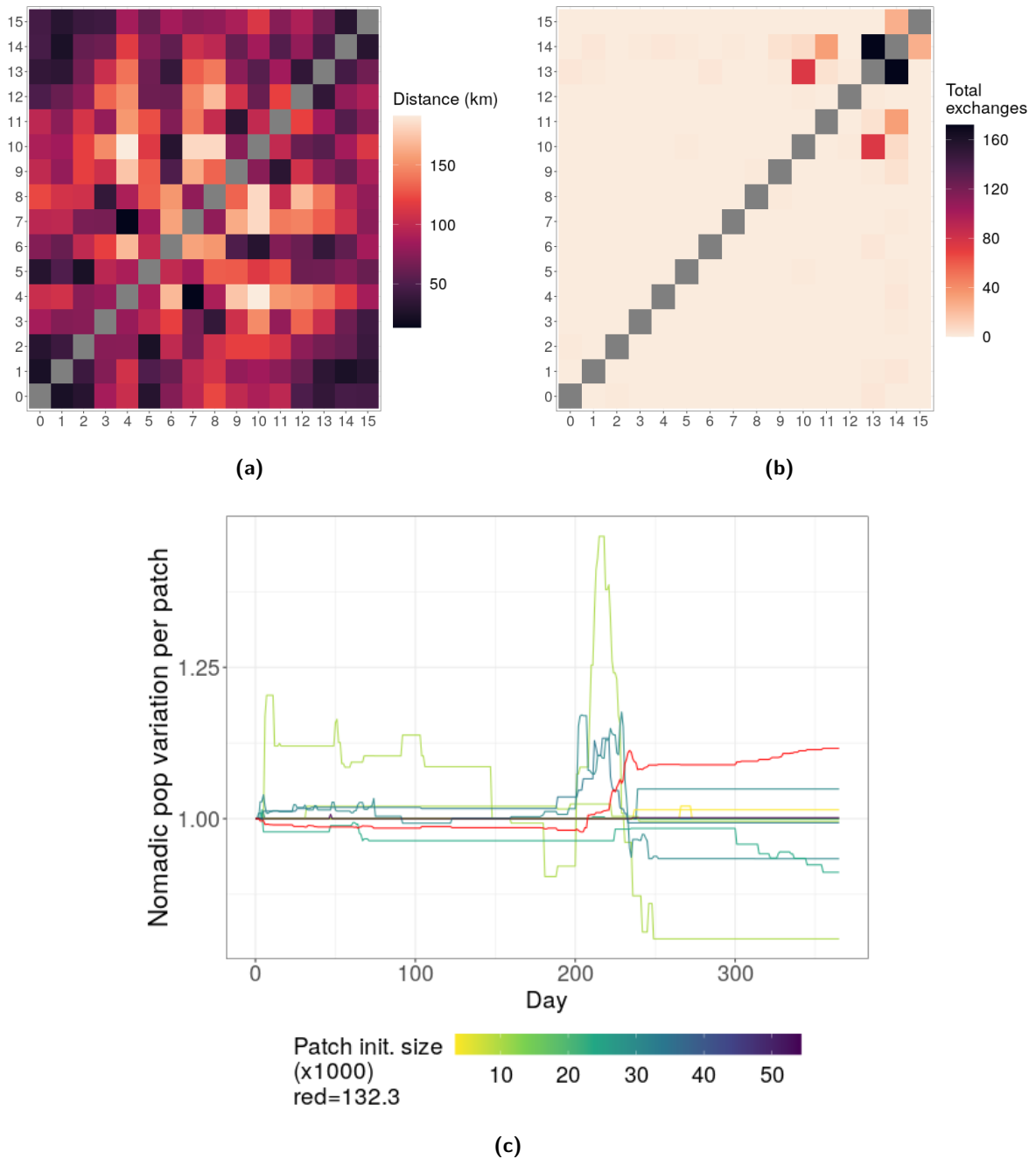


**Figure 5.3** – Description of the network, and resulting patch dynamics when applying the 2015 raw dataset. (a) Distance matrix between the centroids of patches selected for the metapopulation ( $\approx 50\%$  of nodes present in the full dataset by Belkhiria et al., 2019). (b) Total number of exchanges between selected patches, as described in the surveys by Belkhiria et al., 2019. (c) Variation of nomadic population per patch, when applying the raw movement dataset for 2015. Color indicates the initial size of the population, corresponding to the wet-season size. The red line corresponds to a starting value of 132.3.

## 5.2.2 Metapopulation model

### 5.2.2.1 Within-patch : RVF virus transmission dynamics

We expand the model developed by Cecilia et al., 2020 (Chapter 3). Table 5.1 sums up the main parameter modifications made compared to Cecilia et al., 2020. Figure 5.4 shows the new compartments of our expanded model. To account for infectiousness differences between livestock host species, as estimated in Chapter 4 (Table 5.1), we distinguish cattle, sheep and goats, compared to cattle and small ruminants initially. In addition, infectiousness varies with time since infection, in relationship with viral loads (Chapter 4). This is incorporated through consecutive I states, each lasting a day and with their own infectiousness to vectors (Figure 5.4, Table 5.1). We only include vectorial transmission, and keep a reservoir frequency-dependent force of infection (Wonham et al., 2006) as in the initial model. Sedentary and nomadic animals do not differ in their exposure to mosquito bites. All animals suffer disease-induced mortality rates. For sheep, the parametrization is based on estimates from Chapter 4, showing that individuals dying from RVF are more infectious than those less severely affected. As a consequence, a distinction is made between infected sheep surviving the infection and those selected to die from it, with different infectiousness (Figure 5.4, Table 5.1). We do not incorporate demographic parameters such as birth and death for animals, because we simulate only 1 year scenarios.

Definition	Value		Source
<b>Vectors</b>			
Feeding preference	sheep	0.135	Ba et al., 2006
	cattle	0.730	
	goat	0.135	
Biting rate	1/3 day <sup>-1</sup>		†
Extrinsic incubation period	9 days		†
<b>Sheep</b>			
RVF-induced death rate (proba to go in $I_{d,1}$ state)	30%		Bird et al., 2009
$I_{d,i}$ states			
proba to die from RVF	day 1	0%	Chapter 4
	day 2	0%	
	day 3	2.21%	
	day 4	7.49%	
	day 5	17.64%	
	day 6	30.88%	
	day 7	100%	
Proba to infect a vector	<i>Aedes Culex</i>		Chapter 4
	day 1	1.6% 0.3%	
	day 2	5.3% 1.5%	
	day 3	27.1% 12.8%	
	day 4	45.2% 25.4%	
	day 5	31.3% 15.2%	
	day 6	17% 6.7%	
day 7	6.8% 2%		
$I_{s,i}$ states			
Proba to infect a vector	day 1	1.7% 0.2%	Chapter 4
	day 2	4.2% 1.2%	
	day 3	21.5% 9.2%	
	day 4	30.8% 14.8%	
	day 5	8.6% 2.8%	
	day 6	0.2% 0.02%	
<b>Cattle</b>			
RVF-induced death rate	10%		Bird et al., 2009
Proba to infect a vector	<i>Aedes Culex</i>		Chapter 4
	day 1	0.4% 0.07%	
	day 2	1% 0.2%	
	day 3	9.5% 3.2%	
	day 4	19.2% 8%	
day 5	3.9% 1.1%		
<b>Goat</b>			
RVF-induced death rate	10%		
Proba to infect a vector	<i>Aedes Culex</i>		Chapter 4
	day 1	1.8% 0.4%	
	day 2	4.9% 1.3%	
	day 3	17.6% 6.9%	
	day 4	5.4% 1.6%	
day 5	0.2% 0.03%		

**Table 5.1** – Parameter values of the within-patch model, added or modified compared to Cecilia et al., 2020. † : consistent with temperature-dependent equations used in Cecilia et al., 2020 applied with the mean temperature of patches.

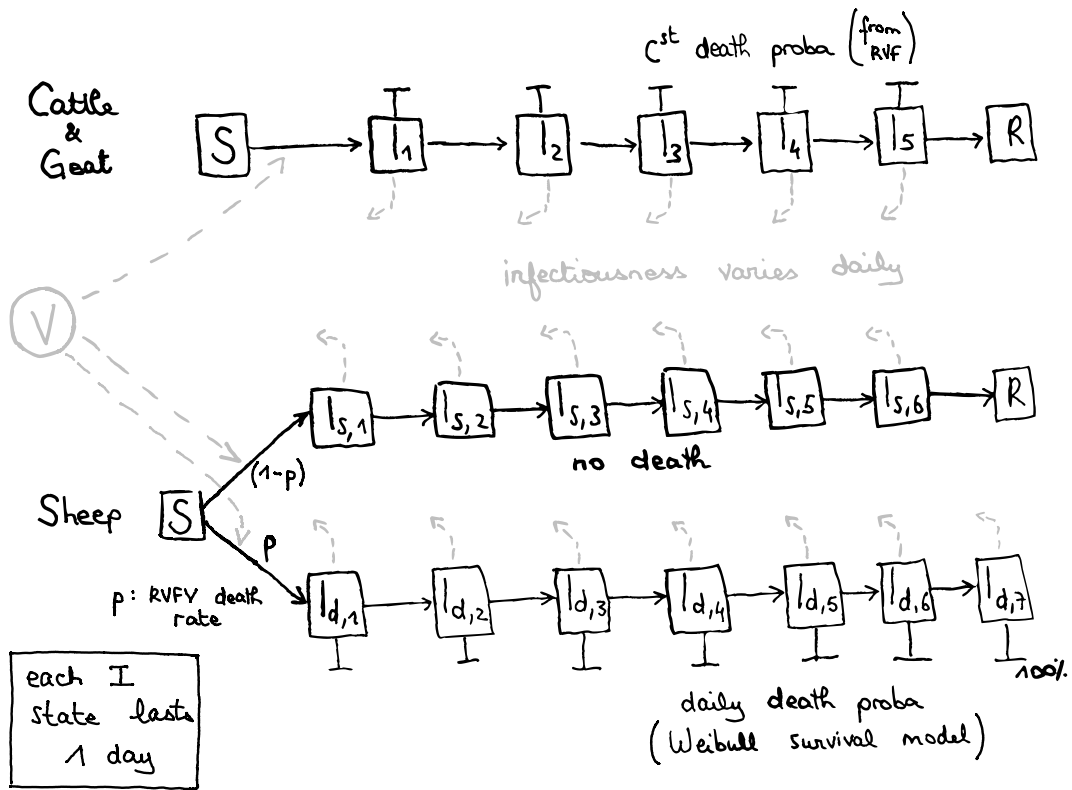


**Figure 5.4** – Schematic representation of how the within-patch model incorporates heterogeneity between livestock hosts, in terms of infectious period duration and infectiousness to mosquitoes, as evidenced in Chapter 4. Grey dashed arrows from I states represent infectiousness to vectors, but were not extended through the corresponding compartment for readability. For more details on vector compartments and force of infection, see Cecilia et al., 2020. Parameter values can be found in Table 5.1.

Vector population dynamics are based on Tran et al., 2019 entomological model outputs, provided weekly. We linearise the variations to update the population daily. If the vector population increases from one week to the other, new susceptible individuals are added, as we do not consider vertical transmission in our model. If the vector population decreases, individuals are removed from all health states, according to their current repartition in compartments. We do not directly incorporate environmental variables into our model. Therefore, vector extrinsic incubation period and biting rate are set as constant instead of temperature-dependent in Cecilia et al., 2020. In each patch, vector population dynamics, which are impacted by rainfall and temperature through the entomological model, determine the beginning and end dates of the wet season. As in Durand et al., 2020, the beginning of the wet season is set as the first date when *Aedes* go above a third of their yearly maximum value, and the end of the wet season is set as the first date when *Culex* go below a third of their yearly maximum value. Figure 5.5A-B shows the maximum number of *Aedes* and *Culex* within patches for the year 2015, taken as a reference scenario because it corresponds to the year with most movement data from Belkhiria

et al., 2019 (maps for 2014 and 2016 are shown in Figures S.1,S.2). Resulting beginning and end dates are shown in Figure 5.5C-D, and corresponding durations in Figure S.2. These dates are used to inform nomadic host movements, as described in the next section.

2015

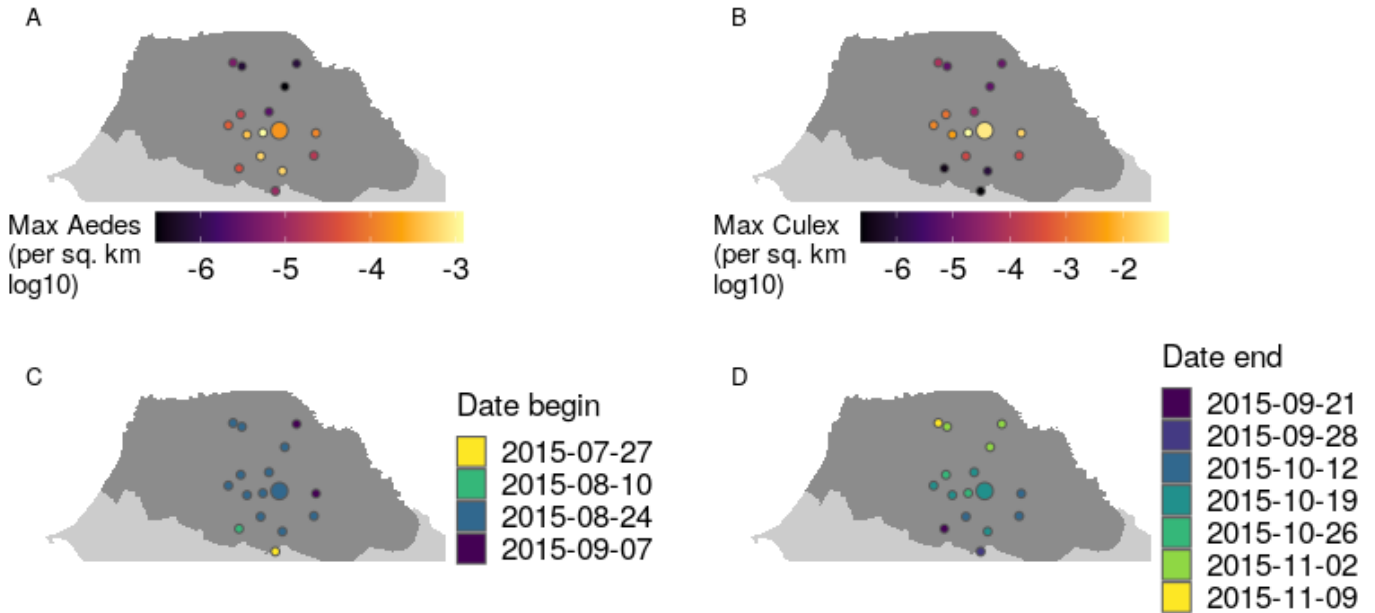


**Figure 5.5** – Maximum number of *Aedes* and *Culex* per patch in 2015 (A-B). These maxima inform the beginning and end dates of the wet season (C-D), used to generate the synthetic animal movement dataset (see 5.2.2.2). In 2015, the wet season lasts 35 to 77 days depending on patches (Figure S.2).

The model is implemented stochastically using the Emulsion generic simulation engine (Picault et al., 2019), which minimizes the amount of code to write and ease subsequent modifications by non modelers. The number of patches, vector densities, and movements, are incorporated as input data which can be modified as needed, making the model flexible and adaptable to other case studies.

### 5.2.2.2 Between-patch : animal mobility

In addition to the possibility of strictly applying an available movement dataset (Figure 5.3c), we also implement an algorithm to generate synthetic movement data for nomadic animals. The targeted dynamics (Figure 5.6) can be described as follows:

The nomadic population is initialized at its dry season level, as described in section 5.2.1.3. It remains stable over the dry season, with a constant renewal rate corresponding to an average stay of 9.8 days (Durand et al., 2020). Animals coming in and out of the patch at that time are only exchanged with outside the metapopulation. Shortly before the beginning of the

wet season, a progressive increase in the nomadic population takes place, again through exchanges with outside the metapopulation, until the wet season population level (section 5.2.1.3) is reached. During the wet season, the renewal rate corresponds to an average stay of 16.3 days (Durand et al., 2020). Animals are mostly exchanged with outside the metapopulation, with a given proportion assigned to movements between patches of the metapopulation. When the wet season ends, the population progressively goes back to its dry season level, through exchange with outside the metapopulation. It settles to the dry season level, again with a renewal rate of  $1/9.8 \text{ day}^{-1}$ .

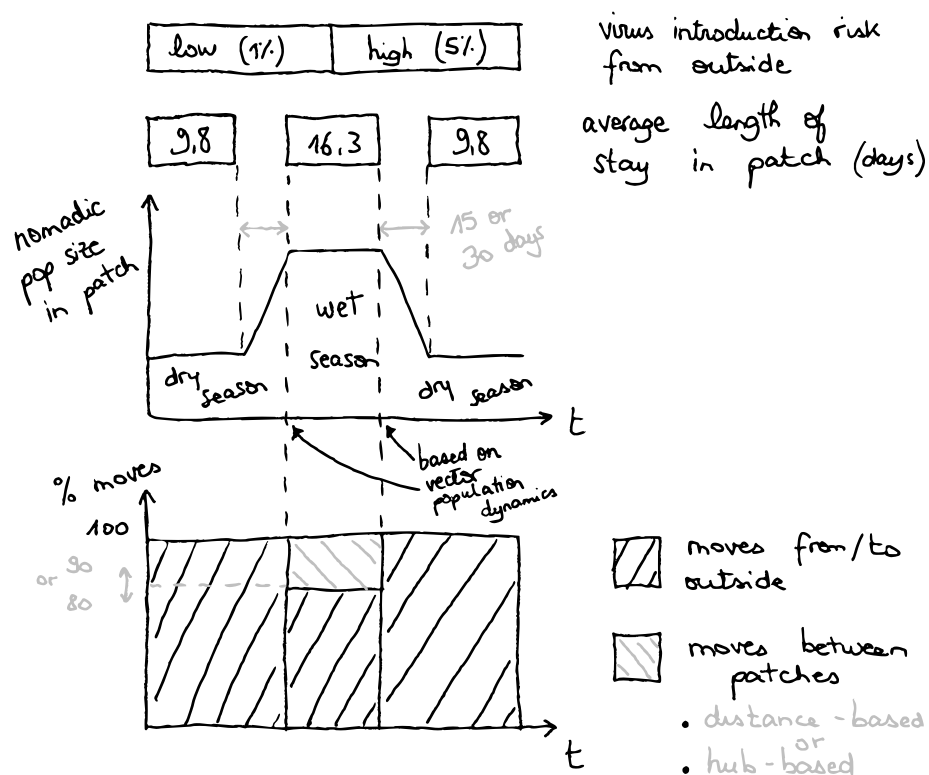


**Figure 5.6** – Schematic representation of the targeted synthetic within-patch nomadic population dynamics. It consists of a trapezoidal dynamics, with a low population during the dry season and a high population during the wet season, as in Durand et al., 2020. Introductions in the metapopulation are the source of RVFV introduction in the system, with a low risk until the middle of the wet season, and a higher level after. Movements between patches of the metapopulation only take place during the wet season.

Movements from/to outside the metapopulation are used because our metapopulation is not representative of all transhumance stops nor does it include regions outside the Ferlo where herders doing long-distance, country-level migration come from. These movements are the only source of RVFV introduction in our model. The prevalence among animals entering the metapopulation has two possible levels. A low level from January to the middle of the wet



season (exact date patch-specific, see 5.2.2.1), and a higher level from the middle of the wet season to December, to reflect the origin of animals (low risk when coming from their dry season camp in the south, higher risk when coming from their native village in the Senegal river delta and valley, see Introduction).

For movements between patches of the metapopulation, the repartition of animals can follow a distance-based or a hub-based distribution. From one patch to the others, the distribution of animals can be weighted based on the distance between patches (distance-based, Figure 5.3a), or weighted based on true animal flows described in the surveys (hub-based, Figure 5.3b). In that case, the adjacency matrix from the network is used, where a non-null entry means a link exists between two patches, and the exact value is the total number of movements (undirected) between those two patches, used as a weight. This matrix is meant to implicitly include various factors playing a role in herders' itinerary choice.

It should be noted that the synthetic movement dataset is generated before the simulation, independently for each patch. This means that regarding intra-metapopulation movements, for each patch, the algorithm sets the destination of outgoing animals, but cannot control whether arrivals will match departures. It is therefore not guaranteed that the population will stay stable during the wet season, and might instead climp up (source) or crumble (sink) disproportionately. Then, the decreasing phase will maintain the status of the population which could therefore stabilize way above or below its dry season level. To control these possible source-sink dynamics, we add constraints during the simulation, so that movements which would make the local nomadic population go 10% above their wet season level or 10% below their dry season level are not operated. This can cause a cascade of events (a patch which stops receiving induce others to stop emptying etc.). Alternatively, we could re-assign movements to/from outside the metapopulation, when the assigned destination/source of the movement cannot send/receive more animals.

### 5.2.3 Scenarios of animal movements

All scenarios are simulated for one year, with a daily timestep. They are run 10 times, starting with no infection within patches.

#### 5.2.3.1 Raw movements

In the scenario applying the raw movement dataset, populations are set to their wet season level from the start of the year so that it is not a limiting factor in the dynamics. We test

3 tuples of values (applied during the 1st half and 2nd half of the wet season) for the RVFV prevalence in animals coming from outside the metapopulation: [1-5]%, [1-10]%, and [5-5]%

### 5.2.3.2 *Synthetic movements*

For scenarios applying synthetic movement datasets, the outside prevalence is set to 1% during the first half of the season and 5% during the second half of the season. We test the effect of spreading arrivals and departures of animals at the beginning and end of the wet season across 15 or 30 days (length of the linear increasing and decreasing phases in Figure 5.6). We test the impact of setting 10% or 20% of movements within the metapopulation during the wet season (Figure 5.6). We see how applying distance-based or hub-based movements affects the nomadic population dynamics in patches. We examine the variability between runs, the heterogeneity between patches, how RVFV spreads from nomadic to sedentary populations, and the contributions of livestock and vector species to infections and transmission.

## 5.3 Results

### 5.3.1 *Raw movements*

The raw movement dataset cannot induce a substantial RVFV spread in the metapopulation. For all levels of outside risk tested, RVFV prevalence in nomadic population stays below 1% at all times, in all patches. The temporal dynamics at the metapopulation scale is shown in Figure S.3. We do not analyze these scenarios further.

### 5.3.2 *Synthetic movements*

Synthetic movement datasets succeed to induce a trapezoidal nomadic population dynamics, starting and ending at different dates among patches (Figure 5.7, other scenarios in Figure S.5). This is only possible when controlling movements during the simulation ( $\pm 10\%$  of wet/dry season level). When the synthetic movement dataset is applied as is, some patches receive far more individuals than they send, their population skyrockets and do not return to reasonable numbers (Figure S.4). Even with control, the total metapopulation has increased almost by a factor 5 at the end of the simulation (black line in Figure S.4). The dynamics and heterogeneity among patches is overall similar between distance-based and hub-based movements (Figure 5.7). Variability between runs in terms of patch prevalence is marginal (Figures 5.8,S.6,S.7), so we aggregate model outputs in median per timestep in further analyses.

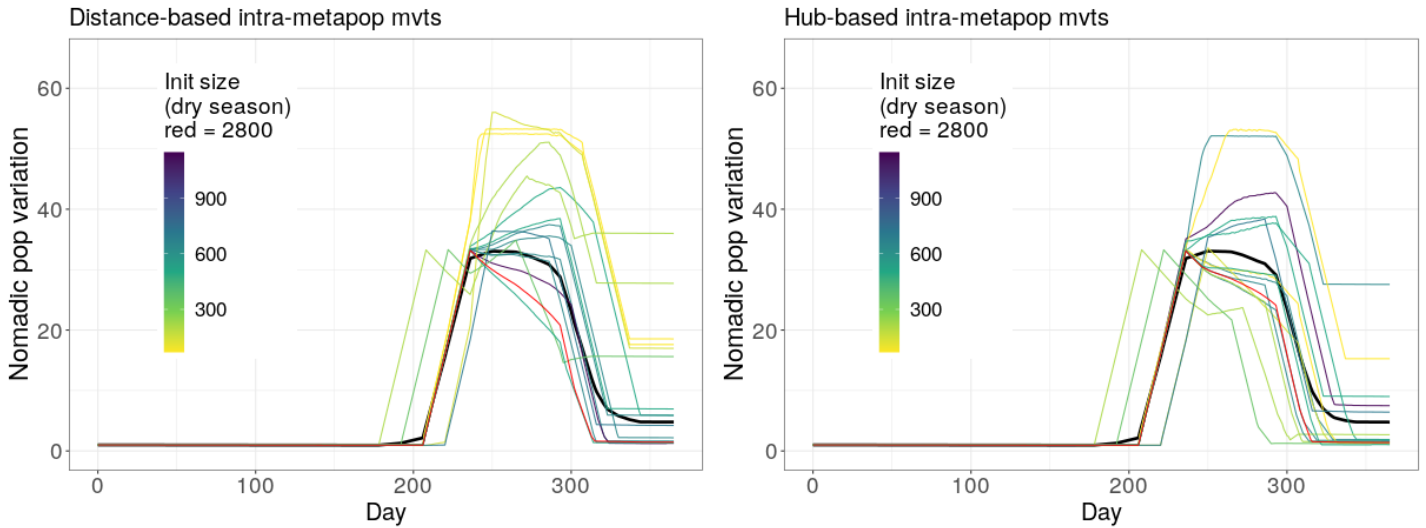


**Figure 5.7** – Example of nomadic population dynamics per patch, when intra-metapopulation movements are distance-based (left) or hub-based (right). Each patch is normalized by its starting value (all lines start at 1), shown by color. The red line corresponds to a starting value of 2800. The black line shows the variation at the metapopulation scale. Scenario is 10% intra-metapopulation movements, with 30 day progression in-between seasons. One run showed.

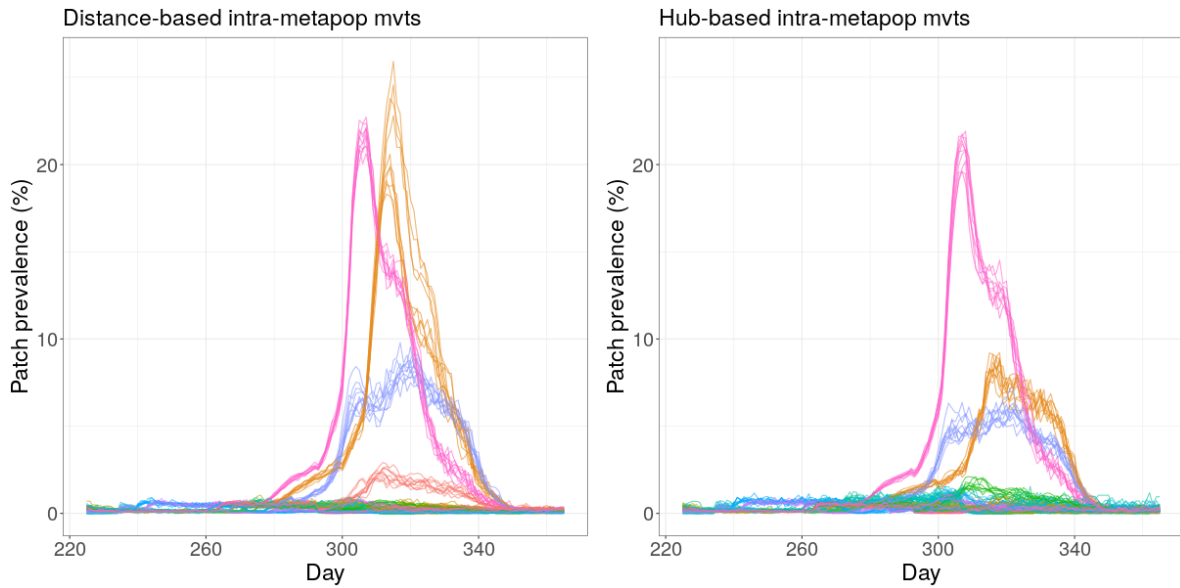


**Figure 5.8** – Example of variability in patch prevalence (%) between 10 stochastic runs. Scenario is 10% intra-metapopulation movements, with 15 day progression in-between seasons. Distance-based movements (left) means that movements going out of a patch are distributed in other patches based on distance. Hub-based movements (right) means that movements going out of a patch are distributed in other patches based on what is observed in the initial dataset of surveyed itineraries. A line represents a patch prevalence over time for a given run. All lines with the same color correspond to the same patch. Note that we only show timesteps after 225 because prevalence is low before.

The same three patches (1 diagali, 11 ranerou, and 14 younoufere) stand out with the highest prevalences in all scenarios (Figures 5.8,S.6,S.7). These correspond to the locations with the most water-positive pixels (Table S.2) and therefore, the highest host and vector densities. Patch 14 is also quite central, with on average small distances to other patches (Figure 5.3a) and more strongly connected than other patches according to field surveys (Figure 5.3b). The timing of peaks is similar for distance-based and hub-based movements when comparing similar scenarios, but the number of infections can vary strongly (Figures 5.8,S.6,S.7).

Sedentary infections peak later than nomadic infections (Figures 5.9,S.8). Nomadic infections peak towards the end of the wet season, while sedentary infections peak when nomads are leaving. The maximum value of sedentary infections can in some instance be higher than the maximum value of nomadic infections (Figures 5.9,S.8).

Increasing the length of the transition phase between seasons from 15 to 30 days lowers the peak infection value in sedentary populations and also delays it (Figures 5.9,S.8), resulting in fewer infections in total. This pattern is less systematic for nomadic infections (Figures 5.9,S.8).

Livestock species get infected sequentially, with cattle infections systematically peaking earlier than goats and sheep infections (Figures 5.10,S.9). Maximum cattle infections are most of the time lower than maximum sheep infections (Figure 5.10), but can be higher in some patches (Figure S.9). Goat and sheep infections always peak at the same time (Figures 5.10,S.9). At the time of peak host infections, *Culex* vectors are always the main contributors to transmission (Figures 5.10,S.9).

Livestock host species contribution to transmission vary over time (Figures 5.10,S.9). Cattle are responsible of the first vector infections and sheep then take over (Figures 5.10,S.9). *Culex* always outnumber *Aedes* infections by far in the time period considered (Figures 5.10,S.9).

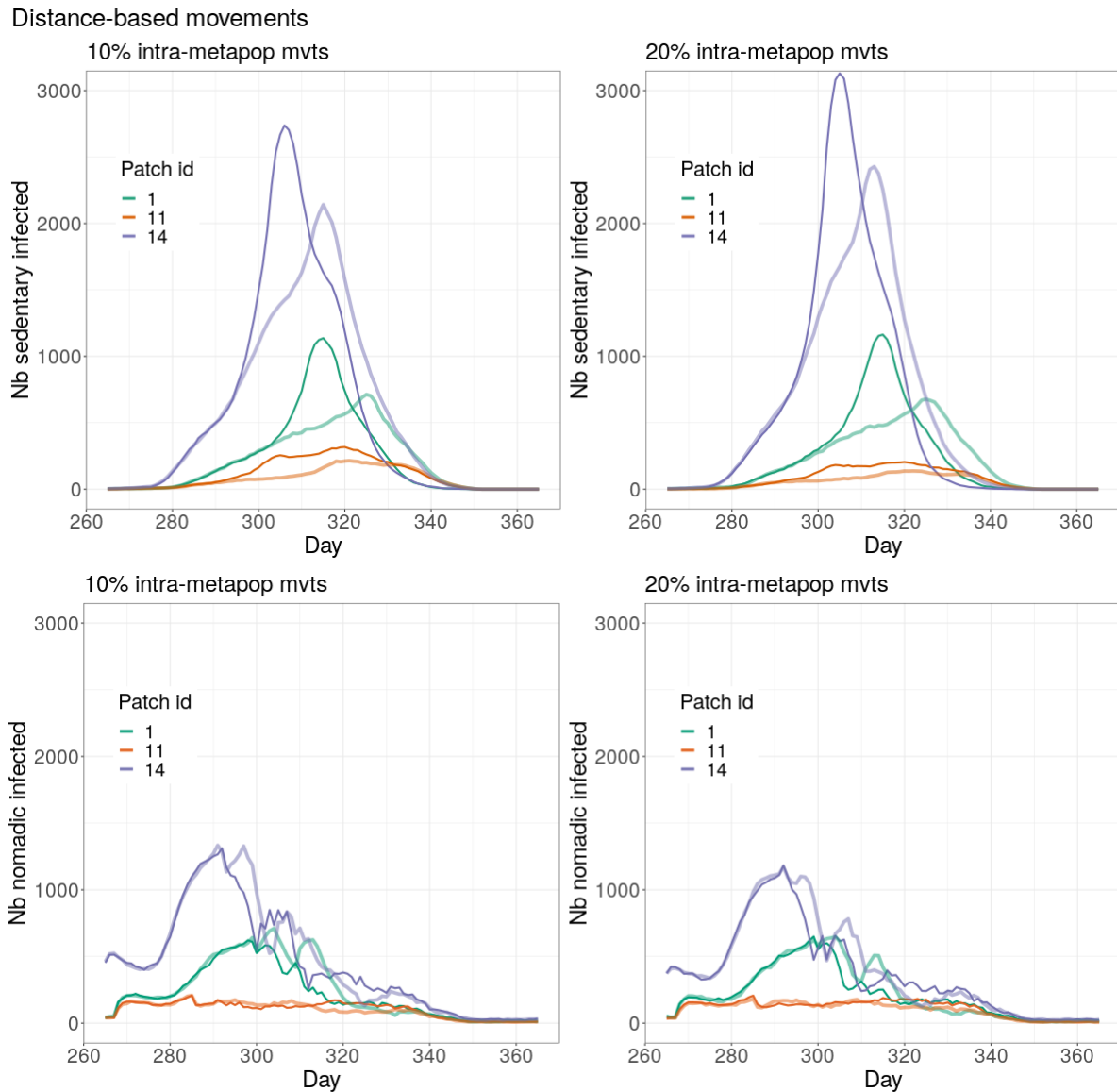


**Figure 5.9** – Number of infected sedentary (top) and nomadic (bottom) animals over time, per patch. Intra-metapopulation movements are distance-based, and represent a proportion of 10% (left) or 20% (right) of total movements during the wet season. Colors indicate patch. Darker lines represent scenarios with 15 day transition phase between seasons, and thicker, lighter lines represent scenarios with 30 day transition phase between seasons. Timesteps after 260. Median of 10 runs.

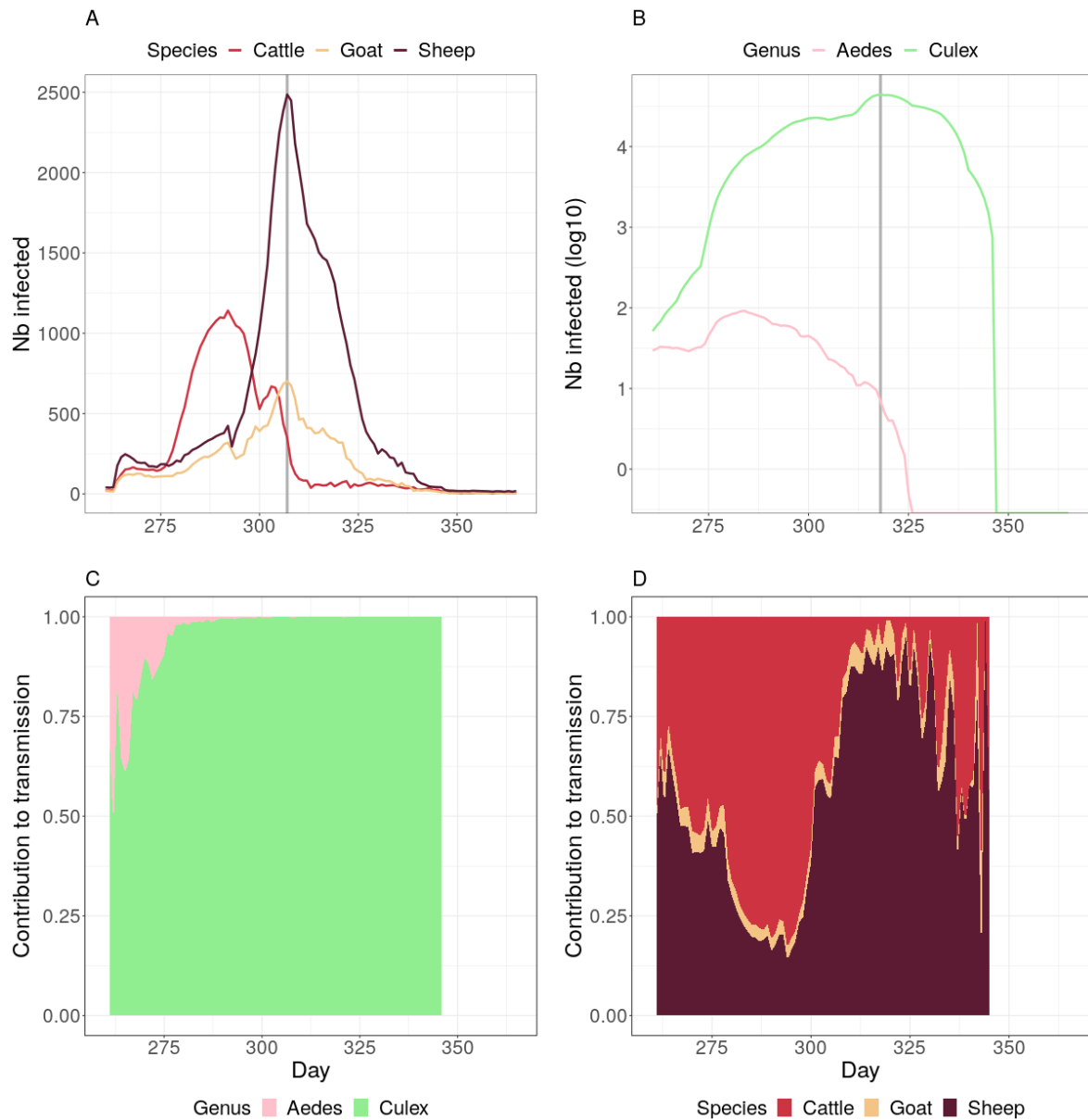


**Figure 5.10** – Example of host and vector contribution to infections and transmission. Patch 14, 10% distance-based intra-metapopulation movements, 15 day transition between seasons. A: Number of infected animals per species over time. Vertical grey line shows time of maximum animal infections. C: Contribution of vector species to host infections (% of force of infection) over time. Blank plot at the last timesteps means transmission has stopped (no new cases). B: Number of infected vectors per species over time, log10 scale. Vertical grey line shows time of maximum vector infections. D: Contribution of host species to vector infections (% of force of infection) over time. Timesteps after 260. Median of 10 runs.

## 5.4 Discussion

Following a data-driven, integrative approach, we have developed a metapopulation model of RVFV transmission dynamics in northern Senegal, taking into account seasonal herd movements, the specificities of nomadic and sedentary populations, heterogeneity in livestock species' infectiousness, and two vector species population dynamics. Applying currently available movement datasets cannot induce RVFV spread in our model, while synthetic datasets based on qualitative, knowledge-driven patterns, can. Even though all patches receive infected animals from outside the metapopulation, only a few locations see their prevalence increase to significant levels. The spatial spread is therefore limited, but infections do arise in sedentary populations, with a delay compared to nomadic populations. In particular, the pace at which nomadic herds arrive at and leave from the Ferlo region influences the timing and level of peak infections in sedentary populations. Animal infections arise in significant numbers towards the end of the wet season, and transmission continues until the dry season is fully established. Cattle infections climb up earlier than other species, while goat and sheep infections are synchronized and peak later on. Cattle and sheep are sequentially the main contributors to vector infections, which mostly consist of *Culex* from mid-wet season onwards.

This study has methodological and operational implications. Regarding model development, we have seen that, in data-scarce settings, combining quantitative and qualitative (knowledge-driven) approaches is needed to assess the role of animal mobility in the spread of emerging diseases. In our case study, infections remain localized, which could simplify the implementation of control measures, as long as key hotspots of the network are properly identified. Both nomadic and sedentary populations are at risk, therefore animal health practitioners should ensure that they reach both communities. As the first species reaching important prevalence, cattle could be envisioned as sentinel animals, provided their clinical expression of the disease is strong enough to be noticeable. Investigating whether cattle vaccination could protect other species stands out as a priority, but some additional steps are needed to move towards a fine evaluation of possible control strategies.

A sensitivity analysis is required to evaluate the impact of parameter variations on model outputs. In particular, the species composition of herds as well as the synchronicity of transhumance with vector population dynamics (i.e the duration of contacts) are possibly important factors kept constant in our scenarios so far. The choice of outputs should be carefully done, as a too restrictive set of outputs might mask important interactions. For instance, the role

of *Aedes* vectors currently seem minimal in our analyses but could be important for the emergence phase of the outbreak, when case numbers are small. Similarly, when designing control strategies, some important criteria will need to be incorporated. For vaccination, minimizing the number of doses (cost priority) or cases (health priority) will likely change the strategy deemed most efficient (Adongo et al., 2013). Regarding surveillance scenarios, the tool used to detect cases (symptoms, tests) will also influence the outcome. Control strategies aim to bring down infections to low levels, which supports our decision to develop a stochastic model, suited to study extinction rates properly (Finkenstadt, 2002; Allen and Lahodny, 2012).

Additional assumptions might be needed to improve the accuracy of our model. The renewal of herds was neglected in the present study because of short simulations, but is expected to be important when examining multi-year dynamics, which rely on the replenishment of susceptible populations. Similarly, the introduction of immune animals, or their presence within the metapopulation, could impact RVFV spread. We presently considered fully naive populations, which can be seen as a worst-case scenario. Besides, direct transmission between animals by contact with abortion or birth products has been shown to play a role in RVFV transmission dynamics (Nicolas et al., 2014; Durand et al., 2020). In the absence of empirical hypotheses about inter-species or inter-herds transmission for this pathway, we preferred not to include it. Incorporating this transmission route would be particularly relevant for an evaluation of human risk of infection.

Finally, adjacent research questions could require modeling choices to be revisited. Between patches, the identity of individuals moving across a network has a significant impact on the infection dynamics (Keeling et al., 2010). In our scenario applying the raw movement dataset, the species composition of movements was maintained, but not the identity of herds. In addition to a highly enriched dataset, this would likely require an agent-based model (ABM, with agents consisting of herds), which is more computationally costly. However, by enabling the exploration of different choice of itineraries between herds, this would move us closer to considering the decision-making of pastoralists in epidemiological modeling. Within patches, variability in mosquito exposure along with fine-grained interactions between nomadic and sedentary herds might impact transmission dynamics, due to daily navigation between camps, ponds, and drillings. This could be examined first in a dedicated ABM at the patch scale, building on the one by Paul et al., 2014, to decide whether non-homogeneous mixing is rele-



vant within patches at the metapopulation scale (Watts et al., 2005; Perkins et al., 2013).

Overall, our model incorporates major sources of heterogeneity between hosts and sets the groundwork for a future exploration of their contribution to the spread of multi-host vector-borne diseases. Our present conclusions are specific to RVFV in northern Senegal, but the model can easily be adapted to other case studies, provided relevant input are available.

## 5.5 Supplementary information

Buffer size (radius, km)	Number of nodes close to at least 1 water-positive pixel	Number of independent intersections (involving 2 or more node buffers)	Number of independent patches
1	10	0	10
2	14	1	13
3	19	3	16
4	21	3	16
5	24	3	19
<b>6</b>	<b>26</b>	<b>3</b>	<b>20</b>
7	26	4	19
8	26	5	17
9	26	5	17
10	27	5	18

**Table S.1** – Number of intersections depending on buffer radius chosen for the determination of metapopulation patches.

Node centroid (long;lat)	Region(s)	Number of water-positive pixel in buffer
-14.44105 ; 15.32959	younoufere, wendou nayi, mboul djolof, belal dewe, belel kedde	39
-14.65850 ; 15.30206	diagali	16
-13.95826 ; 15.29718	ranerou	10
-14.86795 ; 15.27774	barkedji	9
-14.95117 ; 15.53504	dodji	9
-15.11401 ; 15.39766	linguere	9
-14.68788 ; 15.00371	velingara ferlo	9
-15.05138 ; 16.19222	kaowel	7
-14.57846 ; 15.56786	lougre thioly, wendou aliou	7
-14.40136 ; 14.81564	mbem-mbem	7
-14.97271 ; 14.85014	thiel	5
-13.98563 ; 15.01159	oudalaye	3
-14.49401 ; 14.56192	payar	3
-14.21450 ; 16.17963	medina ndiatbe	2
-14.36874 ; 15.88737	gaye kadar	1
-14.93596 ; 16.14555	mbiddi	1

**Table S.2** – Name and location of selected metapopulation patches, with number of water-positive pixels they contain.

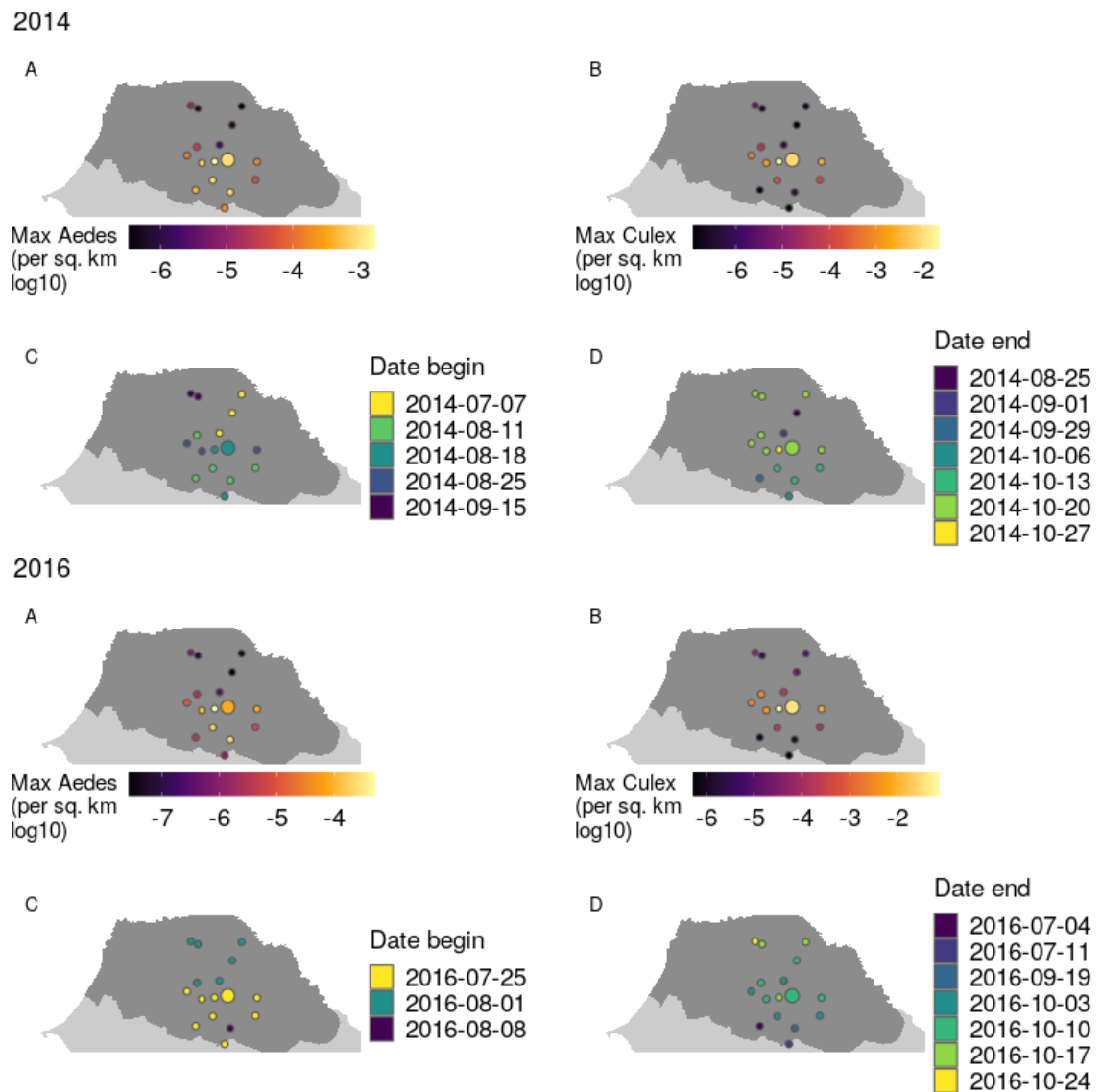


**Figure S.1** – Maximum number of *Aedes* and *Culex* per patch in 2014 and 2016 (A-B). Resulting beginning and end dates for the wet season (C-D). Note that in 2016, 2 patches (south west) have their end date earlier than their start date, indicating that the vector population dynamics might not be the most appropriate proxy of migration in some cases.

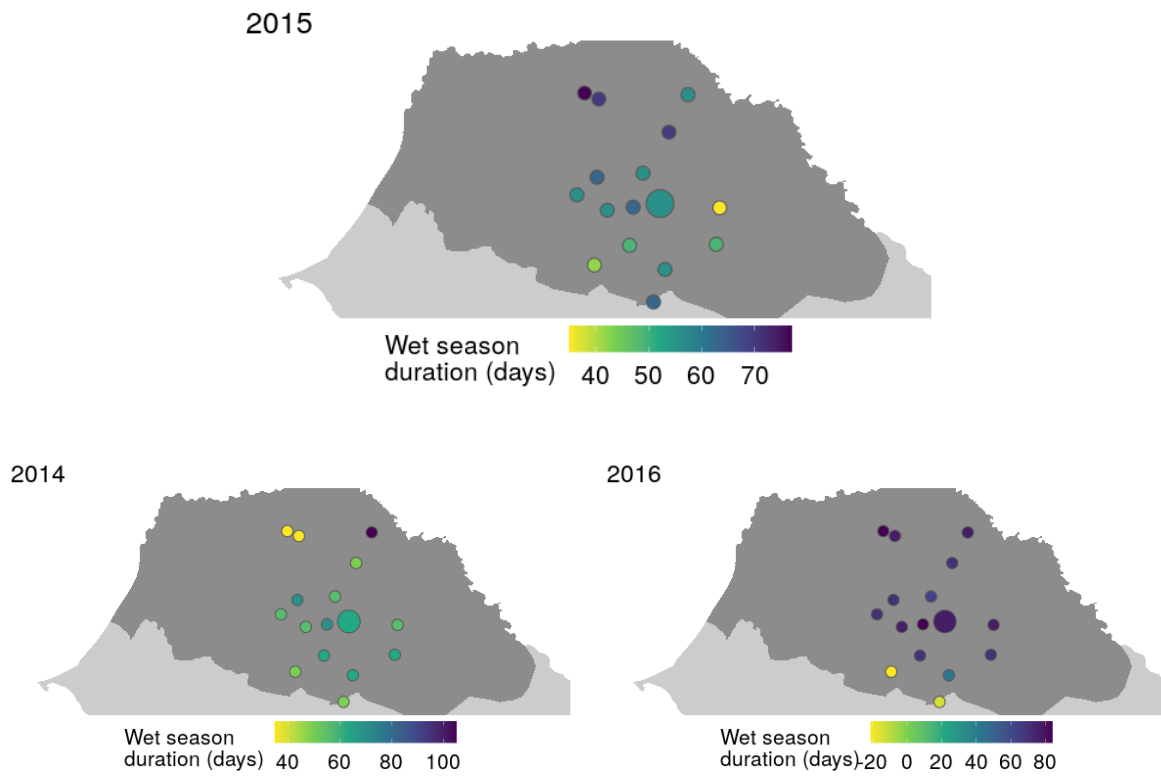


**Figure S.2** – Duration of the wet season per patch per year, as computed based on vector population dynamics.

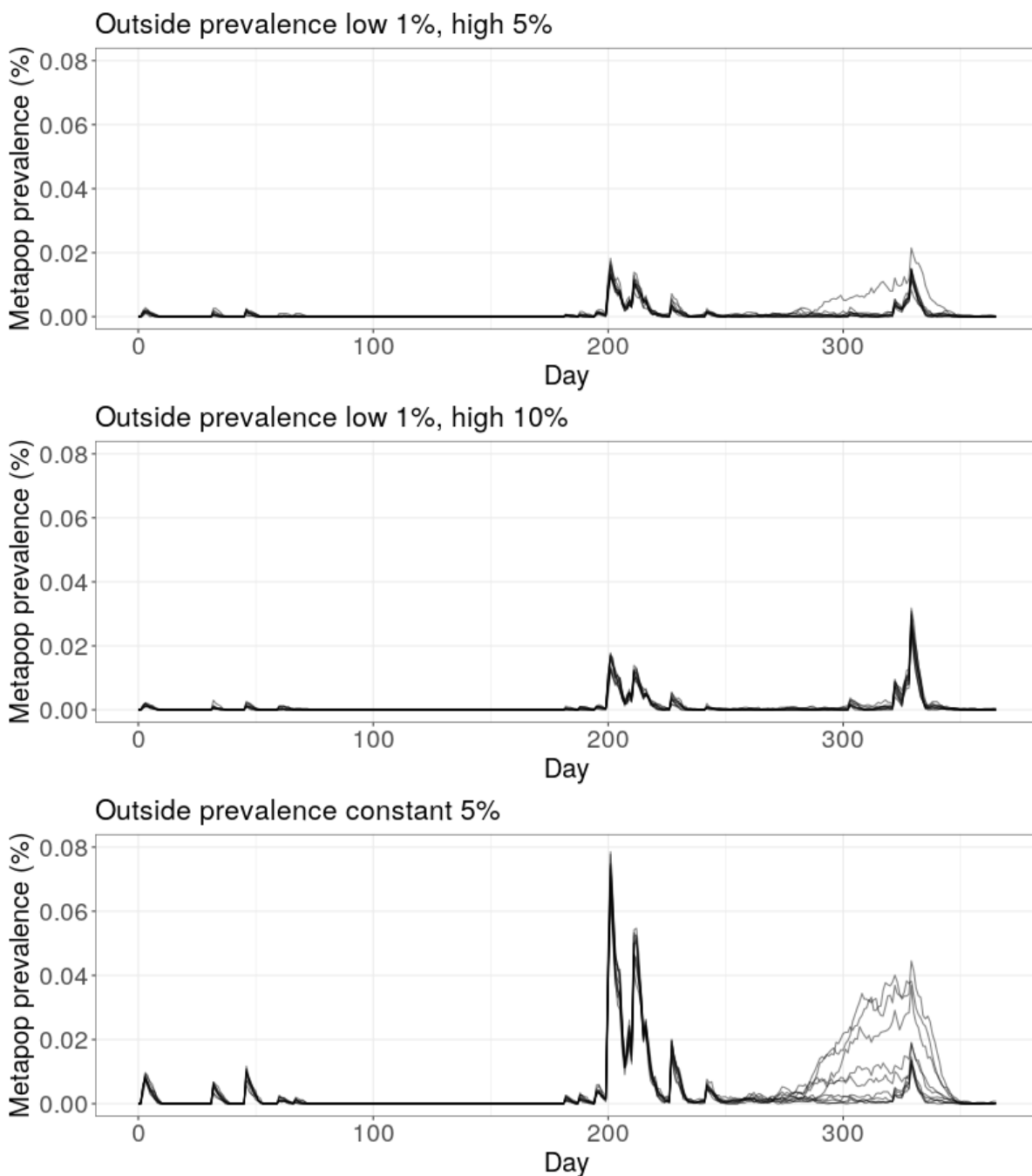


**Figure S.3** – Total prevalence (%) in the metapopulation over time when applying the raw movement dataset. Titles indicate the prevalence in animals coming from outside the metapopulation. For scenarios with a low and a high level, the change is made in the middle of the wet season. The dates of the wet season are defined per patch, depending on the density of vectors (see 5.2.2.2). Lines represent runs of the model (10 per scenario).

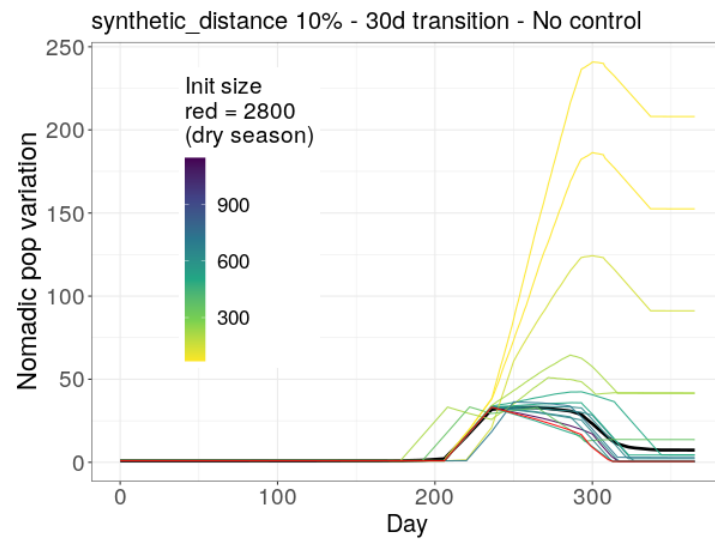


**Figure S.4** – Example of nomadic population dynamics when movements are not controlled in the simulation (synthetic dataset applied as is). One run showed.

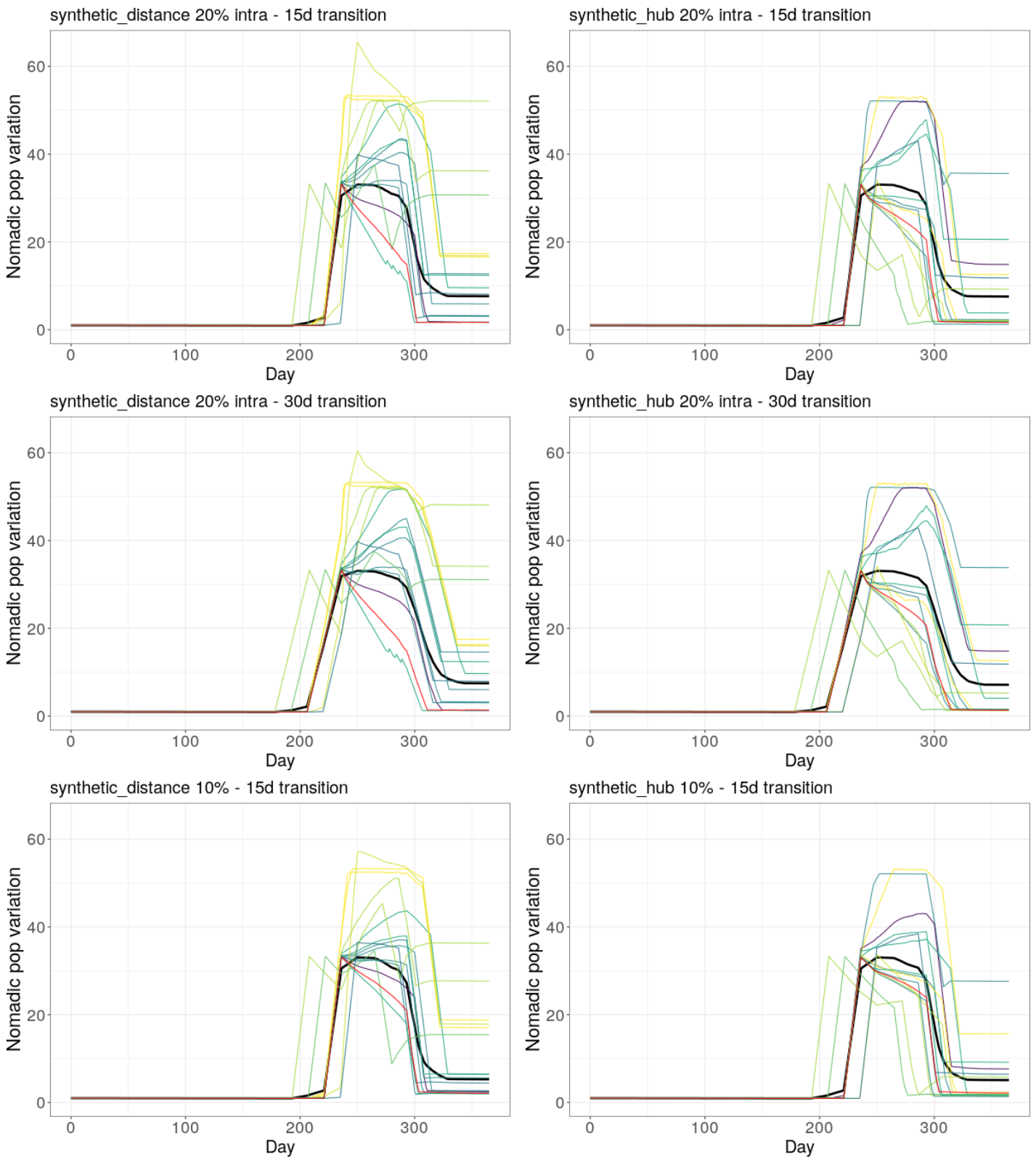


**Figure S.5** – Nomadic population variations per scenario (see title). Each patch is normalized by its starting value (all lines start at 1), shown by color. Color scale is the same as in Figure 5.7. The black line shows the variation at the metapopulation scale. One run showed.

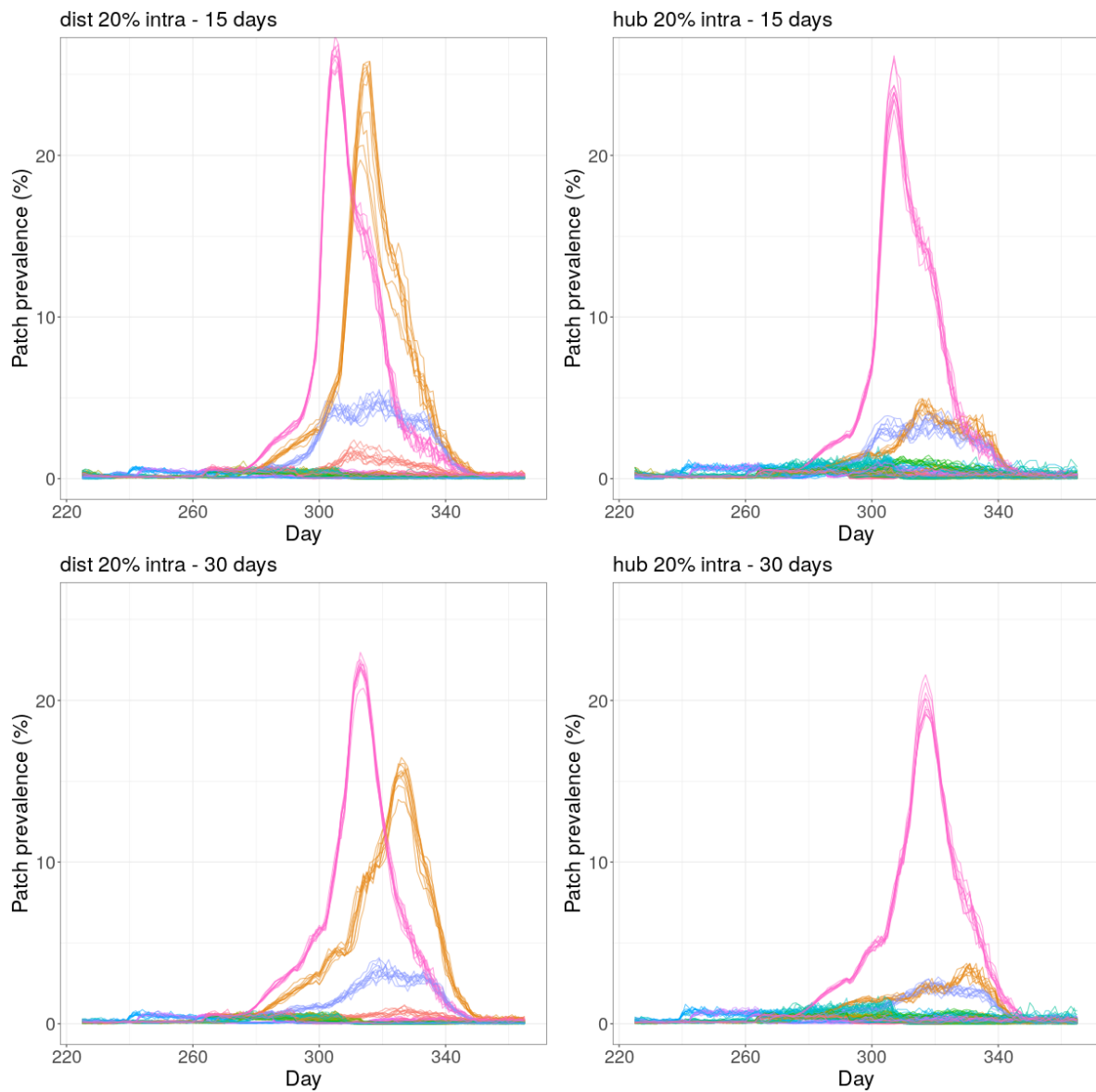


**Figure S.6** – Variability in patch prevalence between 10 stochastic runs for scenarios applying 20% intra-metapopulation movements, comparing distance-based (left) and hub-based (right) typologies. A line represents a patch prevalence over time for a given run. All lines with the same color correspond to the same patch. Note that we only show timesteps after 225 because prevalence is low before.



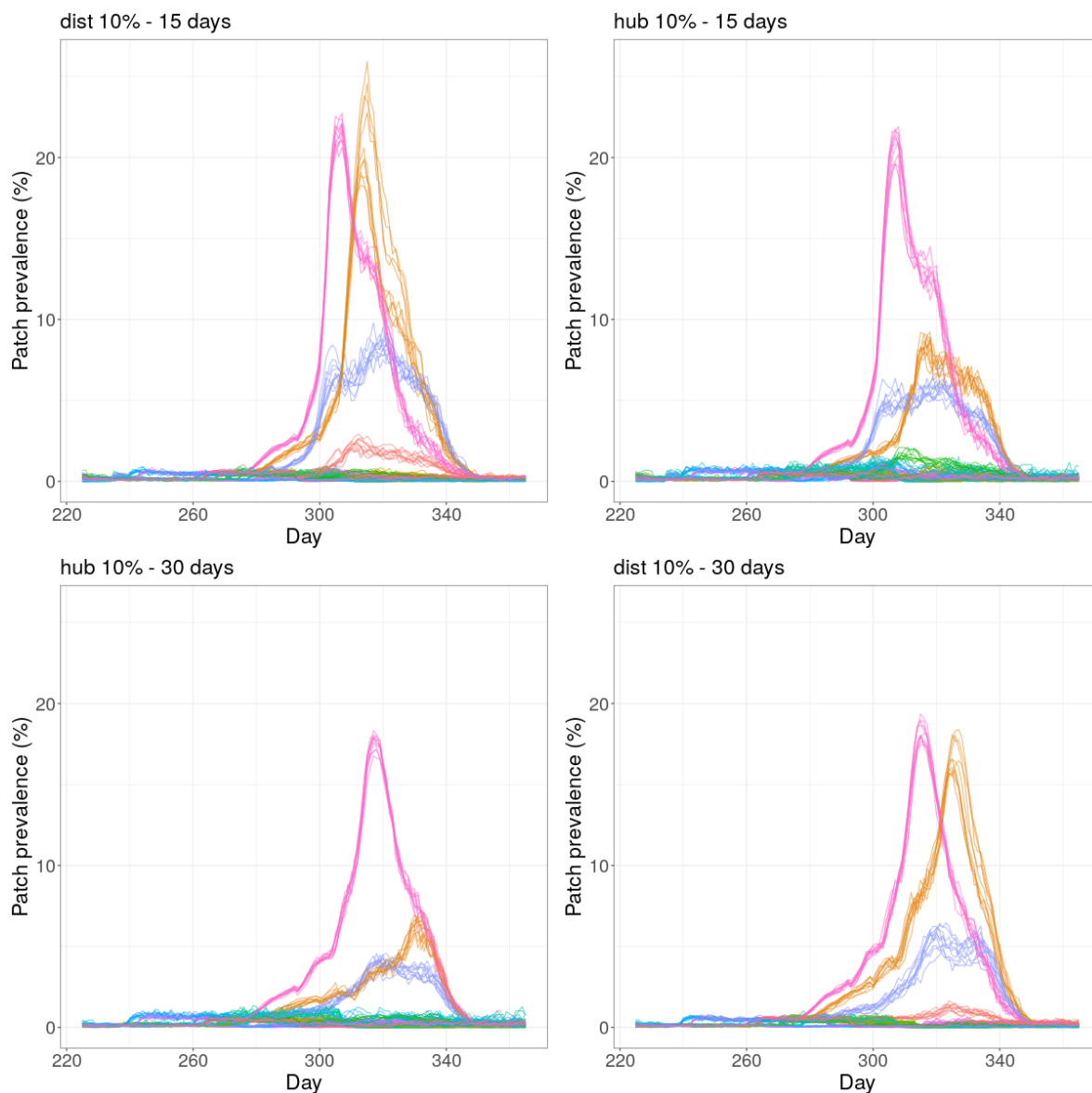


**Figure S.7** – Variability in patch prevalence between 10 stochastic runs for scenarios applying 10% intra-metapopulation movements, comparing distance-based (left) and hub-based (right) typologies. A line represents a patch prevalence over time for a given run. All lines with the same color correspond to the same patch. Note that we only show timesteps after 225 because prevalence is low before.

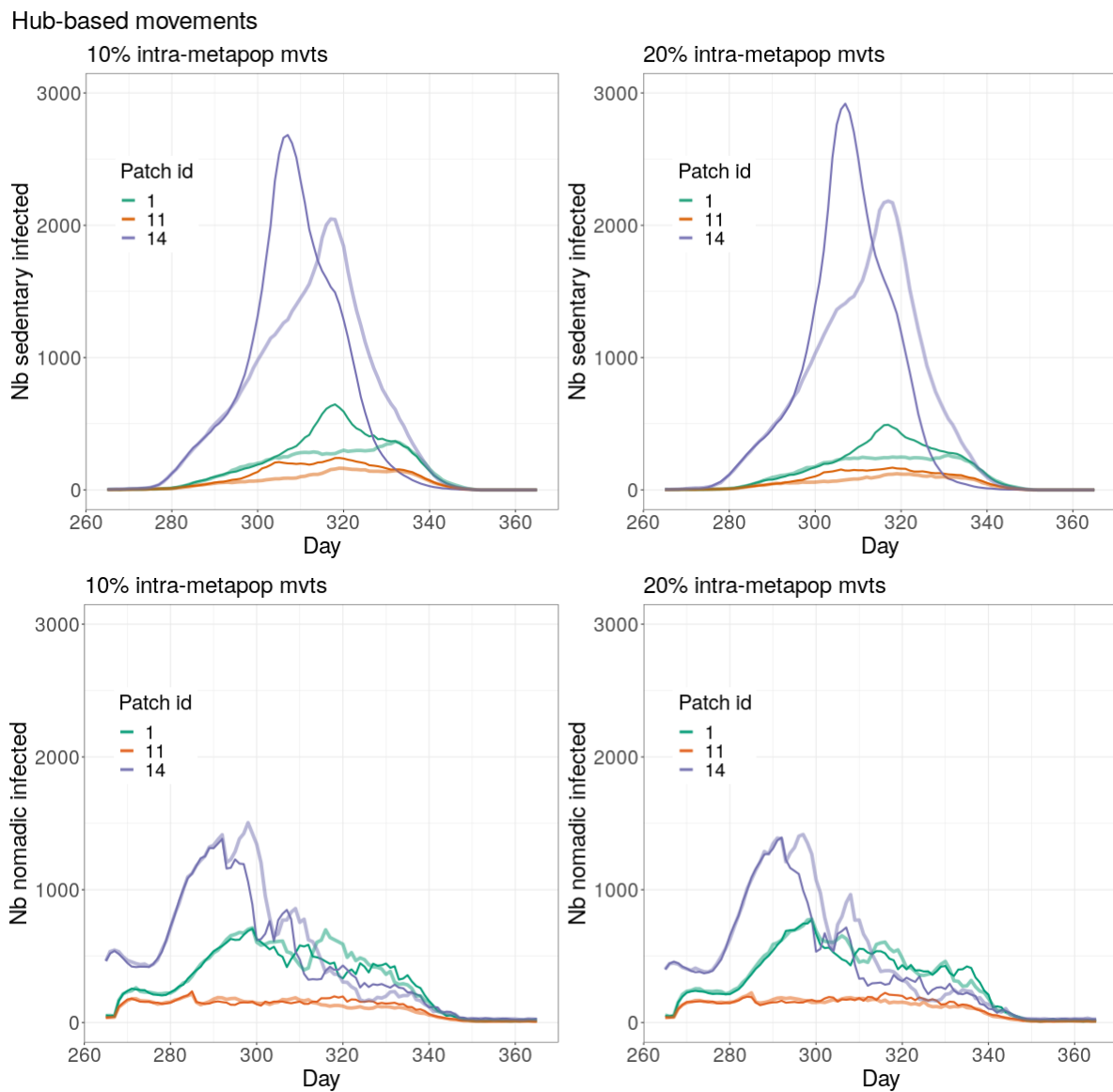


**Figure S.8** – Number of infected sedentary (top) and nomadic (bottom) animals over time, per patch. Intra-metapopulation movements are hub-based, and represent a proportion of 10% (left) or 20% (right) of total movements during the wet season. Colors indicate patch. Darker lines represent scenarios with 15 day transition phase between seasons, and thicker, lighter lines represent scenarios with 30 day transition phase between seasons. Median of 10 runs.

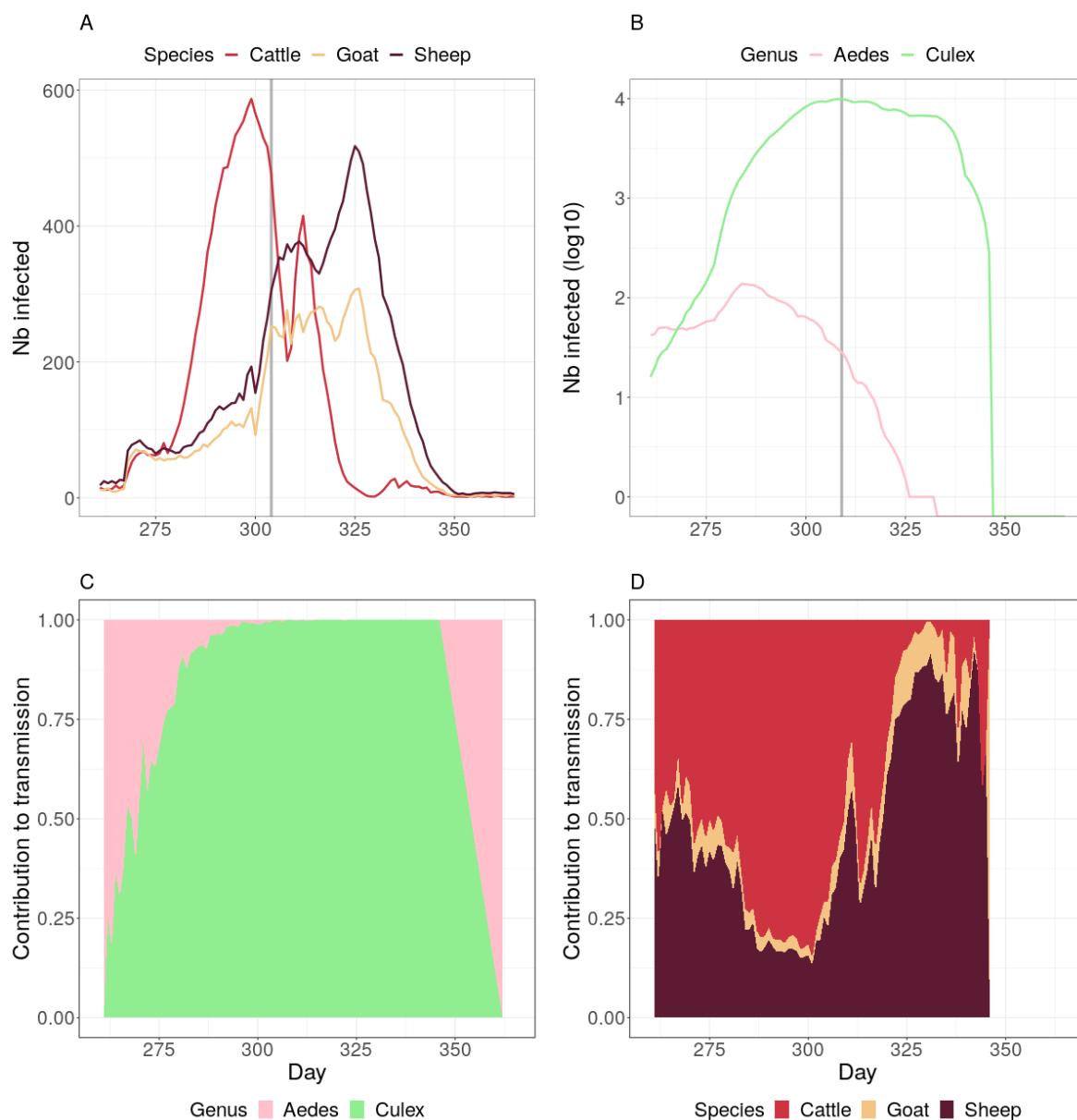


**Figure S.9** – Example of host and vector contribution to infections and transmission. Patch 1, 10% distance-based intra-metapopulation movements, 30 day transition between seasons. A: Number of infected animals per species over time. Vertical grey line shows time of maximum animal infections. C: Contribution of vector species to host infections (% of force of infection) over time. Blank plot at the last timesteps means transmission has stopped (no new cases). B: Number of infected vectors per species over time, log10 scale. Vertical grey line shows time of maximum vector infections. D: Contribution of host species to vector infections (% of force of infection) over time. Timesteps after 260. Median of 10 runs.



# 6

## Discussion

The goal of this PhD was to create new knowledge on the eco-epidemiology of Rift Valley fever virus transmission dynamics. Specifically, we aimed at gaining new insights on the role played by the different livestock host species on RVFV emergence and spread. We explored this question at various spatio-temporal scales and resolutions, in an integrative attempt to capture the major components shaping this role, with a case study located in the West African Sahel, a RVF endemic region.

### 6.1 Main contributions

We reflected on existing RVFV mechanistic models, to study their methodological diversity, their contribution to RVFV epidemiology, and identify questions left unaddressed (Chapter 2). There has been a profusion of new models published in the last five years, and overall an equilibrium seems to exist between theoretical, grey, and applied models. Although using different tools to analyse their models, or different hypotheses, they can contribute in complementary ways to the understanding, anticipation, and control, of RVFV. We highlighted important knowledge gaps, some of which were tackled in my PhD. First, the heterogeneity between vertebrate RVFV hosts seemed understudied, both at the population- and individual-level. Second, in Senegal, a spatial model at large scale, including host movements, was lacking.

An important component of RVFV eco-epidemiology which this PhD intended to address was the role of the different livestock host species in RVFV emergence, transmission, and spread. First, in Chapter 3, we showed that, when considering them equal in susceptibility and transmission, the contribution of hosts to vector-borne RVFV emergence was driven by vector feeding preferences and host relative densities. Therefore, in northern Senegal, the immunity of

cattle, favoured by vectors and less numerous than small ruminants, was identified as a possible way to mitigate the epidemic potential. However, when focusing on individual-level transmission potential in Chapter 4, we showed that the net infectiousness in young hosts was higher in sheep than in cattle and goats. Besides, fatal infections induced a higher transmission potential than less severe infections in lambs, leaving the overall effect on population-level transmission undetermined. Finally, the role of seasonal livestock mobility had to be considered. In Chapter 5, incorporating the interaction of processes at multiple scales, we showed that in northern Senegal, cattle infections precede sheep and goats' infections, and that cattle and sheep are sequentially the main contributors to transmission. To our knowledge, estimations of infectiousness made in Chapter 4, and temporal patterns of infection and transmission highlighted in Chapter 5, are entirely new results absent from previous literature on RVFV.

To map the epidemic potential of RVFV in northern Senegal over time, we developed a model and showed the existence of a period of high risk in September across the territory from 2014 to 2016 (Chapter 3), consistent with observations made during the 2013-2014 outbreak (Sow et al., 2016). We quantified the contrast between the Ferlo region and the Senegal river delta and valley (SRDV), in agreement with the enzootic-epizootic dynamics observed in Senegal. An analytical formula of the basic reproduction number was extracted from the model, through the next generation matrix approach. This approach is not new (Diekmann et al., 1990; Driessche and Watmough, 2002; Diekmann et al., 2010), although its use for vector-borne disease risk mapping is not widespread (19 articles identified through a systematic review by Cheng et al., 2020). Thanks to a deep knowledge of local drivers of transmission, acquired through numerous field studies (Traoré-lamizana et al., 2001; Ndione et al., 2008; Bop et al., 2014; Oumar, 2015; Biteye et al., 2018, 2019), as well as large scale estimations of host and vector densities becoming available (Gilbert et al., 2018; Tran et al., 2019), local dynamics could be scaled up by our model. The identification of spatio-temporal patterns provided a broader understanding of the suitability of SRDV and the Ferlo for RVFV emergence. Concretely, we provided detailed insights on time periods, locations, and durations of high risk, achieving both large scales (northern Senegal, 3 consecutive rainy seasons) and fine resolutions (3.5 km<sup>2</sup> pixels, introduction dates assessed weekly).

To study individual-level differences in livestock host infectiousness, we intended to examine the full cycle of events from one mosquito bite to the next (Chapter 4). We developed a model of within-host viral load dynamics, fitted to a unique experimental dataset. Using a sampling-

based approach and a composite likelihood, we performed parameter estimations for groups of animals differing by their species or survival outcome. Our results provided mechanistic insights on possible processes explaining the observed heterogeneity, such as the efficiency of viral replication and the lifespan of infectious viral particles. A simple yet insightful meta-analysis of competence studies calibrated the relationship between vertebrate host infectious viral loads and vector infection rates, revealing the importance of the mosquito genus involved, with *Aedes* spp. vectors being more easily infected than *Culex* spp. vectors. Such a difference had not been quantified across a large range of dosage before.

Finally, to complete the set of epidemiological processes relevant for our case study, we developed an original metapopulation model simulating connexions in a network of major transhumance hubs in the Ferlo region of Senegal (Chapter 5). Within each patch, we expanded the model from Chapter 3 to integrate knowledge from Chapter 4. We showed that the progressivity of the animal flow conditioned the way RVFV introductions through nomadic herds spread into sedentary populations, and that *Culex* vectors were largely responsible for livestock infections at the time of the outbreaks. The spatial aggregation level was chosen to accommodate heterogeneous vector populations along with large- and small-scale movements of hosts. This chapter used new data made available during the course of the PhD, and provides a flexible tool to further explore complex scenarios of transmission between the endemic region of SRDV and the fragmented Ferlo region of heterogeneous suitability.

## 6.2 Implications

The results of this PhD have several kinds of implications. Firstly, at the micro-scale, the role of experimental, controlled infections appears crucial to understand at a finer grain both the host and vector response to infection, and all the factors influencing their competence. Progress on the modeling side will necessarily be conditioned on advances made in fundamental research on those aspects. Secondly, in the field, the description of pastoralists movements and factors influencing their decision-making must continue. When both of these directions are further explored, models will be able to provide insights on the design of efficient control strategies. To do so, such modeling efforts will need to focus on feasible and acceptable animal- and public health measures, taking into account the economic and cultural value of animals (Craighead et al., 2021) along with the limits of available vaccines (Chamchod et al., 2016; Nielsen et al., 2020).

The role of data (or absence thereof) is paramount in shaping the structure of mathematical models and the questions they aim to answer, and this PhD has been no exception. We have used multiple types of data : routinely collected, remotely-sensed, meteorological data, experimental, laboratory data on vector and host infection, host demographic data transformed through a model, entomological model outputs validated on capture data, field surveys, expert knowledge. This list is obviously lacking an important category : epidemiological data, in the sense of case reports, or a proxy such as serological data. As noted in the systematic review by Bron et al., 2021<sup>1</sup>, the quality and availability of epidemiological data on Rift Valley fever is highly heterogeneous, and efforts need to be made on the standardization of reporting (case definition, spatial and temporal sampling information) in order to accurately inform mathematical models. Guidelines have been designed for the management of scientific data, known as the FAIR principles (Findable, Accesible, Interoperable, Reusable, Wilkinson et al., 2016). A recent review on the status of veterinary epidemiological research regarding these principles concluded that none of the datasets met all the FAIR requirements (Meyer et al., 2021). In particular, most non-molecular epidemiological datasets were not “findable”, and interoperability, which requires specific data management skills, was also problematic (Meyer et al., 2021). In the case of vector-borne diseases in the Sahel, the accessibility of field sites and the preservation of samples are important hurdles not easily overcome.

Throughout this PhD, dynamical patterns emerged from a combination of drivers included in the models, which could not have been captured with individual indicators alone. This emphasizes the need for integrative approaches and systems thinking, without which important interactions between processes might be neglected (Xia et al., 2017). This is the basis of the One Health approach (Mackenzie and Jeggo, 2019), and we argue that the diversity of modeling approaches can assist in the implementation of this concept to battle vector-borne and zoonotic diseases. Phenomenological models can play a key role in selecting relevant processes to include or characterize suitable habitats, by highlighting significant correlations in complex datasets (Cianci et al., 2015; Pigott et al., 2015; Sindato et al., 2016). Such phenomenological models can then be nested into mechanistic models for specific processes (e.g temperature-dependency, density-dependency). Only when and if the impact of interactions or entire processes turns out to be negligible (which might be the case only in specific contexts, e.g. zones with stable temperatures year-round), can the complexity be reevaluated and downgraded. For this last step, the role of sensitivity analyses is crucial and still too often neglected (Saltelli et al., 2019).

---

<sup>1</sup> I am a co-author of Bron et al. 2021, you can find the paper in Appendix A



Overall, the right balance must be found between realism, needed for a model to be practically useful, and parcimony, essential for a model to be tractable and well supported by empirical knowledge.

Closely related to the choice of drivers/processes to include in a model, is the choice of the most relevant way to group and link entities. In this PhD, this question was raised in two ways. First, for a given type of entity, with clearly identified biological boundaries (e.g. a host, a vector), the degree of heterogeneity to incorporate within entity types should be chosen according to the context modeled: in our case, we found that the existing taxonomic diversity (species, genus) at the host- and vector-level was compelling enough to make it a focus of this PhD. Second, organization levels and associated degree of complexity must be chosen with regards to the research question being investigated, as mentioned in the Introduction (Box 1.2). Infectious disease systems are by essence multiscale systems, but not every multiscale system has to lead to multiscale models (Garabed et al., 2019). Pathogens' life cycle take place (in part or fully) within-individuals, where their impact can be witnessed at the cell-, tissue-, or organ-level (Gommet et al., 2011; Odendaal et al., 2019; Oymans et al., 2020). Pathogens then spread between individuals, or can survive in the environment. Individuals can themselves be organized into various social and spatial aggregation levels, be it families, herds, neighborhoods, batches etc., in between which they can move. In this PhD, scales were first treated separately (Chapter 3 and 4). Then, some approximations were made to retain the most relevant aspects of each (Chapter 5). This was done because timescales differed strongly (an individual infection is way shorter than the duration of an entire outbreak), and because of the absence of cross-scale data (Garabed et al., 2019). Our work therefore cannot strictly be defined as multiscale modeling, as there was no bidirectional interactions between the smaller and the larger scale. A whole body of theoretical work is being developed to define levels, resolutions, scales and categorize types of multiscale models (Garira, 2017). For vector-borne disease systems, such models could for instance enable the comparison of control strategies targeting the reduction of pathogen load within hosts or vectors to strategies aiming at controlling the vector population or its contact with the host population (Garira and Chirove, 2019).

The diversity of processes, scales, and data, inevitably raises the question of pluridisciplinarity. Epidemiology is inherently a highly diverse discipline (Lynch, 2006), and epidemiological modeling, which I tend to see as a “concentrator of knowledge”, strongly rely on all epidemiological disciplines. In this PhD, I have been lucky to work with veterinarians, geomaticians,

climatologists, virologists, and entomologists, to name a few. In such interdisciplinary contexts, communication is key. I could probably come up with my own set of guidelines, which could be Repeat, Reformulate, Ask Again. Indeed, interactions are not always smooth, as we tend to use different words for the same thing, or misuse the vocabulary of the other discipline. We might also not pursue the same goals, or be held back by the same constraints. It is therefore crucial to make sure that you are on the same page before concretely diving into model implementation, unless you want to risk starting all over again because of a misunderstanding. Overall, I feel like while I clearly benefited from the knowledge exchanged during those interdisciplinary meetings, with colleagues kindly willing to invest time in my project, it sometimes felt like a one-way street, with some colleagues not always seeing that they could also get something out of this collaboration. In other words, mathematical models might still be seen as a finality, or in the best case an iterative, integrative process which can be updated with new knowledge, but rarely as something that can inform the design of new experiments or field work. For instance, details provided in case reports, or the sampling design used for serosurveys, are not currently suited to confirm or deny our conclusions on the role of livestock host species. Again, guidelines have been formulated to favor a more holistic approach, with the example of model-guided fieldwork in research on wildlife ecological and epidemiological dynamics (Restif et al., 2012). In my view, this vision of research is needed if we hope to achieve anything close to transdisciplinarity, a trendy although illdefined word (Lynch, 2006).

### 6.3 Perspectives

This work opened several new avenues to explore, from possible model refinements and transferability to complementary research questions to address.

By focusing on short-term amplification following virus introduction into a given geographical area (Chapter 3), we provided the basis for a surveillance system at large scale in northern Senegal. To make such a tool operational, the immune status of herd would need to be assessed regularly by repeated field surveys, to make sure that the size of susceptible host populations is monitored over time and estimated accurately. Besides, for diseases inducing lifelong immunity, the renewal rate of herds should also be taken into account (Hammami et al., 2016). However, the traceability of livestock trade and herd demographics in the region is poor (Lesnoff, 2013; Jahel et al., 2020). From a modeler's point of view, the systematic identification of animals would be highly desirable. This might not be achievable operationally, nor accepted culturally, as *peul* do not count what they cherish (animals or kids, Pin-Diop, 2006). Still, demographic models

have been developed in such settings, requiring some methodological compromises (Lesnoff, 2008; Lesnoff, 2013). Finally, a better characterization of animal flows in the region, in addition to improving the model developed in Chapter 5, could allow the estimation of a likelihood associated with each introduction date, assessed as equiprobable in Chapter 3. Currently, forecasting models used for RVFV are strictly based on anomaly detection in environmental variables (FAO-WHO, 2008), and could benefit from a more mechanistic approach such as the one we developed.

To fully grasp the transmission dynamics of RVFV in the West African Sahel, the models developed in this PhD should be extended to Mauritania. Indeed, outbreaks in Mauritania usually precede RVFV detection in Senegal (Lancelot et al., 2019). Although studies do exist on climatic drivers of RVFV and livestock mobility in the affected regions (Caminade et al., 2014; Apolloni et al., 2018), no mechanistic model has been developed so far for this context. For our approach to be transferred, one major component missing is the adaptation of the entomological model by Tran et al., 2019. Several steps are needed to achieve this. First, to precisely locate permanent and seasonal water-bodies, remotely-sensed images have to be retrieved and processed by combining specific spectral bands, suited for a given vegetation cover and turbidity. Several Normalized Difference Water Indexes exist, and the one used to detect temporary ponds in the Ferlo region (MNDWI or  $NDWI_{G/MIR}$ ) by Tran et al., 2019 has been shown to perform well in the Mauritanian context (Campos et al., 2012). Second, for the hydrological model to be adapted (Soti et al., 2010), measures of ponds in Mauritania are needed to calibrate parameters such as runoff coefficient and soil moisture. Last but not least, while field data show that *Ae. vexans* and *Cx. poicilipes* are present in regions of active RVFV circulation in Mauritania, a lot of anopheline specimens are also reported (Mint Mohamed Lemine et al., 2017). Further investigations would need to determine which species to include to achieve the most relevant entomological model for RVFV transmission dynamics in Mauritania. Alternatively, the use of an environmental proxy could be envisioned, as in Métras et al., 2017, 2020, but requires detailed epidemiological data to parametrize the relationship between the proxy and transmission.

Finally, the livestock trade between the West African Sahel and the Maghreb, and within the mediterranean basin, makes our work directly relevant to study the risk of RVFV introduction into new areas, such as the EU (Chevalier, 2013; Durand et al., 2013). A promising method for surveillance is the use of Early Warning Signals (EWS). It consists of a suite of summary

statistics which undergo characteristic changes as critical transitions are approaching. It is therefore intended to detect possible disease emergence before  $R_0 > 1$ , and elimination before  $R_0 < 1$  (O'Regan and Drake, 2013). The theory, developed using mechanistic models, has yet to accommodate all flaws inherent to case report data (Brett et al., 2018). For vector-borne diseases in particular, the impact of seasonality and how it could hinder EWS use is still subject to debate (Williamson et al., 2016; Miller et al., 2017). In the meantime, our work could contribute to improving the existing MINTRISK model (Nielsen et al., 2020), currently in use to assess risk of RVFV introduction into the EU. This model sets four possible levels for the basic reproduction ratio (very low :  $< 0.3$ , to very high :  $> 10$ , Nielsen et al., 2020), and could therefore gain in accuracy by adopting a data-driven mapping approach such as ours.

## 6.4 Questions pending

A number of processes remain unexplored in mathematical models of RVFV transmission, and for other vector-borne pathogens to some extent. Possible explanations include a shallow understanding of some processes, which might require more fundamental research before being synthesized into model equations. Moreover, the lack of data might be discouraging to modellers, who feel like simplifying assumptions and large uncertainty in parameter values could diminish the added value of incorporating a given process.

Regarding micro-scale processes, the role of virus strains and co-infections seem like leads worth investigating. Even though there is only one serotype for RVFV, different strains have been shown to induce distinct virulence, at least in mice (Ikegami et al., 2017). In addition, evolutionary pressures, driving pathogen adaptation, might result in a counterintuitive trade-off balancing between-host transmission and within-host replication (Althouse and Hanley, 2015). Similarly, interferences can arise in the case of co-infections, which are not uncommon (Muturi et al., 2021). At the within-host scale, viral interference involving RVFV has been shown to impact both replication and immune response (Safini et al., 2021). At the between-host scale, the competition for susceptible hosts might also produce unexpected outbreak patterns, as shown through modeling (Rohani et al., 2003; Barfield et al., 2015).

Genetic diversity is also a marker of a pathogen's history, testifying of past spread and paths taken. Thanks to the development of next-generation sequencing, strains can be more easily sequenced and become openly accessible. Phylogenetic approaches have been used to understand RVFV introduction into new areas, by identifying clades (Pepin et al., 2010; Ikegami, 2012;

Samy et al., 2017). Recently, phylodynamic approaches have gained momentum, using information on genetic diversity to enrich mathematical models and gain a deeper understanding of pathogen spread (Volz et al., 2009; Layan et al., 2021). In particular, phylogeographic models are becoming more and more sophisticated (Dellicour et al., 2021), and the incorporation of inference frameworks has brought mechanistic insights into the spatial distribution of cases for vector-borne diseases such as dengue (Salje et al., 2021). These are promising methods possibly helpful to understand the large scale dynamics of RVFV spread.

The field of infectious disease epidemiology, like many others, has made important progress in the era of big data. Indeed, new sources of data can now be exploited to enrich models. In Senegal, mobile phone call records highlighted the role of mass gatherings in the spread of cholera (Finger et al., 2016). In Latin America, the use of Google searches, social media, and news reports improved the forecasting of Zika incidence (McGough et al., 2017). Such datasets might be relevant for RVFV, e.g because religious events such as Tabaski are thought to increase its transmission to humans (Lancelot et al., 2019). However, outside urban areas, it is not guaranteed that pastoralists all possess a phone with access to the internet. Moreover, the use of such data might raise ethics concern in the general population, and accessibility issues with private companies collecting them. Besides, data processing requires the development of a dedicated expertise, e.g. in text-mining (Valentin et al., 2020). Ultimately, this leaves us wondering whether any individual modeling project could ever succeed in combining all the relevant datasets and state-of-the-art methods to achieve the most reliable analysis in a timely manner.

## 6.5 Lessons learned from the community

The diversity of modeling methods and data appears as a unique opportunity to produce an accurate understanding and possible forecasting of pathogen spread, as well as the evaluation of complex control strategies. To get the most out of this diversity of expertise, collective efforts such as modeling challenges (several teams modelling a similar pathogen with similar data, Shaman and Karspeck, 2012; Viboud et al., 2018) or ensemble models (combining a set of plausible models with their uncertainty to outperform individual models, Lindström et al., 2015; Chowell et al., 2020) are becoming more frequent. For dengue, such methods were used to evaluate forecasts of seasonal outbreaks in Peru and Puerto Rico (Yamana et al., 2016; Johansson et al., 2019). Models showed different strenghts and weaknesses when assessing their ability to predict peak incidence, the week of the peak, and total incidence (Yamana et al.,

2016; Johansson et al., 2019). When combined, individual biases were reduced while retaining reliable aspects of each model (Yamana et al., 2016; Johansson et al., 2019). For chikungunya, a challenge was organized using data from epidemics across the Americas, and showed that simpler approaches outperformed more complex ones, because biases in reporting could mislead some models, such as those incorporating transportation dynamics (Valle, 2018).

Mathematical modelling has now established itself as a key tool for outbreak response as well as the control of endemic diseases (Lofgren et al., 2014; Ezanno et al., 2020). However, the world *in silico* is still often oversimplified, and does not take into account real-world constraints which could hamper the feasibility of model recommendations. A recent review identified models incorporating such constraints into their analyses, e.g. vaccine stockouts or nurse shortage (Bozzani et al., 2021). By contrast, some models underestimate the resilience of a system, e.g. when projecting future distributions of neglected tropical diseases solely under the effect of climate change, discarding any possible offsetting through socioeconomic development (Béguin et al., 2011). Finally, several studies have assessed the use and acceptability of models as public health decision tools, and unanimously recommend the integration of modellers and model-building into the policy process, which entails frequent and qualitative exchanges with practitioners, the clear communication of the limits of modeling, along with the creation of a cycle where results inform decisions and vice versa (Kitching et al., 2006; Metcalf et al., 2015; Doms et al., 2018).

## 6.6 Conclusion

In this PhD, we used mechanistic modelling to explore a complex pathosystem, involving multiple hosts and vectors. We tailored model hypotheses, implementation, and analyses to chapter-specific research questions, to ensure the most appropriate degree of complexity was reached, while getting the most out of available data sources. These chapters together also tell a story : a story about biotic and abiotic processes, individuals and populations, which all interact across scales and from which stems the eco-epidemiological dynamics of Rift Valley fever virus. Iteratively, we built a global vision of the system, which we hope will be helpful to guide future research and modestly contribute to limit the burden of vector-borne and zoonotic diseases.

# Bibliography

- Achee, N. L. et al. (2019). “Alternative strategies for mosquito-borne arbovirus control”. In: *PLOS Neglected Tropical Diseases* 13.1. DOI: 10.1371/journal.pntd.0006822.
- Adams, B. and D. D. Kapan (2009). “Man Bites Mosquito: Understanding the Contribution of Human Movement to Vector-Borne Disease Dynamics”. In: *PLoS ONE* 4.8. DOI: 10.1371/journal.pone.0006763.
- Adongo, D., K. R. Fister, H. Gaff, and D. Hartley (2013). “Optimal Control Applied to Rift Valley Fever”. In: *Natural Resource Modeling* 26.3. DOI: 10.1111/nrm.12006.
- Adriansen, H. K. (2008). “Understanding pastoral mobility: the case of Senegalese Fulani”. In: *The geographical journal* 174.3.
- Ahmad, K. (2000). “More deaths from Rift Valley fever in Saudi Arabia and Yemen”. In: *The Lancet* 356.9239. DOI: 10.1016/S0140-6736(05)74068-X.
- Allen, L. J. S. and G. E. Lahodny (2012). “Extinction thresholds in deterministic and stochastic epidemic models”. In: *Journal of Biological Dynamics* 6.2. DOI: 10.1080/17513758.2012.665502.
- Althouse, B. M. and K. A. Hanley (2015). “The tortoise or the hare? Impacts of within-host dynamics on transmission success of arthropod-borne viruses”. In: *Philosophical Transactions of the Royal Society B: Biological Sciences* 370.1675. DOI: 10.1098/rstb.2014.0299.
- Andraud, M., N. Hens, C. Marais, and P. Beutels (2012). “Dynamic Epidemiological Models for Dengue Transmission: A Systematic Review of Structural Approaches”. In: *PLoS ONE* 7.11. DOI: 10.1371/journal.pone.0049085.
- Anyamba, A. et al. (2009). “Prediction of a Rift Valley fever outbreak”. In: *Proceedings of the National Academy of Sciences* 106.3. DOI: 10.1073/pnas.0806490106.
- Anyamba, A. et al. (2012). “Climate Teleconnections and Recent Patterns of Human and Animal Disease Outbreaks”. In: *PLoS Neglected Tropical Diseases* 6.1. DOI: 10.1371/journal.pntd.0001465.
- Anzo-Hernández, A., B. Bonilla-Capilla, J. Velázquez-Castro, M. Soto-Bajo, and A. Fraguera-Collar (2019). “The risk matrix of vector-borne diseases in metapopulation networks and its relation with local and global  $R_0$ ”. In: *Communications in Nonlinear Science and Numerical Simulation* 68. DOI: 10.1016/j.cnsns.2018.06.006.

- Apolloni, A. et al. (2018). “Towards the description of livestock mobility in Sahelian Africa: some results from a survey in Mauritania”. In: *PLoS ONE* 13.1. DOI: 10.1371/journal.pone.0191565.
- Apolloni, A., C. Corniaux, C. Coste, R. Lancelot, and I. Touré (2019). “Livestock Mobility in West Africa and Sahel and Transboundary Animal Diseases”. In: *Transboundary Animal Diseases in Sahelian Africa and Connected Regions*. Springer International Publishing. DOI: 10.1007/978-3-030-25385-1\_3.
- Azar, S. R. and S. C. Weaver (2019). “Vector Competence: What Has Zika Virus Taught Us?” In: *Viruses* 11.9. DOI: 10.3390/v11090867.
- Ba, Y., D. Diallo, C. M. F. Kebe, I. Dia, and M. Diallo (2005). “Aspects of bioecology of two Rift Valley fever virus vectors in Senegal (West Africa): *Aedes vexans* and *Culex poicilipes* (Diptera: Culicidae)”. In: *Journal of Medical Entomology* 42.5.
- Ba, Y., D. Diallo, I. Dia, and Diallo, M (2006). “Comportement trophique des vecteurs du virus de la fièvre de la vallée du Rift au Sénégal : implications dans l'épidémiologie de la maladie.” In: *Bull Soc Pathol Exot* 99.4.
- Bacaër, N. (2011). *A Short History of Mathematical Population Dynamics*. Springer London. DOI: 10.1007/978-0-85729-115-8.
- Bacigalupo, S. A., L. K. Dixon, S. Gubbins, A. J. Kucharski, and J. A. Drewe (2020). “Towards a unified generic framework to define and observe contacts between livestock and wildlife: a systematic review”. In: *PeerJ* 8.e10221.
- Bah, A., I. Touré, C. Le Page, A. Ickowicz, and A. Diop (2006). “An agent-based model to understand the multiple uses of land and resources around drillings in Sahel”. In: *Mathematical and Computer Modelling* 44.5-6. DOI: 10.1016/j.mcm.2005.02.014.
- Balcan, D., V. Colizza, B. Goncalves, H. Hu, J. J. Ramasco, and A. Vespignani (2009). “Multiscale mobility networks and the spatial spreading of infectious diseases”. In: *Proceedings of the National Academy of Sciences* 106.51. DOI: 10.1073/pnas.0906910106.
- Balenghien, T. et al. (2013). “Towards a better understanding of Rift Valley fever epidemiology in the south-west of the Indian Ocean”. In: *Veterinary Research* 44.1. DOI: 10.1186/1297-9716-44-78.
- Bardosh, K. L., S. J. Ryan, K. Ebi, S. Welburn, and B. Singer (2017). “Addressing vulnerability, building resilience: community-based adaptation to vector-borne diseases in the context of global change”. In: *Infect Dis Poverty* 6.1. DOI: 10.1186/s40249-017-0375-2.
- Barfield, M., M. E. Orive, and R. D. Holt (2015). “The role of pathogen shedding in linking within- and between-host pathogen dynamics”. In: *Mathematical Biosciences* 270. DOI: 10.1016/j.mbs.2015.04.010.
- Barker, C. M., T. Niu, W. K. Reisen, and D. M. Hartley (2013). “Data-Driven Modeling to Assess Receptivity for Rift Valley Fever Virus”. In: *PLoS Neglected Tropical Diseases* 7.11. DOI: 10.1371/journal.pntd.0002515.



- Bartlow, A. W., C. Manore, C. Xu, K. A. Kaufeld, S. Del Valle, A. Ziemann, G. Fairchild, and J. M. Fair (2019). “Forecasting Zoonotic Infectious Disease Response to Climate Change: Mosquito Vectors and a Changing Environment”. In: *Veterinary Sciences* 6.2. DOI: 10.3390/vetsci6020040.
- Beechler, B. R., C. A. Manore, B. Reininghaus, D. O’Neal, E. E. Gorsich, V. O. Ezenwa, and A. E. Jolles (2015). “Enemies and turncoats: bovine tuberculosis exposes pathogenic potential of Rift Valley fever virus in a common host, African buffalo ( *Syncerus caffer* )”. In: *Proceedings of the Royal Society B: Biological Sciences* 282.1805. DOI: 10.1098/rspb.2014.2942.
- Begon, M., M. Bennett, R. Bowers, N. French, S. Hazel, and J. Turner (2002). “A clarification of transmission terms in host-microparasite models: numbers, densities and areas”. In: *Epidemiology and Infection* 129.01. DOI: 10.1017/S0950268802007148.
- Belkhiria, J., M. M. Lo, F. Sow, B. Martínez-López, and V. Chevalier (2019). “Application of exponential random graph models to determine nomadic herders’ movements in Senegal”. In: *Transboundary and Emerging Diseases* 66. DOI: 10.1111/tbed.13198.
- Bergren, N. A., E. M. Borland, D. A. Hartman, and R. C. Kading (2021). “Laboratory demonstration of the vertical transmission of Rift Valley fever virus by *Culex tarsalis* mosquitoes”. In: *PLoS Negl Trop Dis* 15.3. DOI: 10.1371/journal.pntd.0009273.
- Bicout, D. J. and P. Sabatier (2004). “Mapping Rift Valley Fever vectors and prevalence using rainfall variations”. In: *Vector Borne Zoonotic Dis.* 4.1. DOI: 10.1089/153036604773082979.
- Bicout, D. J., M. Vautrin, C. Vignolles, and P. Sabatier (2015). “Modeling the dynamics of mosquito breeding sites vs rainfall in Barkedji area, Senegal”. In: *Ecological Modelling* 317. DOI: 10.1016/j.ecolmodel.2015.08.027.
- Bird, B. H., T. G. Ksiazek, S. T. Nichol, and N. J. MacLachlan (2009). “Rift Valley fever virus”. In: *JAVMA* 234.7.
- Birnberg, L., S. Talavera, C. Aranda, A. I. Núñez, S. Napp, and N. Busquets (2019). “Field-captured *Aedes vexans* (Meigen, 1830) is a competent vector for Rift Valley fever phlebovirus in Europe”. In: *Parasites & Vectors* 12.1. DOI: 10.1186/s13071-019-3728-9.
- Biteye, B., A. G. Fall, M. Ciss, M. T. Seck, A. Apolloni, M. Fall, A. Tran, and G. Gimonneau (2018). “Ecological distribution and population dynamics of Rift Valley fever virus mosquito vectors (Diptera, Culicidae) in Senegal”. In: *Parasit Vectors* 11.1. DOI: 10.1186/s13071-017-2591-9.
- Biteye, B., A. G. Fall, M. T. Seck, M. Ciss, M. Diop, and G. Gimonneau (2019). “Host-feeding patterns of *Aedes* (*Aedimorphus*) *vexans arabiensis*, a Rift Valley Fever virus vector in the Ferlo pastoral ecosystem of Senegal”. In: *PLOS ONE* 14.10. DOI: 10.1371/journal.pone.0215194.
- Bodian, A. (2014). “Caractérisation de la variabilité temporelle récente des précipitations annuelles au Sénégal (Afrique de l’Ouest)”. In: *Physio-Géo* Volume 8. DOI: 10.4000/physio-geo.4243.

- Bop, M., A. Amadou, O. Seidou, C. M. F. Kéb  , J. A. Ndione, S. Sambou, and I. S. Sanda (2014). “Modeling the hydrological dynamic of the breeding water bodies in Barkedji’s zone”. In: *Journal of Water Resource and Protection* 06.08. DOI: 10.4236/jwarp.2014.68071.
- Bornmann, L. and R. Mutz (2015). “Growth rates of modern science: A bibliometric analysis based on the number of publications and cited references: Growth Rates of Modern Science: A Bibliometric Analysis Based on the Number of Publications and Cited References”. In: *J Assn Inf Sci Tec* 66.11. DOI: 10.1002/asi.23329.
- Boutayeb, A. (2010). “The impact of infectious diseases on the development of Africa”. In: Springer Science. Chap. Disease burdens and economic impacts.
- Bozzani, F. M., A. Vassall, and G. B. Gomez (2021). “Building resource constraints and feasibility considerations in mathematical models for infectious disease: A systematic literature review”. In: *Epidemics* 35. DOI: 10.1016/j.epidem.2021.100450.
- Brett, T. S., E. B. O’Dea, Marty, P. B. Miller, A. W. Park, J. M. Drake, and P. Rohani (2018). “Anticipating epidemic transitions with imperfect data”. In: *PLoS Comput Biol* 14.6. DOI: 10.1371/journal.pcbi.1006204.
- Bron, G. M., K. Strimbu, H. Cecilia, A. Lerch, S. Moore, Q. Tran, T. A. Perkins, and Q. A. ten Bosch (2021). “Over 100 years of Rift Valley Fever: a patchwork of data on pathogen spread and spillover”. In: *Pathogens* 10.708. DOI: 10.3390/pathogens10060708.
- Bruckmann, L. (2018). “Crue et d  veloppement rural dans la vall  e du S  n  gal : entre marginalisation et r  silience”. In: *Belgeo* 2. DOI: 10.4000/belgeo.23158.
- Brustolin, M. et al. (2017). “Rift Valley fever virus and European mosquitoes: vector competence of *Culex pipiens* and *Stegomyia albopicta* (= *Aedes albopictus*): European mosquitoes as vectors of RVFV”. In: *Medical and Veterinary Entomology* 31.4. DOI: 10.1111/mve.12254.
- B  guin, A., S. Hales, J. Rockl  v, C.   str  m, V. R. Louis, and R. Sauerborn (2011). “The opposing effects of climate change and socio-economic development on the global distribution of malaria”. In: *Global Environmental Change* 21.4. DOI: 10.1016/j.gloenvcha.2011.06.001.
- Cabral, J. S., L. Valente, and F. Hartig (2017). “Mechanistic simulation models in macroecology and biogeography: state-of-art and prospects”. In: *Ecography* 40.2. DOI: 10.1111/ecog.02480.
- Caminade, C. et al. (2011). “Mapping Rift Valley fever and malaria risk over West Africa using climatic indicators”. In: *Atmospheric Science Letters* 12.1. DOI: 10.1002/asl.296.
- Caminade, C., J. Ndione, M. Diallo, D. MacLeod, O. Faye, Y. Ba, I. Dia, and A. Morse (2014). “Rift Valley fever outbreaks in Mauritania and related environmental conditions”. In: *International Journal of Environmental Research and Public Health* 11.1. DOI: 10.3390/ijerph110100903.
- Campbell-Lendrum, D., L. Manga, M. Bagayoko, and J. Sommerfeld (2015). “Climate change and vector-borne diseases: what are the implications for public health research and policy?”

- In: *Philosophical Transactions of the Royal Society B: Biological Sciences* 370.1665. DOI: 10.1098/rstb.2013.0552.
- Campos, J. C., N. Sillero, and J. C. Brito (2012). “Normalized difference water indexes have dissimilar performances in detecting seasonal and permanent water in the Sahara–Sahel transition zone”. In: *Journal of Hydrology* 464-465. DOI: 10.1016/j.jhydro1.2012.07.042.
- Cavalerie, L., M. V. P. Charron, P. Ezanno, L. Dommergues, B. Zumbo, and E. Cardinale (2015). “A Stochastic Model to Study Rift Valley Fever Persistence with Different Seasonal Patterns of Vector Abundance: New Insights on the Endemicity in the Tropical Island of Mayotte”. In: *PLOS ONE* 10.7. DOI: 10.1371/journal.pone.0130838.
- Cecilia, H., R. Métras, A. G. Fall, M. M. Lo, R. Lancelot, and P. Ezanno (2020). “It’s risky to wander in September: Modelling the epidemic potential of Rift Valley fever in a Sahelian setting”. In: *Epidemics* 33. DOI: 10.1016/j.epidem.2020.100409.
- Chamchod, F., R. S. Cantrell, C. Cosner, A. N. Hassan, J. C. Beier, and S. Ruan (2014). “A Modeling Approach to Investigate Epizootic Outbreaks and Enzootic Maintenance of Rift Valley Fever Virus”. In: *Bull Math Biol* 76.8. DOI: 10.1007/s11538-014-9998-7.
- Chamchod, F., C. Cosner, R. S. Cantrell, J. C. Beier, and S. Ruan (2016). “Transmission Dynamics of Rift Valley Fever Virus: Effects of Live and Killed Vaccines on Epizootic Outbreaks and Enzootic Maintenance”. In: *Front. Microbiol.* 6. DOI: 10.3389/fmicb.2015.01568.
- Cheng, Y., N. B. Tjaden, A. Jaeschke, S. M. Thomas, and C. Beierkuhnlein (2020). “Deriving risk maps from epidemiological models of vector borne diseases: State-of-the-art and suggestions for best practice”. In: *Epidemics* 33. DOI: 10.1016/j.epidem.2020.100411.
- Chevalier, V. (2013). “Relevance of Rift Valley fever to public health in the European Union”. In: *Clinical Microbiology and Infection* 19.8. DOI: 10.1111/1469-0691.12163.
- Chevalier, V., S. d. La Rocque S., T. Baldet, L. Vial, and F. Roger (2004). “Epidemiological processes involved in the emergence of vector-borne diseases : West Nile fever, Rift Valley fever, Japanese encephalitis and Crimean-Congo haemorrhagic fever: -EN- -FR- -ES-”. In: *Revue Scientifique et Technique de l’OIE* 23.2. DOI: 10.20506/rst.23.2.1505.
- Chevalier, V., M Pépin, L Plée, and R. Lancelot (2010). “Rift Valley fever - a threat for Europe ?” In: *Clinical Microbiology and Infection* 19.8. DOI: 10.1111/1469-0691.12163.
- Chevalier, V., R. Lancelot, Y. Thiongane, B. Sall, A. Diaté, and B. Mondet (2005). “Rift Valley Fever in Small Ruminants, Senegal, 2003”. In: *Emerging Infectious Diseases* 11.11. DOI: 10.3201/eid1111.050193.
- Chitnis, N., J. M. Cushing, and J. M. Hyman (2006). “Bifurcation Analysis of a Mathematical Model for Malaria Transmission”. In: *SIAM Journal on Applied Mathematics* 67.1. DOI: 10.1137/050638941.
- Chitnis, N., J. M. Hyman, and C. A. Manore (2013). “Modelling vertical transmission in vector-borne diseases with applications to Rift Valley fever”. In: *Journal of Biological Dynamics* 7.1. DOI: 10.1080/17513758.2012.733427.

- Chowell, G., R. Luo, K. Sun, K. Roosa, A. Tariq, and C. Viboud (2020). “Real-time forecasting of epidemic trajectories using computational dynamic ensembles”. In: *Epidemics* 30. DOI: 10.1016/j.epidem.2019.100379.
- Cianci, D., N. Hartemink, and A. Ibáñez-Justicia (2015). “Modelling the potential spatial distribution of mosquito species using three different techniques”. In: *International Journal of Health Geographics* 14.1. DOI: 10.1186/s12942-015-0001-0.
- Clapham, H. E., V. Tricou, N. Van Vinh Chau, C. P. Simmons, and N. M. Ferguson (2014). “Within-host viral dynamics of dengue serotype 1 infection”. In: *Journal of The Royal Society Interface* 11.96. DOI: 10.1098/rsif.2014.0094.
- Clark, M. H. A., G. M. Warimwe, A. Di Nardo, N. A. Lyons, and S. Gubbins (2018). “Systematic literature review of Rift Valley fever virus seroprevalence in livestock, wildlife and humans in Africa from 1968 to 2016”. In: *PLOS Neglected Tropical Diseases* 12.7. DOI: 10.1371/journal.pntd.0006627.
- Clements, A. C., D. U. Pfeiffer, V. Martin, C. Pittiglio, N. Best, and Y. Thiongane (2007). “Spatial Risk Assessment of Rift Valley Fever in Senegal”. In: *Vector-Borne and Zoonotic Diseases* 7.2. DOI: 10.1089/vbz.2006.0600.
- Coffey, L. L., N. Forrester, K. Tsetsarkin, N. Vasilakis, and S. C. Weaver (2013). “Factors shaping the adaptive landscape for arboviruses: implications for the emergence of disease”. In: *Future Microbiology* 8.2. DOI: 10.2217/fmb.12.139.
- Colizza, V., A. Barrat, M. Barthélemy, and A. Vespignani (2007). “Predictability and epidemic pathways in global outbreaks of infectious diseases: the SARS case study”. In: *BMC Med* 5.1. DOI: 10.1186/1741-7015-5-34.
- Courtejoie, N., G. Zanella, and B. Durand (2018). “Bluetongue transmission and control in Europe: A systematic review of compartmental mathematical models”. In: *Preventive Veterinary Medicine* 156. DOI: 10.1016/j.prevetmed.2018.05.012.
- Craighead, L., J. M. Cardwell, B. C. Prakashbabu, E. Ba, I. Musallam, R. B. Alambédji, J. Ayih-Akakpo, J. Guitian, and B. Häsler (2021). ““Everything in this world has been given to us from cows”, a qualitative study on farmers’ perceptions of keeping dairy cattle in Senegal and implications for disease control and healthcare delivery”. In: *PLoS ONE* 16.2. DOI: 10.1371/journal.pone.0247644.
- Danzetta, M. L., R. Bruno, F. Sauro, L. Savini, and P. Calistri (2016). “Rift Valley fever transmission dynamics described by compartmental models”. In: *Preventive Veterinary Medicine* 134. DOI: 10.1016/j.prevetmed.2016.09.007.
- Daubney, R. and J. R. Hudson (1931). “Enzootic hepatitis or rift valley fever. An undescribed virus disease of sheep cattle and man from east africa”. In: *The Journal of Pathology and Bacteriology* 34.4. DOI: 10.1002/path.1700340418.
- Davies, F. G. (2010). “The Historical and Recent Impact of Rift Valley Fever in Africa”. In: *The American Journal of Tropical Medicine and Hygiene* 83.2\_Suppl. DOI: 10.4269/ajtmh.2010.83s2a02.

- Davies, F. G. and V. Martin (2003). “Recognizing Rift Valley fever”. In: *FAO Animal Health Manual* 17.
- De Angelis, D., A. M. Presanis, P. J. Birrell, G. S. Tomba, and T. House (2015). “Four key challenges in infectious disease modelling using data from multiple sources”. In: *Epidemics* 10. DOI: 10.1016/j.epidem.2014.09.004.
- Dellicour, S., M. S. Gill, N. R. Faria, A. Rambaut, O. G. Pybus, M. A. Suchard, and P. Lemey (2021). “Relax, Keep Walking — A Practical Guide to Continuous Phylogeographic Inference with BEAST”. In: *Molecular Biology and Evolution*. DOI: 10.1093/molbev/msab031.
- Diallo, D., C. Talla, Y. Ba, I. Dia, A. A. Sall, and M. Diallo (2011). “Temporal distribution and spatial pattern of abundance of the Rift Valley fever and West Nile fever vectors in Barkedji, Senegal”. In: *Journal of Vector Ecology* 36.2. DOI: 10.1111/j.1948-7134.2011.00184.x.
- Diekmann, O, J. Heesterbeek, and J. Metz (1990). “On the definition and the computation of the basic reproduction ratio  $R_0$  in models for infectious diseases in heterogeneous populations”. In: *Journal of Mathematical Biology* 28.
- Diekmann, O., J. A. P. Heesterbeek, and M. G. Roberts (2010). “The construction of next-generation matrices for compartmental epidemic models”. In: *Journal of The Royal Society Interface* 7.47. DOI: 10.1098/rsif.2009.0386.
- Diop, A. T., O. Sy, A. Ickowicz, and I. Toure (2003). “Politique d’hydraulique et gestion de l’espace et des ressources dans la région sylvopastorale du Sénégal, Ferlo”. In:
- Doms, C., S. C. Kramer, and J. Shaman (2018). “Assessing the Use of Influenza Forecasts and Epidemiological Modeling in Public Health Decision Making in the United States”. In: *Sci Rep* 8.1. DOI: 10.1038/s41598-018-30378-w.
- Driessche, P. van den and J. Watmough (2002). “Reproduction numbers and sub-threshold endemic equilibria for compartmental models of disease transmission”. In: *Mathematical Biosciences* 180.1-2. DOI: 10.1016/S0025-5564(02)00108-6.
- Duffy, S. (2018). “Why are RNA virus mutation rates so damn high?” In: *PLoS Biol* 16.8. DOI: 10.1371/journal.pbio.3000003.
- Durand, B., S. Lecollinet, C. Beck, B. Martínez-López, T. Balenghien, and V. Chevalier (2013). “Identification of Hotspots in the European Union for the Introduction of Four Zoonotic Arboviroses by Live Animal Trade”. In: *PLoS ONE* 8.7. DOI: 10.1371/journal.pone.0070000.
- Durand, B. et al. (2020). “Rift Valley fever in northern Senegal: A modelling approach to analyse the processes underlying virus circulation recurrence”. In: *PLOS Neglected Tropical Diseases* 14.6. DOI: 10.1371/journal.pntd.0008009.
- Eckhoff, P. A., C. A. Bever, J. Gerardin, E. A. Wenger, and D. L. Smith (2015). “From puddles to planet: modeling approaches to vector-borne diseases at varying resolution and scale”. In: *Current Opinion in Insect Science* 10. DOI: 10.1016/j.cois.2015.05.002.

- EFSA Panel on Animal Health and Welfare (EFSA AHAW Panel) et al. (2020). “Rift Valley Fever – assessment of effectiveness of surveillance and control measures in the EU”. In: *EFSA* 18.11. DOI: 10.2903/j.efsa.2020.6292.
- El Bcheraoui, C. et al. (2020). “Burden of disease in francophone Africa, 1990–2017: a systematic analysis for the Global Burden of Disease Study 2017”. In: *The Lancet Global Health* 8.3. DOI: 10.1016/S2214-109X(20)30024-3.
- Endo, A., E. van Leeuwen, and M. Baguelin (2019). “Introduction to particle Markov-chain Monte Carlo for disease dynamics modellers”. In: *Epidemics* 29. DOI: 10.1016/j.epidem.2019.100363.
- Eriksson, A., F. Elías-Wolff, B. Mehlig, and A. Manica (2014). “The emergence of the rescue effect from explicit within- and between-patch dynamics in a metapopulation”. In: *Proc. R. Soc. B.* 281.1780. DOI: 10.1098/rspb.2013.3127.
- Esser, H. J., R. Mögling, N. B. Cleton, H. van der Jeugd, H. Sprong, A. Stroo, M. P. G. Koopmans, W. F. de Boer, and C. B.E. M. Reusken (2019). “Risk factors associated with sustained circulation of six zoonotic arboviruses: a systematic review for selection of surveillance sites in non-endemic areas”. In: *Parasites Vectors* 12.1. DOI: 10.1186/s13071-019-3515-7.
- Evans, A. et al. (2008). “Prevalence of antibodies against Rift Valley fever virus in Kenyan wildlife”. In: *Epidemiology and Infection* 136.9. DOI: 10.1017/S0950268807009806.
- Ezanno, P., M. Andraud, G. Beaunée, T. Hoch, S. Krebs, A. Rault, S. Touzeau, E. Vergu, and S. Widgren (2020). “How mechanistic modelling supports decision making for the control of enzootic infectious diseases”. In: *Epidemics* 32. DOI: 10.1016/j.epidem.2020.100398.
- FAO (2018). *Pastoralism in Africa’s drylands*. Tech. rep. 52 pp. Licence: CC BY-NC-SA 3.0 IGO.
- Fawzy, M. and Y. A. Helmy (2019). “The One Health Approach is Necessary for the Control of Rift Valley Fever Infections in Egypt: A Comprehensive Review”. In: *Viruses* 11.2. DOI: 10.3390/v11020139.
- Finger, F., T. Genolet, L. Mari, G. C. de Magny, N. M. Manga, A. Rinaldo, and E. Bertuzzo (2016). “Mobile phone data highlights the role of mass gatherings in the spreading of cholera outbreaks”. In: *Proceedings of the National Academy of Sciences* 113.23. DOI: 10.1073/pnas.1522305113.
- Finkenstadt, B. F. (2002). “A stochastic model for extinction and recurrence of epidemics: estimation and inference for measles outbreaks”. In: *Biostatistics* 3.4. DOI: 10.1093/biostatistics/3.4.493.
- Fischer, E. A., G.-J. Boender, G. Nodelijk, A. A. de Koeijer, and H. J. van Roermund (2013). “The transmission potential of Rift Valley fever virus among livestock in the Netherlands: a modelling study”. In: *Veterinary Research* 44.1. DOI: 10.1186/1297-9716-44-58.
- Fontaine, A., S. Lequime, I. Moltini-Conclois, D. Jiolle, I. Leparç-Goffart, R. C. Reiner, and L. Lambrechts (2018). “Epidemiological significance of dengue virus genetic variation in

- mosquito infection dynamics”. In: *PLOS Pathogens* 14.7. DOI: 10.1371/journal.ppat.1007187.
- Fontenille, D., C. Lagneau, S. Lecollinet, R. Lefait Robin, M. Setbon, B. Tirel, and A. Yébakima (2009). *La lutte antivectorielle en France*. IRD Editions. DOI: 10.4000/books.irdeditions.1214.
- Fouque, F. and J. C. Reeder (2019). “Impact of past and on-going changes on climate and weather on vector-borne diseases transmission: a look at the evidence”. In: *Infectious Diseases of Poverty* 8.1. DOI: 10.1186/s40249-019-0565-1.
- Fritzsche McKay, A. and B. J. Hoyer (2016). “Are Migratory Animals Superspreaders of Infection?: An Introduction to the Symposium”. In: *Integr. Comp. Biol.* 56.2. DOI: 10.1093/icb/icw054.
- Gachohi, J. M., M. K. Njenga, P. Kitala, and B. Bett (2016). “Modelling Vaccination Strategies against Rift Valley Fever in Livestock in Kenya”. In: *PLoS Negl Trop Dis* 10.12. DOI: 10.1371/journal.pntd.0005049.
- Gaff, H., C. Burgess, J. Jackson, T. Niu, Y. Papelis, and D. Hartley (2011). “Mathematical Model to Assess the Relative Effectiveness of Rift Valley Fever Countermeasures:” in: *International Journal of Artificial Life Research* 2.2. DOI: 10.4018/jalr.2011040101.
- Gaff, H. D., D. M. Hartley, and N. P. Leahy (2007). “AN EPIDEMIOLOGICAL MODEL OF RIFT VALLEY FEVER”. In: *Electronic Journal of Differential Equations*.
- Gao, D., C. Cosner, R. S. Cantrell, J. C. Beier, and S. Ruan (2013). “Modeling the Spatial Spread of Rift Valley Fever in Egypt”. In: *Bull Math Biol* 75.3. DOI: 10.1007/s11538-013-9818-5.
- Garabed, R. B., A. Jolles, W. Garira, C. Lanzas, J. Gutierrez, and G. Rempala (2019). “Multi-scale dynamics of infectious diseases”. In: *Interface Focus*. 10.1. DOI: 10.1098/rsfs.2019.0118.
- Garira, W. (2017). “A complete categorization of multiscale models of infectious disease systems”. In: *Journal of Biological Dynamics* 11.1. DOI: 10.1080/17513758.2017.1367849.
- Garira, W. and F. Chirove (2019). “A general method for multiscale modelling of vector-borne disease systems”. In: *Interface Focus*. 10.1. DOI: 10.1098/rsfs.2019.0047.
- Gates, M. C. and M. E. Woolhouse (2015). “Controlling infectious disease through the targeted manipulation of contact network structure”. In: *Epidemics* 12. DOI: 10.1016/j.epidem.2015.02.008.
- Gerdes, G. H. (2004). “Rift Valley fever”. In: *Rev. sci. tech. Off. int. Epiz.* 23.2.
- Giannini, A. (2003). “Oceanic Forcing of Sahel Rainfall on Interannual to Interdecadal Time Scales”. In: *Science* 302.5647. DOI: 10.1126/science.1089357.
- Gil, H., W. A. Qualls, C. Cosner, D. L. DeAngelis, A. Hassan, A. M. Gad, S. Ruan, S. R. Cantrell, and J. C. Beier (2016). “A model for the coupling of the Greater Bairam and local environmental factors in promoting Rift-Valley Fever epizootics in Egypt”. In: *Public Health* 130. DOI: 10.1016/j.puhe.2015.07.034.

- Gilbert, M., G. Nicolas, G. Cinardi, T. P. Van Boeckel, S. O. Vanwambeke, G. R. W. Wint, and T. P. Robinson (2018). “Global distribution data for cattle, buffaloes, horses, sheep, goats, pigs, chickens and ducks in 2010”. In: *Scientific Data* 5. DOI: 10.1038/sdata.2018.227.
- Gog, J. R., L. Pellis, J. L. Wood, A. R. McLean, N. Arinaminpathy, and J. O. Lloyd-Smith (2015). “Seven challenges in modeling pathogen dynamics within-host and across scales”. In: *Epidemics* 10. DOI: 10.1016/j.epidem.2014.09.009.
- Gomez, O. S. (1979). “Contribution à l’étude la transhumance au Sénégal : ses conséquences sur l’exploitation du cheptel et sur le développement économique et social des populations pastorales”. PhD thesis. Ecole inter-états des sciences et medecine veterinaires de Dakar.
- Gommet, C. et al. (2011). “Tissue Tropism and Target Cells of NSs-Deleted Rift Valley Fever Virus in Live Immunodeficient Mice”. In: *PLoS Neglected Tropical Diseases* 5.12. DOI: 10.1371/journal.pntd.0001421.
- Gorsich, E. E., B. R. Beechler, P. M. van Bodegom, D. Govender, M. M. Guarido, M. Venter, and M. Schrama (2019). “A comparative assessment of adult mosquito trapping methods to estimate spatial patterns of abundance and community composition in southern Africa”. In: *Parasites Vectors* 12.1. DOI: 10.1186/s13071-019-3733-z.
- Grace, D., M. Songe, and T. Knight-Jones (2015). “IMPACT OF NEGLECTED DISEASES ON ANIMAL PRODUCTIVITY AND PUBLIC HEALTH IN AFRICA”. In: *Africa - OIE Regional Commission*.
- Grenfell, B. and J. Harwood (1997). “(Meta)population dynamics of infectious diseases”. In: *TREE* 12.
- Grossi-Soyster, E. N., J. Lee, C. H. King, and A. D. LaBeaud (2019). “The influence of raw milk exposures on Rift Valley fever virus transmission”. In: *PLOS Neglected Tropical Diseases* 13.3. DOI: 10.1371/journal.pntd.0007258.
- Gubler, D. J. (2006). “Human Arbovirus Infections Worldwide”. In: *Annals of the New York Academy of Sciences* 951.1. DOI: 10.1111/j.1749-6632.2001.tb02681.x.
- Guilloteau, C., M. Gosset, C. Vignolles, M. Alcoba, Y. M. Tourre, and J.-P. Lacaux (2014). “Impacts of Satellite-Based Rainfall Products on Predicting Spatial Patterns of Rift Valley Fever Vectors\*”. In: *Journal of Hydrometeorology* 15.4. DOI: 10.1175/JHM-D-13-0134.1.
- Hammami, P., R. Lancelot, and M. Lesnoff (2016). “Modelling the dynamics of post-vaccination immunity rate in a population of Sahelian sheep after a vaccination campaign against Peste des Petits Ruminants virus”. In: *PLoS ONE* 11.9. DOI: 10.1371/journal.pone.0161769.
- Hanafi, H. et al. (2010). “Rift Valley Fever Virus Epidemic in Kenya, 2006/2007: The Entomologic Investigations”. In: *The American Journal of Tropical Medicine and Hygiene* 83.2\_Suppl. DOI: 10.4269/ajtmh.2010.09-0319.
- Handel, A., N. L. La Gruta, and P. G. Thomas (2020). “Simulation modelling for immunologists”. In: *Nature Reviews Immunology* 20.3. DOI: 10.1038/s41577-019-0235-3.
- Hanski, I. (1998). “Metapopulation dynamics”. In: *Nature* 396.



- Hartig, F., J. M. Calabrese, B. Reineking, T. Wiegand, and A. Huth (2011). “Statistical inference for stochastic simulation models - theory and application: Inference for stochastic simulation models”. In: *Ecology Letters* 14.8. DOI: 10.1111/j.1461-0248.2011.01640.x.
- Hartman, A. (2017). “Rift Valley Fever”. In: *Clinics in Laboratory Medicine* 37.2. DOI: 10.1016/j.cll.2017.01.004.
- Haydon, D., S. Cleaveland, L. H. Taylor, and M. K. Laurenson (2002). “Identifying Reservoirs of Infection: A Conceptual and Practical Challenge”. In: *Emerg. Infect. Dis.* 8.12. DOI: 10.3201/eid0812.010317.
- Hayes, B. H., M. Andraud, L. G. Salazar, N. Rose, and T. Vergne (2021). “Mechanistic modelling of African swine fever: A systematic review”. In: *Preventive Veterinary Medicine* 191. DOI: 10.1016/j.prevetmed.2021.105358.
- Hidano, A., T. E. Carpenter, M. A. Stevenson, and M. C. Gates (2016). “Evaluating the efficacy of regionalisation in limiting high-risk livestock trade movements”. In: *Preventive Veterinary Medicine* 133. DOI: 10.1016/j.prevetmed.2016.09.015.
- Hoch, T., S. Touzeau, A.-F. Viet, and P. Ezanno (2018). “Between-group pathogen transmission: From processes to modeling”. In: *Ecological Modelling* 383. DOI: 10.1016/j.ecolmodel.2018.05.016.
- Hollings, T., M. Burgman, M. van Andel, M. Gilbert, T. Robinson, and A. Robinson (2018). “How do you find the green sheep? A critical review of the use of remotely sensed imagery to detect and count animals”. In: *Methods in Ecology and Evolution* 9.4. DOI: 10.1111/2041-210X.12973.
- Hollingsworth, T. D., J. R. Pulliam, S. Funk, J. E. Truscott, V. Isham, and A. L. Lloyd (2015). “Seven challenges for modelling indirect transmission: Vector-borne diseases, macroparasites and neglected tropical diseases”. In: *Epidemics* 10. DOI: 10.1016/j.epidem.2014.08.007.
- Hopkins, S. R., A. E. Fleming-Davies, L. K. Belden, and J. M. Wojdak (2020). “Systematic review of modelling assumptions and empirical evidence: Does parasite transmission increase nonlinearly with host density?” In: *Methods in Ecology and Evolution*. DOI: 10.1111/2041-210X.13361.
- Huyvaert, K., R. Russell, K. Patyk, M. Craft, P. Cross, M. Garner, M. Martin, P. Nol, and D. Walsh (2018). “Challenges and Opportunities Developing Mathematical Models of Shared Pathogens of Domestic and Wild Animals”. In: *Veterinary Sciences* 5.4. DOI: 10.3390/vetsci5040092.
- Ikegami, T. (2012). “Molecular biology and genetic diversity of Rift Valley fever virus”. In: *Antiviral Research* 95.3. DOI: 10.1016/j.antiviral.2012.06.001.
- Ikegami, T. et al. (2017). “Distinct virulence of Rift Valley fever phlebovirus strains from different genetic lineages in a mouse model”. In: *PLoS ONE* 12.12. DOI: 10.1371/journal.pone.0189250.
- ILRI/FAO (2008). *Decision-support tool for prevention and control of Rift Valley fever epizootics in the Greater Horn of Africa*. ILRI Guide. Version 1, p.28.

- International Federation for Animal Health (IFAH) (2014). *The growing threat of vector-borne disease in humans and animals*.
- Jahel, C. et al. (2020). "Mapping livestock movements in Sahelian Africa". In: *Sci Rep* 10.1. DOI: 10.1038/s41598-020-65132-8.
- Jesse, M., P. Ezanno, S. Davis, and J. Heesterbeek (2008). "A fully coupled, mechanistic model for infectious disease dynamics in a metapopulation: Movement and epidemic duration". In: *Journal of Theoretical Biology* 254.2. DOI: 10.1016/j.jtbi.2008.05.038.
- Jesse, M. and H. Heesterbeek (2011). "Divide and conquer? Persistence of infectious agents in spatial metapopulations of hosts". In: *Journal of Theoretical Biology* 275.1. DOI: 10.1016/j.jtbi.2011.01.032.
- Johansson, M. A. et al. (2019). "An open challenge to advance probabilistic forecasting for dengue epidemics". In: *Proc Natl Acad Sci USA* 116.48. DOI: 10.1073/pnas.1909865116.
- Jouan, A., B. Le Guenno, J. Digoutte, B. Philippe, O. Riou, and F. Adam (1988). "An RVF epidemic in Southern Mauritania". In: *Annales de l'Institut Pasteur / Virologie* 139. DOI: 10.1016/S0769-2617(88)80046-7.
- Jourdain, F. et al. (2020). "From importation to autochthonous transmission: Drivers of chikungunya and dengue emergence in a temperate area". In: *PLoS Negl Trop Dis* 14.5. DOI: 10.1371/journal.pntd.0008320.
- Jupp, P. G., A. Kemp, A. Grobbelaar, P. Leman, F. J. Burt, A. M. Alahmed, D. A. Mujalli, M. A. Khamees, and R. Swanepoel (2002). "The 2000 epidemic of Rift Valley fever in Saudi Arabia: mosquito vector studies". In: *Medical and Veterinary Entomology* 16.3. DOI: 10.1046/j.1365-2915.2002.00371.x.
- Keeling, M. J., L. Danon, M. C. Vernon, and T. A. House (2010). "Individual identity and movement networks for disease metapopulations". In: *Proceedings of the National Academy of Sciences* 107.19. DOI: 10.1073/pnas.1000416107.
- Keeling, M. J. and P. Rohani (2008). *Modeling infectious diseases in humans and animals*. Princeton University Press.
- Kitching, R., M. Thrusfield, and N. Taylor (2006). "Use and abuse of mathematical models : an illustration from the 2001 foot and mouth disease epidemic in the United Kingdom". In: *Rev. Sci. Tech. OIE* 25.1. DOI: 10.20506/rst.25.1.1665.
- Kortekaas, J., J. Zingeser, P. de Leeuw, S. de La Rocque, H. Unger, and R. Moormann (2011). "Rift Valley fever vaccine development, progress and constraints". In: *Emerg. Infect. Dis.* [serial on the Internet].
- Ksiazek, T. et al. (1989). "Rift Valley fever among domestic animals in the recent West African outbreak". In: *Res Virol.* 140.1. DOI: 10.1016/s0923-2516(89)80086-x.
- La Rocque, S. de and P. Formenty (2014). "Applying the One Health principles: a trans-sectoral coordination framework for preventing and responding to Rift Valley fever outbreaks". In: *Rev. Sci. Tech. OIE* 33.2. DOI: 10.20506/rst.33.2.2288.

- LaBeaud, A. D., J. W. Kazura, and C. H. King (2010). “Advances in Rift Valley fever research: insights for disease prevention:” in: *Current Opinion in Infectious Diseases* 23.5. DOI: 10.1097/QCO.0b013e32833c3da6.
- Lacaux, J., Y. Tourre, C. Vignolles, J. Ndione, and M. Lafaye (2007). “Classification of ponds from high-spatial resolution remote sensing: application to Rift Valley fever epidemics in Senegal”. In: *Remote Sensing of Environment* 106.1. DOI: 10.1016/j.rse.2006.07.012.
- Lambin, E. F., A. Tran, S. O. Vanwambeke, C. Linard, and V. Soti (2010). “Pathogenic landscapes: Interactions between land, people, disease vectors, and their animal hosts”. In: *International Journal of Health Geographics* 9.1. DOI: 10.1186/1476-072X-9-54.
- Lancelot, R. et al. (2019). “Rift Valley Fever: One Health at Play?” In: *Transboundary Animal Diseases in Sahelian Africa and Connected Regions*. Springer International Publishing. DOI: 10.1007/978-3-030-25385-1\_8.
- Larsen, P. O. and M. von Ins (2010). “The rate of growth in scientific publication and the decline in coverage provided by Science Citation Index”. In: *Scientometrics* 84.3. DOI: 10.1007/s11192-010-0202-z.
- Laughlin, L. W., J. M. Meegan, L. J. Strausbaugh, D. M. Morens, and R. H. Watten (1979). “Epidemic Rift Valley fever in Egypt: observations of the spectrum of human illness”. In: *Transactions of the Royal Society of Tropical Medicine and Hygiene* 73.6. DOI: 10.1016/0035-9203(79)90006-3.
- Layan, M., S. Dellicour, G. Baele, S. Cauchemez, and H. Bourhy (2021). “Mathematical modelling and phylodynamics for the study of dog rabies dynamics and control: A scoping review”. In: *PLoS Negl Trop Dis* 15.5. DOI: 10.1371/journal.pntd.0009449.
- Leedale, J., A. E. Jones, C. Caminade, and A. P. Morse (2016). “A dynamic, climate-driven model of Rift Valley fever”. In: *Geospat Health* 11.1 Suppl. DOI: 10.4081/gh.2016.394.
- Lequime, S., R. E. Paul, and L. Lambrechts (2016). “Determinants of Arbovirus Vertical Transmission in Mosquitoes”. In: *PLOS Pathogens* 12.5. DOI: 10.1371/journal.ppat.1005548.
- Lequime, S., J.-S. Dehecq, S. Matheus, F. de Laval, L. Almeras, S. Briolant, and A. Fontaine (2020). “Modeling intra-mosquito dynamics of Zika virus and its dose-dependence confirms the low epidemic potential of *Aedes albopictus*”. In: *PLOS Pathogens* 16.12. DOI: 10.1371/journal.ppat.1009068.
- Lesnoff, M (2008). *DynMod: a tool for demographic projections of tropical livestock populations under Microsoft Excel, User’s manual - Version 1*. CIRAD (French Agricultural research Centre for International Development), ILRI (International Livestock Research Institute).
- Lesnoff, M. (2013). “Méthodes d’enquête pour l’estimation des taux démographiques des cheptels de ruminants domestiques tropicaux. Synthèse, limites et perspectives”. In: *Rev. Elev. Med. Vet. Pays Trop.* 66.2. DOI: 10.19182/remvt.10142.
- Lessler, J., W. Edmunds, M. Halloran, T. Hollingsworth, and A. Lloyd (2015). “Seven challenges for model-driven data collection in experimental and observational studies”. In: *Epidemics* 10. DOI: 10.1016/j.epidem.2014.12.002.

- Lessler, J., A. S. Azman, M. K. Grabowski, H. Salje, and I. Rodriguez-Barraquer (2016). “Trends in the Mechanistic and Dynamic Modeling of Infectious Diseases”. In: *Curr Epidemiol Rep* 3.3. DOI: 10.1007/s40471-016-0078-4.
- Leta, S., T. J. Beyene, E. M. De Clercq, K. Amenu, M. U. Kraemer, and C. W. Revie (2018). “Global risk mapping for major diseases transmitted by *Aedes aegypti* and *Aedes albopictus*”. In: *International Journal of Infectious Diseases* 67. DOI: 10.1016/j.ijid.2017.11.026.
- Liberati, A. et al. (2009). “The PRISMA statement for reporting systematic reviews and meta-analyses of studies that evaluate healthcare interventions: explanation and elaboration”. In: *BMJ* 339.jul21 1. DOI: 10.1136/bmj.b2700.
- Lindström, T., M. Tildesley, and C. Webb (2015). “A Bayesian Ensemble Approach for Epidemiological Projections”. In: *PLoS Comput Biol* 11.4. DOI: 10.1371/journal.pcbi.1004187.
- Linthicum, K. J., F. G. Davies, A. Kairo, and C. L. Bailey (1985). “Rift Valley fever virus (family Bunyaviridae, genus Phlebovirus). Isolations from Diptera collected during an interepizootic period in Kenya”. In: *Journal of Hygiene* 95.01. DOI: 10.1017/S0022172400062434.
- Linthicum, K. J., S. C. Britch, and A. Anyamba (2016). “Rift Valley fever: an emerging mosquito-borne disease”. In: *Annual Review of Entomology* 61.1. DOI: 10.1146/annurev-ento-010715-023819.
- Lo Iacono, G., A. A. Cunningham, B. Bett, D. Grace, D. W. Redding, and J. L. N. Wood (2018). “Environmental limits of Rift Valley fever revealed using ecoepidemiological mechanistic models”. In: *Proc. Natl. Acad. Sci. U.S.A.* 115.31. DOI: 10.1073/pnas.1803264115.
- Lofgren, E. T. et al. (2014). “Opinion: Mathematical models: A key tool for outbreak response”. In: *Proc Natl Acad Sci USA* 111.51. DOI: 10.1073/pnas.1421551111.
- Lumley, S., D. L. Horton, L. L. M. Hernandez-Triana, N. Johnson, A. R. Fooks, and R. Hewson (2017). “Rift Valley fever virus: strategies for maintenance, survival and vertical transmission in mosquitoes”. In: *Journal of General Virology* 98.5. DOI: 10.1099/jgv.0.000765.
- Lumley, S., L. M. Hernández-Triana, D. L. Horton, M. D. M. Fernández de Marco, J. M. Medlock, R. Hewson, A. R. Fooks, and N. Johnson (2018). “Competence of mosquitoes native to the United Kingdom to support replication and transmission of Rift Valley fever virus”. In: *Parasites Vectors* 11.1. DOI: 10.1186/s13071-018-2884-7.
- Lynch, J. (2006). “It’s not easy being interdisciplinary”. In: *International Journal of Epidemiology* 35.5. DOI: 10.1093/ije/dy1200.
- Macdonald, G. (1956a). “Epidemiological basis of malaria control”. In: *Bull. World Health Org.* 15.
- (1956b). “Theory of the eradication of malaria”. In: *Bull. World Health Org.* 15.
- Macdonald, G. and G. W. Gockel (1964). “The malaria parasite rate and interruption of transmission”. In: *Bull. World Health Org.* 31.
- Mackenzie, J. S. and M. Jeggo (2019). “The One Health Approach—Why Is It So Important?” In: *TropicalMed* 4.2. DOI: 10.3390/tropicalmed4020088.

- Madani, T. A. et al. (2003). "Rift Valley Fever Epidemic in Saudi Arabia: Epidemiological, Clinical, and Laboratory Characteristics". In: *Clinical Infectious Diseases* 37.8. DOI: 10.1086/378747.
- Manore, C. A. and B. R. Beechler (2015). "Inter-Epidemic and Between-Season Persistence of Rift Valley Fever: Vertical Transmission or Cryptic Cycling?" In: *Transbound Emerg Dis* 62.1. DOI: 10.1111/tbed.12082.
- Manore, C. A., K. S. Hickmann, J. M. Hyman, I. M. Foppa, J. K. Davis, D. M. Wesson, and C. N. Mores (2015). "A network-patch methodology for adapting agent-based models for directly transmitted disease to mosquito-borne disease". In: *Journal of Biological Dynamics* 9.1. DOI: 10.1080/17513758.2015.1005698.
- Marino, S., I. B. Hogue, C. J. Ray, and D. E. Kirschner (2008). "A methodology for performing global uncertainty and sensitivity analysis in systems biology". In: *Journal of Theoretical Biology* 254.1. DOI: 10.1016/j.jtbi.2008.04.011.
- Martens, W., T. Jetten, J. Rotmans, and L. Niessen (1995). "Climate change and vector-borne diseases. A global modelling perspective". In: *Fuel and Energy Abstracts* 36.6. DOI: 10.1016/0140-6701(95)98058-Y.
- Martin, L. B. et al. (2019). "Extreme Competence: Keystone Hosts of Infections". In: *Trends in Ecology & Evolution* 34.4. DOI: 10.1016/j.tree.2018.12.009.
- Massó Sagüés, E., E. Fernández-Carrión, and J. M. Sánchez-Vizcaíno (2019). "Risk of Introduction of Infectious Animal Diseases for Europe Based on the Health Situation of North Africa and the Arabian Peninsula". In: *Frontiers in Veterinary Science* 6. DOI: 10.3389/fvets.2019.00293.
- McCallum, H., N. Barlow, and J. Hone (2001). "How should pathogen transmission be modelled?" In:
- McGough, S. F., J. S. Brownstein, J. B. Hawkins, and M. Santillana (2017). "Forecasting Zika Incidence in the 2016 Latin America Outbreak Combining Traditional Disease Surveillance with Search, Social Media, and News Report Data". In: *PLoS Negl Trop Dis* 11.1. DOI: 10.1371/journal.pntd.0005295.
- McMahon, B., C. Manore, J. Hyman, M. LaBute, and J. Fair (2014). "Coupling Vector-host Dynamics with Weather Geography and Mitigation Measures to Model Rift Valley Fever in Africa". In: *Mathematical Modelling of Natural Phenomena* 9.2. DOI: 10.1051/mmnp/20149211.
- Meegan, J. M. (1979). "The Rift Valley fever epizootic in Egypt 1977–1978 1. Description of the epizootic and virological studies". In: *Transactions of the Royal Society of Tropical Medicine and Hygiene* 73.6. DOI: 10.1016/0035-9203(79)90004-X.
- Metcalfe, C., W. Edmunds, and J. Lessler (2015). "Six challenges in modelling for public health policy". In: *Epidemics* 10. DOI: 10.1016/j.epidem.2014.08.008.
- Metelmann, S., C. Caminade, A. E. Jones, J. M. Medlock, M. Baylis, and A. P. Morse (2019). "The UK's suitability for *Aedes albopictus* in current and future climates". In: *Journal of The Royal Society Interface* 16.152. DOI: 10.1098/rsif.2018.0761.

- Meyer, A., C. Faverjon, M. Hostens, A. Stegeman, and A. Cameron (2021). “Systematic review of the status of veterinary epidemiological research in two species regarding the FAIR guiding principles”. In: *BMC Vet Res* 17.1. DOI: 10.1186/s12917-021-02971-1.
- Miller, E. and A. Huppert (2013). “The Effects of Host Diversity on Vector-Borne Disease: The Conditions under Which Diversity Will Amplify or Dilute the Disease Risk”. In: *PLoS ONE* 8.11. DOI: 10.1371/journal.pone.0080279.
- Miller, P. B., E. B. O’Dea, P. Rohani, and J. M. Drake (2017). “Forecasting infectious disease emergence subject to seasonal forcing”. In: *Theor Biol Med Model* 14.1. DOI: 10.1186/s12976-017-0063-8.
- Mint Mohamed Lemine, A. et al. (2017). “Mosquitoes (Diptera: Culicidae) in Mauritania: a review of their biodiversity, distribution and medical importance”. In: *Parasites & Vectors* 10.1. DOI: 10.1186/s13071-017-1978-y.
- Miron, R., G. Giordano, A. Kealey, and R. Smith (2016). “Multiseason transmission for Rift Valley fever in North America”. In: *MATHEMATICAL POPULATION STUDIES*.
- Mondet, B., A. Diaïté, J.-A. Ndione, A. G. Fall, V. Chevalier, R. Lancelot, M. Ndiaye, and N. Ponçon (2005). “Rainfall patterns and population dynamics of *Aedes (Aedimorphus) vexans arabiensis*, Patton 1905 (Diptera: Culicidae), a potential vector of Rift Valley fever virus in Senegal”. In: *Journal of Vector Ecology* 30.1.
- Mordecai, E. A. et al. (2019). “Thermal biology of mosquito-borne disease”. In: *Ecology Letters*. DOI: 10.1111/ele.13335.
- Morel-Journel, T., S. Assié, E. Vergu, J.-B. Mercier, F. Bonnet-Beaugrand, and P. Ezanno (2021). “Minimizing the number of origins in batches of weaned calves to reduce their risks of developing bovine respiratory diseases”. In: *Vet Res* 52.1. DOI: 10.1186/s13567-020-00872-z.
- Morvan, J., J.-F. Saluzzo, D. Fontenille, P. Rollin, and P. Coulanges (1991). “Rift valley fever on the east coast of Madagascar”. In: *Research in Virology* 142.6. DOI: 10.1016/0923-2516(91)90070-J.
- Moulay, D. and Y. Pigné (2013). “A metapopulation model for chikungunya including populations mobility on a large-scale network”. In: *Journal of Theoretical Biology* 318. DOI: 10.1016/j.jtbi.2012.11.008.
- Moutailler, S., G. Krida, F. Schaffner, M. Vazeille, and A.-B. Failloux (2008). “Potential Vectors of Rift Valley Fever Virus in the Mediterranean Region”. In: *Vector-Borne and Zoonotic Diseases* 8.6. DOI: 10.1089/vbz.2008.0009.
- Mpeshe, S. C., H. Haario, and J. M. Tchuente (2011). “A Mathematical Model of Rift Valley Fever with Human Host”. In: *Acta Biotheoretica* 59.3-4. DOI: 10.1007/s10441-011-9132-2.
- Mpeshe, S. C., L. S. Luboobi, and Y. Nkansah-Gyekye (2014). *Modeling the Impact of Climate Change on the Dynamics of Rift Valley Fever*. Research article. DOI: 10.1155/2014/627586.

- Muturi, M. et al. (2021). “Serological evidence of single and mixed infections of Rift Valley fever virus, *Brucella* spp. and *Coxiella burnetii* in dromedary camels in Kenya”. In: *PLoS Negl Trop Dis* 15.3. DOI: 10.1371/journal.pntd.0009275.
- Métras, R., L. M. Collins, R. G. White, S. Alonso, V. Chevalier, C. Thurania-McKeever, and D. U. Pfeiffer (2011). “Rift Valley Fever Epidemiology, Surveillance, and Control: What Have Models Contributed?” In: *Vector-Borne and Zoonotic Diseases* 11.6. DOI: 10.1089/vbz.2010.0200.
- Métras, R. et al. (2017). “Drivers for Rift Valley fever emergence in Mayotte: A Bayesian modelling approach”. In: *PLOS Neglected Tropical Diseases* 11.7. DOI: 10.1371/journal.pntd.0005767.
- Métras, R. et al. (2020). “Estimation of Rift Valley fever virus spillover to humans during the Mayotte 2018–2019 epidemic”. In: *Proceedings of the National Academy of Sciences* 117.39. DOI: 10.1073/pnas.2004468117.
- Napp, S. et al. (2018). “Understanding the legal trade of cattle and camels and the derived risk of Rift Valley Fever introduction into and transmission within Egypt”. In: *PLoS Negl Trop Dis* 12.1. DOI: 10.1371/journal.pntd.0006143.
- Ndiaye, E. H. et al. (2016). “Vector competence of *Aedes vexans* (Meigen), *Culex poicilipes* (Theobald) and *Cx. quinquefasciatus* Say from Senegal for West and East African lineages of Rift Valley fever virus”. In: *Parasites & Vectors* 9. DOI: 10.1186/s13071-016-1383-y.
- Ndiaye, P., D. Bicout, B. Mondet, and P. Sabatier (2006). “Rainfall triggered dynamics of *Aedes* mosquito aggressiveness”. In: *Journal of Theoretical Biology* 243.2. DOI: 10.1016/j.jtbi.2006.06.005.
- Ndione, J.-A., M. Diop, J.-P. Lacaux, and A. T. Gaye (2008). “Variabilité intra-saisonnière de la pluviométrie et émergence de la fièvre de la vallée du Rift dans la vallée du fleuve Sénégal : nouvelles considérations”. In: *Climatologie* 5. DOI: 10.4267/climatologie.794.
- Ndione, J.-A., J.-P. Lacaux, Y. Tourre, C. Vignolles, D. Fontanaz, and M. Lafaye (2009). “Mares temporaires et risques sanitaires au Ferlo: contribution de la télédétection pour l'étude de la fièvre de la vallée du Rift entre août 2003 et janvier 2004”. In: *Sécheresse* 20.1. DOI: 10.1684/sec.2009.0170.
- Nepomichene, T. N.J. J., F. N. Raharimalala, S. F. Andriamandimby, J.-P. Ravalohery, A.-B. Failloux, J.-M. Heraud, and S. Boyer (2018). “Vector competence of *Culex antennatus* and *Anopheles coustani* mosquitoes for Rift Valley fever virus in Madagascar: Vector competence for RVFV in Madagascar”. In: *Medical and Veterinary Entomology* 32.2. DOI: 10.1111/mve.12291.
- Nicholas, D. E., K. H. Jacobsen, and N. M. Waters (2014). “Risk factors associated with human Rift Valley fever infection: systematic review and meta-analysis”. In: *Trop Med Int Health* 19.12. DOI: 10.1111/tmi.12385.
- Nicolas, G., V. Chevalier, L. M. Tantely, D. Fontenille, and B. Durand (2014). “A Spatially Explicit Metapopulation Model and Cattle Trade Analysis Suggests Key Determinants for the

- Recurrent Circulation of Rift Valley Fever Virus in a Pilot Area of Madagascar Highlands”. In: *PLOS Neglected Tropical Diseases* 8.12. DOI: 10.1371/journal.pntd.0003346.
- Nielsen, S. S. et al. (2020). “Rift Valley Fever – epidemiological update and risk of introduction into Europe”. In: *EFSA Journal* 18.3. DOI: 10.2903/j.efsa.2020.6041.
- Niu, T., H. D. Gaff, Y. E. Papelis, and D. M. Hartley (2012). “An Epidemiological Model of Rift Valley Fever with Spatial Dynamics”. In: *Computational and Mathematical Methods in Medicine* 2012. DOI: 10.1155/2012/138757.
- Njenga, M. K. et al. (2015). “Randomized Controlled Field Trial to Assess the Immunogenicity and Safety of Rift Valley Fever Clone 13 Vaccine in Livestock”. In: *PLoS Negl Trop Dis* 9.3. DOI: 10.1371/journal.pntd.0003550.
- Odendaal, L., S. J. Clift, G. T. Fosgate, and A. S. Davis (2019). “Lesions and Cellular Tropism of Natural Rift Valley Fever Virus Infection in Adult Sheep”. In: *Vet Pathol* 56.1. DOI: 10.1177/0300985818806049.
- Olive, M.-M., S. M. Goodman, and J.-M. Reynes (2012). “THE ROLE OF WILD MAMMALS IN THE MAINTENANCE OF RIFT VALLEY FEVER VIRUS”. In: *Journal of Wildlife Diseases* 48.2. DOI: 10.7589/0090-3558-48.2.241.
- Olive, M.-M. et al. (2016). “Integrated Analysis of Environment, Cattle and Human Serological Data: Risks and Mechanisms of Transmission of Rift Valley Fever in Madagascar”. In: *PLoS Negl Trop Dis* 10.7. DOI: 10.1371/journal.pntd.0004827.
- Oumar, S. (2015). *Dynamique de la transhumance et perspectives d’un développement intégré dans les régions agro-sylvo-pastorales du Ferlo (Sénégal)*. DOI: 10.13140/rg.2.1.3683.3446.
- Oymans, J., P. J. Wichgers Schreur, L. van Keulen, J. Kant, and J. Kortekaas (2020). “Rift Valley fever virus targets the maternal-foetal interface in ovine and human placentas”. In: *PLoS Negl Trop Dis* 14.1. DOI: 10.1371/journal.pntd.0007898.
- O’Regan, S. M. and J. M. Drake (2013). “Theory of early warning signals of disease emergence and leading indicators of elimination”. In: *Theor Ecol* 6.3. DOI: 10.1007/s12080-013-0185-5.
- Parham, P. E. et al. (2015). “Climate, environmental and socio-economic change: weighing up the balance in vector-borne disease transmission”. In: *Philosophical Transactions of the Royal Society B: Biological Sciences* 370. DOI: 10.1098/rstb.2013.0551.
- Paul, P. N. T., A. Bah, P. I. Ndiaye, and J. A. Ndione (2014). “An Agent-Based Model for Studying the Impact of Herd Mobility on the Spread of Vector-Borne Diseases: The Case of Rift Valley Fever (Ferlo Senegal)”. In: *Open Journal of Modelling and Simulation* 02.03. DOI: 10.4236/ojmsi.2014.23012.
- Paul, P. N. T., P. I. Ndiaye, A. Bah, D. Dione, and J. A. Ndione (2020). “Coupling an Agent-Based Model with a Mathematical Model of Rift Valley Fever for Studying the Impact of Animal Migrations on the Rift Valley Fever Transmission”. In: *Computational Science*



- and Its Applications – ICCSA 2020*. Vol. 12250. Series Title: Lecture Notes in Computer Science. Springer International Publishing. DOI: 10.1007/978-3-030-58802-1\_34.
- Pedro, S. A., S. Abelman, F. T. Ndjomatchoua, R. Sang, and H. E. Z. Tonnang (2014). “Stability, Bifurcation and Chaos Analysis of Vector-Borne Disease Model with Application to Rift Valley Fever”. In: *PLoS ONE* 9.10. DOI: 10.1371/journal.pone.0108172.
- Pedro, S. A., S. Abelman, and H. E. Z. Tonnang (2016). “Predicting Rift Valley Fever Inter-epidemic Activities and Outbreak Patterns: Insights from a Stochastic Host-Vector Model”. In: *PLOS Neglected Tropical Diseases* 10.12. DOI: 10.1371/journal.pntd.0005167.
- (2017). “The Role of *Hyalomma truncatum* on the Dynamics of Rift Valley Fever: Insights from a Mathematical Epidemic Model”. In: *Acta Biotheor.* 65.1. DOI: 10.1007/s10441-016-9285-0.
- Pepin, M., M. Bouloy, B. H. Bird, A. Kemp, and J. Paweska (2010). “Rift Valley fever virus (*Bunyaviridae: Phlebovirus*): an update on pathogenesis, molecular epidemiology, vectors, diagnostics and prevention”. In: *Veterinary Research* 41.6. DOI: 10.1051/vetres/2010033.
- Perkins, T. A., T. W. Scott, A. Le Menach, and D. L. Smith (2013). “Heterogeneity, Mixing, and the Spatial Scales of Mosquito-Borne Pathogen Transmission”. In: *PLoS Computational Biology* 9.12. DOI: 10.1371/journal.pcbi.1003327.
- Peyre, M., V. Chevalier, S. Abdo-Salem, A. Velthuis, N. Antoine-Moussiaux, E. Thiry, and F. Roger (2015). “A Systematic Scoping Study of the Socio-Economic Impact of Rift Valley Fever: Research Gaps and Needs”. In: *Zoonoses and Public Health* 62.5. DOI: 10.1111/zph.12153.
- Phiri, D., M. Simwanda, S. Salekin, V. Nyirenda, Y. Murayama, and M. Ranagalage (2020). “Sentinel-2 Data for Land Cover/Use Mapping: A Review”. In: *Remote Sensing* 12.14. DOI: 10.3390/rs12142291.
- Picault, S., Y.-L. Huang, V. Sicard, S. Arnoux, G. Beaunée, and P. Ezanno (2019). “EMULSION: Transparent and flexible multiscale stochastic models in human, animal and plant epidemiology”. In: *PLoS Computational Biology* 15.9. DOI: 10.1371/journal.pcbi.1007342.
- Pigott, D. M., N. Golding, A. Mylne, Z. Huang, D. J. Weiss, O. J. Brady, M. U. G. Kraemer, and S. I. Hay (2015). “Mapping the zoonotic niche of Marburg virus disease in Africa”. In: *Trans R Soc Trop Med Hyg* 109.6. DOI: 10.1093/trstmh/trv024.
- Pin-Diop, R. (2006). “Spatialisation du risque de transmission de la fièvre de la Vallée du Rift en milieu agropastoral sahélien du Sénégal septentrional”. PhD thesis. Université d’Orléans.
- Pomposi, C., A. Giannini, Y. Kushnir, and D. E. Lee (2016). “Understanding Pacific Ocean influence on interannual precipitation variability in the Sahel: PACIFIC OCEAN INFLUENCE ON SAHEL PRECIPITATION”. In: *Geophysical Research Letters* 43.17. DOI: 10.1002/2016GL069980.
- Radchuk, V., S. Kramer-Schadt, and V. Grimm (2019). “Transferability of Mechanistic Ecological Models Is About Emergence”. In: *Trends in Ecology & Evolution* 34.6. DOI: 10.1016/j.tree.2019.01.010.

- Reiner, R. C. et al. (2013). “A systematic review of mathematical models of mosquito-borne pathogen transmission: 1970–2010”. In: *Journal of The Royal Society Interface* 10.81. DOI: 10.1098/rsif.2012.0921.
- Restif, O. et al. (2012). “Model-guided fieldwork: practical guidelines for multidisciplinary research on wildlife ecological and epidemiological dynamics”. In: *Ecol Lett* 15.10. DOI: 10.1111/j.1461-0248.2012.01836.x.
- Rich, K. M. and F. Wanyoike (2010). “An Assessment of the Regional and National Socio-Economic Impacts of the 2007 Rift Valley Fever Outbreak in Kenya”. In: *The American Journal of Tropical Medicine and Hygiene* 83.2\_Suppl. DOI: 10.4269/ajtmh.2010.09-0291.
- Rift Valley fever outbreaks forecasting models* (2008). Joint FAO - WHO experts consultation.
- Rissmann, M., F. Stoek, M. J. Pickin, and M. H. Groschup (2020). “Mechanisms of inter-epidemic maintenance of Rift Valley fever phlebovirus”. In: *Antiviral Research* 174. DOI: 10.1016/j.antiviral.2019.104692.
- Roberts, M. G. and J. A. P. Heesterbeek (2018). “Quantifying the dilution effect for models in ecological epidemiology”. In: *Journal of The Royal Society Interface* 15.140. DOI: 10.1098/rsif.2017.0791.
- Roche, B., M Eric Benbow, R. Merritt, R. Kimbirauskas, M. McIntosh, P. L. C. Small, H. Williamson, and J.-F. Guégan (2014). “Identifying the Achilles heel of multi-host pathogens: the concept of keystone ‘host’ species illustrated by *Mycobacterium ulcerans* transmission”. In: *Environ. Res. Lett.* 8.4. DOI: 10.1088/1748-9326/8/4/045009.
- Rohani, P., C. J. Green, N. B. Mantilla-Beniers, and B. T. Grenfell (2003). “Ecological interference between fatal diseases”. In: *Nature* 422.6934. DOI: 10.1038/nature01542.
- Romoser, W. (2011). “Rift Valley fever virus-infected mosquito ova and associated pathology: possible implications for endemic maintenance”. In: *Research and Reports in Tropical Medicine*. DOI: 10.2147/RRTM.S13947.
- Ross, S. R. (1908). *Report on the prevention of malaria in Mauritius*. London, UK: Waterlow and Sons Limited.
- (1911). *The prevention of malaria*. New York, NY:Dutton.
- Rostal, M. K., J. E. Liang, D. Zimmermann, R. Bengis, J. Paweska, and W. B. Karesh (2017). “Rift Valley Fever: Does Wildlife Play a Role?” In: *ILAR Journal* 58.3. DOI: 10.1093/ilar/ilx023.
- Safini, N., Z. Bamouh, J. Hamdi, M. Jazouli, K. O. Tadlaoui, and M. El Harrak (2021). “In-vitro and in-vivo study of the interference between Rift Valley fever virus (clone 13) and Sheeppox/Lumpy Skin disease viruses”. In: *Sci Rep* 11.1. DOI: 10.1038/s41598-021-91926-5.
- Saker, L, L Kelley, B Cannito, A Gilmore, and D Campbell-Lendrum (2004). *Globalization and infectious diseases: a review of the linkages*. Tech. rep. TDR/STR/SEB/ST/04.2.
- Salje, H. et al. (2021). “Reconstructing unseen transmission events to infer dengue dynamics from viral sequences”. In: *Nat Commun* 12.1. DOI: 10.1038/s41467-021-21888-9.

- Saltelli, A., K. Aleksankina, W. Becker, P. Fennell, F. Ferretti, N. Holst, S. Li, and Q. Wu (2019). “Why so many published sensitivity analyses are false: a systematic review of sensitivity analysis practices”. In: *Environmental Modelling & Software* 114. DOI: 10.1016/j.envsoft.2019.01.012.
- Samy, A. M., A. T. Peterson, and M. Hall (2017). “Phylogeography of Rift Valley Fever Virus in Africa and the Arabian Peninsula”. In: *PLOS Neglected Tropical Diseases* 11.1. DOI: 10.1371/journal.pntd.0005226.
- Scoglio, C. M., C. Bosca, M. H. Riad, F. D. Sahneh, S. C. Britch, L. W. Cohnstaedt, and K. J. Linthicum (2016). “Biologically Informed Individual-Based Network Model for Rift Valley Fever in the US and Evaluation of Mitigation Strategies”. In: *PLOS ONE* 11.9. DOI: 10.1371/journal.pone.0162759.
- Sedda, L. et al. (2019). “Improved spatial ecological sampling using open data and standardization: an example from malaria mosquito surveillance”. In: *Journal of The Royal Society Interface* 16. DOI: 10.1098/rsif.2018.0941.
- Sekamatte, M., M. H. Riad, T. Teklehiorghis, K. J. Linthicum, S. C. Britch, J. A. Richt, J. P. Gonzalez, and C. M. Scoglio (2019). “Individual-based network model for Rift Valley fever in Kabale District, Uganda”. In: *PLOS ONE* 14.3. DOI: 10.1371/journal.pone.0202721.
- Sellers, R. F. (1980). “Weather, host and vector – their interplay in the spread of insect-borne animal virus diseases”. In: *Journal of Hygiene* 85.1. DOI: 10.1017/S0022172400027108.
- Seufi, A. M. and F. H. Galal (2010). “Role of Culex and Anopheles mosquito species as potential vectors of rift valley fever virus in Sudan outbreak, 2007”. In: *BMC Infectious Diseases* 10.1. DOI: 10.1186/1471-2334-10-65.
- Shaman, J. and A. Karspeck (2012). “Forecasting seasonal outbreaks of influenza”. In: *Proceedings of the National Academy of Sciences* 109.50. DOI: 10.1073/pnas.1208772109.
- Simpson, J. E., P. J. Hurtado, J. Medlock, G. Molaei, T. G. Andreadis, A. P. Galvani, and M. A. Diuk-Wasser (2012). “Vector host-feeding preferences drive transmission of multi-host pathogens: West Nile virus as a model system”. In: *Proceedings of the Royal Society B: Biological Sciences* 279.1730. DOI: 10.1098/rspb.2011.1282.
- Sindato, C., E. Karimuribo, and E. Mboera (2011). “The epidemiology and socio-economic impact of Rift Valley fever epidemics in Tanzania: A review”. In: *Onderstepoort J Vet Res* 13.2. DOI: 10.4314/thrb.v13i5.1.
- Sindato, C., K. B. Stevens, E. D. Karimuribo, L. E. G. Mboera, J. T. Paweska, and D. U. Pfeiffer (2016). “Spatial Heterogeneity of Habitat Suitability for Rift Valley Fever Occurrence in Tanzania: An Ecological Niche Modelling Approach”. In: *PLoS Negl Trop Dis* 10.9. DOI: 10.1371/journal.pntd.0005002.
- Smith, D. L. et al. (2014). “Recasting the theory of mosquito-borne pathogen transmission dynamics and control”. In: *Transactions of the Royal Society of Tropical Medicine and Hygiene* 108.4. DOI: 10.1093/trstmh/tru026.

- Soti, V., C. Puech, D. Lo Seen, A. Bertran, C. Vignolles, B. Mondet, N. Dessay, and A. Tran (2010). “The potential for remote sensing and hydrologic modelling to assess the spatio-temporal dynamics of ponds in the Ferlo Region (Senegal)”. In: *Hydrology and Earth System Sciences* 14.8. DOI: 10.5194/hess-14-1449-2010.
- Soti, V., A. Tran, J.-S. Bailly, C. Puech, D. L. Seen, and A. Bégué (2009). “Assessing optical earth observation systems for mapping and monitoring temporary ponds in arid areas”. In: *International Journal of Applied Earth Observation and Geoinformation* 11.5. DOI: 10.1016/j.jag.2009.05.005.
- Soti, V., A. Tran, P. Degenne, V. Chevalier, D. Lo Seen, Y. Thiongane, M. Diallo, J.-F. Guégan, and D. Fontenille (2012). “Combining Hydrology and Mosquito Population Models to Identify the Drivers of Rift Valley Fever Emergence in Semi-Arid Regions of West Africa”. In: *PLoS Neglected Tropical Diseases* 6.8. DOI: 10.1371/journal.pntd.0001795.
- Soti, V., V. Chevalier, J. Maura, A. Bégué, C. Lelong, R. Lancelot, Y. Thiongane, and A. Tran (2013). “Identifying landscape features associated with Rift Valley fever virus transmission, Ferlo region, Senegal, using very high spatial resolution satellite imagery”. In: *International Journal of Health Geographics* 12. DOI: 10.1186/1476-072X-12-10.
- Sow, A. et al. (2016). “Widespread Rift Valley fever emergence in Senegal in 2013–2014”. In: *Open Forum Infectious Diseases*. DOI: 10.1093/ofid/ofw149.
- St. Maurice, A. de et al. (2018). “Rift valley fever viral load correlates with the human inflammatory response and coagulation pathway abnormalities in humans with hemorrhagic manifestations”. In: *PLOS Neglected Tropical Diseases* 12.5. DOI: 10.1371/journal.pntd.0006460.
- Sumaye, R., F. Jansen, D. Berkvens, B. De Baets, E. Geubels, E. Thiry, and M. Krit (2019). “Rift Valley fever: An open-source transmission dynamics simulation model”. In: *PLOS ONE* 14.1. DOI: 10.1371/journal.pone.0209929.
- Talla, C., D. Diallo, I. Dia, Y. Ba, J.-A. Ndione, A. A. Sall, A. Morse, A. Diop, and M. Diallo (2014). “Statistical Modeling of the Abundance of Vectors of West African Rift Valley Fever in Barkédji, Senegal”. In: *PLoS ONE* 9.12. DOI: 10.1371/journal.pone.0114047.
- Talla, C., D. Diallo, I. Dia, Y. Ba, J.-A. Ndione, A. P. Morse, A. Diop, and M. Diallo (2016). “Modelling hotspots of the two dominant Rift Valley fever vectors (*Aedes vexans* and *Culex poicilipes*) in Barkédji, Sénégal”. In: *Parasites & Vectors* 9. DOI: 10.1186/s13071-016-1399-3.
- Taylor, D., M. Hagenlocher, A. E. Jones, S. Kienberger, J. Leedale, and A. P. Morse (2016). “Environmental change and Rift Valley fever in eastern Africa: projecting beyond HEALTHY FUTURES”. In: *Geospatial Health* 11.1s. DOI: 10.4081/gh.2016.387.
- Thiemann, T. C., S. S. Wheeler, C. M. Barker, and W. K. Reisen (2011). “Mosquito Host Selection Varies Seasonally with Host Availability and Mosquito Density”. In: *PLoS Neglected Tropical Diseases* 5.12. DOI: 10.1371/journal.pntd.0001452.

- Thiongane, D. Y. (2000). “Système sous régional d’alerte et de contrôle de la fièvre de la Vallée du Rift au Mali, en Mauritanie et au Sénégal”. In: 2.
- Thonnon, J., M. Picquet, Y. Thiongane, M. Lo, R. Sylla, and J. Vercruyssen (1999). “Rift valley fever surveillance in the lower Senegal river basin: update 10 years after the epidemic”. In: *Tropical Medicine and International Health* 4.8. DOI: 10.1046/j.1365-3156.1999.00437.x.
- Tourre, Y. M., J.-P. Lacaux, C. Vignolles, and M. Lafaye (2012). “Remote Sensing and Public Health Issues in a Changing Climate and Environment: The Rift Valley Fever Case”. In: *National Security and Human Health Implications of Climate Change*. Springer Netherlands. DOI: 10.1007/978-94-007-2430-3\_19.
- Tourre, Y. M., J.-P. Lacaux, C. Vignolles, J.-A. Ndione, and M. Lafaye (2008). “Mapping of zones potentially occupied by *Aedes vexans* and *Culex poicilipes* mosquitoes, the main vectors of Rift Valley fever in Senegal”. In: *Geospatial health* 3.1. DOI: 10.4081/gh.2008.233.
- Tran, A., A. G. Fall, B. Biteye, M. Ciss, G. Gimonneau, M. Castets, M. T. Seck, and V. Chevalier (2019). “Spatial modeling of mosquito vectors for Rift Valley fever virus in northern Senegal: integrating satellite-derived meteorological estimates in population dynamics models”. In: *Remote Sensing* 11. DOI: 10.3390/rs11091024.
- Traoré-lamizana, M., D. Fontenille, M. Diallo, Y. Bâ, H. G. Zeller, M. Mondo, F. Adam, J. Thonon, and A. Maïga (2001). “Arbovirus Surveillance from 1990 to 1995 in the Barkedji Area (Ferlo) of Senegal, a Possible Natural Focus of Rift Valley Fever Virus”. In: *Journal of Medical Entomology* 38.4. DOI: 10.1603/0022-2585-38.4.480.
- Tuncer, N., H. Gulbudak, V. L. Cannataro, and M. Martcheva (2016). “Structural and Practical Identifiability Issues of Immuno-Epidemiological Vector-Host Models with Application to Rift Valley Fever”. In: *Bulletin of Mathematical Biology* 78.9. DOI: 10.1007/s11538-016-0200-2.
- Tusting, L. S., B. Willey, H. Lucas, J. Thompson, H. T. Kafy, R. Smith, and S. W. Lindsay (2013). “Socioeconomic development as an intervention against malaria: a systematic review and meta-analysis”. In: *The Lancet* 382.9896. DOI: 10.1016/S0140-6736(13)60851-X.
- Valentin, S., E. Arsevska, S. Falala, J. de Goër, R. Lancelot, A. Mercier, J. Rabatel, and M. Roche (2020). “PADI-web: A multilingual event-based surveillance system for monitoring animal infectious diseases”. In: *Computers and Electronics in Agriculture* 169. DOI: 10.1016/j.compag.2019.105163.
- Valle, S. D. (2018). “Summary Results of the 2014-2015 DARPA Chikungunya Challenge”. In: Vazquez-Prokopec, G. M., T. A. Perkins, L. A. Waller, A. L. Lloyd, R. C. Reiner, T. W. Scott, and U. Kitron (2016). “Coupled Heterogeneities and Their Impact on Parasite Transmission and Control”. In: *Trends in Parasitology* 32.5. DOI: 10.1016/j.pt.2016.01.001.
- Viboud, C. et al. (2018). “The RAPIDD ebola forecasting challenge: Synthesis and lessons learnt”. In: *Epidemics* 22. DOI: 10.1016/j.epidem.2017.08.002.

- Vignolles, C., J.-P. Lacaux, Y. M. Tourre, G. Bigeard, J.-A. Ndione, and M. Lafaye (2009). “Rift Valley fever in a zone potentially occupied by *Aedes vexans* in Senegal: dynamics and risk mapping”. In: *Geospatial health* 3.2. DOI: 10.4081/gh.2009.221.
- Volz, E. M., S. L. Kosakovsky Pond, M. J. Ward, A. J. Leigh Brown, and S. D. W. Frost (2009). “Phylogenetics of Infectious Disease Epidemics”. In: *Genetics* 183.4. DOI: 10.1534/genetics.109.106021.
- Walsh, M. G., A. Willem de Smalen, and S. M. Mor (2017). “Wetlands, wild Bovidae species richness and sheep density delineate risk of Rift Valley fever outbreaks in the African continent and Arabian Peninsula”. In: *PLOS Neglected Tropical Diseases* 11.7. DOI: 10.1371/journal.pntd.0005756.
- Wandiga, S. O. et al. (2010). “Vulnerability to epidemic malaria in the highlands of Lake Victoria basin: the role of climate change/variability, hydrology and socio-economic factors”. In: *Climatic Change* 99.3-4. DOI: 10.1007/s10584-009-9670-7.
- Watts, D. J., R. Muhamad, D. C. Medina, and P. S. Dodds (2005). “Multiscale, resurgent epidemics in a hierarchical metapopulation model”. In: *Proceedings of the National Academy of Sciences* 102.32. DOI: 10.1073/pnas.0501226102.
- Weaver, S. C. and W. K. Reisen (2010). “Present and future arboviral threats”. In: *Antiviral Research* 85.2. DOI: 10.1016/j.antiviral.2009.10.008.
- Weaver, S. C., N. L. Forrester, J. Liu, and N. Vasilakis (2021). “Population bottlenecks and founder effects: implications for mosquito-borne arboviral emergence”. In: *Nat Rev Microbiol* 19.3. DOI: 10.1038/s41579-020-00482-8.
- Webster, J. P., A. Borlase, and J. W. Rudge (2017). “Who acquires infection from whom and how? Disentangling multi-host and multi-mode transmission dynamics in the ‘elimination’ era”. In: *Phil. Trans. R. Soc. B* 372.1719. DOI: 10.1098/rstb.2016.0091.
- Wilkinson, M. D. et al. (2016). “The FAIR Guiding Principles for scientific data management and stewardship”. In: *Sci Data* 3.1. DOI: 10.1038/sdata.2016.18.
- Williamson, M. S., S. Bathiany, and T. M. Lenton (2016). “Early warning signals of tipping points in periodically forced systems”. In: *Earth Syst. Dynam.* 7.2. DOI: 10.5194/esd-7-313-2016.
- Wilson, M. L. et al. (1994). “Rift Valley Fever in Rural Northern Senegal: Human Risk Factors and Potential Vectors”. In: *The American Journal of Tropical Medicine and Hygiene* 50.6. DOI: 10.4269/ajtmh.1994.50.663.
- Wonham, M. J., M. A. Lewis, J. Renclawowicz, and P. van den Driessche (2006). “Transmission assumptions generate conflicting predictions in host-vector disease models: a case study in West Nile virus”. In: *Ecology Letters* 9.6. DOI: 10.1111/j.1461-0248.2006.00912.x.
- World Health Organization (WHO) (2014). *A global brief on vector-borne diseases*. (Accessed 17 February 2020).
- Wright, D., J. Kortekaas, T. A. Bowden, and G. M. Warimwe (2019). “Rift Valley fever: biology and epidemiology”. In: *Journal of General Virology* 100.8. DOI: 10.1099/jgv.0.001296.

- Xia, S., X.-N. Zhou, and J. Liu (2017). “Systems thinking in combating infectious diseases”. In: *Infect Dis Poverty* 6.1. DOI: 10.1186/s40249-017-0339-6.
- Xiao, Y., J. C. Beier, R. S. Cantrell, C. Cosner, D. L. DeAngelis, and S. Ruan (2015). “Modelling the Effects of Seasonality and Socioeconomic Impact on the Transmission of Rift Valley Fever Virus”. In: *PLOS Neglected Tropical Diseases* 9.1. DOI: 10.1371/journal.pntd.0003388.
- Xue, L. and C. Scoglio (2013). “The network level reproduction number for infectious diseases with both vertical and horizontal transmission”. In: *Mathematical Biosciences* 243.1. DOI: 10.1016/j.mbs.2013.02.004.
- Xue, L., H. M. Scott, L. W. Cohnstaedt, and C. Scoglio (2012). “A network-based meta-population approach to model Rift Valley fever epidemics”. In: *Journal of Theoretical Biology* 306. DOI: 10.1016/j.jtbi.2012.04.029.
- Xue, L., L. W. Cohnstaedt, H. M. Scott, and C. Scoglio (2013). “A hierarchical network approach for modeling Rift Valley fever epidemics with applications in North America”. In: *PLoS ONE* 8.5. arXiv: 1110.1611. DOI: 10.1371/journal.pone.0062049.
- Yamana, T. K., S. Kandula, and J. Shaman (2016). “Superensemble forecasts of dengue outbreaks”. In: *J. R. Soc. Interface.* 13.123. DOI: 10.1098/rsif.2016.0410.
- Yang, C.-X. and L.-F. Nie (2016). “Modelling the use of impulsive vaccination to control Rift Valley Fever virus transmission”. In: *Advances in Difference Equations* 2016.1. DOI: 10.1186/s13662-016-0835-1.
- Zeilinger, A. R. and M. P. Daugherty (2014). “Vector preference and host defense against infection interact to determine disease dynamics”. In: *Oikos* 123.5. DOI: 10.1111/j.1600-0706.2013.01074.x.
- Özkan, et al. (2016). “Challenges and priorities for modelling livestock health and pathogens in the context of climate change”. In: *Environmental Research* 151. DOI: 10.1016/j.envres.2016.07.033.

# Appendices



## Article

# Over 100 Years of Rift Valley Fever: A Patchwork of Data on Pathogen Spread and Spillover

Gebbienna M. Bron <sup>1,\*</sup>, Kathryn Strimbu <sup>2</sup>, H el ene Cecilia <sup>3</sup>, Anita Lerch <sup>2</sup>, Sean M. Moore <sup>2</sup>, Quan Tran <sup>2</sup>, T. Alex Perkins <sup>2</sup> and Quirine A. ten Bosch <sup>1,\*</sup>

<sup>1</sup> Quantitative Veterinary Epidemiology, Wageningen University and Research, 6708 PB Wageningen, The Netherlands

<sup>2</sup> Department of Biological Sciences and Eck Institute for Global Health, University of Notre Dame, Notre Dame, IN 46556, USA; kstrimbu@nd.edu (K.S.); alerch2@nd.edu (A.L.); smoore15@nd.edu (S.M.M.); qtran4@nd.edu (Q.T.); taperkins@nd.edu (T.A.P.)

<sup>3</sup> BIOPAR, INRAE, Oniris, 44300 Nantes, France; helene.cecilia@oniris-nantes.fr

\* Correspondence: bieneke.bron@wur.nl (G.M.B.); quirine.tenbosch@wur.nl (Q.A.t.B.); Tel.: +31-(0)-317-482335 (G.M.B. & Q.A.t.B.)

**Abstract:** During the past 100 years, Rift Valley fever virus (RVFV), a mosquito-borne virus, has caused potentially lethal disease in livestock, and has been associated with significant economic losses and trade bans. Spillover to humans occurs and can be fatal. Here, we combined data on RVF disease in humans (22 countries) and animals (37 countries) from 1931 to 2020 with seroprevalence studies from 1950 to 2020 (n = 228) from publicly available databases and publications to draw a more complete picture of the past and current RVFV epidemiology. RVFV has spread from its original locus in Kenya throughout Africa and into the Arabian Peninsula. Throughout the study period seroprevalence increased in both humans and animals, suggesting potentially increased RVFV exposure. In 24 countries, animals or humans tested positive for RVFV antibodies even though outbreaks had never been reported there, suggesting RVFV transmission may well go unnoticed. Among ruminants, sheep were the most likely to be exposed during RVF outbreaks, but not during periods of cryptic spread. We discuss critical data gaps and highlight the need for detailed study descriptions, and long-term studies using a one health approach to further convert the patchwork of data to the tale of RVF epidemiology.

**Keywords:** bunyavirales; mosquito-borne disease; notifiable disease; Rift Valley fever phlebovirus; ProMED



**Citation:** Bron, G.M.; Strimbu, K.; Cecilia, H.; Lerch, A.; Moore, S.M.; Tran, Q.; Perkins, T.A.; ten Bosch, Q.A. Over 100 Years of Rift Valley Fever: A Patchwork of Data on Pathogen Spread and Spillover. *Pathogens* **2021**, *10*, 708. <https://doi.org/10.3390/pathogens10060708>

Academic Editors:  
V eronique Chevalier,  
Philippe Dussart and Benoit Durand

Received: 29 January 2021

Accepted: 1 June 2021

Published: 5 June 2021

**Publisher's Note:** MDPI stays neutral with regard to jurisdictional claims in published maps and institutional affiliations.



**Copyright:**   2021 by the authors. Licensee MDPI, Basel, Switzerland. This article is an open access article distributed under the terms and conditions of the Creative Commons Attribution (CC BY) license (<https://creativecommons.org/licenses/by/4.0/>).

## 1. Introduction

Over 100 years ago, in June 1912, an outbreak of “an obscure disease [that] caused heavy mortality in lambs” was described which, temporarily, had a discouraging effect on the sheep industry in Kenya [1]. Eighteen years later, in 1930, the likely causative agent, Rift Valley fever virus (RVFV), was isolated by Daubney and colleagues [2]. Nearly 100 years later, this primarily mosquito-transmitted virus, now known as Rift Valley fever phlebovirus [3], still causes morbidity and mortality in animals with spillover to people throughout the African continent, Indian Ocean, and Middle East. Outbreaks can lead to severe recurring economic losses, disrupting the livelihoods of often poor communities. Due to its economic impact, pathogenicity, and unpredictable (re)emergence, RVFV is recognized as a danger for both human and animal populations [4]. A better understanding of the eco-epidemiology of RVF could help inform intervention and surveillance strategies to reduce the burden of disease and minimize pathogen range expansion.

In the face of climate change, range expansions and redistributions of mosquito-borne viruses are expected [5]. RVFV, mostly transmitted by *Culex* and *Aedes* spp. mosquitoes, first expanded its range outside Africa in 2000, when it caused major outbreaks on the Arabian

Peninsula [6–9]. The suitable geographical ranges for competent mosquito and ruminant populations that are conducive to pathogen introduction and spread are changing, alarming Europe and the Americas [10,11]. Historically, the emergence of RVFV in new areas has been unpredictable, but it has frequently been linked to animal trade [12–14]. As “a transmissible disease that has the potential for very serious and rapid spread, without regards for national borders, and with serious socio-economic and public health consequence as well as major importance in the international trade of animals and animal products,” the World Organization for Animal Health (OIE) recognizes RVF as a notifiable animal disease of concern. Similarly, the World Health Organization’s research and development blueprint named RVFV a priority pathogen due to its “epidemic potential” [4].

The impact and disease burden of RVF on local economies and livelihoods exemplifies the potential devastating consequences that RVFV could have on the global food supply and population health. Outbreak sizes in humans have been estimated to range from a few cases to thousands of cases, with case fatality risk ranging from 1 to 30% [15]. Human cases—ranging from mild to flu-like symptoms to hemorrhagic fever and death—are most common in individuals with close contact with animals and those consuming raw meat [16], often in rural communities. In Africa, more than 740 million individuals are currently living in rural, mostly agricultural communities, and this is expected to increase to 1039 million by 2050 [17], placing them and their animals potentially at risk for RVF. Outbreaks in animals are recognized by abortion storms and high mortality in young animals [2]. Although sheep and goats are most susceptible, RVFV also affects cattle, camels, and, sporadically, wildlife [18,19]. No RVFV treatments are registered for humans or animals, and medical treatments, when available, are limited to supportive care.

The strategies for RVF outbreak prevention and control are limited [20]. At a local level, communities and livestock owners could implement strategies to reduce mosquito bites, e.g., mosquito-control, moving animals to high-elevations pastures during peak mosquito seasons. In addition, individual animals can be protected and herd immunity can be accomplished by vaccinating animals [21,22]. However, preventative vaccination can be challenging due to a low burden of disease in the absence of outbreaks, and logistical and economical barriers, in part due to limitations of the currently available vaccines. For example, the most commonly used vaccine in livestock is a live-attenuated vaccine (i.e., Smithburn vaccine) which is highly effective [23] but can cause abortion and birth defects when vaccinating pregnant animals [24]. When RVFV is suspected in animals, control measures include, for example, announcements for hygiene measures, awareness, and vaccination campaigns [25]. However, when cases are confirmed in humans, a widespread outbreak is generally suspected and more expensive and intense measures are used, ranging from vector control to ruminant trade bans [25,26]. These interventions can disrupt local, regional, and national economies. For example, the estimated economic impact of a RVF outbreak from 2006 to 2007 ranged from 0.01% of the gross domestic product (GDP) in Tanzania (6.7 million US\$) to 5.5% of the GDP in Somalia (471 million US\$), making outbreak prevention a potentially more cost-effective strategy [27,28]. To strengthen RVF outbreak prevention, predictive modeling could be used to facilitate early community communication, targeted mosquito control interventions, and even localized vaccination campaigns [29].

RVF outbreaks in animals and humans are associated with a variety of factors, but the eco-epidemiology is not fully understood. RVFV circulates through different transmission routes; infection may occur through an infectious mosquito bite, or by contact with infected tissues and fluids (e.g., aborted tissues, exposure during slaughter). Outbreaks in animals, and subsequently in people, are often associated with increased rainfall in historically endemic areas, most notably the foci along the Great Rift Valley [30,31]. The virus, capable of vertical transmission, likely survives in *Aedes* spp. eggs in the environment. When infected eggs hatch during rainfall and flooding events, the virus might be able to re-emerge. Next, flooded areas provide ample breeding habitat for mosquitoes, further amplifying transmission. These patterns have been seen during, for example, the 1973–1975 South

African, and the 1997–1998 and 2006–2007 Eastern Africa outbreaks, which were associated with El Niño rain events [32,33]. In other areas, RVFV may be introduced via the live-animal trade. Movements of infected animals from endemic regions with year-long presence of mosquitoes, can (re)introduce the virus to more seasonal ecosystems, in a source-sink fashion. Trade-related introductions and outbreaks are frequently associated with large gatherings, whereby large numbers of potentially infected animals are brought in for slaughter [12,34,35]. Despite the recognition of the underlying factors, the complexity of the dynamics together with a scarcity in data hamper actionable risk assessments.

To improve our understanding of the historic and current epidemiology of RVF, and to aid in planning future surveillance and intervention strategies, we compiled historical RVF data (including grey and white literature) on outbreak reporting and seroprevalence studies of both humans and animals. We examined patterns in the data associated with the occurrence of outbreaks and cryptic spread, including the seroprevalence in ruminant species, and examined if and how indicators of RVFV occurrence in animal populations are correlated to spillover to humans. As the data used largely come from outbreak reporting, which is highly heterogeneous across regions and over time, one should be careful in drawing hard conclusions from these analyses. Rather, this work should be regarded as hypothesis generating and aims to identify research gaps and needs based on a comprehensive overview of different data sources on this emerging zoonotic disease.

## 2. Materials and Methods

To explore the temporal and spatial activity of Rift Valley fever virus (RVFV) in Africa and beyond, we combined human and animal (domesticated animals and wildlife) case records and serological studies. To create a dataset as complete as possible, we included information sources beyond peer-reviewed (experimental) studies (an integrative literature review) but refrained from expert consultation and interviews. We extracted data from case reports, outbreak reports, and serological studies available in openly accessible, online databases, and in peer-reviewed journals. We then explored relationships among these records. Mosquito records were excluded.

### 2.1. Data Acquisition Strategy

Data was extracted in five steps, A to E, by hand (Figure 1). First, we obtained RVF case data from databases on outbreaks in humans and animals (step A), complemented with data from systematic literature reviews (step B). Next, we extracted seroprevalence data from systematic literature reviews by cross-referencing the included studies (described in more detail later) (step C). We updated existing reviews to the current date (step D) and confirmed the absence of RVFV evidence for selected countries (step E, Figure 1). The database was last updated on 13 January 2021, and includes publications published up until 31 December 2020, including data pertaining to 2020 and earlier.

In step A, RVF case records were extracted from posts from the Program for Monitoring Emerging Diseases (ProMED) from the International Society for Infectious Diseases (ISID) and the public databases from the World Organization for Animal Health's (OIE). ProMED was established in 1994 and archived posts were accessible from 1996 onward [36]. The OIE's Handistatus 2.0 database [37] contained data from 1995 to 2004, after which it was replaced by the current World Animal Health Information System (WAHIS/WAHID) interface [38]. RVF case data were compared against the World Health Organization's Rift Valley fever outbreak bulletins [39] and the Centers for Disease Control and Prevention (CDC) outbreak summaries [40] from 2000 onward to ensure no human RVF cases were omitted. Next, in step B, additional case records were extracted from historical review papers and reports [33,41–44].

To identify and extract data from original seroprevalence studies, we built on existing systematic literature reviews [45,46], and cross-referenced references within these publications (step C). Hereby, we included all geographical regions, e.g., studies from outside Africa and the Arabian Peninsula were included. Next, we used the search strategy

from the most recent RVFV seroprevalence review, Clark et al., (2018) [45], to include publications published after 2016. Using the search term (“Rift Valley Fever” OR “rvf”) AND (“prevalence OR “incidence” OR “sero”) in PubMed and Web of Knowledge, 102 and 162 publications were identified, respectively. There were 88 duplicates between the two searches. Of the 176 unique publications, 34 were already in our dataset (i.e., obtained through cross referencing); 88 were excluded based on their title (e.g., not relating to RVF); for 54 publications, the abstract was assessed after which 21 were excluded as they did not contain information pertaining to RVF or did not include original or new data, and data from 33 publications were added to the dataset. In addition, we conducted an absence of evidence search (step E) to explore if publications were available for countries from African, Southern and Western Asian United Nations (UN) regions [47] with neither serological nor outbreak data (Google Scholar search terms: (“country name”, “Rift Valley fever virus”, serology)). For 30 countries, no RVFV data was found, including six countries on mainland Africa: Algeria, Burundi, Eritrea, Guinea Bissau, Lesotho and Liberia.

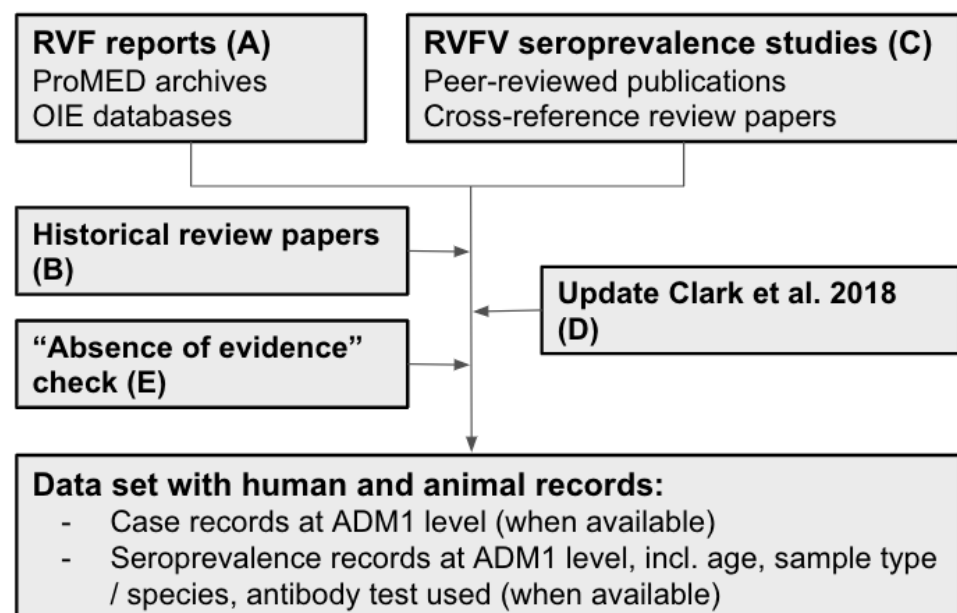


**Figure 1.** Flowchart of the source and data acquisition. A total of 275 sources ((A) two OIE databases and ProMED, and (B–E): 272 publications) were used to inform the RVF case and RVFV seroprevalence dataset for humans and animals. RVF reports were extracted from databases (A) and supplemented with historical review papers (B). Seroprevalence data was first extracted from publications identified through cross-referencing review papers (C) and the search strategy of Clark et al., 2018 was repeated to identify and add publications from 2017 to 2020 (D). In step (E), a search was conducted to explore if publications were available for African, Southern and Western Asian countries without RVF reports and RVFV seroprevalence studies to confirm absence of RVFV evidence. Data was included until 31 December 2020; the last update was conducted on 13 January 2021 by repeating step A and D. ADM1: Administrative Level 1, e.g., districts, provinces.

## 2.2. Dataset

Information parsed from the different sources was summarized in four data types: human RVF cases, animal RVF cases, human serology, and animal serology.

### 2.2.1. RVF Case Definition

Case definitions for RVF vary between agencies, reporting countries, and reports. As such, we did not use a standardized case definition and included any reported and suspected cases. Broadly, a case is defined as an individual infected with RVFV, with or without clinical symptoms. Cases of RVF in animals are often recognized by clinical symptoms in the herd but may go unnoticed. Determining the number of infected animals

is therefore challenging. The OIE includes records on suspected transmission without case confirmation in their HandiStatus 2.0 and WAHIS database. We included those entries in our animal RVF dataset as well. In contrast, a human case of RVF is often defined as an individual with moderate to severe clinical symptoms who sought medical care. For both animals and humans, case numbers were included in the datasets, when available, but again, it is important to note that these cases represent varying levels of certainty. Cases were not always associated with a confirmatory diagnostic test. Speculations by authors on the total outbreak size were not included as cases, but these estimates were noted in a 'notes' column in the database (Supplementary Table S1).

A year with RVF cases was defined as any calendar year for which positive case numbers in humans or animals were reported or suspected for a country. We used this term synonymously with RVF outbreak, as an outbreak year was defined as any calendar year for which case data were reported. Laboratory-based cases were not considered. Inter-epizootic cases were included, whereas travel-related cases were excluded. Sometimes, an outbreak year only had one reported case. RVF outbreaks that spanned two calendar years (e.g., November to February) were marked in both years. When data sources reported a year from July to June (sometimes referred to as collating by season) and no additional information was available about the time of the observation (i.e., month or week), we also marked the observations in both calendar years.

### 2.2.2. Geographical Information

Countries were grouped according to UN geographical regions [47]. The Canary Islands (ES-IC) were grouped with Northern Africa. Countries were abbreviated using three-letter codes and, when possible, information was parsed to administrative level 1 (ADM1) using the regions, districts, and provinces included in the Database of Global Administrative Areas (GADM) [48]. ADM2 and other smaller locations referenced (e.g., farm names) were collated at the ADM1 level. Since our database spans 91 years, including the period of decolonisation in Africa, when many nations (re)gained their independence, country names changed, borders were adjusted, and new nations were formed. To address this, we matched countries with the current UN and GADM database (e.g., Rhodesia, now Zimbabwe). In addition, historic RVF cases and serological studies may have taken place in an area of a country which is now recognized as an independent country by the UN. We used the current country names based on ADM1 level information or general regional directions of the data (e.g., South Sudan). Hence, older studies can be linked to countries that were not formally established at the time the study was conducted.

### 2.2.3. Serological Records

Reports on the presence of RVFV antibodies in humans and animals were summarized by country (ADM0), ADM1 (when available), year(s) of sample collection (if this information was not available, authors were contacted), the number of individuals tested, number positive, and study sample characteristics. Data were further characterized including the age of human participants, animal species, or people-sampling strategies (e.g., random sampling of a general population; sampling of febrile, hospitalized or suspected patients; testing of high-risk individuals; unclear strategies or mixed samples), the type of antibody test used (e.g., enzyme-linked immunosorbent assay, immunofluorescent antibody test, virus neutralization test, complement fixing, plaque reduction neutralization tests), and antibody type targeted. If both IgM and IgG results were available, we included the IgG results and marked IgM availability in the notes. It is important to note that the presence of IgG antibodies does not mean the virus is circulating in the area where the sample was taken, and that movements and vaccination status of individuals should be accounted for. Cross-reactivity with other circulating viruses may also interfere with the interpretation of seroprevalence estimates, depending on the test used (e.g., African phleboviruses cross-reacting in haemagglutination-inhibition assays). In areas without known cases, the

presence of RVFV should be confirmed, and paired sera should, ideally, be taken to confirm seroconversion and thereby recent exposure.

### 2.3. Statistical Analyses

Summary statistics regarding the temporal and spatial extent of each of the datasets are presented first. To further explore the aggregated data at the country and year level, we assessed how RVFV seroprevalence, and case data of animals and humans were associated to each other in regression analyses.

#### 2.3.1. Data Preparation

For our statistical analyses, we aggregated data at the country level, because for about a quarter of the entries, ADM1 was unknown (394 of 1507 records). Seroprevalence data were cleaned prior to analysis, excluding IgM-only records, records with missing data (e.g., study year or exact number of positives), and data points that could not be categorized as either outbreak- or non-outbreak-associated (e.g., data points reporting multiple years only partly overlapping an outbreak). A serological record was considered associated with RVF outbreaks if the samples were taken during the year in which RVF cases were recorded in humans or animals in the same country, or in the year after. Here, we made the assumption that post-outbreak serology is typically performed in the outbreak region. We test this assumption on the subset of data for which sufficient information is available. For those instances that this cannot be verified, we discuss the impact of the assumption. We limited outbreak-associated serology to those surveys performed up to one year post-outbreak.

#### 2.3.2. Annual RVF Case and Serological Study Availability

We estimated the increase in annual data availability for the four data types to quantify the progress made in data availability over time. For each data type, the response variable denoting if RVFV cases or a serological study was available in a given year (1) or not (0) was regressed against year: 1930 to 2020 for RVF cases and 1930 to 2017 for serological studies. We report the estimated slope of the logistic regression models.

#### 2.3.3. Seroprevalence over Time, and across Regions and Outbreaks

We compared seroprevalence between samples that were or were not associated with recent RVF cases (outbreak-associated: yes or no) using logistic regression models weighted by sample size. In these models, we accounted for differences between geographic regions (reference level: Eastern Africa) and over time. Time was rescaled to 10-year time steps. The start year of sample collection was used when a study reported multiple sampling years combined. The logistic regression analysis of human seroprevalence data was conducted for a subset of data including randomly sampled individuals only. The regression analysis of animal seroprevalence data was conducted for the full dataset and a subset of data including ruminant samples only (including camels, but excluding mixed samples with horses, mixed wildlife samples, and donkey, pig and rodent samples). Model estimates were exponentiated to calculate the adjusted odds ratios (aOR) of finding a positive sample in a group compared to the reference group.

#### 2.3.4. Ruminant Species' Seroprevalence and the Association with Reported Outbreaks

To further dissect possible species contribution to RVFV, the logistic regression was repeated on a subset of data including only records for single ruminant species (sheep-reference level, buffalo, camels, cattle, goats). The species model accounted for differences in time (i.e., the year of sample collection) and geographical region (reference level: Eastern Africa), as above (Section 2.3.3), and assessed the association of species, recent RVF cases (yes or no), and their interaction with seroprevalence. The model was weighted by sample size. Variance inflation factors were assessed (<3 was accepted). Model estimates were exponentiated to calculate aOR. The interaction between species and outbreak was displayed using aORs with sheep in the absence of an outbreak as the reference level. The

likelihood of detecting a positive buffalo, camels, cattle, and goats in the absence of an outbreak was calculated by exponentiating the model estimates. The effect of an outbreak on seroprevalence of sheep was calculated by exponentiating the outbreak estimate. The aORs for the other species during an outbreak were calculated by exponentiating the sum of three model estimates: the estimates for the species (1), outbreak (2) and the interaction of the species and outbreak (3).

### 2.3.5. Exploring Cryptic Spread: RVFV Activity Prior to RVF Case Reporting

To assess if cryptic RVFV transmission may be present (i.e., animals were exposed to RVFV, but no cases were reported), we extracted all seroprevalence data when RVF had never been reported in the country. We compared, by ANOVA, if the mean seroprevalence (by country and year) was different based on the current, 2020, RVF status of the country (i.e., RVF cases have been reported since the seroprevalence study was conducted, or no cases have been reported to date).

### 2.3.6. Exploring Pathogen Spillover: Concurrent Animal and Human RVFV Activity

To assess if animal case investigations were more likely when human RVF outbreaks occurred, we compared, by Fisher's exact test, if the proportion of animal case records with case counts was different when human outbreaks had or had not occurred in the same year and country. To determine if countries with higher seroprevalence in animals were more likely to have higher human seroprevalence, we summarized seroprevalence by country and year for randomly collected human samples and ruminant animal samples and assessed the Spearman's rank-based statistic. As above, we acknowledge that the spatial scale of RVF outbreaks is typically smaller than the country level. We further examine the limited number of studies for which ADM1-level information is available for both human and animal studies to answer two questions: (i) how likely are studies in humans and animals from the same year to have been performed in the same ADM1, and (ii) for those records, can we distinguish patterns between human and animal seroprevalence and are those consistent with conclusions from the larger dataset?

### 2.3.7. Software

All statistical analyses were conducted in R Statistical Computing Software [49]. Package *lme4* [50] was used for regression models. Figures were created using packages *rnaturalearth* [51] and *ggplot2* [52], and organized using *cowplot* [53].

## 3. Results

Information from OIE databases and ProMED archives was supplemented with data from 273 peer reviewed publications (Table 1). The dataset consists of 1507 records of four data types: 125 on human RVF cases extracted from 59 sources, 415 on RVF cases in animals from 38 sources, 294 on human serology from 106 sources, and 673 records on animal serology extracted from 144 sources (Supplementary Table S1).

**Table 1.** Peer-reviewed publications by region. The median year of publication and range are included. The OIE databases ( $n = 2$ ) and ProMED archive (available since 1996) are not included in this table.

Continent	Region	Sources	Year of Publication of Used Sources		
			Earliest	Median	Most Recent
Africa	Central	22	1965	2008	2019
	Eastern	102	1931	2013	2020
	Northern	35	1978	1999	2020
	Southern	33	1951	2011	2020
	Western	47	1980	2009	2020
Asia	Southern	2	1995	2000	2005
	Western	21	1984	2013	2020
Multiple and other regions *		11	1969	2011	2020
Total		273	1931	2011	2020

\* One publication from Poland, Europe, is available [54].

### 3.1. Data Availability

#### 3.1.1. Data Availability over Time

A total of 91 years were included in the dataset (1930 to 2020), with the first publication in 1931 [2] (Table 1, Figure 2). Publications on human and animal RVF cases were first available in 1931. The first publication on human seroprevalence estimates was published in 1956 [55], and on animal seroprevalence estimates in 1958 [56]. The average lag between study-end year and publication year of the manuscript for seroprevalence studies was three years for both human and animal studies. RVF cases that occurred prior to 1990 often had a lag in their publication, as case records were published in peer-reviewed sources (e.g., historical reviews, compared to current near real-time reporting). During the 1990s, this transitioned to predominantly same-year reporting. Over 40% of human and animal RVF reports we extracted came from archived ProMED posts (37 of 89 human, and 125 of 279 animal RVF records published after 1996, respectively), which were mostly reported the same year as the outbreaks occurred.

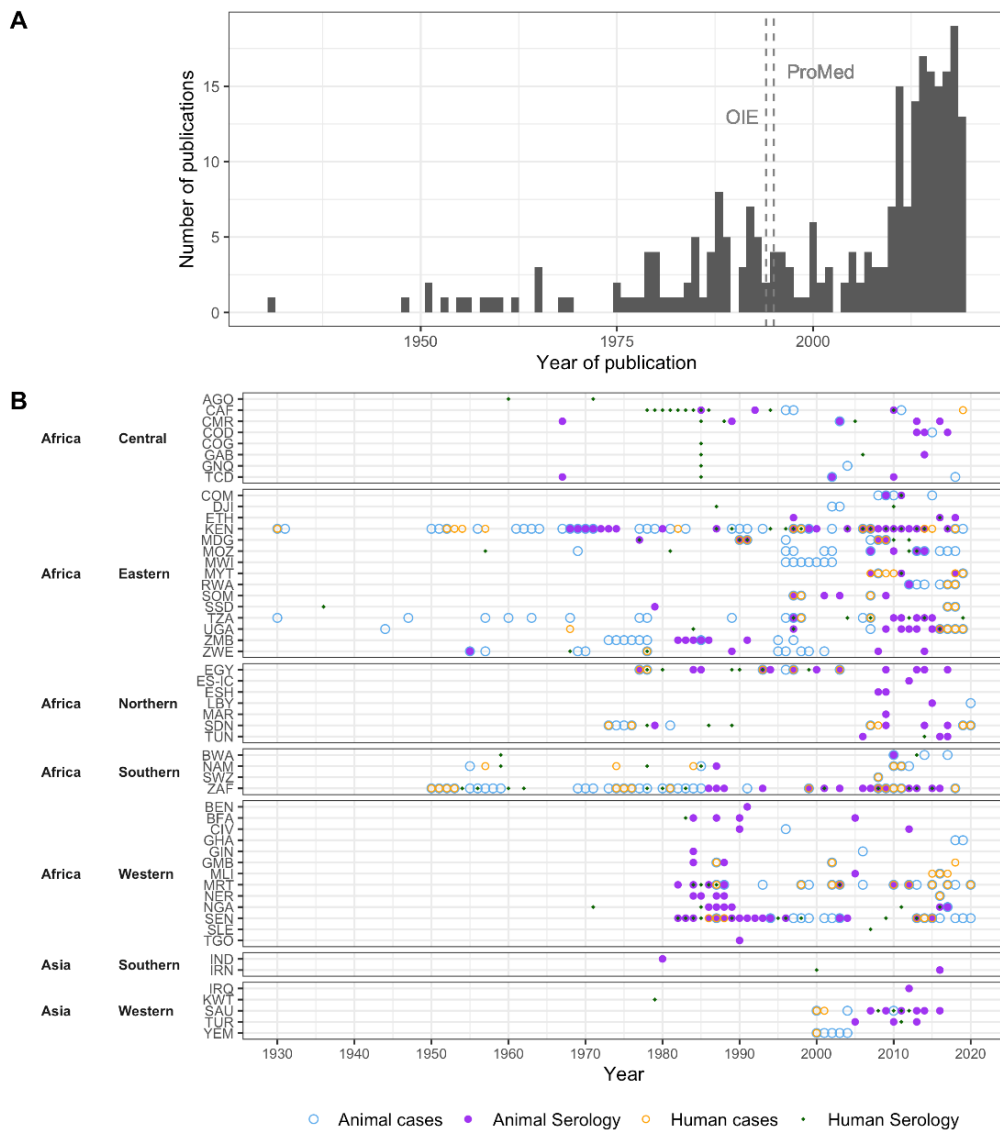


**Figure 2.** Regional variation in RVF reports and seroprevalence studies over time. (A) Number of included publications by year. Vertical lines represent the first year during which OIE and ProMED reports were included. (B) For each country, the years during which Rift Valley fever cases were reported, and the years during which Rift Valley fever virus seroprevalence data were collected are marked for animals and humans. When results from multiple years were reported as one, e.g., 1991–2000, we marked the first year in the figure. Serological data also include studies where no RVFV antibodies were detected; note that this is not a RVFV detection chart.



The number of RVFV publications increased over time (Figure 2A). For all four data types, the probability of there being at least one record in a given year increased significantly ( $p < 0.001$ ), although the rate of increase differed between data types. This increase in publications was steepest for animal serology (beta = 0.124, 95% Confidence Interval [CI]: 0.082, 0.184) in comparison to human serology (beta = 0.089, 95%CI: 0.058, 0.129), human RVF cases (beta = 0.054, 95%CI: 0.033, 0.079), and RVF cases in animals (beta = 0.064, 95%CI: 0.038, 0.098) (Supplementary Figure S1).

### 3.1.2. Spatial Distribution of Data

All five African regions, and about 80% of African countries, were represented in the dataset and thus had either RVF cases reported or seroprevalence studies conducted (Figure 3). In addition, Southern and Western Asia were included with two (Iran and India) and five countries (Saudi Arabia, Yemen, Iraq, Kuwait, and Turkey), respectively (Figure 3). Of the 52 countries in the dataset, human and animal RVF case records were found for 22 and 37 countries, respectively (Figure 3C,D). Human and animal seroprevalence studies were conducted in 33 and 45 countries, respectively (Figure 3E,F). Most human and animal serological publications ( $n = 106$  and  $n = 142$ ) originated from Kenya (22 and 15) or South Africa (10 and 13), followed by Egypt (7 and 12). For 15 countries, both human RVF cases and human seroprevalence data were available. For twice the number of countries (31 countries), both animal RVF cases and animal seroprevalence have been reported.

### 3.2. RVF Outbreaks and Number of Cases Affected

A total of 605,005 animal and 10,944 human RVF cases were reported during 68 and 45 years, respectively (Supplementary Table S1). Animal and human cases were most often reported in Kenya (32 and 13 years, respectively) and South Africa (31 and 14 years, respectively) (Figure 3C,D). Most animal cases were also reported from Kenya (507,996, 84% of total cases), followed by Tanzania (38,167) and South Africa (19,543). Most human cases were reported from Sudan (2534), Egypt (1267) and Kenya (1187).

A total of 224 animal and 95 human RVF case records were available after aggregating data by country and year. For 152 of the 319 aggregated records, case counts were available (47.6%). Most of the records with case counts (126 of 152, 82.9%) occurred in 2000 or later. The number of RVF cases in animals ranged from a single animal succumbing to RVFV (e.g., an antelope in Senegal in 2020) up to estimates of 250,000 animals affected during the 1950 to 1951 outbreaks in Kenya. Human case counts also ranged from one individual to about 1500, but it was noted that an estimated 20,000 to 100,000 people may have been infected in South Africa in the 1950s.

### 3.3. Variation in Seroprevalence

Over 250,000 individuals (human and animals) were represented in the seroprevalence data and 210,074 of which met the inclusion criteria: 131,378 animals and 80,406 humans. The percentage of individuals that tested positive for RVFV antibodies by country and year ranged from 0% (93 to 4590 individuals tested) to 40% (30 individuals tested) in humans, and 0% (1 to 1344 animals tested) to 70% (150 individuals sampled) in animals (Figure 4A,C).

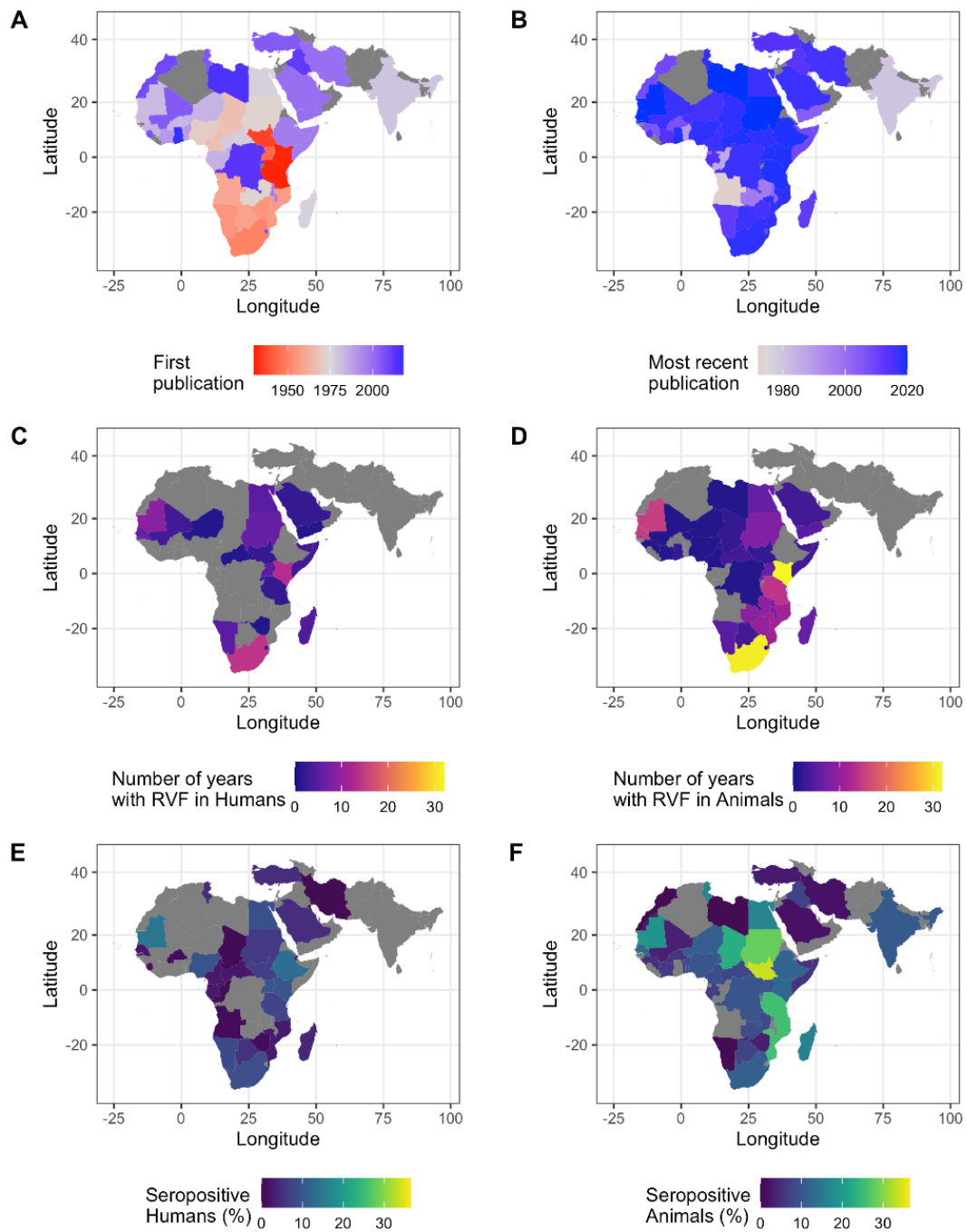


**Figure 3.** RSV reporting and activity. (A,B) The year of the first (A) and most recent (B) RSV publication by country. The studies on the Canary Islands, Comoros Islands, and Mayotte are not shown. No publications were found for the countries in grey. (C,D) Number of years with human (C) or animal (D) RSV case records per country. (E,F) Percent of individuals positive for RSV antibodies of all individuals sampled per country for human samples (E) and animal samples (F). All samples, except IgM-only records, were included. Gray indicates that no RSV case reports or seroprevalence studies were found for this country. It should be noted that the presence of individuals with a positive RSV antibody test does not ascertain local circulation of the virus and should be interpreted with caution, particularly for countries with no confirmed cases.

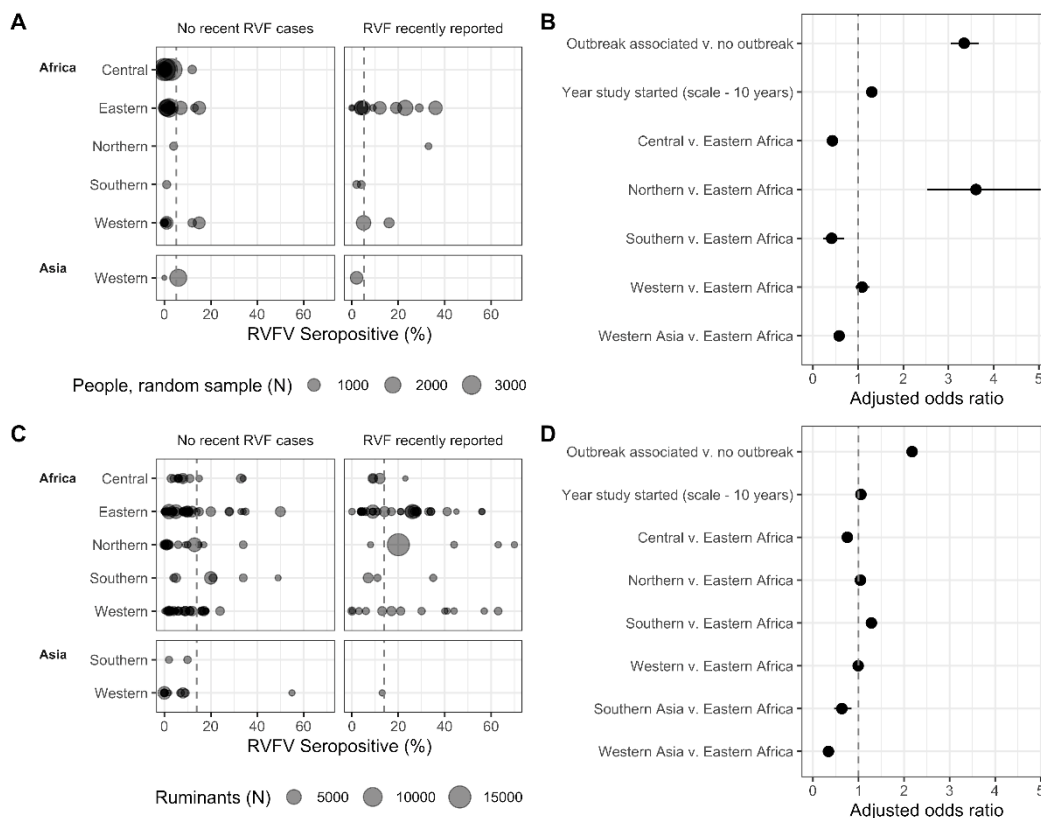


**Figure 4.** Regional human, individuals selected by random sampling, (A,B) and ruminant (C,D) RVFV seroprevalence in the absence of recent human and/or animal RVF cases or within the same year, or year post, reported RVF cases. (A,C) Sample size and seroprevalence per country and year. The grey, dashed vertical lines represent the mean seropositivity (A,C) and equal odds (B,D). Horizontal lines represent confidence intervals around the point estimate (B,D). Southern Asia is represented by studies from Iran and India; Western Asia is represented by Iraq, Saudi Arabia, Turkey and Yemen.

### 3.3.1. The Association of Seroprevalence with Time, Region, and Outbreaks

A subset with data on 48,702 randomly selected human individuals remained, after excluding those studies that targeted individuals with high-risk lifestyles and professions, febrile patients, and studies that had mixed or unclear sample selection. Similarly, 122,419 ruminant samples remained (including camels), after excluding studies with non-ruminants (e.g., rodents, horses, pigs, donkeys), and mixed samples of ruminants and non-ruminants (e.g., “pig and sheep”).

Among all the included samples, 5.2% of human samples and 13.9% of ruminant samples were positive for RVFV antibodies (Figure 4A,C). Of samples associated with an outbreak (i.e., human and/or animal cases in the same or previous year), 12.6% of human samples and 19.8% of ruminant samples were positive for RVFV antibodies. This was substantially lower for samples not associated with outbreaks, with 2.7% of human samples and 9.8% of ruminant samples positive for RVFV antibodies (Figure 4A,C). Indeed, when assessing the subset of randomly selected individuals, the adjusted odds (aOR) of finding a positive serum sample was 3.35 times higher (95%CI: 3.06, 3.67,  $p < 0.001$ ) when sampling was conducted in the same year or the year after RVF cases were reported in the country compared to sampling conducted in the absence of recently reported RVF cases (Figure 4B). A similar, yet smaller effect was observed for ruminants, with aOR = 2.18 (95%CI: 2.10, 2.25,  $p < 0.001$ ), indicating that more individuals are exposed to the virus during outbreak years than during cryptic cycles (Figure 4D). As expected, the proportion of individuals who tested positive for RVFV antibodies also varied over time and by region (Figure 4). Every 10 years, the probability for a sample to be positive increased 1.30 times (95%CI: 1.24, 1.37,  $p < 0.001$ ) for the subset of randomly selected humans and, similarly, 1.05 times

per 10-year timestep for ruminants (95%CI: 1.04, 1.07,  $p < 0.001$ ) (Figure 4B,D). In addition, relative to Eastern Africa, the proportion of individuals who tested positive was higher in people in northern Africa, largely driven by a study conducted in an area affected by RVFV 13 years prior, (aOR: 3.61, 95%CI: 2.53, 5.04) and lower in individuals from central and southern Africa and western Asia (i.e., Kuwait, Saudi Arabia, Turkey) (aOR: 0.43, 0.41 and 0.58, 95%CI: 0.36, 0.51; 0.23, 0.69 and 0.49, 0.68) (Figure 4B, Supplementary Table S2). The probability for a ruminant being seropositive in central Africa, and southern (i.e., Iran and India) and western Asia (i.e., Iraq, Saudi Arabia, Turkey) was lower than in eastern Africa (Figure 4D, Supplementary Table S3). The seropositivity in the ruminant populations in north, west, and south African regions was similar to slightly higher than, eastern Africa. Observed patterns of time and outbreaks on the proportion of individuals who tested positive in ruminants were robust to using the full dataset (i.e., the dataset with non-ruminants included. Supplementary Table S4). For most records, it was not possible to verify if the seroprevalence studies were performed in the same ADM1-level as where the outbreaks occurred. About half of human outbreak records (65 of 125), and about a third of animal outbreak records (135 of 415 records) did not have ADM1-levels reported. When looking at the seroprevalence subsets for which ADM1-level were available (77.7% of randomly selected humans records (80 of 103 records containing 32,434 individuals), and 80% of ruminant records (410 of 515 records containing 79,112 individuals), and taking a conservative approach to considering a sample outbreak associated (i.e., if an outbreak occurred in the country, and the ADM1 was not known, the sample was not outbreak-associated), the general conclusions are robust, though effect sizes vary, and some regional associations changed (Supplementary Tables S5 and S6).

### 3.3.2. Ruminant Species' Seroprevalence and the Association with Reported Outbreaks

The percentage of animals testing positive varied between the different ruminant species sampled, with sheep having the lowest seroprevalence in the absence of recent RVF cases (Table 2). However, the interaction between species and outbreak-associated sampling was strongly significant ( $p < 0.001$ ). While the odds of detecting a seropositive sheep in association with recent RVF cases tripled, the odds of finding positive buffalo, camels, cattle and goats only increased 1.26 to 1.48 times (Table 2, Supplementary Table S7). The higher odds of detecting a positive sheep in association with RVF cases indicates that this species could be more likely to be exposed during outbreaks, possibly amplifying the outbreak.

**Table 2.** Species-specific seroprevalence and adjusted odds ratios for the interaction between species and recent RVF reporting.

Species	No Recent RVF Cases				RVF Recently Reported			
	%	(n)	aOR	95% CI	%	(n)	aOR	95% CI
Sheep	8.1	(17,328)	1	(Reference)	21.6	(10,271)	2.99	(2.77, 3.23)
Buffalo	13.8	(1417)	1.47	(1.25, 1.73)	15.7	(1523)	1.85	(1.16, 2.93)
Camels	10.0	(4938)	1.80	(1.60, 2.03)	20.5	(1451)	2.62	(1.80, 3.82)
Cattle	13.0	(22,288)	1.47	(1.37, 1.58)	18.2	(19,519)	2.12	(1.67, 2.69)
Goats	11.9	(8746)	1.24	(1.14, 1.35)	17.1	(5968)	1.83	(1.38, 2.43)

Common livestock species were compared to sheep tested when RVF had and had not been recently reported in a country. The logistic regression model also accounted for the year the study was started and the region the work was conducted in (Supplementary Table S7). aOR: adjusted odds ratio; CI: confidence interval.

### 3.3.3. Exploring Cryptic Spread: RVFV Activity Prior to RVF Case Reporting

Serological studies took place in 27 countries (including the Canary Islands) without known RVF cases, for a total of 50 aggregated records by country and year (Figure 5). In 24 countries, animals tested positive for RVFV antibodies; in 11 of these countries, RVF cases have never been reported to date, whereas in 13 countries, RVF cases were reported 1 to 38 years later. Notably, animals tested positive for RVFV antibodies in Iraq, Iran, and

Turkey (Figure 3). However, confirmed animal or human cases have not been documented in these countries to date.

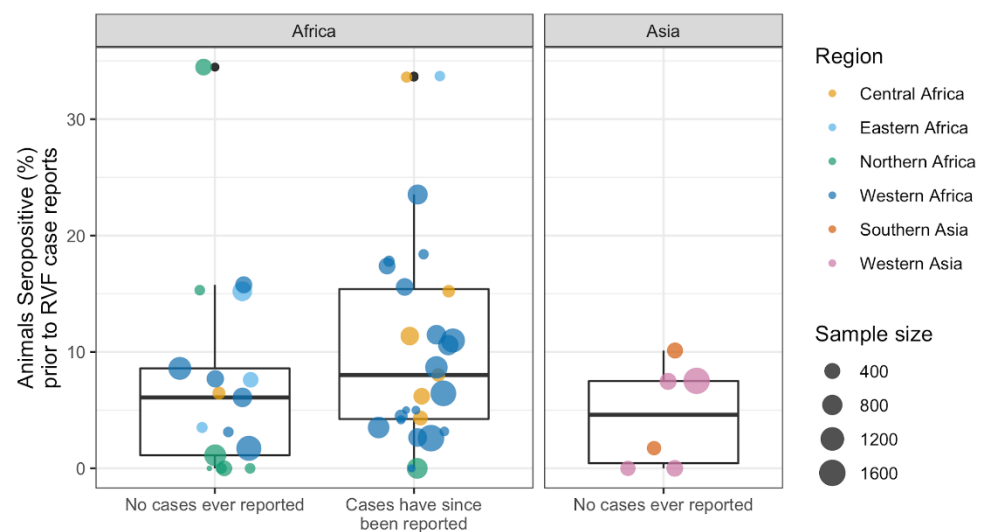


**Figure 5.** Rift Valley fever virus seroprevalence when RVF cases had never been reported in the country (human and/or animal). The outlier with no known RVF cases represents samples from Tunisia collected between 2017 and 2018 (34.5% positive of 470 camels) [57], and two outliers currently known to report RVF cases represent samples collected in South Sudan from 1979 to 1983 (33.7% positive of 92 ruminants, cattle and goats) [58], and Cameroon in 1968 (33.6% of 122 sheep) [59].

A total of 1859 of 24,642 animals tested positive for RVFV antibodies in countries without known RVF cases at the time of the survey (7.5%), 8.8% of animals from countries that later reported RVF cases (1217 of 13,788) and 7.2% of animals sampled in countries that, to date, have not reported RVF cases (827 of 11,454, Figure 5). No difference in seroprevalence, by country and year, was detected between the groups that currently report and do not report RVF cases (ANOVA,  $df$  1,48,  $F = 2.5$ ,  $p = 0.12$ , Figure 5).

### 3.4. Exploring Pathogen Spillover: Concurrent Animal and Human RVFV Activity

#### 3.4.1. Association of Human RVF Outbreaks with Animal RVF Cases

There were 73 concurrent human and animal RVF outbreaks (i.e., human and animal cases reported in the same year and country); 77% of 95 human outbreaks and 33% of 224 animal outbreaks occurred concurrently. Concurrent outbreaks were reported in 21 countries, with most in South Africa (14), Mauritania (9) and Kenya (7).

For about half of the concurrent outbreaks, case counts were available for both humans and animals (38 of the 73 paired records). The human and animal case counts of concurrent outbreaks (38 paired records) were weakly positively correlated (Spearman  $S = 6588$ ,  $\rho = 0.279$ ,  $p = 0.09$ , Supplementary Figure S2). The occurrence of human RVF cases increased the likelihood that case counts were available for animal RVF records: 59% (43 of 73) of concurrent outbreaks and 30% (45 of 151) of animal-only outbreaks had case counts (OR: 3.36, 95%CI: 1.81, 6.30,  $p < 0.001$ ).

Of the 22 human RVF outbreaks without associated animal RVF cases, 16 occurred within two years of an RVF outbreak in animals, leaving six human RVF outbreaks without a link to reported animal RVF cases (6.3% of 96 human RVF outbreaks: 150 cases in Kenya from 2014 to 2015, 15 cases in the Central African Republic in 2019, one case in Gambia in 2018, and an unknown number of cases in Namibia in 1974 and Uganda in 1968).

#### 3.4.2. Correlation between Animal and Human Seroprevalence

A total of 17,269 people (selected using a random sampling strategy) and 11,777 ruminants were sampled in the same year and country. The 19 paired records of concurrent

seroprevalence data include 10 countries (Kenya  $n = 9$ , Senegal  $n = 2$ , Central African Republic, Ethiopia, Madagascar, Mauritania, Mayotte, Tanzania, Uganda and South Africa) and 16 years (earliest 1982, most recent 2017).

Countries with high seroprevalence in animals were not typically associated with high human seroprevalence during the same year (Spearman  $S = 720$ ,  $\rho = 0.368$ ,  $p = 0.12$ , Figure 6). When considering the seroprevalence records that selected for high-risk individuals (e.g., herders, slaughterhouse workers), the association with ruminant seroprevalence was even weaker (12 paired country-year records, Spearman  $S = 120$ ,  $\rho = 0$ ,  $p = 1$ ). The absence of a significant correlation between human and ruminant seroprevalence may, among other factors, result from the fact that not all records originated from the same ADM1-level. ADM1-level information was available for human and ruminant seroprevalence records of 10 paired country-year records. Of those, three country-year records included the same ADM1 for animal and human serological data, a spatial scale which more precisely reflects RVFV outbreaks.

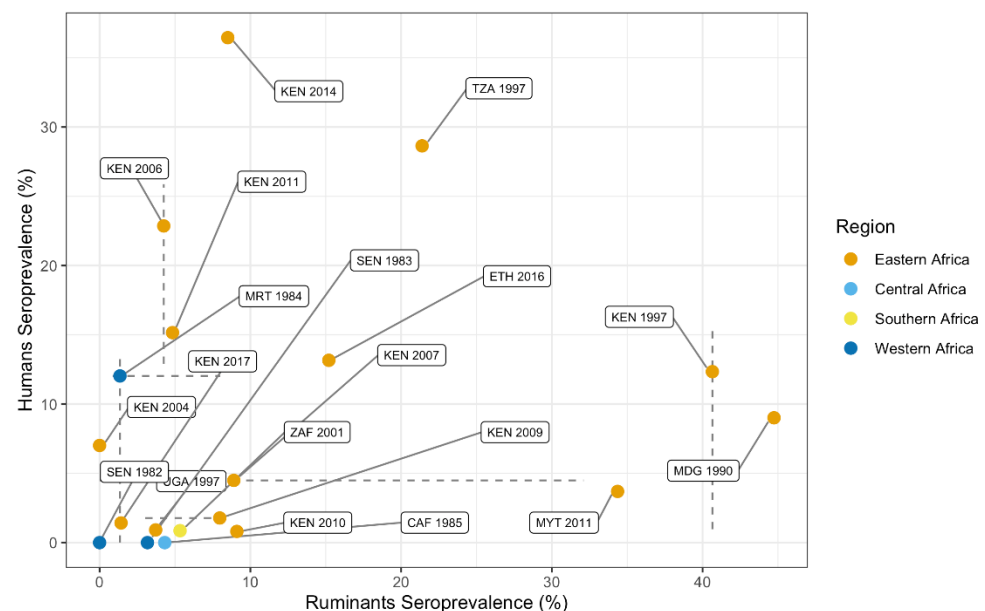


**Figure 6.** Animal and human RVF seroprevalence data from the same year and country. Point estimates represent mean seropositivity (percent of individuals testing positive of the total number of individuals tested) by country and year. The point estimates are color-coded by region. Lines represent the range in seroprevalence estimates reported when multiple publications were included in the prevalence estimate.

#### 4. Discussion

Approximately 90 years of reporting, 70 years of surveillance efforts, and about 20 years of near real-time case report availability allowed us to map the pathogen's geographic distribution, and the extent of co-occurrence of RVF in different host species. Explorations of this patchwork of different data sources allowed for the generation of new hypotheses on the epidemiology of RVF. For instance, analyses showed sheep are the most exposed species during outbreaks. This suggests they may play an important role in transmission of the pathogen, particularly during outbreaks. The dataset generated (Supplementary Table S1) provides the first open-access global human and animal RVF case and RVFV seroprevalence data compilation, and allows researchers to further investigate the epidemiology of the virus.

RVFV spread significantly over the past decades and appears to (re)emerge more frequently. For example, the pathogen spread to Saudi Arabia and Yemen from Africa in 2000. The pathogen was also successfully introduced to Madagascar, Mayotte and the Comoros Islands, with RVF outbreaks in recent years on both islands (2008 onward) [36,38].

Interestingly, evidence of RVFV circulation was described in 1977 in Madagascar, but the first cases were only reported in 1990. In addition, there is serological evidence of viral exposure in animals in Iraq [60], Iran [61] and Turkey [62] in the absence of RVF cases. However, as RVFV confirmation and animal travel histories are incomplete, local RVFV circulation cannot be established based on these records alone. Furthermore, the pathogen recently re-emerged in areas where no cases had been confirmed for over 40 to 50 years [63]. The increase in outbreak reports is in part due to improved reporting systems that are globally accessible, but not exclusively. Greater mobility and trade could facilitate the movement of susceptible and exposed animals. These movements in combination with increased densities of humans and animals, changing mosquito population dynamics, landscapes and weather patterns could all contribute to faster introductions and subsequent transmission. Indeed, animal and human exposure to RVFV appears to have increased over time. The approximate 30% increase in seropositivity in humans and 5% increase in animals every 10 years (e.g., 5% seroprevalence becomes 6.5% or 5.25%) suggests increased exposure to the virus. However, these changes in seropositivity could in part be due to improved, more sensitive diagnostic tools, and changed sampling strategies, whereby cross-sectional studies screening for hemorrhagic fever viruses were replaced by RVFV-specific studies in areas with known or suspected virus activity (e.g., outbreak investigations, intervention evaluations). In addition, an increase in seroprevalence is to be expected in longer-lived species, such as humans, even if the force of infection is relatively stable over time, due to the accumulation of exposed individuals who survived infection (i.e., seropositive individuals). Age-stratified sampling could help disentangle these historical transmission patterns [64], but few studies reported on the age of participants and fewer provided age-stratified data (for examples, see [65–67]). In addition, structured, long-term seroconversion studies that include both humans and main animal hosts could help provide local evidence of the force of infection and how it changes over time.

Our analyses corroborated a prominent role of sheep during outbreaks, finding them to be the most likely species to seroconvert during outbreaks, three times more likely than during cryptic transmission cycles. In comparison, goats were approximately 1.5 times more likely to seroconvert. This aligns with the belief that sheep are the most important host species for RVFV amplification, owing to their high susceptibility and viral loads [2,68]. These characteristics, in addition to sheep experiencing the most severe pathology due to RVFV, could make them the prime vaccine target to minimize economic losses for farmers and to prevent RVF outbreaks. Understanding the species' local contribution to RVFV maintenance and amplification is important for vaccination and surveillance strategies to prevent RVF outbreaks.

Despite several large RVF outbreaks in animals, human case counts remained relatively low, suggesting either limited or geographical variation in spillover, or infections going unrecognized, undiagnosed, or unreported. In people, the probability of asymptomatic infection is estimated to range from 90 to 98% [69,70]. In addition, health care access and diagnostics may be limited, and RVF symptoms overlap with those of other prevalent diseases [71], possibly obscuring case identification and reporting. Similarly to humans, animal RVF cases may also be overlooked, thereby facilitating cryptic transmission of RVFV. The absence of animal cases when human RVF cases were observed suggests that livestock cases also go unreported, or human cases were strictly mosquito-mediated (mosquitoes becoming infected through vertical transmission or by feeding on infected wildlife) or due to slaughter or raw wildlife meat consumption. In a herd, RVF is easy to overlook when few animals are affected, or few animals show signs of disease [72]. As suggested by the greater likelihood of having case counts for animals when human cases occur simultaneously, outbreak investigations among animals are often initiated after human cases have been detected. In addition, the presence of RVFV antibodies without animal or human RVF cases in a country could be explained by cryptic transmission, whereby cases may be mild enough or in small enough numbers to go unnoticed. Some of the presence of antibodies in the absence of cases could be explained by RVFV exposure at different geographical

locations, i.e., in traded animals, and seroconversion due to vaccination. Overall, the evidence of cryptic transmission urges reconsideration of reliance on passive surveillance systems for the detection of RVFV, and other emerging pathogens.

Increased data availability, through historical reviews, studies sharing their (raw) data, and near real-time reporting of RVF cases facilitated the creation of this comprehensive dataset, thereby connecting the patchwork of RVFV data and improving epidemiological inference made in these publications. Our study highlights the value of detailed reviews at a national level that summarize historic local and national database records—many previously unavailable—with as much detail as possible (for example, [41,43]). Furthermore, our dataset illustrates the importance of centralized databases, as many of RVF case records were sourced from ProMED-archives and the OIE. Notably, ProMED combines grey literature with official reporting of cases and outbreaks to international organizations, expanding its reach beyond traditional data sources. We thus purposely expanded our search strategy to go beyond peer-reviewed published (experimental) studies (an integrated approach, e.g., including theses, ProMED, OIE databases), used a broad case definition, and accepted all serological tests detecting IgG. By adopting this strategy, we were able to picture a more complete view of the history of RVF epidemiology. However, the robustness of data and conclusions from the analyses should also be considered in this context. The information gained from patterns in the data should be further explored and investigated in more detail when additional data become available.

Standardization in reporting would strengthen the dataset and the inferences that can be made from the data in future analyses. For example, serological studies were inconsistent in reporting the importation and vaccination history of the animals, possibly inflating seroprevalence. Similarly, the migration and travel history of people was often not included, placing the location of RVFV antibody detection away from the true location of infection. In addition, although districts, regions or provinces of sampling were often reported, the data was not shared at these geographical levels in about a quarter of publications. Therefore, we summarized data by country and year to create a more robust dataset. This aggregation sacrifices the fine-scale information and prevents describing and detecting within-country variation. Since RVF outbreaks are often localized, they can prompt outbreak investigations and seroprevalence studies beyond the affected area; our aggregation of the dataset combined studies from areas with and without RVFV transmission, thereby possibly underestimating seroprevalence associated with outbreaks. Furthermore, we identified samples as outbreak-associated when samples were collected during the outbreak, or the year after the outbreak (reported RVF cases in humans and/or animals). This grouping potentially placed samples collected at outbreak locations two years or more after an outbreak in the non-outbreak group (e.g., sampling in Egypt 13 years post-outbreak [73]). Combined, this meant that our adjusted odds ratios likely underestimated the actual increase in human and animal seroprevalence due to RVF outbreaks.

As the geographical range suitable for RVFV introduction and establishment continues to expand, global efforts should continue to improve surveillance strategies to detect pathogen emergence and prevent pathogen spread. Similarly, with the increasing frequency of outbreaks, both in eastern and western Africa, regional and national programs may adjust their disease surveillance and RVFV intervention program. To evaluate if RVFV activity and exposure is increasing, as suggested by the increased seroprevalence over time, targeted long-term studies in endemic and non-endemic areas could be started. These efforts would be more beneficial if a One Health approach were to be used [74], in which human, animal, and mosquito populations, as well as the environment, are monitored simultaneously. Looking ahead, standardized reporting of serological studies, and uniform case definitions would ensure that on-the-ground, local efforts can be utilized at a larger geographical scale, further informing mathematical models and facilitating a thorough understanding of RVFV epidemiology. Ultimately, these research and reporting efforts combine local interests and international research priorities to limit the burden of RVFV.



**Supplementary Materials:** The following are available online at <https://www.mdpi.com/article/10.3390/pathogens10060708/s1>, Figure S1: Data availability over time (logistic regression plotted), Figure S2: Human and Animal RVF cases, Table S1: Dataset, Table S2: Seroprevalence model output–People, Table S3: Seroprevalence model output–Ruminant, Table S4: Seroprevalence model output–All animals, Table S5: Seroprevalence model output–People matched by ADM1, Table S6: Seroprevalence model output–Ruminant matched by ADM1, Table S7: Seroprevalence model output–Selected ruminant species

**Author Contributions:** Conceptualization, G.M.B., Q.A.t.B., Q.T., T.A.P.; Methodology, G.M.B., K.S., Q.A.t.B., Q.T., T.A.P.; Validation, H.C.; Formal Analysis, G.M.B.; Investigation, G.M.B., K.S.; Data Curation, A.L., G.M.B., K.S.; Writing–Original Draft Preparation, G.M.B., K.S., Q.A.t.B.; Writing–Review & Editing, All authors; Visualization, G.M.B., K.S., T.A.P.; Supervision, Q.A.t.B., S.M.M., TAP; Funding Acquisition, G.M.B., Q.A.t.B., T.A.P. All authors have read and agreed to the published version of the manuscript.

**Funding:** This work was supported by an award from the Coalition for Epidemic Preparedness Innovations to the University of Notre Dame. In addition, TAP received support from USDA-NIFA AFRI Grant 2019-67015-28982 as part of the joint USDA-NSF-NIH-BBSRC-BSF Ecology and Evolution of Infectious Diseases program. HC was supported by FORESEE project funded by INRAE metaprogram GISA (Integrated Management of Animal Health), Région Pays de la Loire, CIRAD. GMB was supported by the Wageningen University Graduate Schools postdoc-talent grant.

**Institutional Review Board Statement:** Ethical review and approval was not obtained for this study, because animal and human data were extracted from published sources.

**Data Availability Statement:** Data is contained within the supplementary material and the Open Science Framework (OSF) repository (DOI 10.17605/OSF.IO/UXRA6), as part of the OSF project (DOI 10.17605/OSF.IO/54UKB). Code to reproduce figures and tables is available in the OSF project (<https://osf.io/uvdjk/>, accessed on 21 January 2021).

**Acknowledgments:** We thank Robert Sumaye for his insightful comments and constructive review of the manuscript. We also thank several authors who kindly provided additional information regarding their studies upon request.

**Conflicts of Interest:** The authors declare no conflict of interest.

## References

1. Harcourt, M.P.; Bowring, C.C. *Annual Report on the East Africa Protectorate for 1912–1913*; Barclay and Fry: Southwark, UK, 1914; p. 27.
2. Daubney, R.; Hudson, J.R.; Garnham, P.C. Enzootic Hepatitis or Rift Valley Fever. An Undescribed Virus Disease of Sheep Cattle and Man from East Africa. *J. Pathol. Bacteriol.* **1931**, *34*, 545–579. [[CrossRef](#)]
3. ICTV Taxonomy History: Rift Valley Fever Phlebovirus. Available online: [https://talk.ictvonline.org/taxonomy/p/taxonomy-history?taxnode\\_id=201900163](https://talk.ictvonline.org/taxonomy/p/taxonomy-history?taxnode_id=201900163) (accessed on 21 January 2021).
4. Mehand, M.S.; Al-Shorbaji, F.; Millett, P.; Murgue, B. The WHO R&D Blueprint: 2018 Review of Emerging Infectious Diseases Requiring Urgent Research and Development Efforts. *Antivir. Res.* **2018**, *159*, 63–67. [[CrossRef](#)]
5. Ryan, S.J.; Carlson, C.J.; Mordecai, E.A.; Johnson, L.R. Global Expansion and Redistribution of Aedes-Borne Virus Transmission Risk with Climate Change. *PLoS Negl. Trop. Dis.* **2019**, *13*. [[CrossRef](#)]
6. US Department of Health and Human Services, Centers for Disease Control and Prevention. Outbreak of Rift Valley Fever–Yemen, August–October 2000. *Morb. Mortal. Wkly. Rep.* **2000**, *49*, 1065–1066.
7. Ahmad, K. More Deaths from Rift Valley Fever in Saudi Arabia and Yemen. *Lancet* **2000**, *356*, 1422. [[CrossRef](#)]
8. Al-Afaleq, A.I.; Hussein, M.F.; Al-Naeem, A.A.; Housawi, F.; Kabati, A.G. Seroepidemiological Study of Rift Valley Fever (RVF) in Animals in Saudi Arabia. *Trop. Anim. Health Prod.* **2012**, *44*, 1535–1539. [[CrossRef](#)]
9. Madani, T.A.; Al-Mazrou, Y.Y.; Al-Jeffri, M.H.; Mishkhas, A.A.; Al-Rabeah, A.M.; Turkistani, A.M.; Al-Sayed, M.O.; Abodahish, A.A.; Khan, A.S.; Ksiazek, T.G.; et al. Rift Valley Fever Epidemic in Saudi Arabia: Epidemiological, Clinical, and Laboratory Characteristics. *Clin. Infect. Dis.* **2003**, *37*, 1084–1092. [[CrossRef](#)]
10. Nielsen, S.S.; Alvarez, J.; Bicout, D.J.; Calistri, P.; Depner, K.; Drewe, J.A.; Garin-Bastuji, B.; Rojas, J.L.G.; Schmidt, C.G.; Michel, V.; et al. Rift Valley Fever—Epidemiological Update and Risk of Introduction into Europe. *EFSA J.* **2020**, *18*, e06041. [[CrossRef](#)] [[PubMed](#)]
11. Hartley, D. Potential Effects of Rift Valley Fever in the United States. *Emerg. Infect. Dis.* **2011**. [[CrossRef](#)]

12. Abdo-Salem, S.; Waret-Szkuta, A.; Roger, F.; Olive, M.-M.; Saeed, K.; Chevalier, V. Risk Assessment of the Introduction of Rift Valley Fever from the Horn of Africa to Yemen via Legal Trade of Small Ruminants. *Trop. Anim. Health Prod.* **2011**, *43*, 471–480. [[CrossRef](#)] [[PubMed](#)]
13. El-Harrak, M.; Martín-Folgar, R.; Llorente, F.; Fernández-Pacheco, P.; Brun, A.; Figuerola, J.; Jiménez-Clavero, M.Á. Rift Valley and West Nile Virus Antibodies in Camels, North Africa. *Emerg. Infect. Dis.* **2011**, *17*, 2372–2374. [[CrossRef](#)]
14. Carroll, S.A.; Reynes, J.-M.; Khristova, M.L.; Andriamandimby, S.F.; Rollin, P.E.; Nichol, S.T. Genetic Evidence for Rift Valley Fever Outbreaks in Madagascar Resulting from Virus Introductions from the East African Mainland Rather than Enzootic Maintenance. *J. Virol.* **2011**, *85*, 6162–6167. [[CrossRef](#)] [[PubMed](#)]
15. Wright, D.; Kortekaas, J.; Bowden, T.A.; Warimwe, G.M. Rift Valley Fever: Biology and Epidemiology. *J. Gen. Virol.* **2019**, *100*, 1187–1199. [[CrossRef](#)]
16. Turkistany, A.-H.; Mohamed, A.G.; Al-Hamdan, N. Seroprevalence of Rift Valley fever Among Slaughterhouse Personnel in Makkah During Hajj1419h (1999). *J. Fam. Community Med.* **2001**, *8*, 53–57.
17. Department of Economic and Social Affairs, Population Division, United Nations. *World Urbanization Prospects: The 2018 Revision*; United Nations: New York, NY, USA, 2019; ISBN 978-92-1-148319-2.
18. Rostal, M.K.; Liang, J.E.; Zimmermann, D.; Bengis, R.; Paweska, J.; Karesh, W.B. Rift Valley Fever: Does Wildlife Play a Role? *ILAR J.* **2017**, *58*, 359–370. [[CrossRef](#)]
19. Bird, B.H.; Ksiazek, T.G.; Nichol, S.T.; MacLachlan, N.J. Rift Valley Fever Virus. *J. Am. Vet. Med. Assoc.* **2009**, *234*, 883–893. [[CrossRef](#)]
20. Breiman, R.F. Decision-Support Tool for Prevention and Control of Rift Valley Fever Epizootics in the Greater Horn of Africa. *Am. J. Trop. Med. Hyg.* **2010**, *83*, 75–85. [[CrossRef](#)]
21. Bird, B.H.; Nichol, S.T. Breaking the Chain: Rift Valley Fever Virus Control via Livestock Vaccination. *Curr. Opin. Virol.* **2012**, *2*, 315–323. [[CrossRef](#)] [[PubMed](#)]
22. World Health Organization. The Use of Veterinary Vaccines for Prevention and Control of Rift Valley Fever: Memorandum from a WHO/FAO Meeting. *Bull. World Health Organ.* **1983**, *61*, 261–268.
23. Smithburn, K.C. Rift Valley Fever: The Neurotropic Adaptation of the Virus and the Experimental Use of This Modified Virus as a Vaccine. *Br. J. Exp. Pathol.* **1949**, *30*, 1–16.
24. Coetzer, J.A.W.; Barnard, B.J.H. Hydrops Amnii in Sheep Associated with Hydranencephaly and Arthrogyrposis with Wesselsbron Disease and Rift Valley Fever Viruses as Aetiological Agents. *Onderstepoort J. Vet. Res.* **1977**, *44*, 119–126.
25. Mariner, J. *Rift Valley Fever Surveillance*; FAO Animal Production and Health Manual No 21; Food and Agriculture Organization of the United Nations: Rome, Italy, 2018; p. 80, ISBN 978-92-5-130244-6.
26. Al-Afaleq, A.I.; Hussein, M.F. The Status of Rift Valley Fever in Animals in Saudi Arabia: A Mini Review. *Vector-Borne Zoonotic Dis.* **2011**, *11*, 1513–1520. [[CrossRef](#)]
27. Peyre, M.; Chevalier, V.; Abdo-Salem, S.; Velthuis, A.; Antoine-Moussiaux, N.; Thiry, E.; Roger, F. A Systematic Scoping Study of the Socio-Economic Impact of Rift Valley Fever: Research Gaps and Needs. *Zoonoses Public Health* **2015**, *62*, 309–325. [[CrossRef](#)] [[PubMed](#)]
28. Tempia, C.; Abdi, A.M. Economic Impact of Rift Valley Fever on the Somali Livestock Industry and a Novel Surveillance Approach in Nomadic Pastoral Systems. In Proceedings of the 11th International Symposium on Veterinary Epidemiology and Economics, Cairns, Australia, 2006.
29. Métras, R.; Collins, L.M.; White, R.G.; Alonso, S.; Chevalier, V.; Thurairanira-McKeever, C.; Pfeiffer, D.U. Rift Valley Fever Epidemiology, Surveillance, and Control: What Have Models Contributed? *Vector-Borne Zoonotic Dis.* **2011**, *11*, 761–771. [[CrossRef](#)]
30. Anyamba, A.; Linthicum, K.J.; Small, J.L.; Collins, K.M.; Tucker, C.J.; Pak, E.W.; Britch, S.C.; Eastman, J.R.; Pinzon, J.E.; Russell, K.L. Climate Teleconnections and Recent Patterns of Human and Animal Disease Outbreaks. *PLoS Negl. Trop. Dis.* **2012**, *6*, e0001465. [[CrossRef](#)] [[PubMed](#)]
31. Williams, R.; Malherbe, J.; Weepener, H.; Majiwa, P.; Swanepoel, R. Anomalous High Rainfall and Soil Saturation as Combined Risk Indicator of Rift Valley Fever Outbreaks, South Africa, 2008–2011. *Emerg. Infect. Dis.* **2016**, *22*, 2054–2062. [[CrossRef](#)]
32. Anyamba, A.; Chretien, J.-P.; Small, J.; Tucker, C.J.; Formenty, P.B.; Richardson, J.H.; Britch, S.C.; Schnabel, D.C.; Erickson, R.L.; Linthicum, K.J. Prediction of a Rift Valley Fever Outbreak. *Proc. Natl. Acad. Sci. USA* **2009**, *106*, 955–959. [[CrossRef](#)] [[PubMed](#)]
33. Davies, F.G.; Linthicum, K.J.; James, A.D. Rainfall and Epizootic Rift Valley Fever. *Bull. World Health Organ.* **1985**, *63*, 941–943. [[PubMed](#)]
34. Lancelot, R.; Cêtre-Sossah, C.; Hassan, O.A.; Yahya, B.; Ould Elmamy, B.; Fall, A.G.; Lo, M.M.; Apolloni, A.; Arsevska, E.; Chevalier, V. Rift Valley Fever: One Health at Play? In *Transboundary Animal Diseases in Sahelian Africa and Connected Regions*; Kardjadj, M., Diallo, A., Lancelot, R., Eds.; Springer International Publishing: Cham, Switzerland, 2019; pp. 121–148, ISBN 978-3-030-25384-4.
35. Davies, F.G. Risk of a Rift Valley Fever Epidemic at the Haj in Mecca, Saudi Arabia. *Rev. Sci. Tech. Off. Int. Epiz.* **2006**, *25*, 137–147. [[CrossRef](#)]
36. Search ProMED Posts-ProMED-Mail. Available online: <https://promedmail.org/promed-posts/> (accessed on 13 January 2021).
37. OIE Handistatus II. Available online: <http://web.oie.int/hs2/report.asp> (accessed on 4 November 2020).

38. OIE WAHIS Interface. Available online: <https://www.oie.int/animal-health-in-the-world/the-world-animal-health-information-system/data-after-2004-wahis-interface/> (accessed on 13 January 2021).
39. WHO. Rift Valley Fever. Available online: [http://www.who.int/csr/don/archive/disease/rift\\_valley\\_fever/en/](http://www.who.int/csr/don/archive/disease/rift_valley_fever/en/) (accessed on 5 November 2020).
40. CDC. Outbreak Summaries. Rift Valley Fever. Available online: <https://www.cdc.gov/vhf/rvf/outbreaks/summaries.html> (accessed on 5 November 2020).
41. Pienaar, N.J.; Thompson, P.N. Temporal and Spatial History of Rift Valley Fever in South Africa: 1950 to 2011. *Onderstepoort J. Vet. Res.* **2013**, *80*, 13. [[CrossRef](#)]
42. Swanepoel, R.; Coetzer, J. Rift Valley Fever. *Infect. Dis. Livest.* **2004**, *2*, 1037–1070.
43. Sindato, C.; Karimuribo, E.D.; Pfeiffer, D.U.; Mboera, L.E.G.; Kivaria, F.; Dautu, G.; Bernard, B.; Paweska, J.T. Spatial and Temporal Pattern of Rift Valley Fever Outbreaks in Tanzania; 1930 to 2007. *PLoS ONE* **2014**, *9*, e0088897. [[CrossRef](#)] [[PubMed](#)]
44. Davies, F.G. Observations on the Epidemiology of Rift Valley Fever in Kenya. *J. Hyg.* **1975**, *75*, 219–230. [[CrossRef](#)]
45. Clark, M.H.A.; Warimwe, G.M.; Di Nardo, A.; Lyons, N.A.; Gubbins, S. Systematic Literature Review of Rift Valley Fever Virus Seroprevalence in Livestock, Wildlife and Humans in Africa from 1968 to 2016. *PLoS Negl. Trop. Dis.* **2018**, *12*, e0006627. [[CrossRef](#)]
46. Clements, A.C.A.; Pfeiffer, D.U.; Martin, V.; Otte, M.J. A Rift Valley Fever Atlas for Africa. *Prev. Vet. Med.* **2007**, *82*, 72–82. [[CrossRef](#)] [[PubMed](#)]
47. UNSD—Methodology. Available online: <https://unstats.un.org/unsd/methodology/m49/> (accessed on 5 November 2020).
48. GADM. Available online: <https://gadm.org/> (accessed on 5 November 2020).
49. R Core Team. *R: A Language and Environment for Statistical Computing*; R Foundation for Statistical Computing: Vienna, Austria, 2020.
50. Bates, D.; Mächler, M.; Bolker, B.; Walker, S. Fitting Linear Mixed-Effects Models Using Lme4. *J. Stat. Softw.* **2015**, *67*, 1–48. [[CrossRef](#)]
51. South, A. Rnaturalearth: World Map Data from Natural Earth. 2017. Available online: <https://cran.r-project.org/web/packages/rnaturalearth/vignettes/rnaturalearth.html> (accessed on 4 June 2021).
52. Wickham, H. *Ggplot2: Elegant Graphics for Data Analysis*; Springer: New York, NY, USA, 2016; ISBN 978-3-319-24277-4.
53. Wilke, C.O. Cowplot: Streamlined Plot Theme and Plot Annotations for “Ggplot2”. 2020. Available online: <https://cran.r-project.org/web/packages/cowplot/index.html> (accessed on 4 June 2021).
54. Bażanów, B.A.; Stygar, D.; Romuk, E.; Skrzep-Poloczek, B.; Pachoń, J.; Gadzała, Ł.; Welz, M.; Paweska, J.T. Preliminary Serological Investigation of Rift Valley Fever in Poland. *J. Vector Borne Dis.* **2018**, *55*, 324–326. [[CrossRef](#)]
55. Kokernot, R.H.; Smithburn, K.C.; Weinbren, M.P. Neutralizing Antibodies to Arthropod-Borne Viruses in Human Beings and Animals in the Union of South Africa. *J. Immunol.* **1956**, *77*, 313–323.
56. Shone, D.K. Rift Valley Fever in Southern Rhodesia. *Cent. Afr. J. Med.* **1958**, *4*, 284–286.
57. Selmi, R. First Serological Evidence of the Rift Valley Fever Phlebovirus in Tunisian Camels. *Acta Trop.* **2020**, *6*, 105462. [[CrossRef](#)] [[PubMed](#)]
58. Eisa, M. Preliminary Survey of Domestic Animals of the Sudan for Precipitating Antibodies to Rift Valley Fever Virus. *J. Hyg.* **1984**, *93*, 629–637. [[CrossRef](#)]
59. Maurice, Y. Baille First Serological Record on the Incidence of Wesselsbronn’s Disease and Rift Valley Fever in Sheep and Wild Ruminants in Chad and Cameroon. *Rev. Elev. Med. Vet Pays. Trop.* **1967**, *20*, 395–405. [[CrossRef](#)] [[PubMed](#)]
60. Saleh Aghaa, O.B.; Rhaymah, M.S. Seroprevalence Study of Rift Valley Fever Antibody in Sheep and Goats in Ninevah Governorate. *Iraqi J. Vet. Sci.* **2013**, *27*, 53–61. [[CrossRef](#)]
61. Fakour, S.; Naserabadi, S.; Ahmadi, E. The First Positive Serological Study on Rift Valley Fever in Ruminants of Iran. *J. Vector Borne Dis.* **2017**, *54*, 348. [[CrossRef](#)]
62. Gür, S.; Kale, M.; Erol, N.; Yapici, O.; Mamak, N.; Yavru, S. The First Serological Evidence for Rift Valley Fever Infection in the Camel, Goitered Gazelle and Anatolian Water Buffaloes in Turkey. *Trop. Anim. Health Prod.* **2017**, *49*, 1531–1535. [[CrossRef](#)]
63. Shoemaker, T.R.; Nyakarahuka, L.; Balinandi, S.; Ojwang, J.; Tumusiime, A.; Mulei, S.; Kyondo, J.; Lubwama, B.; Sekamatte, M.; Namutebi, A.; et al. First Laboratory-Confirmed Outbreak of Human and Animal Rift Valley Fever Virus in Uganda in 48 Years. *Am. J. Trop. Med. Hyg.* **2019**, *100*, 659–671. [[CrossRef](#)] [[PubMed](#)]
64. Métras, R.; Cavalerie, L.; Dommergues, L.; Mérot, P.; Edmunds, W.J.; Keeling, M.J.; Cêtre-Sossah, C.; Cardinale, E. The Epidemiology of Rift Valley Fever in Mayotte: Insights and Perspectives from 11 Years of Data. *PLoS Negl. Trop. Dis.* **2016**, *10*, e0004783. [[CrossRef](#)]
65. Tigoi, C.; Sang, R.; Chepkorir, E.; Orindi, B.; Arum, S.O.; Mulwa, F.; Mosomtai, G.; Limbaso, S.; Hassan, O.A.; Irura, Z.; et al. High Risk for Human Exposure to Rift Valley Fever Virus in Communities Living along Livestock Movement Routes: A Cross-Sectional Survey in Kenya. *PLoS Negl. Trop. Dis.* **2020**, *14*, e0007979. [[CrossRef](#)] [[PubMed](#)]
66. Sumaye, R.D.; Geubbels, E.; Mbeyela, E.; Berkvens, D. Inter-Epidemic Transmission of Rift Valley Fever in Livestock in the Kilombero River Valley, Tanzania: A Cross-Sectional Survey. *PLoS Negl. Trop. Dis.* **2013**, *7*, e0002356. [[CrossRef](#)]
67. Sumaye, R.D.; Abatih, E.N.; Thiry, E.; Amuri, M.; Berkvens, D.; Geubbels, E. Inter-Epidemic Acquisition of Rift Valley Fever Virus in Humans in Tanzania. *PLoS Negl. Trop. Dis.* **2015**, *9*, e0003536. [[CrossRef](#)] [[PubMed](#)]

68. Wichgers Schreur, P.J.; Oreshkova, N.; van Keulen, L.; Kant, J.; van de Water, S.; Soós, P.; Dehon, Y.; Kollár, A.; Péntzes, Z.; Kortekaas, J. Safety and Efficacy of Four-Segmented Rift Valley Fever Virus in Young Sheep, Goats and Cattle. *NPJ Vaccines* **2020**, *5*, 65. [[CrossRef](#)] [[PubMed](#)]
69. World Health Organization. An Outbreak of Rift Valley Fever, Eastern Africa, 1997–1998. *Wkly. Epidemiol. Rec. Relev. Épidémiol. Hebd.* **1998**, *73*, 105–109.
70. CDC. Signs and Symptoms. Rift Valley Fever. Available online: <https://www.cdc.gov/vhf/rvf/symptoms/index.html> (accessed on 21 December 2020).
71. Watts, D.M.; el-Tigani, A.; Botros, B.A.; Salib, A.W.; Olson, J.G.; McCarthy, M.; Ksiazek, T.G. Arthropod-Borne Viral Infections Associated with a Fever Outbreak in the Northern Province of Sudan. *J. Trop. Med. Hyg.* **1994**, *97*, 228–230. [[PubMed](#)]
72. Signs of Rift Valley Fever. Available online: <http://www.fao.org/3/Y4611E/y4611e05.htm> (accessed on 27 January 2021).
73. Corwin, A.; Habib, M.; Watts, D.; Olson, J.; Darwis, M.; Hibbs, R.; Botros, B.; Kleinosky, M.; Shope, R.; Kilpatrick, M. Prevalence of Antibody to Rift Valley Fever Virus in the Nile River Delta of Egypt, 13 Years after a Major Outbreak. *Trans. R. Soc. Trop. Med. Hyg.* **1993**, *87*, 161. [[CrossRef](#)]
74. Rostal, M.K.; Ross, N.; Machalaba, C.; Cordel, C.; Paweska, J.T.; Karesh, W.B. Benefits of a One Health Approach: An Example Using Rift Valley Fever. *One Health* **2018**, *5*, 34–36. [[CrossRef](#)] [[PubMed](#)]



# Hélène Cecilia

My goal is to develop mathematical models across scales to better understand the epidemiology and ecology of infectious diseases, with a special interest for vector borne and zoonotic diseases.

I thrive in pluridisciplinary environments. Oral and visual communication are my strong suits.

@HelCecilia on Twitter - ORCID 0000-0001-5687-3570

## Education

- 2018–Present **PhD - Epidemiology**, BIOEPAR, INRAE (National Research Institute for Agriculture, Food and Environment), ONIRIS (College of Veterinary Medicine, Food Science and Engineering), Nantes, France.  
**Advisors** Pauline Ezanno, Raphaëlle Métras, Renaud Lancelot  
**Jury** Samuel Alizon, Cécile Viboud, Catherine Linard, Sebastian Lequime
- 2010–2015 **Master of Science (BSc, MSc) - Engineering degree in Bioinformatics and Mathematical Modelling**.  
National Institute of Science and Technology (INSA), Lyon, France

## Research positions

- 2018–Present **PhD student - Modelling Rift Valley fever virus dynamics : insights from micro- to macro-scale studies**, BIOEPAR, INRAE, ONIRIS, Nantes, France.  
**Type of models** compartmental, metapopulation, within-host  
**Skills**  $R_0$  (next generation matrix), Metropolis-Hastings MCMC, sensitivity analysis  
**Data handled** spatial data : remotely-sensed temperature, rainfall, water body locations, laboratory data : viral load, vector competence, viral genome segment counts
- October 2019; **Visiting researcher**, Wageningen University and Research, The Netherlands.  
March 2020 Temporarily joined the Quantitative Veterinary Epidemiology group (chaired by Prof. Mart de Jong) and collaborated with Dr. Quirine ten Bosch.
- January 2016 - **Engineer in mathematical biology and programming**, BIOEPAR, INRAE, ONIRIS, Nantes, France.  
October 2017 Developing a computational model of tsetse fly population dynamics in order to evaluate control strategies in Senegal.  
Compartmental, spatially explicit (suitability-driven dispersal), deterministic model. Calibration on field (mark-recapture) and laboratory data (temperature-dependent survival and development rates). Sensitivity analysis. Optimize selection of locations for control.
- February - October 2015 **Engineer in swarm robotics**, Bristol Robotics Laboratory, United Kingdom,  
6 month internship followed by 3 month contract.  
Computational modelling of nanoparticles convection-enhanced delivery against brain cancer.  
Agent-based stochastic model. Application with a swarm of Kilobots.

## Publications

### Peer-reviewed

1. Bron GM, Strimbu K, [Cecilia H](#), Lerch A, Moore S, Tran Q, Perkins TA, ten Bosch QA **2021** Over 100 years of Rift Valley fever : a patchwork of data on pathogen spread and spillover. *Pathogens* 10, 708. [10.3390/pathogens10060708](https://doi.org/10.3390/pathogens10060708)
2. [Cecilia H](#), Arnoux S, Picault S, Dicko A, Seck MT, Sall B, Bassène M, Vreysen M, Pagabeleguem S, Bancé A, Bouyer J and Ezanno P. **2021** Dispersal in heterogeneous environments drives population dynamics and control of tsetse flies. *Proceedings of the Royal Society Biology* 288 : 20202810. [10.1098/rspb.2020.2810](https://doi.org/10.1098/rspb.2020.2810) - extended version of 4.
3. [Cecilia H](#), Métras R, Fall AG, Lo MM, Lancelot R, Ezanno P. **2020** It's risky to wander in September : modelling the epidemic potential of Rift Valley fever in a Sahelian setting. *Epidemics* 33 100409. [10.1016/j.epidem.2020.100409](https://doi.org/10.1016/j.epidem.2020.100409)
4. [Cecilia H](#), Arnoux S, Picault S, Dicko A, Seck MT, Sall B, Bassène M, Vreysen M, Pagabeleguem S, Bancé A, Bouyer J and Ezanno P. **2019** Environmental heterogeneity drives tsetse fly population dynamics and control. bioRxiv 493650., ver. 3 peer-reviewed and recommended by *PCI Ecology*. [10.11101/493650](https://doi.org/10.11101/493650)

### In preparation

[Cecilia H](#), Vriens R, Métras R, Kortekaas J, Wichgers Schreur P, de Wit M, Ezanno P, ten Bosch QA **Submission summer 2021** A model-based analysis of host viral load and vector infection reveals Rift Valley fever virus transmission potential across livestock species

[Cecilia H](#), Drouin A, Métras R, Chevalier V, Durand B, Ezanno P **Submission autumn 2021** A systematic review of Rift Valley fever virus mechanistic models of transmission

[Cecilia H](#), Arnoux S, Durand B, Métras R, Lancelot R, Chevalier V, Ezanno P **Submission winter 2021** Seasonal herd movements and Rift Valley fever in the Sahel : insights from a metapopulation model

## Conferences & seminars

Oral communications [Cecilia H](#), Vriens R, Métras R, Kortekaas J, Wichgers Schreur P, de Wit M, Ezanno P, ten Bosch QA - Not created equal : Exploring Rift Valley fever transmission potential across livestock species. Modelling in Animal Health conference (MODAH) - 27 May 2021, online.

[Cecilia H](#), Métras R, Lancelot R, Ezanno P - Epidemic potential of Rift Valley fever in a Sahelian setting. BioHasard. 26-29 Aug 2019 | Rennes, France.

[Cecilia H](#), Dicko A, Arnoux S, Picault S, Bancé A, Bouyer J, Ezanno P - Controlling the spatio-temporal population dynamics of tsetse flies, vectors of nagana disease, in a cattle breeding region of Senegal. Modelling in Animal Health conference (MODAH), 14-16 Jun 2017 | Nantes, France.

[Cecilia H](#), Dicko A, Arnoux S, Picault S, Bancé A, Bouyer J, Ezanno P - A mechanistic model of tsetse fly population dynamics in space and time calibrated on observed data in Senegal. 8th Workshop on Dynamical Systems Applied to Biology and Natural Sciences (DSABNS), 31 Jan - 03 Feb 2017 | Evora, Portugal. [10.13140/RG.2.2.11037.31208](https://doi.org/10.13140/RG.2.2.11037.31208)

Invited talks [Cecilia H](#). Examples of resilience in epidemiological and ecological systems in Senegal. PhD course, Resilience of living systems, Wageningen University and Research - 2021

[Cecilia H](#), Bermúdez Méndez E, ten Bosch QA. Rift Valley fever : how missing pieces of a three-segment puzzle impact infection in sheep. Quantitative Veterinary Epidemiology colloquium, Wageningen University and Research - 2020

Poster presentations [Cecilia H](#), Arnoux S, Durand B, Métras R, Lancelot R, Chevalier V, Ezanno P - Seasonal herd movements and Rift Valley fever in the Sahel : insights from a metapopulation model. Accepted for *Epidemics*<sup>8</sup>, 30 nov - 3 dec 2021, online

Cecilia H, Vriens R, Ezanno P, Kortekaas J, Wichgers Schreur P, de Wit M, Métras R, ten Bosch QA - Infect or Die Tryin' - Estimation of Rift Valley fever virus species-specific transmission potential. EEID 2021, online.

Cecilia H, Vriens R, Ezanno P, Kortekaas J, Wichgers Schreur P, de Wit M, Métras R, ten Bosch QA - Rift Valley fever virus hosts are not equal - Modelling infectiousness at the individual level. SVEPM 2021, online - **Awarded the poster prize**

Ezanno P, Cecilia H, Dicko A, Arnoux S, Picault S, Bancé A, Bouyer J - A temperature and mortality driven population dynamics of tsetse flies in endemic area : insights from a mechanistic spatio-temporal model calibrated on observed data. Epidemics<sup>6</sup> - International Conference on Infectious Disease Dynamics, 29 Nov - 1 Dec 2017 | Sitges, Spain

Bouyer J, Cecilia H, Dicko A, Arnoux S, Picault S, Bancé A, Ezanno P - Controlling the spatio-temporal dynamics of tsetse flies : insights from a mechanistic model. Third FAO-IAEA International Conference on Area-wide Management of Insect Pests : Integrating the Sterile Insect and Related Nuclear and Other Techniques, 22-26 May 2017 | Vienna, Austria.

## Service

BIOEPAR unit  
scientific council  
Representative of PhD students

BIOEPAR unit  
internal council  
Representative of fixed-term  
contract employees

## Grants

CIRAD Fellowship 1500 € (2019) 2000 € (2020) 500 € (2021)

INRAE Fellowship 2500 €

EGAAL Graduate School Fellowship 400 €

## Software skills

In decreasing order  
of expertise  
R, Python, Bash, Git, C++, Java

## Languages

Mothertongue French  
High level English (TOEIC 960/990)  
Basic Italian, Spanish, Indonesian

## Teaching experience

University Institute  
of Technology,  
Nantes : 24h - 2018  
Object-oriented programming in Java

## Trainings

Nature Masterclass Scientific writing and publishing

MOOC Institut Pasteur Medical entomology

University of Washington Summer Institute in Statistics and Modeling in Infectious Diseases - 2 modules

1. Infectious diseases, immunology and within-host models
2. Statistics and modeling with novel data streams

## Interests and achievements

- Football, futsal, rugby (5-a-side, no tackle)
- Half-marathon : did it once, won't do it again ;)
- 2018 : Gap year to live in Indonesia (3 months) and travel across South-East Asia (5 months)

## Science outreach activities

### In french

- Labo des Savoirs Volunteering for a scientific radio program. President of the association for 1 year, volunteering since 2018 [labodessavoirs.fr](http://labodessavoirs.fr)
- Youtube video Present your PhD in 150 seconds. Part of PhD seminar by Agreenium. [Click here to see it](#)
- La nuit blanche des chercheurs Science-dating : 5x8 minutes sessions (on Zoom) presenting your research and answering questions [nbc.univ-nantes.fr](http://nbc.univ-nantes.fr)
- Pint of Science Member of the organizing committee in Nantes (France). Recruiting speakers, event communication and animation. [pintofscience.com](http://pintofscience.com)
- March for Science Member of the organizing committee for the satellite march in Nantes (France), 400 participants. Worldwide event defending the role of science in policy and society. [marchforscience.com](http://marchforscience.com)

### In english

- Skype a scientist Skype session with a classroom of the American International School of Guangzhou, China (16 years old students), to talk about my research. [skypeascientist.com](http://skypeascientist.com)
- SoapBox Science Bristol, UK : Presenting the use of modelling in natural sciences. "Replicate nature in computer programs : it's not as scary as it seems!" [soapboxscience.org](http://soapboxscience.org)
- London Science Museum Presentation of swarm robotics : hands-on experiments with kids and demos with coin-sized Kilobots.
- University of West England Organization and animation of Ada Lovelace Day : teaching basic programming with a Thymio robot
- Take Aim competition 3rd prize awarded by the Smith Institute : Describe your research in 250 words.



**Rapport de mobilité**  
**Bourse de l'école doctorale EGAAL**  
**Hélène CECILIA**

23 mars 2020

Dans le cadre de ma thèse, je me suis inscrite à l'Ecole Internationale de Recherche Agreenium (EIR-A) pour obtenir un label certifiant la dimension internationale et professionnalisante de ma thèse. Je dois pour cela effectuer un séjour de 3 mois dans un laboratoire étranger. C'est dans ce contexte que j'ai obtenu l'aide de l'école doctorale EGAAL pour financer mon séjour, qui devait initialement se dérouler du 24 février au 27 mars 2020.

Cette mobilité a eu lieu dans l'équipe Quantitative Veterinary Epidemiology de l'université et institut de recherche de Wageningen (communément appelé WUR), aux Pays-Bas, dirigée par Prof. Mart de Jong. Cette collaboration est née grâce à Twitter, et plus particulièrement grâce à ce post de Dr Quirine ten Bosch :



Traduire le Tweet



J'ai décidé de la contacter pour lui proposer de travailler avec moi sur la modélisation de la fièvre de la Vallée du Rift (FVR). Ses publications reflétaient une expertise dans la modélisation des maladies vectorielles, appliquée à la dengue, Zika, ou encore Chikungunya, mais aucune ne faisait mention de la FVR. J'ai donc été d'autant plus surprise lorsqu'elle a répondu à mon mail en m'expliquant que certains virologues de WUR possédaient des données expérimentales inédites sur la FVR et qu'il serait intéressant que nous travaillions ensemble dessus ! Le projet était né.

J'ai effectué un premier séjour de deux semaines en octobre 2019 pour rencontrer l'équipe et réfléchir ensemble au contenu de notre collaboration. J'ai pu présenter le premier chapitre de ma thèse qui était en cours de finalisation, et avoir des retours constructifs qui m'ont aidé pour l'écriture de la publication associée. Ce premier chapitre traitait de la cartographie du risque épidémique de la FVR au Nord du Sénégal. Il s'agit donc d'une approche populationnelle : estimer le risque que le virus se transmette et provoque une épidémie, en fonction des populations de bovins, de petits ruminants et de moustiques présentes, des conditions météo (température, pluviométrie) qui affectent les paramètres biologiques des moustiques, et ce, dans le temps et dans l'espace.

Le projet permis par les données expérimentales disponibles à WUR se place à une autre échelle, complémentaire et tout aussi cruciale pour comprendre la dynamique de transmission du virus : l'échelle intra-hôte. L'idée est d'être capable de modéliser la quantité de virus présente dans le temps dans le sang de l'hôte (dans notre cas, un mouton) après qu'il ait été infecté par une piqûre de moustique. C'est important car il a été montré pour d'autres maladies vectorielles que cette quantité de virus présente dans le sang influe sur la probabilité que l'hôte transmette à son tour le virus à un moustique non porteur qui viendrait le piquer. Par ailleurs, ce modèle a également pour objectif d'expliquer pourquoi la grande partie du matériel viral trouvé dans le sang est en fait constitué de particules incomplètes (qui n'ont pas les 3 segments du génome) et donc non infectieuses, ne pouvant pas rentrer dans de nouvelles cellules du mouton pour se multiplier et proliférer. Cela paraît être une étrange stratégie de la part du virus, et on ne sait pas si c'est dû à la réponse immunitaire innée du mouton ou à cause d'un mécanisme de réplication « auto-limitante » de la part du virus. Ces hypothèses pourront être testées dans le modèle.

Lorsque je suis arrivée pour le deuxième séjour fin février, nous avions donc déjà une première idée de la structure du modèle et des questions auxquelles nous souhaitions répondre. Les 3 premières semaines de ce second séjour ont permis de coder l'algorithme qui servira à estimer les paramètres du modèle. Celui-ci se base sur une méthode statistique que je n'avais jusque là pas eu l'occasion de mobiliser et qui a donc demandé pas mal d'investissement, mais qui constitue une réelle plus-value pour mon éventail de compétences à l'issue de ma thèse. J'ai également pu échanger avec les virologues sur leurs données et affiner les hypothèses qui structurent le modèle. Il n'est pas toujours facile de se comprendre entre modélisateurs et virologues car nos langages sont différents mais c'est une expérience enrichissante pour les deux disciplines à mon sens.

J'ai réellement pu m'autonomiser pendant ce séjour, car j'échangeais peu avec mes co-encadrants en France et je pouvais mener ma barque comme je l'entendais, en ayant l'impression d'être une collaboratrice à part entière et pas une étudiante. J'ai pu nouer des liens avec de nouveaux collaborateurs aux compétences et méthodes de travail différentes, ce qui m'a ouvert l'esprit.

La crise sanitaire due au coronavirus m'a malheureusement contrainte à avancer mon retour en France de deux semaines. Vivre la propagation du virus depuis l'étranger a également été une expérience particulière : loin de ses proches, à comparer les mesures prises par les deux pays, comparer le nombre de cas, se demander si on va pouvoir rentrer. Je suis de retour, et j'espère pouvoir repartir au deuxième semestre pour finir ce projet, lorsque la crise sera derrière nous.

# Infect or Die Tryin' - Estimation of Rift Valley fever virus species-specific transmission potential

Hélène Cecilia\* Roosmarie Vriens Raphaëlle Métras Jeroen Kortekaas  
Paul Wichgers Schreur Mariken de Wit Pauline Ezanno Quirine ten Bosch

\*I'm looking for a postdoc ! helene.cecilia3@gmail.com

@HelCecilia on Twitter

## Context

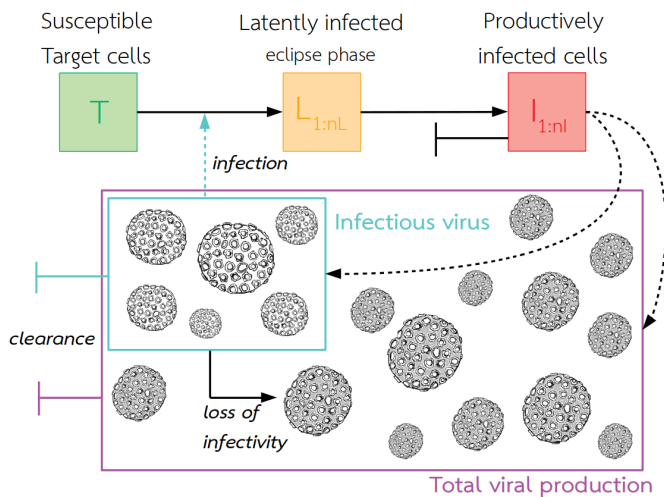
- Rift Valley fever virus (RVFV) is vector-borne and zoonotic
- RVFV affects sheep, goats, cattle, and humans
- RVFV is present throughout Africa, in the South West Indian Ocean islands, and the Arabian Peninsula
- The main mosquitoes involved in RVFV transmission are *Aedes* and *Culex* spp.

## Step 1 : Data, model, and fit

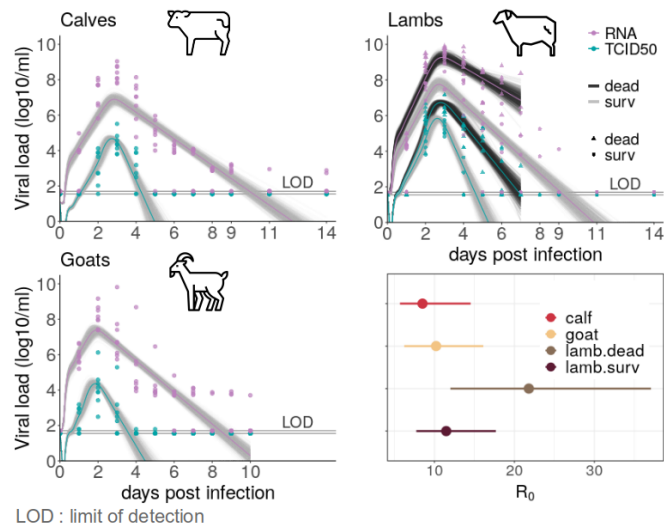
**Protocol** : 16 lambs got exposed (8 calves, 8 young goats), all animals got infected, 10 out of 16 lambs died (0 calves and goats)

**Data** : total viral loads (RNA measured by RT-qPCR) and infectious titers (measured by TCID<sub>50</sub>) in plasma following laboratory infection by RVFV

### Within-host model



### Fit to viral kinetics data of 3 livestock species



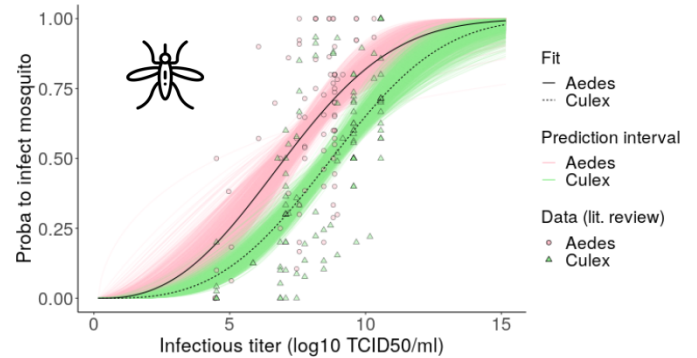
LOD : limit of detection

R<sub>0</sub> : average number of cells getting infected by one infected cell introduced into an entirely susceptible population

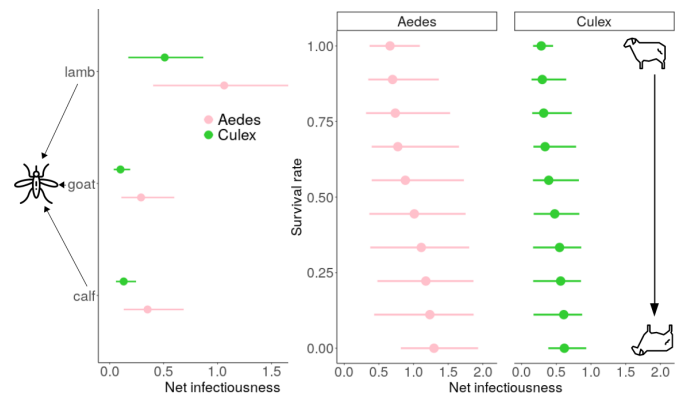
## Goal

Investigate whether some livestock species are more infectious than others

## Step 2 : Probability to infect mosquitoes



## Step 3 : Net infectiousness



Net infectiousness : average number of mosquitoes infected by a host over its infectious period

## Take-home messages

- Lambs have the highest infectiousness to mosquitoes, due to higher peak viremia and a longer infection
- Despite reduced lifespan, lambs dying from RVF are more infectious overall than surviving ones
- Together with vector feeding preferences, husbandry and trading practices, net infectiousness determines species' contribution to overall transmission



## E Pictures taken during my field trip in Senegal - December 2019



Example of a pond during the dry season (the only one I saw!)

*Exemple de mare pendant la saison sèche (la seule que j'ai vu du séjour!)*



Our camp for the first night. In the background, the pen where animals spend the night.

*Notre camp pour la première nuit. Au fond, l'enclos où les animaux passent la nuit.*



Lunch visit at the second herder's camp. In the background, the temporary house built for the dry season.

*Visite chez le deuxième éleveur pour le déjeuner. Au fond, la case fabriquée pour la saison sèche.*



Our car, with mattresses at the back. A small village in the background. The best field buddies I could have hoped for : Ibra Toure (front), Moustapha Dia (right, back) and Diam Sow (left, back).

*Notre voiture, avec les matelas à l'arrière. Au fond, un petit village. Les meilleurs compagnons de terrain : Ibra Toure (premier plan), Moustapha Dia (au fond à droite) et Diam Sow (au fond à gauche).*



Camp of the third herder, where we stayed for the second night. Close to the border with The Gambia, there is a bit more vegetation than during the rest of the trip.

*Campement du troisième éleveur, où nous avons passé la deuxième nuit. Près de la frontière gambienne, il y a un peu plus de végétation que précédemment dans le séjour.*



All set for a second night under the stars!  
*Prêts pour une deuxième nuit sous les étoiles!*



Donkeys are used to carry the family's belongings and bring back the water from the well/drilling.  
*Les ânes sont utilisés pour transporter les affaires de la famille et pour ramener l'eau du puit/fôrage.*







**Titre :** Dynamique de transmission du virus de la fièvre de la Vallée du Rift : modélisation mathématique de l'échelle micro à l'échelle macro

**Mots clés :** fièvre de la Vallée du Rift ; modélisation mathématique ; maladie vectorielle ; multi-hôte ; Senegal

**Résumé :** La fièvre de la Vallée du Rift (FVR) est une maladie virale, vectorielle, et zoonotique. Elle touche principalement les animaux d'élevage : bovins, chèvres, moutons. Nous visons à mieux comprendre la contribution des différentes espèces d'hôtes à la transmission du virus de la FVR, en prenant comme zone d'étude le Sénégal. Une revue de la littérature nous a permis de caractériser la diversité des modèles mathématiques existants, et les questions que ces derniers n'ont pas encore abordé concernant la FVR. Nous avons ensuite cartographié le potentiel épidémique de la FVR au nord du Sénégal, et avons montré que pendant 3 saisons des pluies consécutives (2014-2016), le mois de Septembre était la période la plus à risque. Pour quantifier de potentielles différences d'infectiosité entre espèces d'hôtes à l'échelle individuelle, nous avons développé un modèle intra-hôte de la

dynamique virale, et avons fait le lien avec la probabilité d'infecter les vecteurs. Nos résultats montrent que les moutons sont l'espèce la plus infectieuse, et que les moustiques du genre *Aedes* s'infectent plus facilement que les *Culex*. Enfin, nous avons incorporé cette hétérogénéité dans une métapopulation modélisant les mouvements de transhumance saisonniers au nord du Sénégal. Cela nous a permis de quantifier le délai entre l'introduction du virus de la FVR par les populations nomades et la propagation de l'infection chez les sédentaires. Nous avons également mis en évidence une infection systématiquement plus précoce chez les bovins que chez les petits ruminants. Cette thèse a ainsi permis de mieux comprendre la dynamique de transmission d'un pathogène multi-hôtes et d'identifier des pistes pour l'élaboration de stratégies de maîtrise ciblées et efficaces.

**Title :** Modeling Rift Valley fever transmission dynamics : insight from micro- to macro-scale studies

**Keywords :** Rift Valley fever virus, mathematical modeling, vector-borne disease, multi-host, Senegal

**Abstract :** Rift Valley fever (RVFV) is a viral, vector-borne, zoonotic disease. It affects multiple hosts, mainly livestock such as cattle, sheep, and goats. We aimed at enhancing knowledge on the relative contribution of host species to transmission, focusing on Senegal, a region with recurring RVFV circulation. With a systematic review of existing mechanistic models of RVFV transmission dynamics, we identified critical knowledge gaps and characterised the diversity of modelling approaches. We mapped RVFV epidemic potential in northern Senegal for three consecutive rainy seasons (2014-2016), using the basic reproduction number. September was identified as a period of high risk of amplification following RVFV introduction. To quantify differences in infectiousness between host species, we developed the first within-host model of RVFV production by host cells, and

estimated the relationship between host infectious viral loads and the probability to infect mosquitoes. The results showed that sheep were the most infectious host species, and that *Aedes* vectors were more likely to get infected than *Culex* when fed with similarly infectious bloodmeals. We incorporated this heterogeneity into a metapopulation model representing seasonal herd movements in northern Senegal. We quantified the delay between RVFV introduction through nomadic herds and infection of sedentary populations. We highlighted a systematic earlier infection in cattle than goats and sheep. This PhD used modeling to disentangle the complex transmission dynamics of a multi-host multi-vector pathogen, highlighting possible avenues for the development of efficient and targeted control strategies, crucial to ultimately prevent human cases.